

Cover

February Cover —

The PB-2022 one-kilowatt amplifier provides 50 dB of gain in one modular "supercomponent." The PB-2022, and many other products, will be exhibited at RF TECHNOLOGY EXPO 85. Cover photograph courtesy of Acrian.

Features

26 Special Report: Modules Lead the Way at RF TECHNOLOGY EXPO

Modular "supercomponents" can simplify life for the design engineer. Also a preview of the exhibits at RF TECHNOLOGY EXPO 85. Kiyoshi Akima.

36 The SAW Resonator: How It Works

The first part of this two-part series provides an introduction to the subject of surface acoustic wave resonators. A TI-59 program is given to model the responses of these devices. Jeff Schoenwald.

46 The Phase/Frequency Detector

This article discusses the design of phase-locked loops employing phase/frequency detectors. James Crawford.

Departments

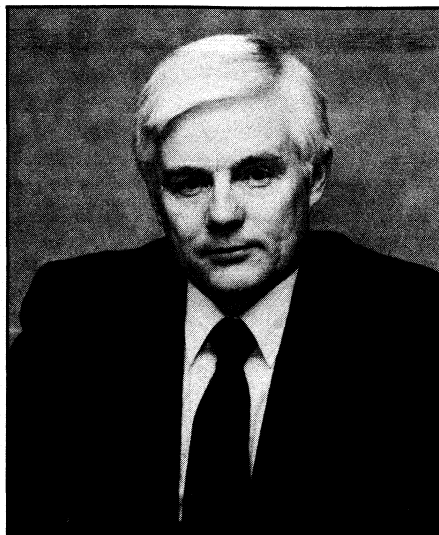
- 6 Editorial
- 8 Publisher's Notes
- 11 Letters
- 16 News
- 61 RFI/EMI Corner
- 62 The Digital Connection
- 64 RF Designer's Notebook
- 67 Info Card
- 71 Product of the Month
- 72 New Products
- 88 New Literature
- 94 Advertisers Index

Special Report p. 26

R.F. DESIGN (ISSN: 0163-321X USPS: 453-490) is published monthly plus one extra issue in June. February 1985, Volume 8, No. 2. Copyright 1985 by Cardiff Publishing Company, a subsidiary of Argus Press Holdings, Inc., 6530 S. Yosemite Street, Englewood, CO 80111 (303) 694-1522. Contents may not be reproduced in any form without written permission. Second-Class Postage paid at Englewood, CO and at additional mailing offices. Subscription office: 1 East First Street, Duluth, MN 55802, (1-800-346-0085). Subscriptions are sent free to qualified individuals responsible for the design and development of communications equipment. Other subscriptions are: \$15 per year in the United States; \$25 per year in Canada and Mexico; \$25 per year for foreign countries. Additional cost for first class mailing. Payment must be made in U.S. funds and accompany request. If available, single copies and back issues are \$5.00 each (in the U.S.). This publication is available on microfilm/fiche from University Microfilms International, 300 N. Zeeb Road, Ann Arbor, MI 48106 USA (313) 761-4700.

POSTMASTER & SUBSCRIBERS: Please send address changes to: R.F. Design, P.O. Box 6317, Duluth, MN 55806.

The Boom in RF Communications



Jim MacDonald
Editor

A news item in last month's issue told about the sales a new California company anticipates in communication systems operating below 2 GHz. Many companies are expecting a growing market for RF communications equipment, especially overseas.

Much of the world depends on the RF spectrum for local communications. The Europeans have been using cellular radio for years, getting their components from American firms. *RF Design* has learned that one African nation has contracted with an American firm for a nationwide RF telephone system.

We at *RF Design* expect to see an RF communications boom in the next few years to rival the computer phenomenon of the last 20 years. People in ordinary occupations are finding they need to communicate faster. Stock brokers in New York, for example, can no longer rely on the telephone or the "tape" for the kind of minute-by-minute stock and bond quotations they need in a volatile market. They are turning to radio as highly selective narrowband antennas make radio communication possible in the canyon-like streets.

Even the military, the largest user of satellite communications, is a large-

volume buyer of RF equipment. Tactical battlefield communications and control systems still use VHF to a large extent, partly because short-range, line-of-sight communications are more secure.

Information exchange in the civilian sector is becoming increasingly time-sensitive. The speed at which we can access information and perform calculations with digital equipment is mind-boggling, but how valuable is the information unless it can be communicated to the right people when they need it? America, with the best telephone system in the world, will probably continue to develop and improve satellite communications, but other nations may not have this capability for years.

Futurists talk about the decentralized workplace. They predict people will work at home on computers tied to a central office mainframe. If this does come about, think how important short-range radio and telephone communication may become. Electronic mail is no substitute for person-to-person conversation, either for conveying complex ideas or for that contact with other people we all need.

We are flooded with information about the world, but we have little communication with each other. Most of us probably know more about the health of the latest Russian leader than we do about the health of our next door neighbor. Sociologists may know why we isolate ourselves — maybe it is necessary. The recent growth in amateur radio, however, and the tenacity with which CB radio has held on in spite of its problems indicate a deep desire to communicate with our fellow human beings, even when we have nothing important to say.

As this issue goes to press the *RF Design* staff is preparing for the RF Technology Expo, January 23-25, bringing together engineers, physicists and manufacturers in the RF field. We hope this exposition and symposium will provide the foundation for a continuing exchange of information. *RF Design* will provide a forum for this ongoing exchange.

A handwritten signature of Jim MacDonald in dark ink. The signature is stylized, with 'Jim' written above 'MacDonald'.

Dear Sir:

I read with great interest the two-part article by John Hatchett and Bill Howell beginning with the September/October edition. I would like to offer some additional information concerning the use of the MC3356 chip for RF modems.

In some modem designs I have used a carrier frequency low enough to use just the IF portion of the MC3356 without frequency conversion. One example of such an arrangement would be the use of the carrier frequency of 10.7 MHz using a ceramic filter as a front-end filter rather than an IF filter. Some of the sensitivity of the MC3356 is lost because the balanced mixer provides gain. An effective method of retrieving this gain is to reconnect the mixer as an RF amplifier.

The frequency conversion section of the MC3356 contains an oscillator and a balanced mixer. Referring to the diagram, Q2 is non-conducting state by connecting the emitter directly to the positive supply and the collector through the input inductor to the same supply voltage. One-half of the balanced mixer is put into the non-conducting state by connecting pin 20 to ground or pin 1. This eliminates all current flow in Q9, Q5 and Q6. Once the mixer balance is so completely upset what remains is a differential amplifier consisting of Q7, Q8 and Q10.

More than 30 dB of gain has been obtained from the circuit shown in the figure.

Sincerely,
Albert D. Helfrick
Boonton, NJ 07005

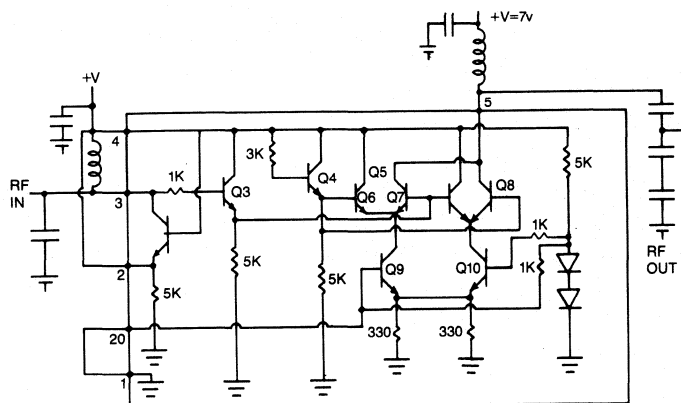


Fig. 1. Schematic of the RF section of the MC3356 receiver chip showing the connections for operating the mixer as an amplifier.

Dear Mr. Akima:

May I take this opportunity of wishing you considerable success in producing *RF Design* monthly. I for one will be very pleased to see the publication more frequently.

Your interesting article on Synthesized Generators in the Nov./Dec. issue covered in some detail recent lower cost product introductions. These generators are ideal for general purpose sources and for limited testing of communications systems, but they do not have the necessary parameters for critical performance testing.

New FCC proposals to create more channels and ease congestion in the mobile radio bands are now being discussed in

the mobile communications industry. These proposals call for channel spacings of as low as 7.5 KHz using various forms of single sideband modulation. (Channel spacing of 12.5 KHz are already common in Europe in the VHF bands.) With most signal generators only just having acceptable performance at 20 KHz carrier offset (the current channel spacing), it is debatable that these generators will be able to perform off-channel tests or be useful for development work on the proposed new systems. Synthesized signal generators such as the Racal-Dana Model 9087 or Hewlett Packard 8662 feature similar phase noise at 3 or 5 KHz carrier offset as at 20 or even 100 KHz from carrier.

Very close to carrier, offsets of less than 1 KHz, the phase noise becomes important when working with low deviation phase modulation and/or when multiplying to microwave frequencies. Again, it is only the multi-loop sophisticated signal generators that can meet these demanding requirements.

Most modern FM communications systems feature either digital data transmission modes or selective calling with digital coding. To evaluate these systems under all operating conditions requires the ability to frequency modulate the carrier with very low rates, or in some cases even DC. The lower cost synthesized signal generators often only use a single phase locked loop which requires closed loop DC operation to maintain frequency stability. These systems usually can only FM at rates above 20 or 50 Hz. The more sophisticated multi-loop systems available from some manufacturers allow true DC coupled frequency modulation.

Switching speed/setting time is perhaps the third important

area that may demand the consideration of a higher cost signal generator. For general purpose applications, a faster switching speed means that more tests may be made in a shorter period of time which can be important when, for example, fully characterizing a filter or checking a receiver for spurious responses. There are other applications particularly in the electronic warfare area that necessitate using a fast switching signal generator. Radio jammers often use a commercial synthesizer as the local oscillator. The response time of the jammer to track frequency agile systems often depends solely on the switching speed of the synthesizer. Switching speed is also important when checking the new generation of anti-jamming (ECCM) communication systems such as SINCGARS. To test an ECCM receiver dynamically, and with both traceability and repeatability requires that the signal generator can respond faster to a message to change frequency than the receiver. Currently, frequency switching speeds of less than 1 millisecond are required, which again precludes the use of the new economy signal sources.

I look forward to reading a further article on signal generators when the technology breakthroughs that influence performance rather than price/performance will be reviewed and discussed.

Sincerely,
Malcolm Levy
RF Products Manager
Racal-Dana instruments, Inc.
Irvine, CA 92714

The SAW Resonator: How It Works

Part I gives an introduction to the Surface Acoustic Wave resonator and a TI-59 program to model device responses.

*By Jeff Schoenwald
Contributing Editor*

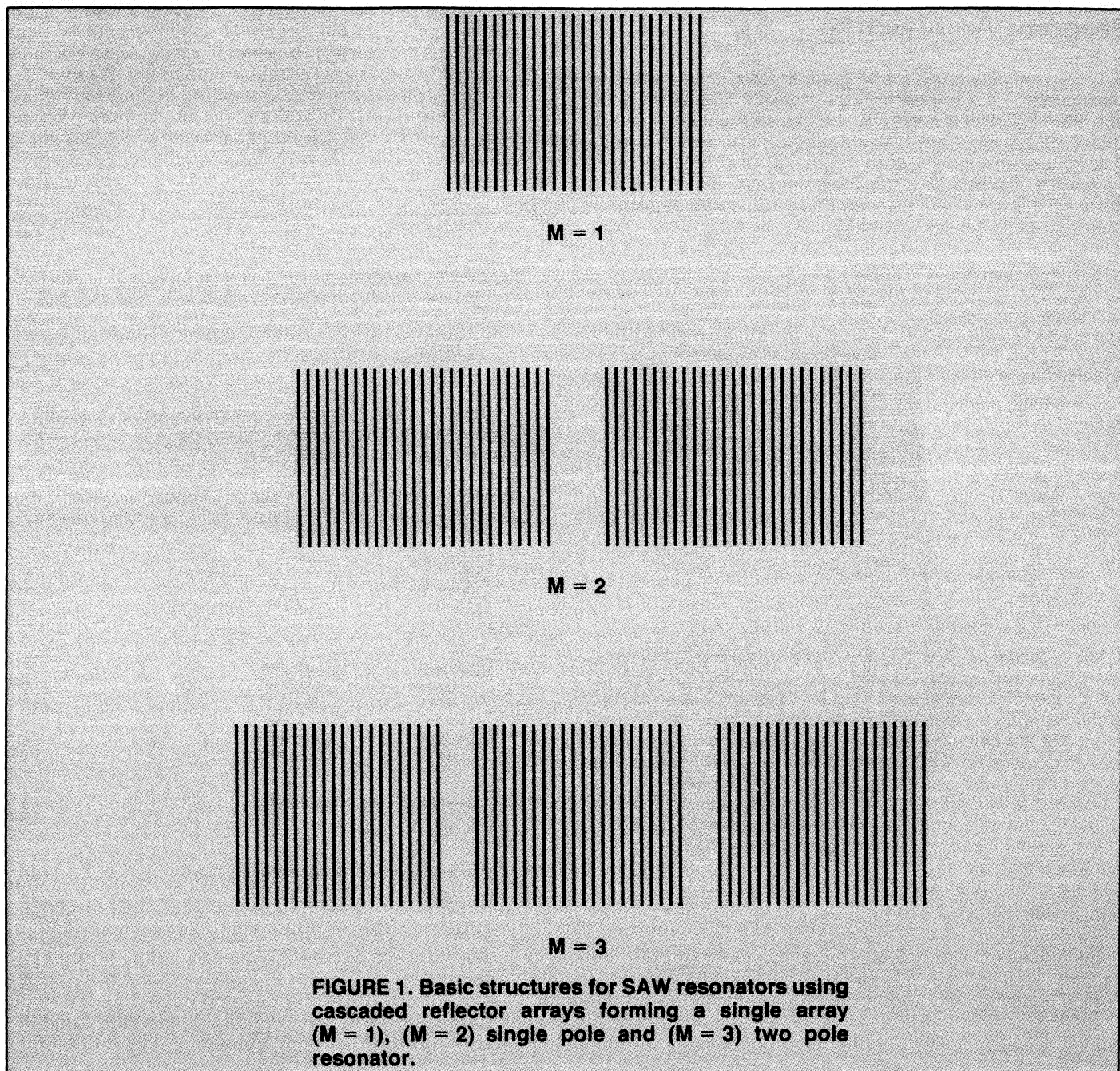
Long-time readers of *RF Design* have encountered the Surface Acoustic Wave (SAW) resonator before^{1,2}. The original concept belongs to Eric Ash, of the Imperial College in London, who made the first attempt to produce a high Q resonant acoustic device that is planar in its fabrication (like all semiconductor circuits today), uses SAW, and can scale the frequency spectrum well beyond the practical limits achievable, then or now, by bulk quartz crystal filters. The first truly successful devices were demonstrated by Texas Instruments, followed soon after by scores of industrial, government and university laboratories in the United States, Europe and Japan. The theory, fabrication and performance of the SAW resonator is well chronicled in some detail and variation in the proceedings of the IEEE Ultrasonics Symposium going to back to 1974.

In this article I have tried to provide the RF engineer with a useful tool — a model with which he can simulate the many different device responses the SAW resonator has been found able to produce. In Part I the theory of the model is presented, along with a listing for the TI-59 calculator equipped with a printer. In Part II we manipulate the model to produce various devices and develop a good feeling for how performance depends on design and material parameters.

The first SAW resonator was a single pole device — a pair of reflecting structures forming a single cavity. Each reflecting structure consists of a repetitive set of lines and gaps — a grating. The grating is formed in various ways but always involves the use of vacuum deposition of metal (mostly aluminum) or occasionally a dielectric, and photolithographic exposure, developing and etching. Sometimes the stripes of the reflector are patterned in etched aluminum; the more reliable technique used today is one in which grooves are plasma etched directly out of

the quartz substrate. Each line and groove is one quarter wavelength long in the direction of propagation of the wave, and is typically 50-200 wavelengths wide, at the designated center frequency. Each pair of line and groove has a very low coefficient of reflection, purposely: too large a coefficient and the surface wave would quickly scatter into the bulk and dissipate. A distributed reflector consisting of several hundreds of lines (sometimes more than a thousand) produces a very efficient phase matched coupling between a SAW wave traveling in one direction and a reflected wave. As we shall see in some of the examples in Part II, the reflectivity can be very nearly 100%. Two such reflectors can form a cavity whose length is an integer number of half wavelengths. This is a Fabry-Perot cavity, and is the fundamental structure known as the single pole resonator. Place an interdigital transducer in the cavity (at the proper position, of course) and we have a way to dump electrical energy into this acoustic cavity through the piezoelectric coupling coefficient of the substrate. Remember that crystal quartz, lithium niobate, zinc oxide and many other materials are piezoelectric. Read my two previous articles^{1,2} for a bit more background, or plow through the rich literature on the subject if you have a few years.

We needn't stop with a single pole resonator. Refer to Fig. 1. A third reflective array properly placed in line with the other two forms a second cavity — the two-pole SAW resonator. This may be continued indefinitely. The calculator is dumb and will not mind. But we, as engineers, can play the program included here like an arcade game and produce interesting and varied results. First, I'll describe the theory behind the program. Second, familiarize yourself with initial data entry procedures and device design. Then, next month, we'll start to build a succession of



devices and look at the power transmission and reflection characteristics of each one and, for a few selected cases, the change in performance of a single design as we make small changes in one of the parameters.

The program comes in two versions. The first one produces a listing of transmitted and reflected power as a function of frequency. The second version, which is run by replacing the last part of the program, will list the phase of the transmitted and reflected waves versus frequency. Unfortunately the TI-59 does not have enough memory to compute both and still be "user friendly" enough to handle all the I/O commands for data entry

and listing on the printer. As a serious TI-59 programmer, you could generate more available memory by loading all the data off-line, eliminating the print commands to list them (jot them down elsewhere), and leave only the appropriate RUN/STOP commands to read important computed parameters as the program generates them at the beginning — you'll understand what I mean when we cover data entry. If you do all this, there should be enough memory space left to compute magnitude *and* phase of transmitted and reflected waves. I have chosen instead to rely on the automation features available on the TI-59 when used with the printer.

An Overview of the Program Architecture

After initial data entry, the program accomplishes its task by transmission line matrix computation methods. The 2x2 transmission matrix (T[1]) of a single line and gap segment is computed. The eigen values of this matrix are determined and the matrix T[N] of an array of N such segments is computed using Sylvester's Theorem (3). This theorem states that if T is a jxj matrix (in this case 2x2), then any polynomial matrix expression in powers of T may be written as:

$$P(T) = \sum_{r=1}^j \left\{ P(\lambda_r) \prod_{\substack{s=1 \\ s \neq r}}^j \left(\frac{T - \lambda_s I}{\lambda_r - \lambda_s} \right) \right\}, \quad I = \begin{bmatrix} 1 & 0 \\ 0 & 1 \end{bmatrix} \quad (1)$$

where I is the 2x2 identity matrix, λ_r is the r'th eigenvalue of the matrix T, and P(λ_r) is the same polynomial as before, but in powers of λ_r , instead of the matrix T. For our 2x2 situation, j=2, T is the matrix of one section (a line and a gap), and P(T)=T_N. Then:

$$\begin{aligned} T^N &= \lambda_1^N \left(\frac{T - \lambda_2 I}{\lambda_1 - \lambda_2} \right) + \lambda_2^N \left(\frac{T - \lambda_1 I}{\lambda_2 - \lambda_1} \right) \\ &= T \left(\frac{\lambda_1^N - \lambda_2^N}{\lambda_1 - \lambda_2} \right) + I \left(\frac{\lambda_1 \lambda_2^N - \lambda_1^N \lambda_2}{\lambda_1 - \lambda_2} \right) \end{aligned} \quad (2)$$

The eigenvalues λ_1 and λ_2 are found by setting the determinant of T-I equal to zero and solving Eq. 2. This approach enables the closed-form, single pass calculation which is independent of the number of sections N in the grating array. The original version of this calculation did not use Sylvester's Theorem and relied instead on a recursive calculation which consumed time proportional to the size of the grating number N(4).

The matrix T[g] representing the gap of length l_g (normalized relative to the wavelength at the specified reference frequency f_0) is computed and the structure cascaded by multiplication of the two matrices

$$T[N] \times T[g] = T[N+g] \quad (3)$$

The composite matrix is then solved for its eigenvalues and Sylvester's Theorem is used again to find the net transmission matrix of M such sections, which form M-1 cavities, or an (M-1) — pole resonator:

$$(T[N+g])^M = T[M] \quad (4)$$

Again, we must compromise because of the calculator's capacity. A practical device could have several cavities with different values of l_g , and the grating arrays between these cavities, referred to as coupling reflectors, might have different sizes. Nevertheless, the symmetric devices we are able to design are instructive, and represent the great majority of designs that have been practically implemented over the past 10 years.

The program assumes the transmission line structure is lossless, i.e., the impedance values are not complex. Making provisions for a complex impedance requires an ability to manipulate them in matrix multiplication, which the TI-59 does not do directly, or doubling the dimension of matrices and increasing the size

of the calculation, which we can't afford. We also assume that the characteristic impedance of the source and load at either end of the grating are the same, and equal to that of the gaps between lines in a grating and between grating arrays where we have formed cavities, i.e., Z(load) = Z(source) = Z(gap) = 1.

Data entry procedures are summarized in the flow diagram in Table 1. After l1, l2, n2 and f0 are entered, fc, the "center frequency" at which the first maximum in reflectivity occurs, is computed:

$$f_c = \frac{f_0}{2(l_1 + n_2 \cdot l_2)} \quad (5)$$

Other reflectivity maxima occur at odd harmonics of fc. The fractional "phase length" of a strip relative to a strip gap pair is

$$t = \frac{n_2 \cdot l_2}{l_1 + n_2 \cdot l_2} \quad (6)$$

If t = 0.5, l1 = n2 * l2 and each segment has equal "optical," or phase thickness. The fractional difference in phase thickness between a gap and a strip is 1-2*t.

Armed with this input and a starting frequency, we may proceed to compute the transmission matrix of a strip-gap pair:

$$T[1] = \begin{bmatrix} A1 & B1 \\ C1 & D1 \end{bmatrix} \quad (7)$$

where

$$A1 = \frac{(Z+1)\cos\gamma}{2} - \frac{(Z-1)\cos(1-2t)\gamma}{2} \quad (7a)$$

$$B1 = j \left(\frac{(Z+1)\sin\gamma}{2} - \frac{(Z-1)\sin(1-2t)\gamma}{2} \right) \quad (7b)$$

$$C1 = j \left(\frac{(Z+1)\sin\gamma}{2Z} + \frac{(Z-1)\sin(1-2t)\gamma}{2Z} \right) \quad (7c)$$

$$D1 = \frac{(Z+1)\cos\gamma}{2Z} + \frac{(Z-1)\cos(1-2t)\gamma}{2Z} \quad (7d)$$

and

$$\gamma = \pi \cdot f_1 / f_c. \quad (8)$$

Once T[1] is obtained, we must find its eigenvalues in order to compute T[1] ^ N = T[N], the equivalent of cascading N sections. We define the quantity 0,

$$\cos \Theta = \frac{A1 + D1}{2} \quad (9)$$

$$\lambda_1 = \cos \Theta + \sqrt{\cos^2 \Theta - 1}$$

$$\lambda_2 = 1/\lambda_1$$

If $\cos^2 \Theta - 1$ is zero or positive, the eigenvalues of t[1] are real. However, it is entirely possible that (A1 + D1)/2 < 0, in which case the eigenvalues are a complex conjugate pair. The distinction is made because the program branches to handle each case differently. If the eigenvalues are real, we obtain:

$$[TN] = \begin{bmatrix} AN & BN \\ CN & DN \end{bmatrix} \quad (10)$$

where

$$AN = A_1 \frac{\lambda_1^N - \lambda_2^N}{\lambda_1 - \lambda_2} - \frac{\lambda_1^{N-1} - \lambda_2^{N-1}}{\lambda_1 - \lambda_2} \quad (11a)$$

$$BN = jB_1 \frac{\lambda_1^N - \lambda_2^N}{\lambda_1 - \lambda_2} \quad (11b)$$

$$CN = jC_1 \frac{\lambda_1^N - \lambda_2^N}{\lambda_1 - \lambda_2} \quad (11c)$$

$$DN = D_1 \frac{\lambda_1^N - \lambda_2^N}{\lambda_1 - \lambda_2} - \frac{\lambda_1^{N-2} - \lambda_2^{N-2}}{\lambda_1 - \lambda_2} \quad (11d)$$

If the eigenvalues are complex, we have instead

$$AN = \frac{D \sin N\theta}{\sin \theta} - \frac{\sin (N-1)\theta}{\sin \theta} \quad (12a)$$

$$BN = \frac{jB_1 \sin N\theta}{\sin \theta} \quad (12b)$$

$$CN = \frac{jC_1 \sin N\theta}{\sin \theta} \quad (12c)$$

$$DN = \frac{D_1' \sin N\theta}{\sin \theta} - \frac{\sin (N-1)\theta}{\sin \theta} \quad (12d)$$

where θ is obtained from (9).

Having constructed a grating array [TN], we must now compute the transmission line that will make up the cavity between two reflectors. The matrix for this section is simple:

$$[Tg] = \begin{bmatrix} \cos y & jZ_1' \sin y \\ j\sin y & \cos y \end{bmatrix} \frac{1}{Z_1} \quad (13)$$

where

$$\gamma = 2\pi \left(\frac{f_1}{f_c} - lg \right) \quad (14)$$

and $Z_1 = 1$.

The matrix for the cascaded reflector and gap is simply obtained using (1). The same calculation is applied to $T[N+g]$ to find its eigenvalues, and then the composite structure is cascaded M times to build a transmission line with M reflectors and M-1 cavities. Note that the tail end of the structure contains a length of transmission line l_q . This will have no effect on the

Program Structure
Data Entry
($l_1, l_2, n_2, f_0, Z, f_1, df, f_2, M, lg$)

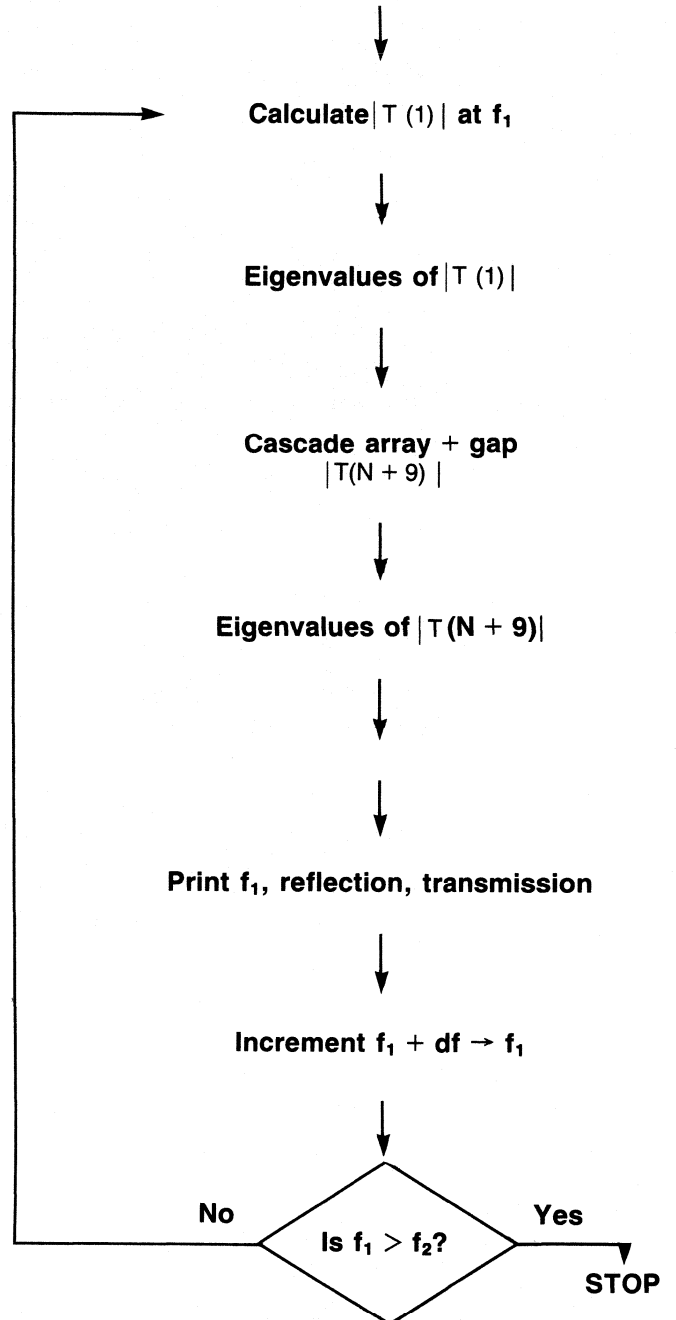


TABLE 1

magnitude of the power transmitted or reflected, but only a phase shift in the transmitted wave.

Once the transmission of matrix T of the entire structure has been computed, the normalized transmission and reflection amplitudes Tf and Rf are easily computed:

$$Tf = \frac{2}{A' + B' + C' + D'} \quad (15a)$$

$$Rf = \frac{A' + B' - C' - D'}{A' + B' + C' + D'} \quad (15b)$$

Since the device is assumed to be lossless only one coefficient need be calculated, say Tf, and

$$RF^2 = 1 - Tf^2 \quad (16)$$

Using the Program for Design and Analysis

The program is listed in Table II. Partition the TI-59 for 30p17 (719.29) and load the program. Two magnetic cards are needed to store it. Enter the data as shown in Table III. Each input parameter is printed as it is entered. After f_0 is entered and printed, f_0 is computed and it too is printed. This is done to aid the user in choosing an appropriate frequency range for analysis. After all input data has been entered, calculation commences, resulting in a listing of the frequency and corresponding normalized reflected and transmitted power (in dB). A complete cycle takes about 20 seconds. The computation is then repeated at the next frequency until the entire frequency domain has been examined. While the program chugs away, take a break.

The user may FIX the number of decimal places desired at the beginning or at any point during data entry, since, for example, the reflection or transmission loss may only be interesting to 0.1 dB accuracy. Care must be taken, however, since the printed listing of input parameters or frequency may appear truncated to less accuracy than was originally specified.

Join us next month for Part II. We will use the program to examine the properties of reflective arrays, single and multiple cavities. As an added bonus, a BASIC version is also provided for the growing number of microcomputer users.

References

1. J. Schoenwald, "Surface Acoustic Waves for the R.F. Design Engineer," *r.f. design*, pp. 11-16, March/April 1981.
2. J. Schoenwald, "Surface Acoustic Waves for the R.F. Design Engineer: The Interdigital Transducer," *r.f. design*, pp. 25-33, July/August, 1981.
3. J. Irving and N. Mullineau, *Mathematics In Physics and Engineering*, pp. 285-288, Academic Press, New York, N.Y. (1959).
4. E.K. Sittig and C.A. Caquin, "Filters and Dispersive Delay Lines Using Repetitively Mismatched Ultrasonic Transmission Lines," *IEEE Transactions on Sonics and Ultrasonics*, Vol. SU-15, pp. 111-119, (1968).

TABLE III
Data Entry

Parameter	Enter	Press
gap length	l_1	A
line length	l_2	R/S
velocity index	n_2	R/S
reference frequency	f_0	R/S
impedance ratio	Z	B
number of sections	N	R/S
start frequency	f_1	C
frequency increment	df	R/S
stop frequency	f_2	R/S
number of reflectors	M	R/S
cavity size	lg	R/S

Table II

000	76	LBL	065	69	69	130	99	PRT
001	50	I x I	066	43	RCL	131	91	R/S
002	43	RCL	067	04	04	132	76	LBL
003	12	12	068	92	RTN	133	12	B
004	22	INV	069	53	(134	42	STO
005	39	COS	070	43	RCL	135	10	10
006	42	STO	071	00	00	136	99	PRT
007	04	04	072	55	÷	137	91	R/S
008	43	RCL	073	02	2	138	42	STO
009	11	11	074	54)	139	11	11
010	42	STO	075	32	$X \rightleftharpoons T$	140	42	STO
011	00	00	076	53	(141	29	29
012	71	SBR	077	43	RCL	142	99	PRT
013	38	SIN	078	00	00	143	53	(
014	42	STO	079	55	÷	144	43	RCL
015	27	27	080	02	2	145	06	06
016	53	(081	54)	146	65	x
017	43	RCL	082	59	INT	147	43	RCL
018	11	11	083	67	EQ	148	07	07
019	75	—	084	00	00	149	55	÷
020	01	1	085	90	90	150	53	(
021	54)	086	43	RCL	151	43	RCL
022	42	STO	087	04	04	152	05	05
023	00	00	088	94	+/-	153	85	+
024	71	SBR	089	92	RTN	154	53	(
025	38	SIN	090	43	RCL	155	43	RCL
026	42	STO	091	04	04	156	06	06
027	28	28	092	92	RTN	157	65	x
028	61	GTO	093	76	LBL	158	43	RCL
029	18	C'	094	11	A	159	07	07
030	76	LBL	095	42	STO	160	54)
031	38	SIN	096	05	05	161	54)
032	53	(097	99	PRT	162	54)
033	53	(098	91	R/S	163	42	STO
034	43	RCL	099	42	STO	164	12	12
035	00	00	100	06	06	165	53	(
036	65	x	101	99	PRT	166	43	RCL
037	43	RCL	102	91	R/S	167	10	10
038	04	04	103	42	STO	168	85	+
039	54)	104	07	07	169	01	1
040	38	SIN	105	99	PRT	170	54)
041	55	÷	106	91	R/S	171	42	STO
042	43	RCL	107	42	STO	172	16	16
043	04	04	108	08	08	173	53	(
044	38	SIN	109	99	PRT	174	24	CE
045	54)	110	55	÷	175	75	—
046	92	RTN	111	53	(176	02	2
047	76	LBL	112	02	2	177	54)
048	45	Y ^x	113	65	x	178	42	STO
049	53	(114	53	(179	17	17
050	43	RCL	115	43	RCL	180	53	(
051	01	01	116	05	05	181	01	1
052	50	I x I	117	85	+	182	75	—
053	45	Y ^x	118	53	(183	02	2
054	43	RCL	119	43	RCL	184	65	x
055	00	00	120	06	06	185	43	RCL
056	54)	121	65	x	186	12	12
057	42	STO	122	43	RCL	187	54)
058	04	04	123	07	07	188	42	STO
059	43	RCL	124	54)	189	18	18
060	01	01	125	54)	190	91	R/S
061	32	$X \rightleftharpoons T$	126	54)	191	76	LBL
062	00	0	127	95	=	192	13	C
063	77	GE	128	42	STO	193	42	STO
064	00	00	129	09	09	194	13	13

Table II continued

195	99	PRT	260	19	19	325	16	16	390	24	24	455	54)	520	43	RCL
196	91	R/S	261	53	(326	85	+	391	35	1/X	456	55	÷	521	05	05
197	42	STO	262	53	(327	53	(392	42	STO	457	53	(522	42	STO
198	14	14	263	43	RCL	328	53	(393	25	25	458	43	RCL	523	19	19
199	99	PRT	264	15	15	329	43	RCL	394	43	RCL	459	24	24	524	92	RTN
200	91	R/S	265	38	SIN	330	15	15	395	11	11	460	75	-	525	76	LBL
201	99	PRT	266	65	x	331	65	x	396	42	STO	461	35	1/x	526	48	EXC
202	53	(267	43	RCL	332	43	RCL	397	00	00	462	54)	527	53	(
203	24	CE	268	16	16	333	18	18	398	53	(463	54)	528	43	RCL
204	85	+	269	75	-	334	54)	399	53	(464	42	STO	529	13	13
205	43	RCL	270	53	(335	39	COS	400	53	(465	28	28	530	99	PRT
206	14	14	271	53	(336	65	x	401	43	RCL	466	76	LBL	531	85	+
207	54)	272	43	RCL	337	43	RCL	402	24	24	467	18	C'	532	43	RCL
208	42	STO	273	15	15	338	17	17	403	42	STO	468	53	(533	14	14
209	26	26	274	65	x	339	54)	404	01	01	469	43	RCL	534	54)
210	91	R/S	275	43	RCL	340	95	=	405	71	SBR	470	19	19	535	42	STO
211	42	STO	276	18	18	341	55	÷	406	45	Yx	471	65	x	536	13	13
212	02	02	277	54)	342	02	2	407	54)	472	43	RCL	537	43	RCL
213	99	PRT	278	38	SIN	343	55	÷	408	75	-	473	27	27	538	02	02
214	91	R/S	279	65	x	344	43	RCL	409	53	(474	75)	539	42	STO
215	42	STO	280	43	RCL	345	10	10	410	43	RCL	475	43	RCL	540	11	11
216	03	03	281	17	17	346	95	=	411	25	25	476	28	28	541	53	(
217	99	PRT	282	54)	347	42	STO	412	42	STO	477	54)	542	02	02
218	98	ADV	283	54)	348	22	22	413	01	01	478	42	STO	543	65	x
219	76	LBL	284	55	÷	349	71	SBR	414	71	SBR	479	05	05	544	43	RCL
220	14	D	285	02	2	350	49	PRD	415	45	Yx	480	53	(545	15	15
221	70	RAD	286	54)	351	61	GTO	416	54)	481	43	RCL	546	65	x
222	53	(287	42	STO	352	48	EXC	417	54)	482	20	20	547	43	RCL
223	89	π	288	20	20	353	76	LBL	418	55	÷	483	65	x	548	03	03
224	65	x	289	53	(354	49	PRD	419	53	(484	43	RCL	549	54)
225	43	RCL	290	53	(355	00	0	420	43	RCL	485	27	27	550	42	STO
226	13	13	291	43	RCL	356	32	$X \leq T$	421	24	24	486	54)	551	27	27
227	55	÷	292	15	15	357	53	(422	75	-	487	42	STO	552	39	COS
228	43	RCL	293	38	SIN	358	53	(423	35	1/x	488	06	06	553	42	STO
229	09	09	294	65	x	359	43	RCL	424	54)	489	53	(554	24	24
230	54)	295	43	RCL	360	19	19	425	54)	490	43	RCL	555	43	RCL
231	42	STO	296	16	16	361	85	+	426	42	STO	491	28	21	556	27	27
232	15	15	297	85	+	362	43	RCL	427	27	27	492	65	x	557	38	SIN
233	53	(298	53	(363	22	22	428	53	(493	43	RCL	558	42	STO
234	53	(299	53	(364	54)	429	43	RCL	494	27	27	559	25	25
235	43	RCL	300	43	RCL	365	65	÷	430	11	11	495	54)	560	53	(
236	15	15	301	15	15	366	02	2	431	75	-	496	42	STO	561	43	RCL
237	39	COS	302	65	x	367	54)	432	01	1	497	07	07	562	19	19
238	65	x	303	43	RCL	368	42	STO	433	54)	498	53	(563	65	x
239	43	RCL	304	18	18	369	12	12	434	42	STO	499	43	RCL	564	43	RCL
240	16	16	305	54)	370	53	(435	00	00	500	22	22	565	24	24
241	75	-	306	38	SIN	371	24	CE	436	53	(501	65	x	566	75	-
242	53	(307	65	x	372	33	X^2	437	53	(502	43	RCL	567	43	RCL
243	53	(308	43	RCL	373	75	-	438	53	(503	27	27	568	20	20
244	43	RCL	309	17	17	374	01	1	439	43	RCL	504	75	-	569	65	x
245	18	18	310	54)	375	54)	440	24	24	505	43	RCL	570	43	RCL
246	65	x	311	54)	376	42	STO	441	42	STO	506	28	28	571	25	25
247	43	RCL	312	55	÷	377	23	23	442	01	01	507	54)	572	54)
248	15	15	313	02	2	378	22	INV	443	71	SBR	508	42	STO	573	42	STO
249	54)	314	55	÷	379	77	GE	444	45	Yx	509	08	08	574	05	05
250	39	COS	315	43	RCL	380	50	$I \times I$	445	54)	510	42	STO	575	53	(
251	65	x	316	10	10	381	53	(446	75	-	511	22	22	576	43	RCL
252	43	RCL	317	54)	382	43	RCL	447	53	(512	43	RCL	577	19	19
253	17	17	318	42	STO	383	12	12	448	43	RCL	513	07	07	578	65	x
254	54)	319	21	21	384	85	+	449	25	25	514	42	STO	579	43	RCL
255	54)	320	43	RCL	385	43	RCL	450	42	STO	515	21	21	580	25	25
256	55	÷	321	15	15	386	23	23	451	01	01	516	43	RCL	581	85	+
257	02	2	322	39	COS	387	34	\sqrt{X}	452	71	SBR	517	06	06	582	43	RCL
258	54)	323	65	x	388	54)	453	45	Yx	518	42	STO	583	20	20
259	42	STO	324	43	RCL	389	42	STO	454	54)	519	20	20	584	65	x

585	43	RCL	650	85	+	652	43	RCL
586	24	24	651	43	RCL	653	07	07
587	54)	652	07	07	654	54)
588	42	STO	653	54)	655	55	÷
589	06	06	654	33	x ²	656	53	(
590	53	(655	95	=	657	43	RCL
591	43	RCL	656	35	1/x	658	05	05
592	21	21	657	65	x	659	33	x ²
593	65	x	658	04	04	660	85	+
594	43	RCL	659	95	=	661	43	RCL
595	24	24	660	42	STO	662	06	06
596	85	+	661	28	28	663	33	x ²
597	43	RCL	662	94	+/-	664	75	-
598	22	22	663	85	+	665	43	RCL
599	65	x	664	01	1	666	07	07
600	43	RCL	665	95	=	667	33	x ²
601	25	25	666	28	LOG	668	75	-
602	54)	667	65	x	669	43	RCL
603	42	STO	668	01	1	670	08	08
604	07	07	669	00	0	671	33	x ²
605	53	(670	95	=	672	54)
606	43	RCL	671	99	PRT	673	54)
607	22	22	672	43	RCL	674	22	INV
608	65	x	673	28	28	675	30	TAN
609	43	RCL	674	28	LOG	676	95	=
610	24	24	675	65	x	677	99	PRT
611	75	-	676	01	1	678	53	(
612	43	RCL	677	00	0	679	43	RCL
613	20	20	678	95	=	680	06	06
614	65	x	679	99	PRT	681	85	+
615	43	RCL	680	98	ADV	682	43	RCL
616	25	25	681	43	RCL	683	07	07
617	54)	682	13	13	684	54)
618	42	STO	683	32	X↔T	685	55	÷
619	08	08	684	43	RCL	686	53	(
620	43	RCL	685	26	26	687	43	RCL
621	05	05	686	67	EQ	688	05	05
622	42	STO	687	19	D'	689	85	+
623	19	19	688	43	RCL	690	43	RCL
624	43	RCL	689	29	29	691	08	08
625	06	06	690	42	STO	692	54)
626	42	STO	691	11	11	693	94	+/-
627	20	20	692	61	GTO	694	22	INV
628	43	RCL	693	14	D	695	30	TAN
629	07	07	694	76	LBL	696	95	=
630	42	STO	695	19	D'	697	99	PRT
631	21	21	696	43	RCL	698	98	ADV
632	43	RCL	697	26	26	699	43	RCL
633	08	08	698	91	R/S	700	13	13
634	42	STO	699	00	0	701	32	X↔T
635	22	22				702	43	RCL
636	71	SBR	638	60	DEG	703	26	26
637	49	PRD	639	53	(704	67	EQ
638	53	(640	02	2	705	19	D'
639	43	RCL	641	65	x	706	43	RCL
640	05	05	642	53	(707	29	29
641	85	+	643	43	RCL	708	42	STO
642	43	RCL	644	08	08	709	11	11
643	08	08	645	65	x	710	61	GTO
644	54)	646	43	RCL	711	14	D
645	33	x ²	647	06	06	712	76	LBL
646	85	+	648	75	-	713	19	D'
647	53	(649	43	RCL	714	43	RCL
648	43	RCL	650	05	05	715	26	26
649	06	06	651	65	x	716	91	R/S

The Phase/Frequency Detector

An analysis of phase-locked loop design employing phase frequency detectors.

By James Crawford

The controversial subject of "Divider Time Delay" in recent *RF Design* issues has prompted the following discussion which was presented at a Hughes Aircraft Co. in-plant class on phase-locked loop design. The following analysis is an endorsement of Dr. Egan's explanation² where he states that the appearance of the delay-like term is due to the sampling process which is taking place in the phase-locked loop, not the transport delay or any other delay through the divider.

The delay-like terms which was mentioned above is shown in equations (3) and (4) of reference [3]. In this reference it is suggested that "the discrepancy between theory and experiment (in phase-locked loop design) was found to be attributed to divider delay which caused a decrease in phase margin significant enough in many cases to cause unstable loop performance." A decrease in loop phase margin does indeed occur in these phase-locked loops but the sole mechanism is a result of the sampling process which is taking place in the closed loop.

A rigorous analysis of phase-locked loop design employing phase-frequency detectors necessitates a detailed examination of the operation fundamentals. Rather than deal immediately with the specifics of phase-locked loop design using the phase/frequency detector, the problem will be dealt with using the following approach:

- 1) A general discussion of sampling phase-locked loops will be given which will display some of the differences between the true open-loop gain function, and the commonly used continuous approximation to the open-loop gain function.
- 2) With the sampling basics now developed, the transfer function for the phase/frequency detector will be found in some detail.
- 3) The phase/frequency detector transfer function is used to write an accurate impulse for the open-loop gain function. Given this function, a band-limited approximation of the open-loop gain function will be found using Z-transforms. The final band-limited expression can be used with conventional continuous transform (Laplace transforms) design methods for phase-locked loops.

Sampling Phase-Locked Loop Fundamentals

In contrast to the continuous mixer-type phase detector, the phase/frequency detector is a sampling phase detector. Phase error information is available at discrete time intervals which are spaced at exact intervals of T seconds, where T is the period of the reference frequency. The phase error at each instant is in the form of an impulse function whose area is proportional to the phase error. In reality, the impulses out of a phase-frequency detector such as the Motorola 4344 are of finite amplitude, but this fact is completely negligible in light of the RC filter time constants which follow the device. The phase detector output pulses may be mathematically viewed as ideal

impulse functions of appropriate area. For the time being, the concept of the phase/frequency detector as an ideal impulse sampler will be deferred and developed momentarily.

The phase-frequency detector is modeled in Figure 1 as an ideal impulse sampler. The function $H(s)$ represents some form of analog "hold" function such as the RC lowpass filters that customarily follow a phase-frequency detector. The function $G(s)$ represents the normal loop filter transfer function.

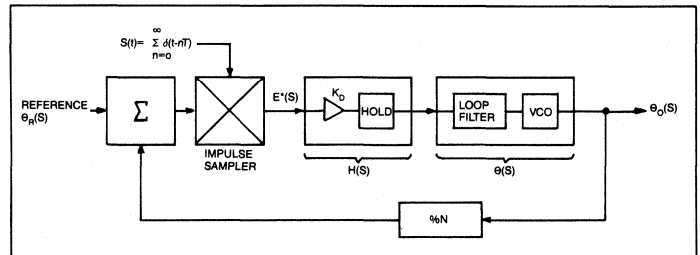


Figure 1. The general Sampled phase-locked loop employs an ideal impulse Sampler which must be followed by some form of "hold" device. (HS).

Before jumping into the loop details, as an aside, consider the time function $f(t)$ which is sampled by an ideal impulse sampler. The sampled time function can be written as in (1) where the asterisk (*) represents the time-sampled form of the function.

$$f^*(t) = f(t) \sum_{n=0}^{\infty} \delta(t - nT) \quad (1)$$

From Laplace platform and convolution theory, (1) may be written in Laplace transforms as in (2) where $F^*(s)$ and $f^*(t)$ are Laplace transform pairs. Note that $F(s)$ and $f(t)$ are also Laplace transform pairs.

$$F^*(s) = F(s) \star L \left\{ \sum_{n=0}^{\infty} \delta(t - nT) \right\} \quad (2)$$

The \star in (2) represents convolution in the frequency domain. Equation (1) may be used with the definition of the forward one-sided Laplace transform to give yet another interpretation of the time-sampled function form in the frequency domain.

$$\begin{aligned} F^*(s) &= \int_0^{\infty} f^*(t) \exp(-st) dt \\ &= \int_0^{\infty} f(t) \sum_{n=0}^{\infty} \delta(t-nT) \exp(-st) dt \end{aligned} \quad (3)$$

$$F^*(s) = \sum_{n=0}^{\infty} \int_0^{\infty} \delta(t-nT) \exp(-st) dt \quad (4)$$

$$F^*(s) = \sum_{n=0}^{\infty} f(nT) \exp(-sT). \quad (5)$$

Equation (5) is actually the defining relationship for the Z-transform of $f(t)$. This fact will be used later in this article for easy calculation of $F^*(s)$.

A very powerful relationship may be found by continuing the convolution calculation in (2). Since the convolution must be performed in the frequency domain, we must know the Laplace transform of the infinite series of impulse functions which are performing the sampling operation. Since

$$\delta(t) \leftrightarrow 1 \quad (6)$$

then

$$\begin{aligned} L \left\{ \sum_{n=0}^{\infty} \delta(t-nT) \right\} &= 1 + \exp(-sT) + \exp(-2sT) + \dots \\ &= \frac{1}{1 - \exp(-sT)} \end{aligned} \quad (7)$$

The convolution of (2) may be rewritten as

$$\begin{aligned} F^*(s) &= F(s) \star \frac{1}{1 - \exp(-sT)} \\ &= \int \frac{F(u) du}{1 - \exp(sT - uT)} \\ &= \int \frac{F(Z)}{1 - \exp(sT)/Z} \frac{dz}{T Z} \end{aligned} \quad (8)$$

where $Z = \exp(uT)$ and $du = dZ/(TZ)$.

Taking this process one step further and using the Residue theorem, this integral may be evaluated as in (9).

$$\begin{aligned} &= \frac{1}{T} \int \frac{F(Z) dZ}{Z - \exp(-sT)} \quad (9) \\ &= \frac{1}{T} \sum_{n=-\infty}^{\infty} F(s+j n Ws) \end{aligned} \quad \text{where } Ws = 2 \pi/T.$$

Equation (9) is a valuable result and although it involves an infinite summation, it may be used to evaluate $F^*(s)$.

These previous transform tools will appear much more valuable if we now return to a discussion of Figure 1. As in classical PLL analysis, the most expedient first step in the loop analysis is to solve for the error function $E^*(s)$. We may write

$$\begin{aligned} E^*(s) &= (\Phi_r - \Phi_o)^* \\ &= \Phi_r^* - \Phi_o^* \\ &= \Phi_r^* - [E^*(s) H(s) G(s)]^* \end{aligned} \quad (10)$$

Those unfamiliar with sampled systems will find [4] particularly useful and easy to understand. As developed in Chapter 4 of [4], the sampling operation in (10) may be brought within the brackets because $E(s)$ is already a sampled function. The sampled error function is then given by

$$E^*(s) = \Phi_r^* - E^*(s) HG^*(s) \quad (11)$$

We finally obtain the desired result for the sampled loop error function.

$$E^*(s) = \frac{\sum_{n=-\infty}^{\infty} \Phi_r(s+j n Ws)/T}{1 + HG^*(s)} \quad (12)$$

In most cases, $\Phi_r(s)$ can be assumed to be effectively bandlimited and aliasing of noise products can be neglected. This gives some simplification to (12) as given in (13).

$$E^*(s) = \frac{\Phi_r(s)/T}{1 + HG^*(s)} \quad (13)$$

where $\Phi^*(s) \sim \Phi_r(s)/T$.

The asterisks would be absent in classical analysis of a phase-locked loop which neglected sampling effects. With rare exception, most systems which use the phase/frequency detector have a small bandwidth compared to the reference frequency in order to obtain reasonably low "sampling spurs." For this reason, the higher order terms (terms other than $n=0$) in equation (9) can largely be ignored for low bandwidth situations. This is precisely why classical analysis ignoring sampling effects still provides excellent results in small bandwidth situations. As the loop bandwidth is increased compared to the reference frequency, however, the higher order terms cannot be ignored.

For large loop bandwidth situations (bandwidth $> 0.1 F_{ref}$), Z-transform techniques should be used to include the higher order effects. If there are true transport time delays within the loop, modified Z-transforms should be used. If the loop bandwidths remain small (say $< 0.1 F_{ref}$), bandlimited forms of the open-loop gain function may be found which very accurately describe sampling effects without resorting to Z-transform analysis. Equation (9) which is repeated below as equation (14) will provide the menu for arriving at a bandlimited form of the open-loop gain function including sampling effects. The continuous Laplace transform impulse response, $G(s)$, must first be found. The continuous open-loop gain function will be re-expressed in terms of Z-transforms and the assumption of small loop bandwidth imposed. The final result will be the bandlimited form of the open-loop gain function with first order sampling effects.

$$F(Z) = \frac{1}{T} \sum_{n=-\infty}^{\infty} F(s+j n Ws) \quad (14)$$

It will be shown that the so called "divider time delay" appears during this step and is solely a result of sampling.

Impulse Response of the Phase/Frequency Detector

A simplistic equivalent circuit of the phase/frequency detector is provided in Figure 2. No attempt has been made here to describe the frequency discriminator mode of operation. In many applications, the phase detector remains in its linear range of operation, because although the phase error may be very large at the VCO, it is reduced by N at the phase detector.

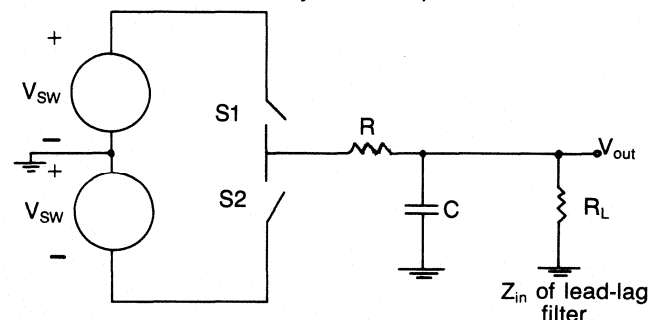


Figure 2

In steady-state operation, the switches in Figure 2 are open 95 percent of each reference period, only closing long enough to replenish the small discharge in capacitor C each reference period. (Since the 4344 type phase detector cannot resolve absolute time difference between the divider and reference pulse trains less than its own internal time delay, some built in offset is needed to avoid the detector's "dead zone" of operation at zero time difference between the two waveform trains.) During the period of frequency acquisition, the proper polarity switch is closed for a length of time which is defined by the time difference between the leading edge of the divide-by-N signal. This signal relationship is shown in Figure 3. The phase detector output pulse width is directly proportional to the phase error within the loop.

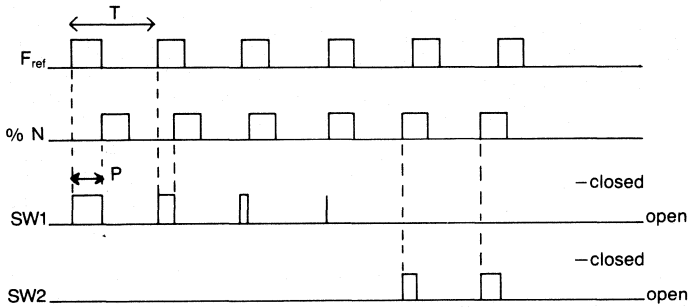


Figure 3

$$\begin{aligned} \phi_e &= \frac{P}{T} 2\pi \\ \text{or} \\ p &= \frac{T}{2\pi} \phi_e \end{aligned} \quad (15)$$

The pulse widths out of the phase detector, p , are very small with respect to the reference period because a Type II loop is always used (zero steady-state phase error) and the VCO phase error is reduced by the divider ratio, N .

We are primarily interested in the impulse response of the phase detector/lowpass filter combination. The transfer function for the lowpass filter alone is given by (16).

$$FL(s) = \frac{R1}{R1 + R} \frac{1}{1 + s \tau 1} \quad (16)$$

$$\text{where } \tau 1 = \frac{R1 R C}{R1 + R}$$

A typical pulse response of the circuit in Figure 2 is presented in Figure 4. The rising edge is very linear because $p \ll \tau 1$. The output voltage, V_{out} , can be easily found from Figure 4. The output voltage during the next reference period is given by (17).

$$\begin{aligned} V_{out}(t) &= V_o \exp(-t/\tau 1) + \\ &\frac{R1}{R1 + R} V_{sw}(1 - \exp(-t/\tau 1)) \end{aligned} \quad (17)$$

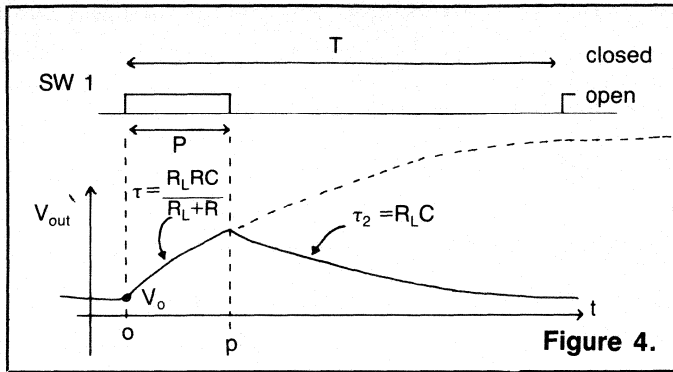


Figure 4.

for $0 < t \leq p$

$$V_{out}(t) = V_{out}(p) \exp(-t/\tau_2) \text{ for } p < t < T.$$

In a properly designed Type II loop under normal linear operation, $p \ll \tau_1$ and equation (17) may be written in a more simple form without the first exponentials.

$$V_{out}(t) \sim V_o + \frac{R_1}{R_1 + R} V_{sw}(t/\tau_1) \quad (18)$$

for $0 < t \leq p$

$$V_{out}(t) = V_{out}(p) \exp(-t/\tau_2) \text{ for } p < t \leq T.$$

It is important to note once more that V_o represents the initial capacitor voltage due to any previous phase sample, Φ_e .

The Laplace transform transfer function can be found by using the above equations directly.

$$V_{out}(s) = L\{(V_o + \frac{R_1}{R_1 + R} V_{sw} \frac{p}{\tau_1}) \exp(-t/\tau_2)\} \quad (19)$$

$$= \frac{V_o}{s + 1/\tau_1} + \frac{R_1 V_{sw} \Phi_e T}{(R_1 + R) \tau_1 2 \pi (s + 1/\tau_2)}$$

where the phase error is $\Phi_e = 2\pi p/T$.

As stated earlier, V_o is a direct result of earlier samples of the phase error, Φ_e . Using this fact, it is possible to show that the output voltage as a function of the input phase error is given by (20).

$$\frac{V_{out}(s)}{\Phi_e(s)} = \frac{K_d T}{(R_1 + R)/R_1 + sRC} \frac{1}{1 - \exp(-sT) \exp(-T/\tau_2)} \quad (20)$$

where $K_d = V_{sw}/(2\pi)$

This is the final result for the phase detector impulse response. The factor T is a direct result of the sampling operation. Notice that if T/τ_2 is not large, the second multiplicative factor cannot be ignored. In this case, the output voltage is a function of the present phase detector error as well as the previous error samples and Z-transform analysis is required. Since the intent of this analysis has been to eventually arrive at a band-limited form of the open-loop gain function, in that vein, T/τ_2 will be assumed to be $\gg 1$ such that Z-transform analysis will not be required in the final end result.

Derivation of the Continuous Band-Limited Open-Loop Gain Function with Sampling

The phase-frequency detector is always used in a Type II phase-locked loop in order to realize reasonable spurious performance and tuning range. In order to simplify the mathematics involved, however, an example using a Type I system will be used. Our approach will be to calculate $Gol(Z)$ and compare it to the continuous form of $Gol(s)$. This will reveal the effects of sampling upon the otherwise continuous open-loop gain expression.

In order to make any connection between an impulse sampled system and a continuous system, the sampled loop must have some form of "hold" device which effectively converts the phase detector impulse functions into smooth time waveforms which have a finite width in time, and a finite height. If the "hold device" is not present, the loop *must* be analyzed as a sampled system. No equivalent continuous system would exist for that case.

The "hold" device may be as simple as an RC lowpass filter, or as complicated as a true 0-order sample/hold. Consider a continuous Type I phase-locked loop with a low pass "hold" as given in (21).

$$Gol(s) = \frac{K_d K_v}{N s} \rightarrow \frac{W_n}{s} \frac{1}{1+s \tau} \quad (21)$$

where

K_d =phase detector gain

K_v =VCO sensitivity

N =feedback divider ratio

τ =low pass filter time constant representing the "hold."

As shown earlier, the sampling effects upon a continuous function may be included by taking the Z-transform of the time function provided that the continuous function is correct of course. In the previous section, it was shown that the impulse response of the phase/frequency detector followed by a simple RC lowpass filter is given by (20). Therefore, assuming that $T \gg \tau$ in equation (20), equation (21) must be multiplied by T to have proper form. Using a table of Z-transforms, equation (21) may be easily converted into $Gol(Z)$.

$$\begin{aligned} \frac{W_n T}{s(1+s\tau)} &\rightarrow W_n (1 - \exp(-t/\tau)) T \\ &\rightarrow \frac{W_n Z T}{Z-1} - \frac{W_n Z T}{Z-A} \end{aligned} \quad (22)$$

Collecting terms in (22), the Z-transform for the Type I system is simply given by (23).

$$Gol(Z) = \frac{W_n Z (1-A) T}{(Z-1)(Z-A)} \quad (23)$$

We can effectively remove any significant effects of the "hold" device upon the system by allowing $\tau \rightarrow 0$, i.e., $A \rightarrow 0$. This is equivalent to making the RC filter time constant negligible compared to the reference period, T . In the limit as $A \rightarrow 0$,

$$Gol(Z) = \frac{W_n Z T}{(Z-1)(Z-0)} = \frac{W_n T}{(Z-1)} \quad (24)$$

Equation (24) may be expressed in terms of the more familiar complex frequency, s , by noting that $Z = \exp(sT)$. Doing so, we obtain (25).

Number of harmonic terms included in summation 5
 Loop reference frequency 10000
 Type I loop Wn 2000
 Loop LPF time constant, nsec 5000
 APPROXIMATION TO SAMPLED OPEN-LOOP GAIN FUNCTION

Summation of Gol Terms			Continuous Gol Exp(-ST/2)	
F	Gol,dB	Ang,Deg		
100	10.06	-91.20	10.06	-91.98
150	6.53	-91.88	6.54	-92.97
200	4.03	-92.40	4.04	-93.96
300	0.51	-93.61	0.51	-95.94
400	-2.00	-94.81	-1.98	-97.92
500	-3.94	-96.03	-3.92	-99.90
700	-6.89	-98.47	-6.85	-103.86
1000	-10.03	-102.21	-9.95	-109.80
1500	-13.65	-108.72	-13.47	-119.70
2000	-16.28	-115.74	-15.98	-129.60
3000	-20.07	-132.17	-19.52	-149.38
4000	-22.55	-153.18	-22.05	-169.16

Number of harmonic terms included in summation 10
 Loop reference frequency 10000
 Type I loop Wn 2000
 Loop LPF time constant, nsec 5000
 APPROXIMATION TO SAMPLED OPEN-LOOP GAIN FUNCTION

Summation of Gol Terms			Continuous Gol Exp(-ST/2)	
F	Gol,dB	Ang,Deg		
100	10.06	-91.46	10.06	-91.98
150	6.54	-92.19	6.54	-92.97
200	4.04	-92.93	4.04	-93.96
300	0.51	-94.39	0.51	-95.94
400	-1.98	-95.86	-1.98	-97.92
500	-3.92	-97.33	-3.92	-99.90
700	-6.84	-100.30	-6.85	-103.86
1000	-9.94	-104.79	-9.95	-109.80
1500	-13.45	-112.49	-13.47	-119.70
2000	-15.92	-120.54	-15.98	-129.60
3000	-19.24	-138.14	-19.52	-149.38
4000	-21.15	-158.08	-22.05	-169.16

Number of harmonic terms included in summation 5
 Loop reference frequency 1000
 Type II loop Wn 2000
 Loop damping factor, eta .707
 APPROXIMATION TO SAMPLED OPEN-LOOP GAIN FUNCTION

Summation of Gol Terms			Continuous Gol Exp(-ST/2)	
F	Gol,dB	Ang,Deg		
100	20.95	-156.41	20.98	-158.03
150	14.77	-147.09	14.67	-149.29
200	10.75	-139.68	10.60	-142.34
300	5.68	-129.45	5.46	-132.82
400	2.48	-123.29	2.22	-127.29
500	0.16	-119.51	-0.11	-124.14
700	-3.13	-115.77	-3.41	-121.69
1000	-6.45	-114.59	-6.72	-122.49
1500	-10.16	-117.17	-10.37	-128.23
2000	-12.79	-122.18	-12.92	-136.02
3000	-16.50	-136.40	-16.49	-153.68
4000	-18.84	-155.59	-19.03	-172.38

Number of harmonic terms included in summation 10
 Loop reference frequency 1000
 Type II loop Wn 1000
 Loop LPF time constant, nsec 5000
 APPROXIMATION TO SAMPLED OPEN-LOOP GAIN FUNCTION

Summation of Gol Terms			Continuous Gol Exp(-ST/2)	
F	Gol,dB	Ang,Deg		
100	10.70	-139.13	10.60	-140.36
150	5.60	-128.39	5.46	-129.85
200	2.38	-121.69	2.22	-123.33
300	-1.73	-114.49	-1.93	-116.51
400	-4.46	-111.20	-4.67	-113.64
500	-6.51	-109.71	-6.72	-112.59
700	-9.53	-109.20	-9.75	-112.99
1000	-12.68	-111.03	-12.98	-116.22
1500	-16.21	-116.62	-16.46	-123.99
2000	-18.67	-123.59	-18.98	-132.82
3000	-21.97	-139.95	-22.53	-151.53
4000	-23.05	-158.98	-25.06	-170.77

(25)

$$Gol(s) = \frac{1}{j2} \frac{Wn \exp(-sT/2)}{\sin(wT/2)}$$

For frequencies which are small compared to the reference frequency, $F_{ref} = 1/T$, the $\sin(x) \sim x$ approximation may be made, reducing (25) to finally (26). This is equivalent to the initial premise that the loop bandwidth is much less than the reference frequency.

(26)

$$Gol(s) = \frac{Wn \exp(-sT/2)}{s}$$

The final result for the bandlimited form of the open-loop gain function is given in (27). This expression includes the first order sampling effects. The appearance of the so-called time delay exponential occurred without introducing any transport time delay whatsoever, only the sampling effects.

(27)

$$Gol(s) = \frac{\exp(-sT/2) Wn}{s}$$

Generalizing, first order sampling effects for phase-locked loops which have a small percentage bandwidth compared to the reference frequency can be analyzed using classical Laplace transform methods provided the new "delay term" is included in the phase detector transfer function.

$$Kd \exp(-sT/2) \quad (28)$$

Further Proof

As further proof of our result above, we may compare this result with that obtained using (9). Only the first few terms of the infinite summation in (9) will be included. The computer program and sample run appear in Appendix I. Notice that the inclusion of the added exponential term of (28) with the normal Type I open-loop gain results in very good agreement between the two mathematical models for frequencies well within the closed-loop bandwidth. The phase of the open-loop gain function would be very inaccurate had the exponential term been left out. As the loop bandwidth increases with respect to the reference frequency, the approximation shows more and more deviation from the true open-loop gain calculated by (9). [Note that for all cases, $T/\tau_1 \gg 1$ has been assumed with loop bandwidth $\ll F_{ref}$.]

In order to be complete, the same calculation was performed for the Type II phase-locked loop with a phase-frequency detector and small RC lowpass filter "hold." The continuous form of the open-loop gain function is given in (29) where T is due to the phase detector transfer function.

(29)

$$Gol(s) = \frac{Kd T}{1 + s\tau} \frac{1 + s\tau_2}{s\tau_1} \frac{Kv}{Ns}$$

Our approximation to $G^*ol(s)$ is found using equation (28).

(30)

$$G^*ol(s) \sim \exp(-sT/2) \frac{Kd}{1 + s\tau} \frac{1 + s\tau_2}{s\tau_1} \frac{Kv}{Ns}$$

The true function $G^*ol(s)$ is found again from substituting equation (29) into (9).

(31)

$$G^*ol(s) = \frac{1}{T} \sum_{n=-\infty}^{\infty} \frac{Kd T}{1 + u\tau} \frac{1 + u\tau_2}{u\tau_1} \frac{Kv}{Nu}$$

where $u = s + jnWs$

February 1985

Reiterating, the T following K_d is due to the phase detector transfer function, (20), whereas the $1/T$ is due to the leading coefficient in (14).

A second computer program and sample run are provided in Appendix I for this Type II phase-locked loop case. Once again, the bandlimited gain expression in (30) closely approximates the true gain function (31) for frequencies well within the closed-loop bandwidth.

In concluding this article, several statements stand out.

- In order to make any correlation between sampled and continuous systems, some form of analog "hold" device impulse response of the hold device is the interpolating waveform between sample points in the time domain.
- The appearance of sampling in any loop with the accompanying "hold" device, causes an exponential phase term to appear, $\exp(-sT/2)$.
- Sampling effects in small percentage bandwidth loop (wrt. F_{ref}) may be quite accurately described by the normal continuous open-loop gain function provided that the additional exponential term is included.

Sampling effects cause the appearance of the exponential delay-like term whenever quantities within the loop are only available at discrete instants in time. Digital dividers within the feedback loop in an otherwise continuous loop will still cause the exponential term to appear. If digital feedback dividers and a digital phase/frequency detector are used within the phase-locked loop together, only one $\exp(-sT/2)$ term results (the continuous first order approximation remains unchanged). True

transport delay within the loop is accounted for by another exponential delay term. (Here, true transport delay refers to delay through op-amps and propagation delay refers to delays through other components, including dividers. These quantities are available in component data books.)

Analysis of the phase/frequency detector in a phase-locked loop can be considerably more complex than the usual continuous analysis which is generally employed. If the loop bandwidth is, say, $< F_{ref}/40$, the loop can be considered continuous for all practical purposes. For higher percentage bandwidths, attention should be given to the added "delay-like" term shown in equation (28) and care should be given to insure that T/τ_2 is > 3 in equation (20). [If $T/\tau_2 < 3$, another integrator in the form of a time variable filter is created which makes the situation much more complex. Of course, keeping $T/\tau_2 > 3$ will result in higher spurs and notch filtering will undoubtedly be required. The time variable filter increases the gain within the loop bandwidth and adds substantial phase as well which can easily lead to instability. For best results, choose $T/\tau_2 > 3$.]

Although the cautious aspects of sampled phase-locked loop design have been brought out for the phase/frequency detector, sampled systems harbor much more capability than first glance indicates. For instance, a Type I sampled loop which employs a zero order sample and hold rather than the phase/frequency detector will theoretically perform phase-lock in only one sample period! An ideal Type II phase-locked loop with a zero order sample and hold phase detector is capable of performing phase-lock in only two sample periods. These speed-optimized phase-locked loops must be analyzed using Z-transforms.⁵

References

1. *RF Design*, "PLL Primer, Part III," A.B. Przedpelski, July/August 1983, pp. 48-58.
2. *RF Design*, Letters to the Editor, Dr. William F. Egan, March/April 1984, pp. 9A-12A.
3. *RF Design*, "Divider Delay: The Missing PLL Analysis Ingredient," Stan Goldman, March/April 1984, pp. 58A-66A.
4. *Digital Control of Dynamic Systems*, Gene F. Franklin, J. David Powell, Addison-Wesley.
5. *Microwaves & RF*, "Sampling Phase-Locked Loops for Frequency Synthesis," J.A. Crawford (to be published).

Appendix I

```

FILE: SAMPLL  71                                PAGE 001
10 '*****
20 '
30 '      Comparison of Sum[ F(s + jnWs) ] with Z-transforms
40 '
50 '*****
60 DIM PTS(20),MAG(20),ANG(20)
62 PI=3.141592654#
70 FOR I%=1 TO 17
80   READ PTS(I%)
90 NEXT I%
100 DATA 100,150,200,300,400,500,700,1000,1500,2000,3000,4000,5000,7000
110 DATA 8000,9000,10000
120 '
130 INPUT "NUMBER OF HARMONICS TO INCLUDE ";NHARM%
135 INPUT "INPUT REFERENCE RATE, HZ ";FREF
136 INPUT "INPUT THE TYPE I LOOP  WN ";WN

```

```

137 INPUT "INPUT THE LOW-PASS FILTER  TIMECONSTANT, NSEC";TAU
138 TAU=TAU*9.999999E-10
140
150 FOR I%=1 TO 17
160   SUMR=0
170   SUMI=0
180   FOR J%=1 TO NHARM%
190     F=PTS(I%) + J%*FREF
200     GOSUB 1000
210     SUMR=SUMR + FR
220     SUMI=SUMI + FI
230     F=PTS(I%) - J%*FREF
240     GOSUB 1000
250     SUMR=SUMR + FR
260     SUMI=SUMI + FI
270   NEXT J%
280   F=PTS(I%)
290   GOSUB 1000
300   SUMR=SUMR + FR
310   SUMI=SUMI + FI
320   MAG(I%)=4.34294*LOG( SUMR^2 + SUMI^2 )
330   ANG(I%)=ATN(SUMI/(SUMR + 1E-08))
340   IF SUMR<0 THEN ANG(I%)=ANG(I%)-PI
350   ANG(I%)=ANG(I%)*180/PI
360 NEXT I%
370 PRINT CHR$(26)
380 LPRINT "Number of harmonic terms included in summation ";NHARM%
390 LPRINT
400 LPRINT "Loop reference frequency ";FREF
410 LPRINT
420 LPRINT "Type I loop  Wn ";WN
430 LPRINT
440 LPRINT "Loop  LPF time constant, nsec ";TAU*1E+09
450 LPRINT
460 LPRINT "APPROXIMATION TO SAMPLED OPEN-LOOP GAIN FUNCTION"
470 LPRINT "
480 LPRINT "      Summation of  Gol Terms      Continuous Gol"
490 LPRINT "      Exp( -ST/2 )"
500 LPRINT "
510 LPRINT "      F      Gol,dB      Ang,Deg  "
520 LPRINT "=====
530 FOR I%=1 TO 17
540   F=PTS(I%)
550   GOSUB 1000
560   NORGAIN=4.34294 * LOG( FR^2 + FI^2 )
570   NORANG=B - WX.5/FREF
580   LPRINT USING "*****      ****.##      ****.##      ****.##      ****
590   .##";PTS(I%),MAG(I%),ANG(I%),NORGAIN,NORANG*180/PI

```

```

10 '*****
20 '
30 '      Comparison of Sum[ F(s + jnWs) ] with Z-transforms
40 '
50 '*****
60 DIM PTS(20),MAG(20),ANG(20)
70 PI=.3141592654#
80 FOR I%=1 TO 17
90   READ PTS(I%)
100 NEXT I%
110 DATA 100,150,200,300,400,500,700,1000,1500,2000,3000,4000,5000,7000
120 DATA 8000,9000,10000
130 '
140 INPUT "NUMBER OF HARMONICS TO INCLUDE ";NHARM%
150 INPUT "INPUT REFERENCE RATE, HZ ";FREF
160 INPUT "INPUT THE TYPE II LOOP WINDING ";WN
170 INPUT "INPUT THE LOOP DAMPING FACTOR ";ETA
180 INPUT "INPUT THE LOW-PASS FILTER TIMECONSTANT, NSEC";TAU
190 TAU=TAU*.999999E-10
200 '
210 FOR I%=1 TO 17
220   SUMR=0
230   SUMI=0
240   FOR J%=1 TO NHARM%
250     F=PTS(I%) + J%*FREF
260     GOSUB 600
270     SUMR=SUMR + FR
280     SUMI=SUMI + FI
290     F=PTS(I%) - J%*FREF
300     GOSUB 600

```

```

310 SUMR=SUMR + FR
320 SUMI=SUMI + FI
330 NEXT J%
340 F=PTS(I%)
350 GOSUB 600
360 SUMR=SUMR + FR
370 SUMI=SUMI + FI
380 MAG(I%)=4.34294XLOG( SUMR^2 + SUMI^2 )
390 ANG(I%)=ATN(SUMI/(SUMR + 1E-08))
400 IF SUMR<0 THEN ANG(I%)=ANG(I%)-PI
410 ANG(I%)=ANG(I%)X180/PI
420 NEXT I%
430 PRINT CHR$(26)
440 LPRINT "Number of harmonic terms included in summation ";NHARM%
450 LPRINT
460 LPRINT "Loop reference frequency ";FREF
470 LPRINT
480 LPRINT "Type II loop Wn ";WN
490 LPRINT
500 LPRINT "Loop damping factor, Eta ";ETA
510 LPRINT
520 LPRINT "Loop LPF time constant, nsec ";TAUX1E+09
530 LPRINT
540 LPRINT "APPROXIMATION TO SAMPLED OPEN-LOOP GAIN FUNCTION"
550 LPRINT "
560 LPRINT " Summation of Gcl Terms
570 LPRINT
580 LPRINT "F Gcl,dB Ang,Deg "
590 LPRINT "-----"
600 FOR I%=1 TO LN
610 F=PTS(I%)
620 GOSUB 600
630 NORGAIN=4.34294 X LOG( FR^2 + FI^2 )
640 NORANG=B - WX.5/FREF
650 LPRINT USING "#####.### #####.### #####.### #####.###"
660 LPRINT "F,PTS(I%),MAG(I%),ANG(I%),NORGAIN,NORANGX180/PI
670 NEXT I%
680 STOP
690 ' *****
700 ' OPEN LOOP GAIN FUNCTION, CONTINUOUS
710 ' *****
720 W=(WN/W)^2 X SQRT( (1 + (2KETAXW/WN)^2) / (1 + (WXTAU)^2) )
730 B=-PI + ATN(2KETAXW/WN) - ATN(WXTAU)
740 FR=XCOS(B)
750 FI=XSIN(B)
760 RETURN

```

A One Transistor FM Transmitter

By William Rynone
Pegasus Data Systems

Last summer, I was requested to design a simple FM transmitter to meet the requirements for a convenient, low cost method of testing a large number of vendor supplied FM receivers that were to be incorporated into a digital data transmission system. The test that had to be performed was intended to make a subjective check of the accuracy of the tuning dial setting and the sensitivity of each receiver unit. Since it might become necessary to perform field tests, interconnecting various pieces of bulky and heavy test equipment was considered to be an undesirable alternative.

To meet the requirement, the transistor circuit shown below was designed, built and tested. The 2N2222 circuitry is a three element phase shift oscillator circuit, designed to yield a 1000 Hz sine wave. The 1000 Hz sine wave is then applied to the TCG-610 varactor diode (6 pF at 4 volts) which changes the tank capacitance, thus varying the RF oscillator frequency at a 1000 Hz rate. The 1000 ohm potentiometer in the collector circuit may be adjusted to enable desired frequency modulation level.

The Hartley RF oscillator, which is designed around a readily available MPF-

102 JFET, has an output that should be relatively stable if it is not enclosed (but without an antenna). When enclosed, a BNC or F connector can be used to feed the RF to a small loop. If you decide to build this unit, be careful. The FCC has regulations regarding the radiation of RF.

One of my colleagues, Bohden Stryzak, modified the transmitter by eliminating the sine wave oscillator portion and replaced it with a carbon microphone as shown below. His children then had a three dollar portable transmitter that could be used with any portable FM receiver as a walkie-talkie.

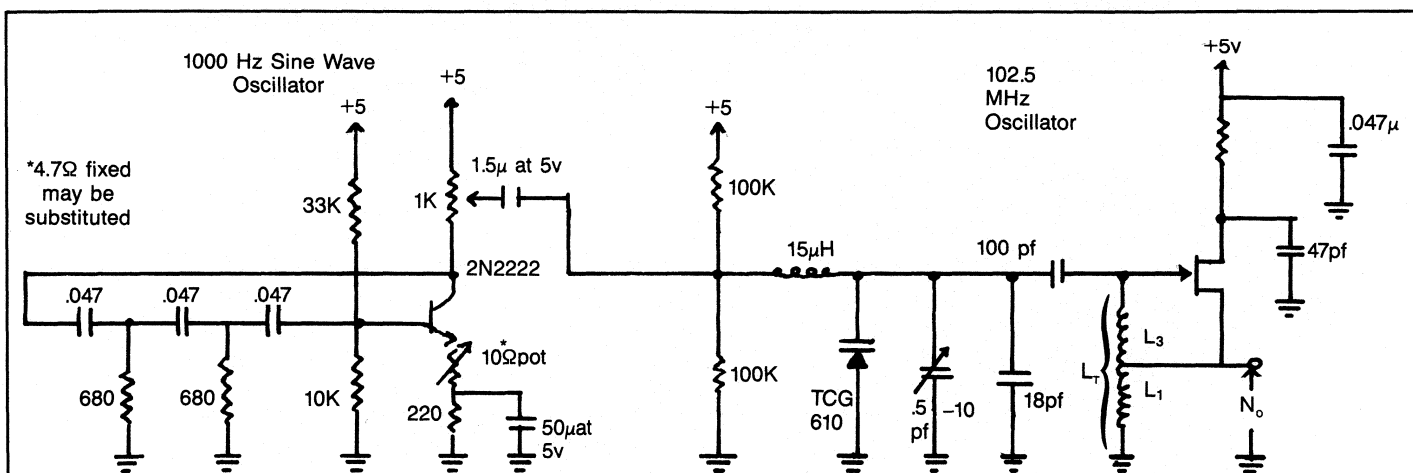


Figure 1

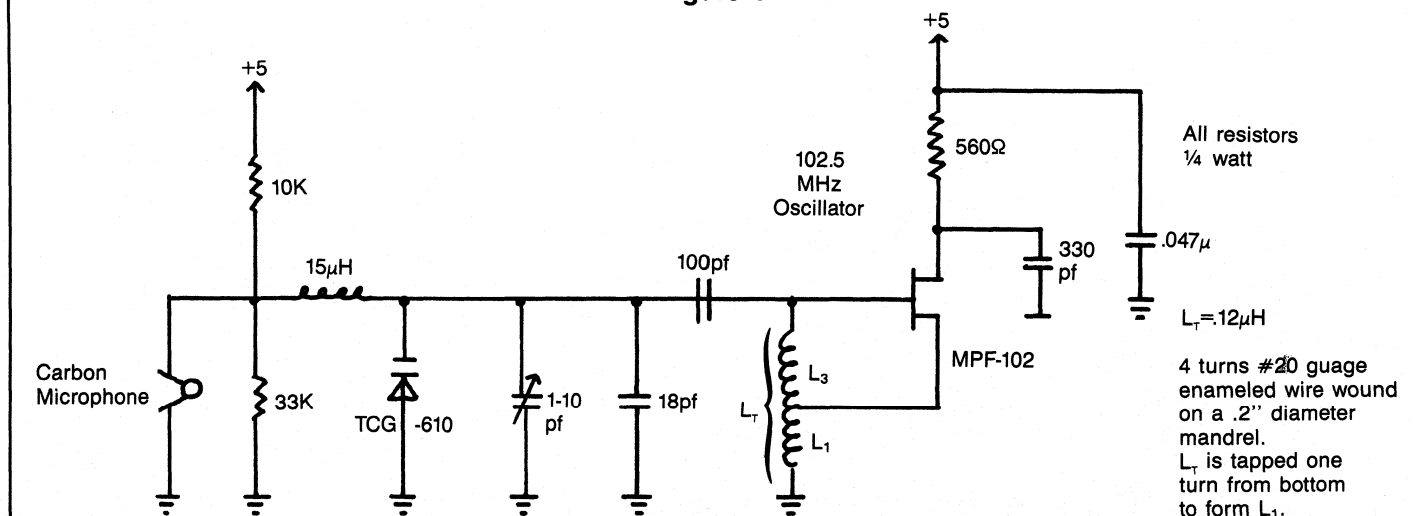


Figure 2.



Cover

This month's cover features Motorola's MDO-2 (left) and the new MDO-3 (right) temperature-compensated crystal oscillators. Motorola considers these MDO products to be the best in TCXO performance in their cost range. The MDO-3 is described in this month's Special Report, along with other recently announced oscillator products. Many of the considerations mentioned in Dennis Marvin's article on frequency-temperature performance determination in crystal oscillators were incorporated in the MDO-2 series. (Photo courtesy of Motorola, Inc.)



Features

20 **Special Report: New Waves in Oscillator Design**

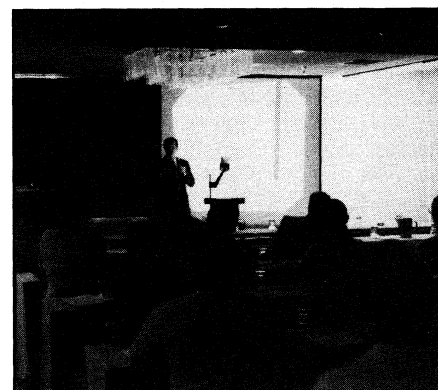
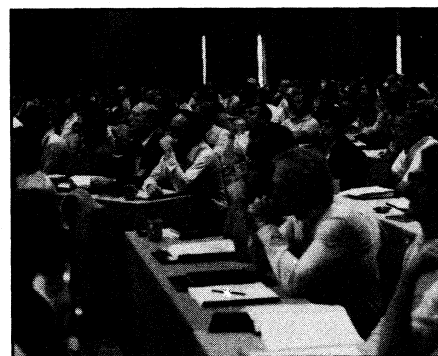
This month's Special Report covers common oscillators designed to operate primarily at frequencies below 2 GHz. Examples of the kinds of improvements being made in crystal and SAW resonator oscillators are described, along with indications of probable trends in oscillator design — James N. MacDonald.

26 **The SAW Resonator: How It Works — Part 2**

The author continues his explanation of the surface acoustic wave resonator and his program to model device responses. He describes how to use the program to examine the properties of reflective arrays and single and multiple cavities. A BASIC version of the program is given for microcomputer users. — Jeffrey S. Schoenwald, Ph.D.

53 **Frequency-Temperature Performance Determination in High Stability TCXOs**

High stability temperature-compensated crystal oscillators are subject to many instabilities not normally considered in the design of lower stability products. The design engineer must carefully consider the system requirements in dynamic environments and as a function of time. The author reviews several second order effects and attempts to quantify the amount of performance debasement that can result. — Dennis Marvin.



Scenes from RF Technology Expo 85 —
Anaheim, Calif.

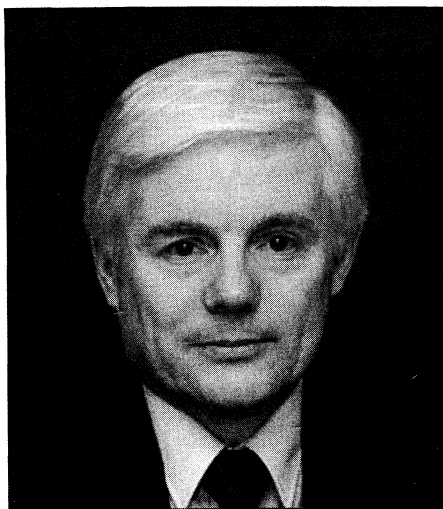
Departments

- 6 Editorial
- 8 Publisher's Notes
- 14 Letters
- 16 News
- 24 RFI/EMI Corner
- 34 Calendar
- 45 Info Card
- 60 The Digital Connection
- 63 New Products
- 72 New Literature
- 76 Advertisers Index

R.F. DESIGN (ISSN: 0163-321X USPS: 453-490) is published monthly plus one extra issue in June. March 1985, Volume 8, No. 3. Copyright 1985 by Cardiff Publishing Company, a subsidiary of Argus Press Holdings, Inc., 6530 S. Yosemite Street, Englewood, CO 80111 (303) 694-1522. Contents may not be reproduced in any form without written permission. Second-Class Postage paid at Englewood, CO and at additional mailing offices. Subscription office: 1 East First Street, Duluth, MN 55802, (1-800-346-0085). Subscriptions are sent free to qualified individuals responsible for the design and development of communications equipment. Other subscriptions are: \$15 per year in the United States; \$25 per year in Canada and Mexico; \$25 per year for foreign countries. Additional cost for first class mailing. Payment must be made in U.S. funds and accompany request. If available, single copies and back issues are \$5.00 each (in the U.S.). This publication is available on microfilm/fiche from University Microfilms International, 300 N. Zeeb Road, Ann Arbor, MI 48106 USA (313) 761-4700.

POSTMASTER & SUBSCRIBERS: Please send address changes to: R.F. Design, P.O. Box 6317, Duluth, MN 55806.

Where Do You Learn About RF Circuits?



James MacDonald
Editor

The biggest surprise at the RF TECHNOLOGY EXPO was the response to the Fundamentals of RF Design course. Based on pre-registrations, the room was set up for a maximum of 350. By starting time the first day the room was filled and more than 100 conference attendees were in the hall hoping to register. We were able to add some chairs, but many who had not pre-registered had to be turned away.

The situation was similar when the course was repeated the next day. By then the room had been expanded to seat 500, anticipating the overflow from the first day. All seats were filled and remained filled throughout the day.

On one hand, this overwhelming response reflected the response to the EXPO as a whole. Attendance exceeded our expectations, if not our hopes. On the other hand, it provided dramatic proof of a serious lack of educational opportunities for RF engineers. The audience composition ranged from young recent graduates to university professors with well-established reputations in electrical engineering.

As I talked with attendees the same fact was mentioned over and over; electrical engineering students have little opportunity or incentive to study RF circuit principles. In many universities the courses simply are not available. Where they are available advisors do not encourage such courses.

Current employment opportunities apparently are greater and salaries higher in the digital and power fields, but this not-very-widely promoted course in RF design fundamentals attracted more than 800 engineers and others involved in designing RF equipment, some from foreign countries. Clearly there is a significant lack of educational opportunities in RF circuit theory and design. We think engineering colleges should take a look at this educational need.

Proceedings of the sessions, including the Fundamentals of RF Design course, will be published soon. RF designers who could not attend the EXPO may want to order a copy. Each session was tape recorded, as well. Tapes may be ordered from Meyer Communications Corp., 13791 E. Rice Place, Aurora, CO 80015.

During World War II many amateur radio operators were hired by defense contractors to build communications gear. Even fewer engineers were trained in RF principles at that time. Amateurs knew how to build equipment, even if they did not thoroughly understand how it worked. Many of them eventually became engineers.

This is one reason so many RF designers are amateur radio enthusiasts. Most of those who worked during WWII are retired, but they passed their enthusiasm on to the younger generation. During EXPO 85 quite a few hams were seen with handheld 2-meter gear and others were heard on the band with mobile and base station rigs.

Carl Lodstrom, SM6MOM/W6, has suggested that we select a frequency for simplex operation during the next EXPO and publicize it. Carl said such a frequency seemed to be chosen by chance at EXPO 85, perhaps because people heard others talking on it and joined the net. He said it was a great way for hams to get together for dinner or meetings.

What do *RF Design* readers think of this idea?

James H. MacDonald

The SAW Resonator Filter: How It Works. Part II

By Jeff Schoenwald
Contributing Editor

Last month, SAW resonator theory and a program for the TI-59 calculator and printer were described. This month, we use the program to learn about SAW resonators. Of special value is the definition and order of parameter entry.

Unless otherwise indicated, certain initial parameters that must be entered will always be the same:

$$\begin{aligned} l_1 &= l_2 = 0.25 \\ n_2 &= 1 \\ f_0 &= 100 \end{aligned}$$

As a first example, consider the characteristics of a single reflector array as a function of changing strip/gap impedance ratio Z at a fixed number of segments $N = 200$. Figures 1a and 1b show the reflection loss and transmission power loss respectively for $Z = 1.005$, 1.01 and 1.015. At frequencies above or below f_c the reflectors are transparent to traveling waves, so the transmission loss is small and the reflected wave loss is quite large. Closer to center frequency, the reflection efficiency of the gratings improves and the transmission loss increases relative to the impedance mismatch Z or number of segments in the array.

In the next example, shown in Figure 2, two reflectors are cascaded. $Z = 1.01$, $N = 100$ in each reflector, and the cavity is 5 wavelengths long (i.e., $l_g = 4.75$). Away from the center frequency, the results are similar to that of the previous examples. Near center frequency, the Fabry Perot cavity becomes resonant and the structure is "transparent," and at f_c the reflected energy is negligible.

While we have assumed no losses due to absorption in the transmission line, we

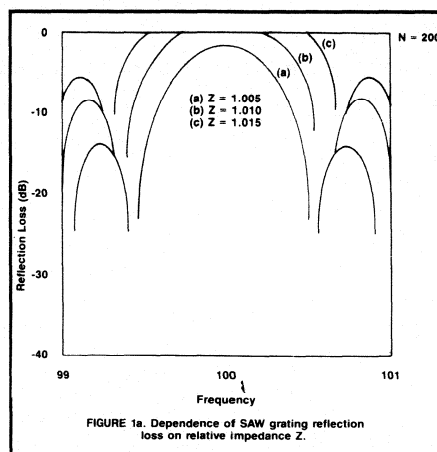


FIGURE 1a. Dependence of SAW grating reflection loss on relative impedance Z .

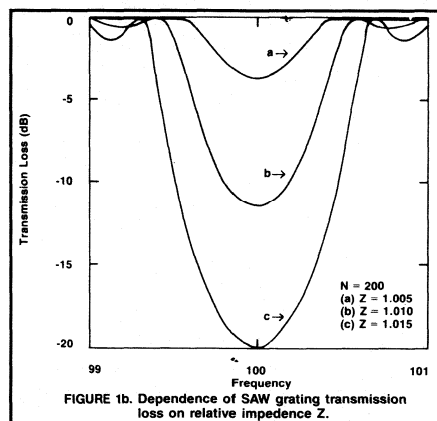


FIGURE 1b. Dependence of SAW grating transmission loss on relative impedance Z .

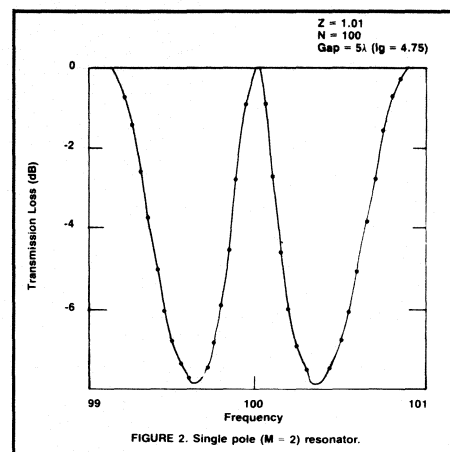


FIGURE 2. Single pole ($M = 2$) resonator.

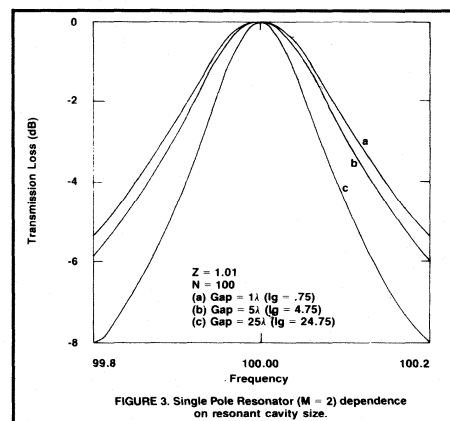


FIGURE 3. Single Pole Resonator ($M = 2$) dependence on resonant cavity size.

will still never obtain an infinite Q factor in a lossless device because a reflective array can never be 100% efficient unless Z or N go to infinity. What we do observe is a resonant peak at the center frequency with the 3 dB fractional bandwidth that determines the unloaded Q ($= f_c / \Delta f_{3\text{ dB}}$) of the resonator. Figure 3 shows the

power transmission characteristics near $f_0 = f_c$ for a single cavity resonator ($M = 2$), with 100 sections/reflector, $Z = 1.01$, with the cavity size as the variable. It is apparent that the 3 dB bandwidth of the resonance decreases and Q increases as the cavity length increases. Figure 4 shows how the Q varies with

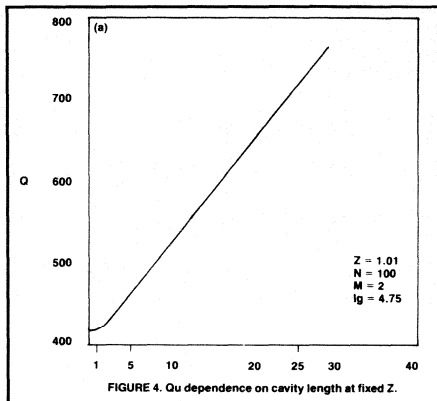


FIGURE 4. Qu dependence on cavity length at fixed Z.

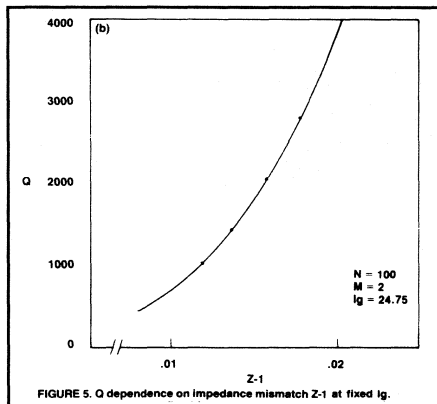


FIGURE 5. Q dependence on impedance mismatch Z-1 at fixed lg.

cavity length while N and Z are held constant. Similar sets of curves can be obtained to determine the dependence of Q or N or Z, which I encourage you to do. Figure 5 shows how Q varies with Z at fixed cavity size.

Cavity Dimension Is Critical

The resonant Fabry-Perot cavity formed by the two reflective arrays will act as an interference filter that efficiently transmits energy at wavelengths which satisfy the cavity relationship:

$$L = \frac{n\lambda_c}{2} \quad (1)$$

where $L = (l_1 + l_2) \cdot \lambda_c$. λ_c is the normalized wavelength at the peak of reflectivity of the grating. If the wavelength is different from λ_c , narrow band transmission through the structure will not occur at the center of the reflection stop-band of the grating. Another way of saying this is, if we let $L = l_1 + l_2$ be equal to some non-integer multiple of $\lambda_c/2$, the transmission spectrum appears non-symmetric. Figure 6 illustrates the effect of advancing the cavity dimension successively by $\lambda_c/8$. If resonance is not precisely

centered at the stop band center of the reflectors the Q, selectivity and efficiency of the resonator suffer.

Another interesting case is worth mentioning before we move on to more complicated structures. If we obey the Fabry-Perot condition of Eq. (1), but make n very large, we encounter a regime in which several longitudinal modes of the cavity can exist, all at slightly different wavelengths (frequencies). This is precisely the case for lasers. A simple laser with two mirrors will have many possible longitudinal cavity modes because the cavity is orders of magnitude larger than wavelength. Special techniques are used to lock the laser into a single mode for added spectral purity. Figure 7 shows some examples of multiple resonances due to oversized cavities.

Designing Multi-Pole Filters

The program is capable of synthesizing device designs that exhibit the essential features of multi-pole SAW resonator filtering behavior. There is no limit to the number of poles one may wish to model, nor does this affect the speed at which the frequency response is synthesized. A design consisting of M grating reflectors will result in an M-1 cavity structure with an M-1 pole response. This assumes, of course that the cavities are kept small enough to avoid more than a single longitudinal mode in each one. The resonances in each cavity will begin to couple and we shall begin to see how this coupling through the grating reflectors that separate each cavity give rise to the very narrow bandpass filtering which has made the SAW resonator popular in the RF and signal processing community.

With this program, all cavities will be the same size and all reflectors will have the same number of strip/gap segments for any one example run. How much can you expect from the TI-59? *C'est la vie*. We will, however, squeeze a bit more out of it.

Figures 8a, b, c and d show the transmission characteristics of 1-, 2-, 3-, and 4-pole resonators. All reflectors have 200 sections, with $Z = 1.01$, and all cavities are $5\lambda_c$ long (i.e., $l_g = 4.75$). The valleys between resonant peaks are very characteristic of the SAW resonator multi-pole filter. Typically, interdigital transducers (idts) are placed within the two outermost cavities of such a structure. This has the property of enhancing the resonance behavior over the broadband response of the idts, since by themselves they have an insertion loss that is often 20 or 30 dB,

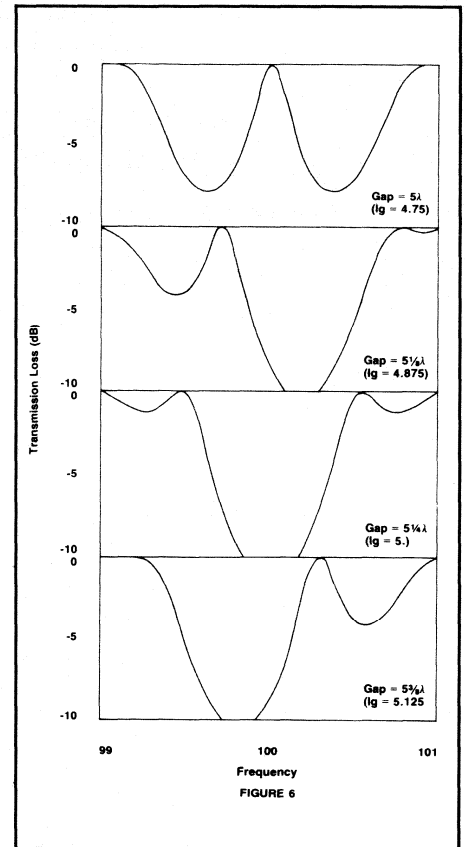


FIGURE 6

whereas the resonances are much stronger because the device impedance drops markedly at those frequencies. Before the idt is properly matched electrically, the resonator response is essentially that of the "unloaded" device and is quite well reproduced by the TI-59 program model. Impedance matching the electrical equivalent circuit of the idt to the cavity impedance will flatten the transmission response over the multipole pass-band.

The Phase of the Reflected and Transmitted Waves

Once the transmission matrix for the entire structure has been calculated, we may easily determine the phase of the reflected and transmitted wave from the transmission factor and reflection factor, T_F and R_F , using equations 2a and 2b.

$$\Phi(\text{refl}) = \arctan \frac{\text{Imag}(R_f)}{\text{Real}(R_f)} \quad (2a)$$

$$\Phi(\text{trans}) = \arctan \frac{\text{Imag}(T_f)}{\text{Real}(T_f)} \quad (2b)$$

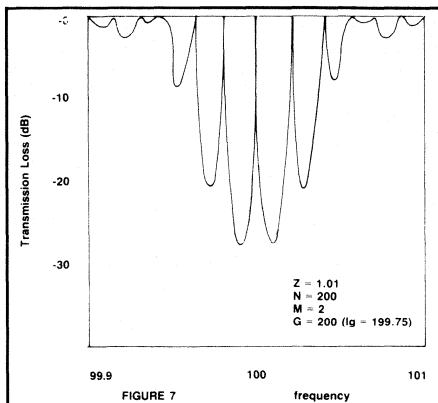


FIGURE 7

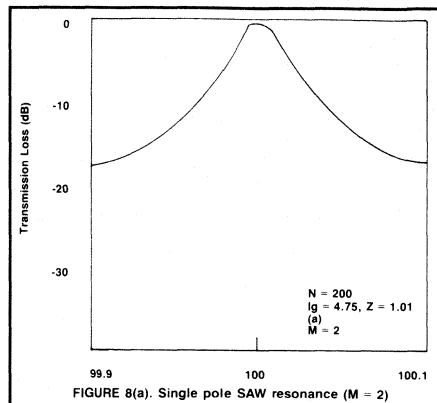


FIGURE 8(a). Single pole SAW resonance (M = 2)

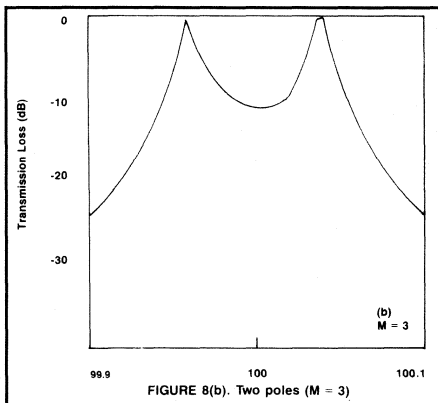


FIGURE 8(b). Two poles (M = 3)

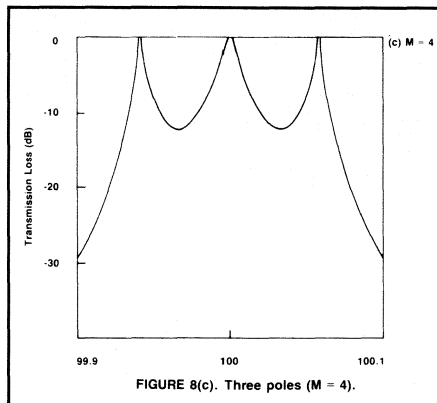


FIGURE 8(c). Three poles (M = 4).

In order to implement this calculation, the listing shown in Table I may be substituted for the last portion of the program, starting at step 638. This may be stored in a simple way. Since the calculator is partitioned for 720 steps, the entire program can be stored in three data banks. The modification occurs only in bank 3. The modified version can be stored on the second edge of the second card (normally used for bank 4). Be sure the calculator is in floating point mode (exit the learn mode and press INV 2nd FIX). Press 3 2nd WRITE but feed in the second magnetic card upside down. Later, when loading the program for phase analysis, the calculator will recognize this as a bank 3 read.

Using this method, power magnitude calculations can be done first, then the third bank replaced with phase calculation, the input parameters re-entered and the calculation repeated, yielding the phase response. Not all registers containing the input parameters are re-used. Look at Table II to determine at which label you must re-enter data. Practically speaking, however, it is easier and safer to re-enter all the data from scratch.

Figures 9 and 10 are examples of the phase response for a single pole resonator. They have identical structures but different values of Z . Rather than short-change the phase computational ability of this program, I will spend a few moments to explain some of the things you can learn from it about SAW resonators. For a plane wave incident on a reflecting surface, the general form of the reflected wave, relative to an incident wave of unit amplitude and zero phase at the front of the reflector, is

$$R_i = r e^{2ik \cdot D} \quad (3)$$

where r is the coefficient of reflection magnitude and D is the distance from the point at which the observation is made to the plane of the reflecting surface. If we imagine that the observation point is the front edge of the distributed grating reflector and D is the distance to a fictitious point at which we may assume a single reflecting mirror is placed, then we are constructing a simple model that represents the distance to the "effective center of reflection."

The phase of the reflected wave is given by the argument of the exponential. If we take the first derivative of this phase with respect to the frequency and convert from radians to degrees, we obtain

$$\Phi_{\text{rad}} = 2 \frac{2\pi}{\lambda} D = \frac{4\pi D f}{v}$$

$$\frac{d\Phi_{\text{rad}}}{df} = 4\pi \frac{D}{v} = \frac{4\pi D}{f\lambda} \quad (4)$$

Therefore,

$$D = \frac{\lambda f}{4\pi} \cdot \frac{d\Phi}{df} = \frac{\lambda f}{4\pi} \frac{\pi}{180} \frac{d\Phi_{\text{deg}}}{df}$$

$$\frac{D}{\lambda} = \frac{f}{720} \frac{\Delta\Phi}{\Delta} \quad (5)$$

Thus, by measuring the slope of phase data we obtain for the reflected wave we are able to compute the distance to the

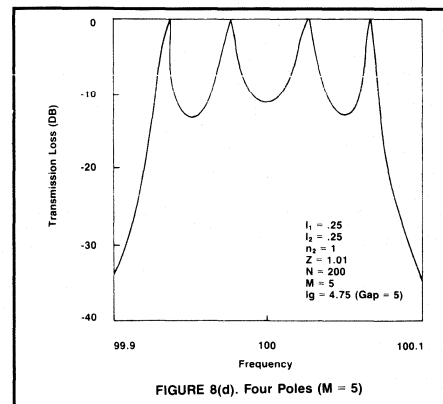


FIGURE 8(d). Four Poles (M = 5)

TABLE I Phase Calculation

638	60	DEG	678	53	(
639	53		679	43	RCL
640	02	2	680	06	06
641	65	x	681	85	+
642	53		682	43	RCL
643	43	RCL	683	07	07
644	08	08	684	54)
645	65	x	685	55	÷
646	43	RCL	686	53	(
647	06	06	687	43	RCL
648	75	-	688	05	05
649	43	RCL	689	85	+
650	05	05	690	43	RCL
651	65	x	691	08	08
652	43	RCL	692	54)
653	07	07	693	94	+/-
654	54)	694	22	INV
655	55	÷	695	30	TAN
656	53	(696	95	=
657	43	RCL	697	99	PRT
658	05	05	698	98	ADV
659	33	x²	699	43	RCL
660	85	+	700	13	13
661	43	RCL	701	32	X-T
662	06	06	702	43	RCL
663	33	x²	703	26	26
664	75	-	704	67	EQ
665	43	RCL	705	19	D'
666	07	07	706	43	RCL
667	33	x²	707	29	29
668	75	-	708	42	STO
669	43	RCL	709	11	11
670	08	08	710	61	GTO
671	33	x²	711	14	D
672	54)	712	76	LBL
673	54)	713	19	D'
674	22	INV	714	43	RCL
675	30	TAN	715	26	26
676	95	=	716	91	R/S
677	99	PRT			

"effective center of reflection." At the peak in reflectivity the center of reflection appears to move toward the front of the reflective array, as evidenced by a decrease in the magnitude of the phase slope. Away from resonance, where the array ultimately looks transparent, the center of reflection moves to the geometric center of the array.

For the cases shown in Figures 10a and 10b, the reflection centers are located, at resonance, a distance of 22 and 17 wavelengths, respectively, inside the array, as viewed from the direction of incidence. Now consider two identical reflectors separated by a distance necessary to produce a single pole resonance. The total length of the cavity is then given by

$$L = (l_g + 1/4) \cdot c + 2D \quad (6)$$

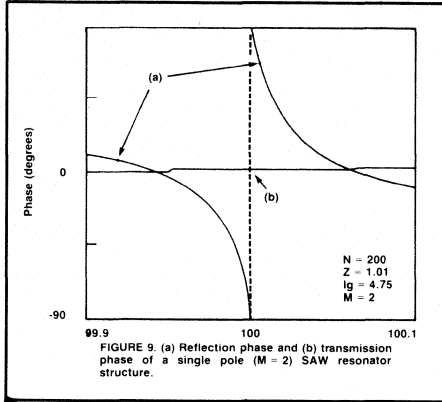


FIGURE 9. (a) Reflection phase and (b) transmission phase of a single pole ($M = 2$) SAW resonator structure.

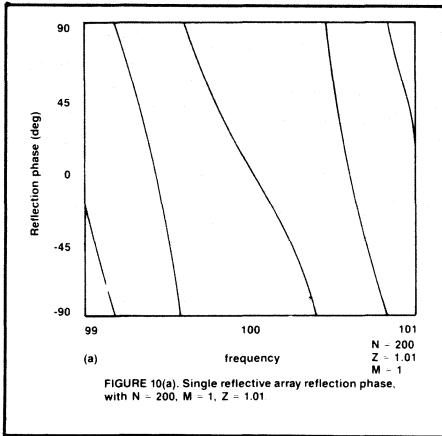


FIGURE 10(a). Single reflective array reflection phase, with $N = 200$, $M = 1$, $Z = 1.01$.

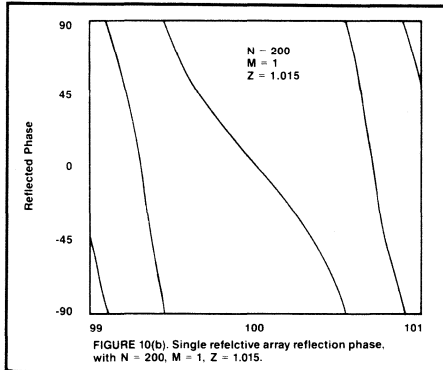


FIGURE 10(b). Single reflective array reflection phase, with $N = 200$, $M = 1$, $Z = 1.015$.

Knowing the value of D is important for determining the frequency spacing between longitudinal modes in the resonant cavity formed by the two arrays. Now we can see that mode spacing is a function of both cavity size and reflective properties of the array, as represented by the distance D . It is possible to derive frequency spacing dependence on effective length of the cavity L , and such derivations abound in books on lasers. The reader is encouraged to do this for the specific case shown in Figure 7. You will indeed find that the mode spacing observed in large SAW resonator cavities,

or in SAW resonators with Z so close to unity that D is sizable, is properly described by taking this reflection distance into account properly. More than once, ignorance of this fact has bitten SAW resonator designers when they least expected it.

Conclusion

I have tried to give the reader a tool for modeling and exploring the behavior of the SAW resonator, a very interesting tool in RF technology. Even if you have no plans for designing such devices you may very likely wish to specify one from a number of vendors that supply them. In that case, you will be better off for having become familiar with the properties of these devices and being an educated customer.

TABLE II

Register	Variable
0	$N, N-1, M, M-1$
1	λ_1, λ_2
2	M
3	lg
4	$\Theta, \lambda_1 \uparrow N, \lambda_3 \uparrow N$
5	$I_1, A(N), A(N+9)$
6	$I_2, B(N), B(N+9)$
7	$n_2, C(N), C(N+9)$
8	$f_0, D(N), D(N+9)$
9	f_c
10	Z
11	N
12	$t, \cos \Theta = (A + D)/2$
13	f_1
14	df
15	$\alpha = \text{Pi} * f_1/f_c$
16	$Z + 1$
17	$Z - 1$
18	$1 - 2t$
19	$A(1), A(N)$
20	$B(1), B(N)$
21	$C(1), C(N)$
22	$D(1), D(N)$
23	$[(A + D)/2 \uparrow 2 - 1]$
24	λ_1
25	λ_2
26	$f_2 + df$
27	$\sin N\Theta$ or $(\lambda_1 \uparrow N - \lambda_2 \uparrow N) / (\lambda_1 - \lambda_2)$
28	$\sin (N - 1)\Theta$ or $(\lambda_1 \uparrow (n - 1) - \lambda_2 \uparrow (N - 1)) / (\lambda_1 - \lambda_2)$
29	N

BONUS!:

A *BASIC* Version

For readers who own or work with a computer, here is a BASIC version of the TI-59 calculator program to model the transmission and reflection power and phase of a SAW resonator type of structure. This program was written on a Commodore 64, which uses a version of BASIC and an ASCII character set that is slightly different from standard ones. I have taken pains to write the program to be as transportable as possible, indicating, when necessary, what lines are not transportable and require change or deletion. The POKEs only pertain to screen or letter color. There are no PEEKs. The printer commands are usable "as is" only on Commodore printers and serve as an example which must be tailored for other brands.

Because memory is not as tight for most micros, power and phase are computed and provisions are made for screen display and hard copy. Disk or tape storage of data files and high resolution plotting are routines that the devoted hacker should add, but these have been left out because of differences between computers in storage procedures and screen addressing.

Data entry is simple and screen prompted. If the velocity in a strip segment is different from the gap velocity the center frequency will be different from the designated reference frequency. I suggest you start with a ratio of 1 and then try small changes to observe the trend. The same advice holds for the impedance ratio and cavity size.

```

10 REM *****
20 REM *   CERTAIN LINES ARE   *
30 REM *   SPECIFIC TO THE    *
40 REM *   COMMODORE 64.     *
50 REM *   DELETE OR ALTER AS DESIRED. *
60 REM *****
70 PI= 3.14159265:REM * C-64 RECOGNIZES SYMBOL FOR PI. USE IT IF YOU CAN *
80 POKE 93281,0:POKE 53280,0:REM *SET BACKGROUND TO BLACK FOR C-64*
90 PRINT CHR$(150):REM *SET SCREEN LETTERS TO YELLOW ON C-64*
100 PRINT CHR$(147)
110 PRINT"SAW RESONATOR TRANSMISSION"
120 PRINT"  LINE SIMULATION"
130 PRINT""
140 PRINT"(C) COPYRIGHT JEFF SCHOENWALD"
150 PRINT"  1984"
160 FOR I = 1 TO 2000
170 NEXT I
180 PRINT CHR$(147)
190 INPUT" GAP SEGMENT LENGTH, L1:L1
200 INPUT" LINE SEGMENT LENGTH, L2:L2
210 INPUT" RELATIVE VELOCITY INDEX OF L2:L2
220 INPUT" REFERENCE FREQUENCY F0:F0
230 INPUT" STRIP/GAP IMPEDANCE RATIO, Z1:Z1
240 INPUT" # OF SEGMENT PAIRS PER REFLECTOR, N:N
250 REM
260 INPUT" START FREQUENCY, F1:F1
270 INPUT" FREQUENCY INCREMENT, DF:DF
280 INPUT" STOP FREQUENCY, F2:F2
290 INPUT" # OF REFLECTOR ARRAY SECTIONS, M:M
300 INPUT" CAVITY SIZE, LG:LG
310 F0=F0/(2*(L1+N*L2))
320 PRINT CHR$(147)
330 PRINT" CENTER FREQUENCY = F0
340 T=N*L2/(L1+N*L2)
350 K=INT((F2-F1)/DF)
360 DIM AN(K),BN(K),CN(K),DN(K),TP(K),RP(K),TF(K),RF(K)
370 FOR K = 0 TO K
380 F = F1 + DF*K
390 LET GAMMA =PI*F/F0
400 A1=((Z+1)/2)*COS(GAMMA)-((Z-1)/2)*COS(GAMMA*(1-2*T))
410 B1=((Z+1)/2)*SIN(GAMMA)-((Z-1)/2)*SIN(GAMMA*(1-2*T))
420 C1=((Z+1)/(2*Z))*SIN(GAMMA)+((Z-1)/(2*Z))*SIN(GAMMA*(1-2*T))
430 D1=((Z+1)/(2*Z))*COS(GAMMA)+((Z-1)/(2*Z))*COS(GAMMA*(1-2*T))
440 N0=N
450 GOSUB 650:REM *COMPUTE EIGENVALUES FOR ONE ARRAY AND COMPUTE T MATRIX*
460 GOSUB 970:REM *COMPUTE CAVITY T MATRIX*
470 GOSUB 1030:REM *MULTIPLY MATRICES*
480 GOSUB 1090:REM *REDEFINE NET T MATRIX*
490 N0=M
500 GOSUB 640
510 REM
520 REM *COMPUTE EIGENVALUES AND MATRIX FOR*
530 AN(K)=AN *M CASCADED REFLECTORS AND CAVITIES*
540 BN(K)=BN
550 CN(K)=CN
560 DN(K)=DN
570 PRINT CHR$(147)
580 PRINT" FREQUENCY PT. #:"K" = "F
590 GOSUB 1180:REM *COMPUTE POWER & PHASE*
600 NEXT K:REM *NEXT FREQUENCY POINT*
610 REM *GOTO OUTPUT MENU*
620 GOTO 1760
630 REM
640 REM**REAL OR COMPLEX EIGENVALUES?**
650 TRIG = (A1+D1)/2
660 IF (TRIG-1)=0 THEN 690
670 IF (TRIG-1)0 THEN 670

```

```

690 RETURN
690 REM T MATRIX FOR COMPLEX EIGENVALUE READY
700 AGL = -ATN(TRIG/SQR(-TRIG*TRIG+1))+(PI/2)
710 IF AGL=0 THEN 780
720 N1=N0-1
730 AN=A1*SIN(N0*AGL)/SIN(AGL)-SIN(N1*AGL)/SIN(AGL)
740 BN=B1*SIN(N0*AGL)/SIN(AGL)
750 CN=C1*SIN(N0*AGL)/SIN(AGL)
760 DN=D1*SIN(N0*AGL)/SIN(AGL)-SIN(N1*AGL)/SIN(AGL)
770 GOTO 790
780 GOSUB 1210
790 RETURN
800 REM *WHEN EIGENVALUES ARE*
810 REM *DEGENERATE*
820 AN=A1-1
830 BN=B1
840 CN=C1
850 DN=D1-1
860 RETURN
870 REM *T MATRIX FOR REAL EIGENVALUES*
880 K1=TRIG*SQR(1-TRIG^2-1)
890 K2=1/K1
900 N1=N0-1
910 AN=A1*(K1*N0-K2*BN)/(K1-K2)-(K1*N1-K2*DN)/(K1-K2)
920 BN=B1*(K1*N0-K2*BN)/(K1-K2)
930 CN=C1*(K1*N0-K2*BN)/(K1-K2)
940 DN=D1*(K1*N0-K2*BN)/(K1-K2)-(K1*N1-K2*DN)/(K1-K2)
950 RETURN
960 REM ***GENERATE CAVITY MATRIX***
970 REM
980 A=COS(2*GAMMA*LG)
990 B=SIN(2*GAMMA*LG)
1000 C=SIN(2*GAMMA*LG)
1010 D=COS(2*GAMMA*LG)
1020 RETURN
1030 REM ***MATRIX MULTIPLICATION***
1040 AP=AN*A-BN*C
1050 BP=AN*B+BN*D
1060 CP=CN*A+DN*C
1070 DP=DN*D-CN*B
1080 RETURN
1090 REM
1100 A1=AP
1110 B1=BP
1120 C1=CP
1130 D1=DP
1140 RETURN
1150 REM ***COMPUTE REFLECTED AND***
1160 REM ***TRANSMITTED POWER AND***
1170 REM ***PHASE***
1180 P=(AN(K)+DN(K))^2+(BN(K)+CN(K))^2

```

```

1190 TP=4/G
1200 TP(K)=10*(LOG(TP))/LOG(10)
1210 RP=1-TP
1220 IF RP = 0 THEN 1280
1230 RP(K)=10*(LOG(RP))/LOG(10)
1240 TF(K)=(180/PI)*ATN(-1*(BN(K)+CN(K))/(AN(K)+DN(K)))
1250 RF=2*(BN(K)+DN(K)+AN(K)+CN(K))/(AN(K)^2-DN(K)^2+BN(K)^2-CN(K)^2)
1260 RF(K)=(180/PI)*ATN(RF)
1270 RETURN
1280 RP(K) = -99.0
1290 GOTO 1240
1300 W=20:REM *STOP SCREEN PRINT EVERY 20 LINES*
1310 PRINT CHR$(147)
1320 PRINT "FREQ. R-PWR T-PWR(DB) R-PHA T-PHA"
1330 PRINT " (DB) (DB) (DEG) (DEG)"
1340 FOR K=0 TO K2
1350 F=F1+DF*K+.000001
1360 B$=STR$(F):GOSUB 1690:F$=B$
1370 R$=STR$(RP(K))
1380 B$=R$:GOSUB 1590:R1$=B$
1390 T1$=STR$(TP(K))
1400 B$=T1$:GOSUB 1590:GOSUB 1670:T1$=B$
1410 R2$=STR$(RF(K))
1420 B$=R2$:GOSUB 1590:R2$=B$
1430 T2$=STR$(TF(K))
1440 B$=T2$:GOSUB 1590:T2$=B$
1450 IF W=K2+2 THEN 2090
1460 PRINT F:TAB(14-LEN(R1$)):R1$:TAB(22-LEN(T1$)):T1$:TAB(30-LEN(R2$)):R2$:TAB(39-LEN(T2$)):T2$
1470 PRINT R2$:TAB(39-LEN(T2$)):T2$
1480 IF K=0 THEN 1510
1490 IF K=K2 THEN 1520
1500 IF W=K2+2 THEN 1920
1510 NEXT K
1520 IF W=K2+2 THEN 2050
1530 PRINT "END OF LISTING. PRESS C FOR MENU"
1540 GET A$
1550 IF A$="" THEN 1540
1560 IF A$="C" THEN 1760
1570 IF A$="Q" THEN 1540
1580 RETURN
1590 REM *MANIPULATE STRINGS TO LINE UP COLUMNS*
1600 FOR U = 1 TO LEN(B$)
1610 IF MID$(B$,U,1)="" THEN 1640
1620 NEXT U
1630 RETURN
1640 B$=LEFT$(B$,U+2)
1650 IF LEN(LEFT$(B$,U+1))<2 THEN B$=B$+"0"
1660 RETURN
1670 IF ABS(TP(K))<.01 THEN B$="-0.00"
1680 RETURN
1690 FOR U = 1 TO LEN(B$)

```

```

1700 IF MID$(B$,U,1)="" THEN 1730
1710 NEXT U
1720 RETURN
1730 B$=LEFT$(B$,U+3)
1740 IF LEN(RIGHT$(B$,U+1))<3 THEN B$=B$+"00"
1750 RETURN
1760 PRINT CHR$(147)
1770 PRINT "  CHOOSE AN OPTION, PLEASE"
1780 PRINT ""
1790 PRINT "1 - REPEAT CALCULATION",CHR$(13)
1800 PRINT "2 - PRINT DATA TO PRINTER",CHR$(13)
1810 PRINT "3 - PRINT DATA TO SCREEN",CHR$(13)
1820 PRINT "4 - QUIT PROGRAM",CHR$(13)
1830 GET A$
1840 IF A$="1" THEN 1890
1850 IF A$="2" THEN 2000
1860 IF A$="3" THEN 1300
1870 IF A$="4" THEN END
1880 IF A$="" THEN 1830

```

```

1890 CLR
1900 GOTO 180
1910 PRINT CHR$(147)
1920 PRINT "PRESS CDS TO CONTINUE"
1930 GET A$
1940 IF A$="C" THEN 1960
1950 IF A$="" THEN 1930
1960 PRINT "FREQ.      R-PWR      T-PWR      R-PHA      T-PHA"
1970 PRINT "          (DB)        (DB)        (DEG)      (DEG)"
1980 GOTO 1510
1990 PRINT CHR$(147)
2000 W=XZ+C
2010 OPEN "4:4:CMD4:" REM * C-64 COMMAND TO OPEN CHANNEL TO COMMODORE PRINTER *
2020 REM * TO SUIT YOUR PRINTER PLEASE ALTER THE FOLLOWING: *
2030 REM * LINES 2010, 2050, 2100 AND 2110 *
2040 GOTO 1330
2050 PRINT#4: CLOSE4

```

```

2060 PRINT CHR$(147)
2070 PRINT "END OF HARD COPY LISTING"
2080 GOTO 1770
2090 REM
2100 PRINT#4: P$=CHR$(16);CHR$(49);CHR$(48);R1$;
CHR$(16);CHR$(49);CHR$(56);T1$;
2110 PRINT#4: CHR$(16);CHR$(50);CHR$(54);R2$;CHR$(
16);CHR$(51);CHR$(52);T2$
2120 GOTO 1480

```



Erratum:

There was an error in equation (13) as printed in Part I. It should have read:

$$[Tg] = \begin{vmatrix} \cos y & jZ_1 \sin y \\ \frac{j \sin y}{Z_1} & \cos y \end{vmatrix}$$

rf calendar

March 11-15 Electromagnetic Interference and Control A Five-day Short Course

Washington, DC

Information: Shirley Forlenzo, George
Washington University; Tel: (202) 676-
8530 or toll-free (800) 424-9773.

March 18-20 Dielectric Resonators A Three-day Short Course

University of Mississippi, Oxford
Campus
Oxford, MS

Information: Dr. Darko Kajfez, Depart-
ment of Electrical Engineering, Univer-
sity, MS 38677; Tel: (601) 232-7231.

March 19-22 Componentes Electronicos '85

Guadalajara, Mexico

Information: Ms. Raquel Polo, Deputy
Project Manager, United States Trade
Center, P.O. Box 3087,
Laredo, TX 78044; Tel: (905) 591-0155.

MODULAR INSERT INFO/CARD #64 ►

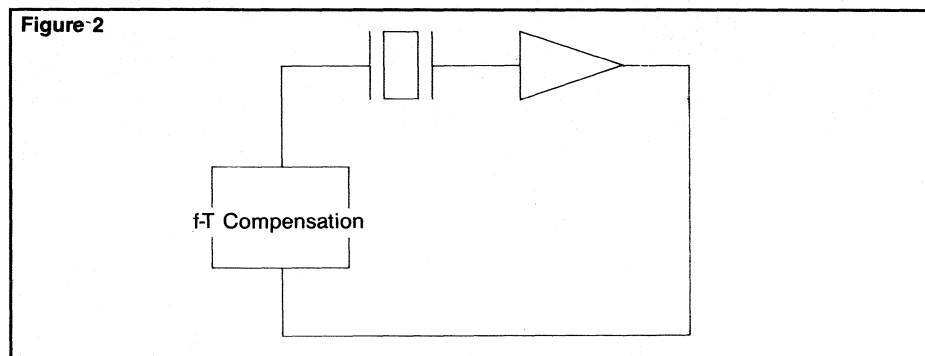
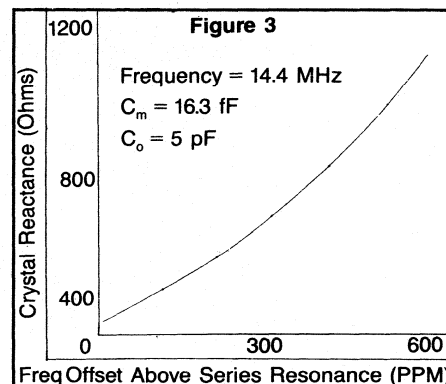
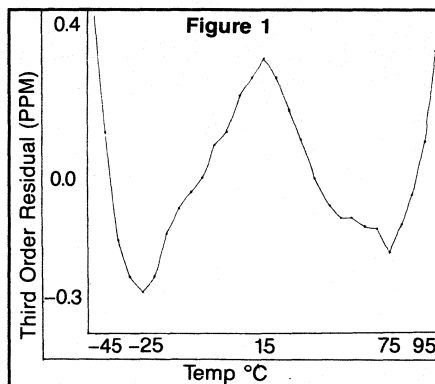
Frequency-Temperature Performance Determination In High Stability TCXOs

By Dennis Marvin
Motorola, Inc.
Communications Systems Division

The temperature compensated crystal oscillator (TCXO) has been with us for over thirty years and is quite often taken for granted. However, as frequency vs. temperature (f-T) stability requirements continue to tighten, many of the previously ignored second order effects will have a significant impact. TCXO stability requirements of 0.5PPM or 2PPM over temperature ranges as wide as -55 to $+95^{\circ}\text{C}$ are becoming commonplace. This article will review several of these second order effects and attempt to quantify the amount of performance debasement that can result.

AT-cut crystals are commonly assumed to have an f-T characteristic that can be represented by a third order polynomial. While this fit is quite adequate for most current applications, it can be inadequate for tight f-T requirements over wide temperature ranges. Figure 1 shows the difference between actual data and the least squares third order curve fit for a typical fundamental crystal. There is a decided, consistent fourth order component. Oscillators with f-T stabilities approaching 1PPM must incorporate a compensation scheme capable of correcting for the fourth order term and crystal evaluation algorithms must do a fourth order fit to insure that good crystals are not discarded.

Tight tolerance TCXO designs are further complicated by component TC and non-linear transfer characteristics. Even though the frequency stability of an AT-cut crystal is almost always less than 1PPM/ $^{\circ}\text{C}$, work at Motorola and by Holbeche and Morley(1) has determined that the motional capacitance, C_m , of a

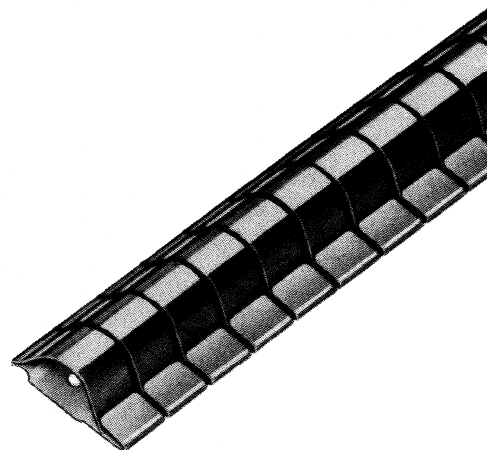


fundamental crystal varies approximately 230PPM/ $^{\circ}\text{C}$. This variability must be addressed during the oscillator design. The varactor and its operating voltage must be carefully selected. If a varactor with a non-linear V-X characteristic is used, the compensation network will have to generate a more complex V-T function to compensate for the distorted varactor transfer function. Similarly, if a nonlinear varactor is used for both temperature compensation and aging adjust, the amount of compensation will change as the aging is corrected.

Background

A fundamental AT-cut (3-20 MHz) TCXO can be simply represented by the block diagram of Figure 2, where the feedback scheme is incorporated into the amplifier block. This block can represent any of the common configurations: Colpitts, Pierce or Clapp. The oscillator operates by meeting Barkhausen's criterion; the sum of the reactances around the loop must equal zero, with the crystal operating at whatever frequency meets this requirement. Figure 3 shows that the crystal reactance is a function of fre-

I nis narrow strip...



quency by following the nonlinear relationship:

$$X = 1/((C_m/2\Delta f/f - C_o)w)$$

Where: C_m is the motional capacitance of the crystal model;
 C_o is the capacitance of the crystal plate, the holder and any associated stray circuit capacitance;
 $\Delta f/f$ is the fractional frequency change of the crystal from series resonance.

Such a circuit can be temperature compensated by having a compensation block that generates a reactance characteristic as a function of temperature such that it causes the crystal to change the operating point on its reactance curve. By carefully designing this block the crystal can be operated so as to cause a net "zero" frequency change over temperature.

There are several networks that are used for the compensation block, both direct and indirect. The preferred circuits are indirect, i.e., a DC voltage is generated external to the oscillator loop and is used to vary the loop reactance via a varactor. Direct compensation, where the compensation is inserted directly in the oscillator loop, has fallen on disfavor, as its use lowers circuit Q. Of the several methods of indirect compensation used, including custom integrated circuits and digital compensa-

tion, the most common and the most easily understood is thermistor-resistor compensation. One embodiment of this is shown in Figure 4(2). Other designs can be similarly analyzed.

If we assume that the varactor has a $\partial = 1$ (not bad for hyperabrupt varactors over a limited voltage range) and that all other parts in the oscillator are constant over temperature ms. characteristic of the crystal. This is a good approximation for initial analysis purposes, with corrections necessary for an exact compensation.

In any case, this thermistor-resistor network has the following transfer function:

$$V_{out} = V_{in} \frac{RT_3(R_1 + RT_1)(R_2 + RT_2)}{(R_1 + RT_1)(R_2 + RT_2)(R_3 + RT_3) + R_2 RT_2(R_1 + RT_1 + R_3 + RT_3)}$$

where RT_1 , RT_2 and RT_3 are the resistances of the three thermistors at a particular temperature.

R_1 and RT_1 affect performance over the entire temperature range, while R_2 and RT_2 primarily affect the cold end and R_3 and RT_3 primarily affect the hot end. Care must be taken to obtain suitable parts values so the appropriate transfer function can be obtained while still maintaining a high degree of independence among the temperature ranges. The use of a personal computer to gather f-T data and process it reduces the need for in-

dependence among the compensation sections.

Parts Aging

When oscillators are being temperature compensated one is normally concerned with passing the specification at a half-dozen or so temperatures with a little margin for measurement error. This is quite adequate for oscillator stabilities of 5PPM or looser, but if a tighter system stability is required parts aging can become very important.

Parts aging can have two effects on the oscillator stability. The first is a positive or negative frequency shift over the entire temperature range, i.e., the oscillator will have the same f-T characteristic after aging has occurred as it did before, but the whole response has a new room tem-

TYPE	AGING
Resistors	
Carbon Comp	>10%
Carbon Film	3 to 5%
Thick Film	1 to 5%
Metal Film	1.5 to 2%
High Precision Metal	
Film Thermistors	0.1 to 0.5%
Non-hermetically sealed	1 to 5%

TABLE 1

perature reference frequency. A more insidious result of parts aging is the distortion done to the f-T response.

Over the life of a product, the resistors and thermistors can age as shown in Table 1.

The effects of parts aging on frequency drift and the f-T characteristic can be determined by inserting a small resistor or thermistor change (e.g., 1%) into the transfer function and analyzing the results. Parts changes of + and - 1% for all of the resistors and thermistors in Figure 4 were inserted and the resulting errors maximized by proper selection of sign. The maximum offset was 36mV or 0.61PPM given a sensitivity of 17PPM/V. Figure 5 is a plot of the maximum f-T distortion. Changes in f-T performance as poor as 0.80PPM/% change are possible. Allowing the 1% aging to occur in a random direction among the resistors and thermistors, there is on average a 0.27PPM/% offset and a 0.41PPM/% f-T distortion to the T.C. curve.

Of these figures the f-T distortion is by far the more serious problem, since a means of frequency adjust can usually be provided to compensate for the frequency drift. With these results now available, the

appropriate resistors and thermistors can be specified and the initial f-T specification appropriately tightened so that system stability can be maintained to allow for compensation aging.

Frequency Adjust Aging

Compensation aging isn't the whole story, unfortunately. The major source of frequency drift is almost always the crystal. This drift is normally corrected by adjusting a capacitor or inductor in the oscillator loop to shift the operating point in the crystal curve and thus return the oscillator to nominal frequency. This shift in operating point also distorts the f-T characteristic and is known as trim effect. Galla and McVey(3) have developed equations to quantify this distortion for both series and parallel adjust circuits (see Figure 6). The values shown are typical for a fundamental frequency equivalent circuit. These equations are:

f-T distortion (PPM)

$$\frac{\text{SERIES}}{4apC_o(C_o+C_1)X10^{-3}} \\ C_1C_m$$

$$\frac{\text{PARALLEL}}{4ap(C_o+C_1)X10^{-3}}$$

C_m

where a is the amount of aging to be corrected (PPM)

p is the amount of temperature compensation (PPM)

C_o is the crystal and holder capacitance (pF)

C_1 is the load capacitance seen by the crystal (pF)

C_m is the motional capacitance of the crystal (fF).

As the distortion in the series adjust configuration is equal to that of the parallel adjust multiplied by C_o/C_1 , and this term is significantly less than 1, the series performance far surpasses that of the parallel. The parallel adjust should never be used in a high stability design if the use of a series is possible. Even if a series adjust is used, an additional 0.17PPM distortion will be generated. Figure 7 shows the f-T characteristic for a series adjust oscillator and its trim effect.

There are several ways that this problem could be alleviated. If C_m were increased, the distortion would decrease. However, all things being equal, C_o would increase in proportion to C_m . Additionally, the larger C_m becomes, the more the variations in the oscillator components affect performance.

The easiest way to reduce this distortion is to reduce p, the amount of temperature compensation, by carefully selecting the crystal angle. It can be further reduced by not overspecifying the temperature range. The smaller the temperature range, the smaller p will be.

Reducing a, the amount of aging to be corrected, is also possible. This can be done by using a better aging design, preaging the crystals or by sorting them for aging. Remember that a reasonably well made crystal will age approximately as much in the first year as it will age in the next ten years combined.

Voltage Regulator Contributing

In addition to the compensation circuitry and the crystal aging, one must also consider the voltage regulator circuit driving the compensation. The regulator is very important, as any voltage variations in it are directly coupled to the varactor and will create drift and distortion problems.

Using the compensation network of Figure 4 and allowing the regulator to vary +1mV/° (a fairly typical value for a fixed commercial regulator) results in an f-T distortion of about 0.4PPM, as shown in

...or this narrower strip...

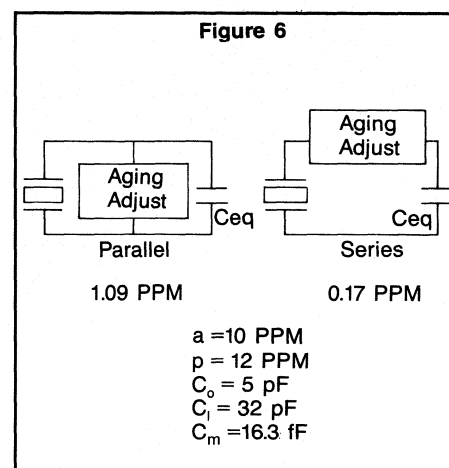
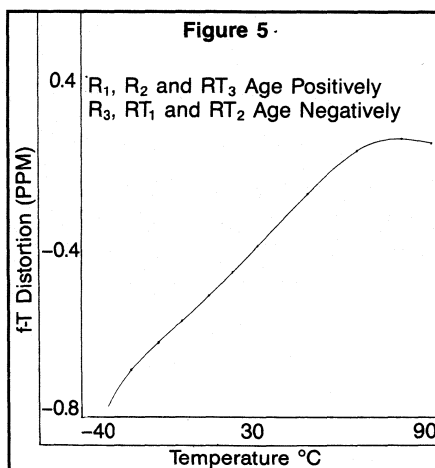
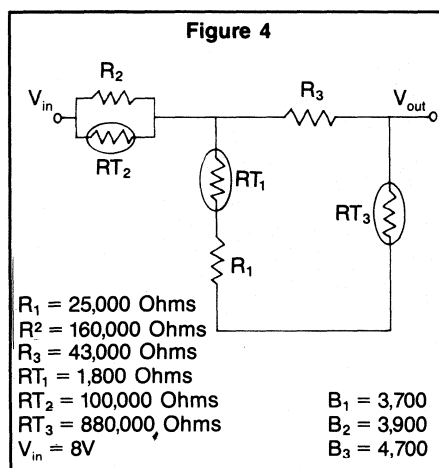
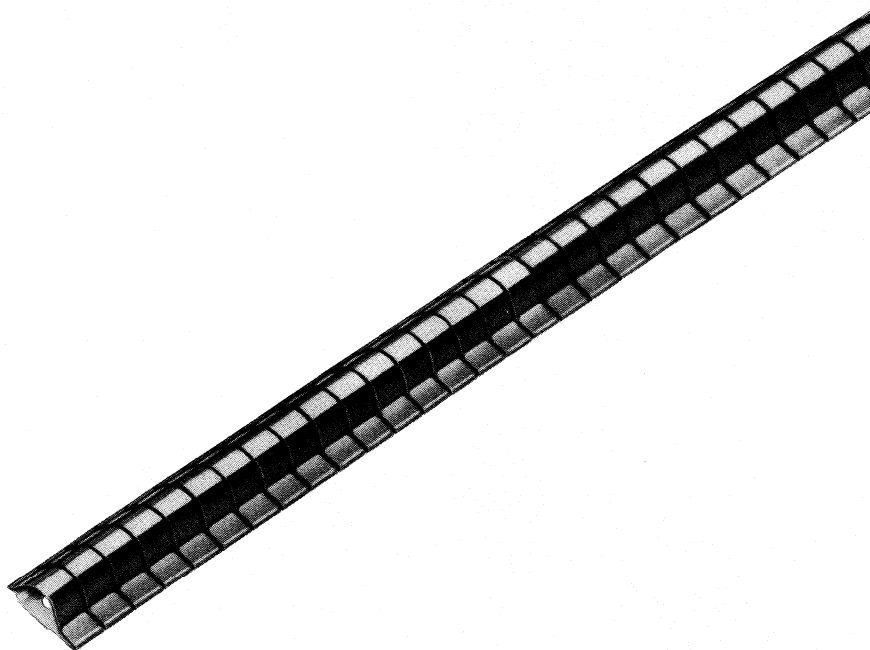


Figure 8. The only way to alleviate the problem of regulator voltage variation with temperature is to temperature compensate the oscillator with an internal regulator so that the temperature variations are compensated out.

Even with a built-in regulator, there is still the potential for aging. Figure 9 shows the distortion for a +1% change in regulator voltage.

Hysteresis

Crystal oscillator frequency performance can be very dependent on environmental dynamics. The designer must consider what dynamic frequency

stability is required and what maximum rate of change of temperature the oscillator will see. The temperature of the oscillator does not normally change nearly as fast as the ambient, as it is generally well isolated inside the system.

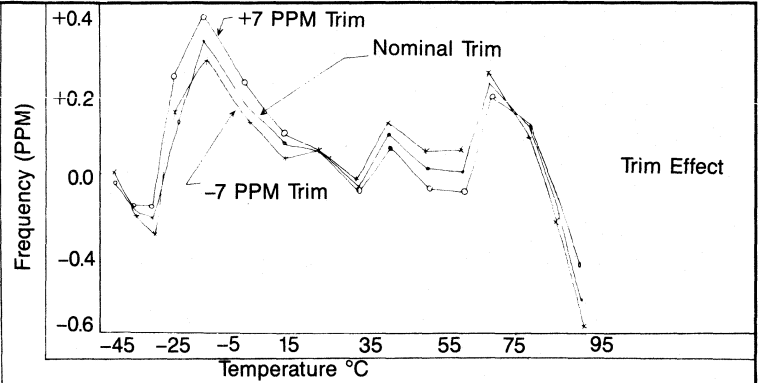
There are two major contributors to the hysteresis problem. The most easily visualized is the imbalance in thermal time constants among the several thermistors and the crystal. Time constants for thermistors in still air range from less than 0.1 sec. for small chips to over 10 sec. for 0.1 inch diameter beads, while typical HC-18 crystals have time constants of from 1 to 2 minutes. There is a

lot of variability in the crystal time constant. Important parameters causing this variability include package, lead and mount material and size, crystal blank size, crystal mounting technique and the type and density of gas sealed in the package.

There are so many variables present that the best way to determine the magnitude of the frequency shift is to measure it for the particular application. Tests performed on a hand-held 2-way radio subjected to a -30 to $+90^\circ$ temperature shock have given shifts as large as 0.3PPM.

If a product will be subjected to severe

Figure 7



swings, this effect can be reduced by better matching time constants through thermally coupling the compensation temperature sensors to the crystal or by increasing the shorter time constant.

The second hysteresis problem lies within the crystal. If an AT-cut crystal undergoes a temperature change, stresses will be set up within it. As the temperature of the crystal is swept back and forth an f-T characteristic is generated that traces a loop about the familiar static characteristic. The direction and magnitude of this offset is dependent upon the particular crystal design, the

temperature range and the speed with which the temperature is changed.

Ballato(4) has modified this effect by changing the familiar crystal model from

$$f/f_0 = a_0 \Delta T + b_0 \Delta T^2 + c_0 \Delta T^3$$

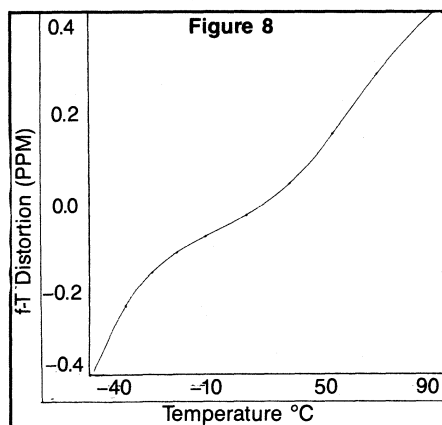
to

$$f(t)/f_0 = a(t) \Delta T(t) + b_0 \Delta T^2(t) + c_0 \Delta T^3(t)$$

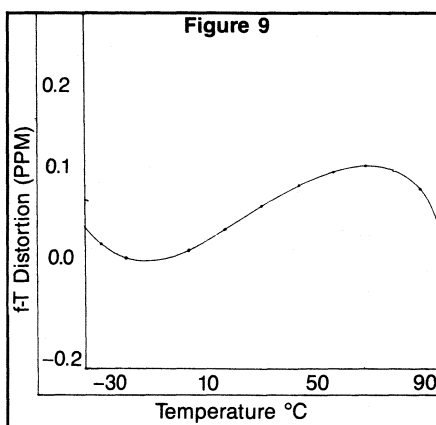
where $a(t) = a_0 + \hat{a}'T(t)$ with \hat{a}' being evaluated separately for each crystal design.

For a particular design where the

...or these even narrower strips...




temperature is varied in a sinusoidal manner + and - 60° about 30° at a frequency of 0.01Hz (an orbital time of 628 sec.) the peak deviation from the static curve was 7.2PPM. As the deviation is linearly related to the frequency of the temperature change for this model, the maximum orbital time to keep the peak deviation below 0.1PPM for this crystal is 12.6 hours. Hence, fast temperature changed can and do affect the desired stability. It should be stressed that the magnitude and direction of this deviation is quite crystal dependent, with this example tending to be worst case, and that this is the peak error over the entire temperature loop.



Conclusion

High stability TCXOs are subject to many instabilities not normally considered in the design of lower stability products. Several of these have been reviewed. The design engineer must carefully consider the system requirements in dynamic environments and as a function of time.

For example, the design Motorola has chosen to use is shown in Figure 10. The as shipped f-T stability requirement is as tight as 1PPM from -40 to +95° with a total system stability of better than 2PPM. In order to accomplish these specification and still maintain a small package size (< 0.3 cu.in.) while minimizing costs, a

custom integrated circuit in a hermetic chip carrier was used (5). The chip consists of a three segment non-linear compensation ms, but has improved isolation between the stages for ease of production. Compensation is achieved with four trimmable resistors. Hermetic sealing of the IC minimizes regulator drift. Parts drift s minimized by utilizing the matched TC characteristics in the IC design while good crystal aging is maintained by pre-aging and then sorting crystals with a curve fit routine using data obtained by actively aging the crystals. Hysteresis is also minimized through crystal sorting and with attention to thermal design. Overall hysteresis and aging are further controlled by hermetically sealing the entire oscillator. 

References

1. Holbeche, R.J. and Morley, P.E., "Investigation into Temperature Variation of Equivalent-circuit Parameters of AT-cut Quartz Crystal Resonators," IEEE Proc., vol 128, pt. A, no.7, October 1981, pp.507-510.
2. Frerking, M.E., *Crystal Oscillator Design and Temperature Compensation*, Van Nostrand Reinhold Co., 1976.
3. Galla, W.D. and McVey, E.S., "TCXO Error Due to Aging Adjustment," PROCEEDINGS OF THE 34th ANNUAL SYMPOSIUM ON FREQUENCY CONTROL, pp.504-508.
4. Ballato, A., "Static and Dynamic Behavior of Quartz Resonators," IEEE TRANSACTIONS ON SONICS AND ULTRASONICS, vol. SU-26, No. 4, July 1979, pp.299-306.
5. Keller, T., Marvin, D. and Steele, R., "Integrated Circuit Compensation of AT Cut Crystal Oscillators," PROCEEDINGS OF THE 34th ANNUAL SYMPOSIUM ON FREQUENCY CONTROL, pp. 498-503.

Digital Signal Processing

By Thomas Callaghan
Watkins-Johnson Company

Digital signal processing is not an easy topic to comprehend. It combines theories of both the analog and the digital disciplines. To ease this understanding, one should remember that all aspects of DSP can be divided into three areas:

- 1) Input Signal
- 2) Digital Processor
- 3) Information Extraction

The input signal must be sampled and quantized before it can be fed to the digital processor. The digital processor can only perform the operations of addition, multiplication and delay (storage) on the signal data. The end result of the digital processor is to extract information from the signal or modify it in some way. This article will explain the input signal.

The input signal, which is analog in nature, can be classified as a continuous time, continuous amplitude signal. To be of a form useful to a digital processor the signal must be converted to a discrete time, discrete amplitude signal.

Sampling

Sampling is the process by which the continuous time, continuous amplitude signal is converted to a discrete time, continuous amplitude signal. This is done by periodically taking minute time chunks out of the analog signal. The output of a sampler is a series of pulses whose envelope approximates the original signal. The process can be represented by multiplying the input signal by a pulse train of uniform amplitude and equal spacing, (Figure 1).

The pulse spacing, T , that is the sampling frequency, $1/T$, cannot be arbitrarily chosen. According to the Sampling Theorem, "If a continuous time function contains only frequency components below F cycles per second, $2F$ samples per second suffice to represent it perfectly and permit perfect recovery." The reason for this is more readily seen in the frequency domain. Referring to Figure 2, one can see that one of the byproducts of sampling is the duplication of the signal every F_s , the sample frequency. If the sample frequency is kept above or equal to $2F$, (Figure 2b), the sampled frequen-

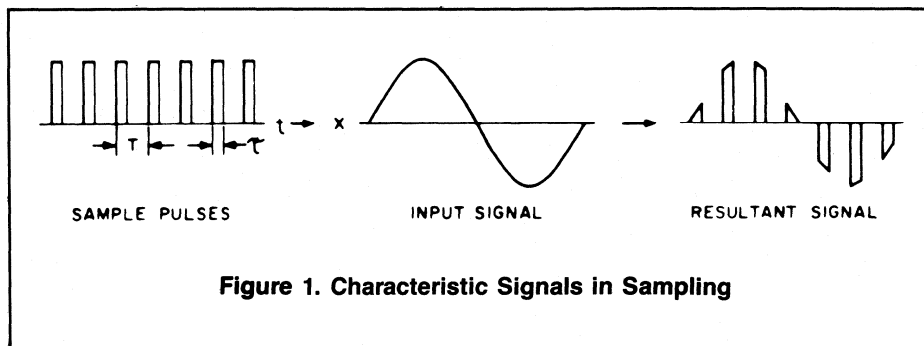


Figure 1. Characteristic Signals in Sampling

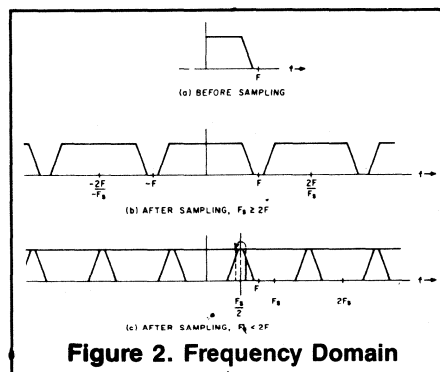


Figure 2. Frequency Domain

cy spectrum produces no overlap and the original signal can be retrieved. If the sample frequency drops below $2F$, the sample frequency spectrum starts to overlap. Any of the frequencies whose spectra are contained in this overlap tend to fold over about $F_s/2$ and into the actual frequency band, as indicated in Figure 2C. This foldover of frequency is called aliasing.

Examples of frequency aliasing are witnessed daily by many unknowing observers. For example, in the old "Westerns," the stage coach rides out of town and its wheels appear to speed up, stop and then go backwards. The backwards revolution is caused by the movie camera not taking sufficient frames per second to dependably capture the wheel's revolution. Another example is when a television or computer terminal is shown in a movie with black bars across the screen. Again, the movie camera is not updating the screen fast enough. In this case, the camera moves at 24 frames per second while the television scans a new frame at

60 times per second.

The sampling theory is all well and good on paper, but in reality it is difficult to remove all unwanted frequencies above the frequency of interest. The most common solution is to place a filter ahead of the sampler to remove unwanted frequencies. The filter, however, has two disadvantages; it alters the signal of interest and unless it has very steep skirts certain unwanted frequencies are passed. A second solution is to sample at a faster rate than $2F$. How much faster is open to debate. Sample too fast and one puts an undue burden on the digital processor.

Another consideration in determining sampling frequency is interpolation errors. Since one is dealing in discrete time, what has happened to the input signal between samples is not known. Naturally, the faster the sample rate the more information known about the signal. When processing is finished, it may be desired to convert back to an analog signal. The conversion is usually done with a D/A converter and some type of low-pass filter to smooth, or interpolate, the discrete points.

So how does one select the sample rate? Gardenhire in [1] presents a good approach to the problem. In his work, the sampling rate is based upon the amount of interpolation error tolerable from the output filter given a specified input filter roll-off characteristic. The input filter roll-off determines the order of the system. Given a certain roll-off, m , the sample rate can be determined from the acceptable interpolation error. The rate is given for a 5% error in Table 1.

...can solve your interference control problems!

Are you involved with FCC Class A and/or Class B Computing Devices—or any other equipment requiring shielding? Instrument Specialties' new, patented* beryllium copper Sticky-Fingers® shielding strips can help you solve your problems!

They offer the attenuation you need, of course. And to attach, you need only peel off the self-adhesive backing strip and press into place. It's there to stay!

What's more, unlike other shielding strips, Sticky-Fingers will not take a set which would reduce performance *after you felt it was satisfactory*. Sticky-Fingers *can't* absorb moisture, are not affected by air, ozone solvents, UV light, or radiation. They *can't* burn, support combustion, outgas; they *can't* stretch or tear, flake or break into small conductive particles to short out electronics.

For more information, write today to Dept. RF-7.

INSTRUMENT SPECIALTIES COMPANY, INC.

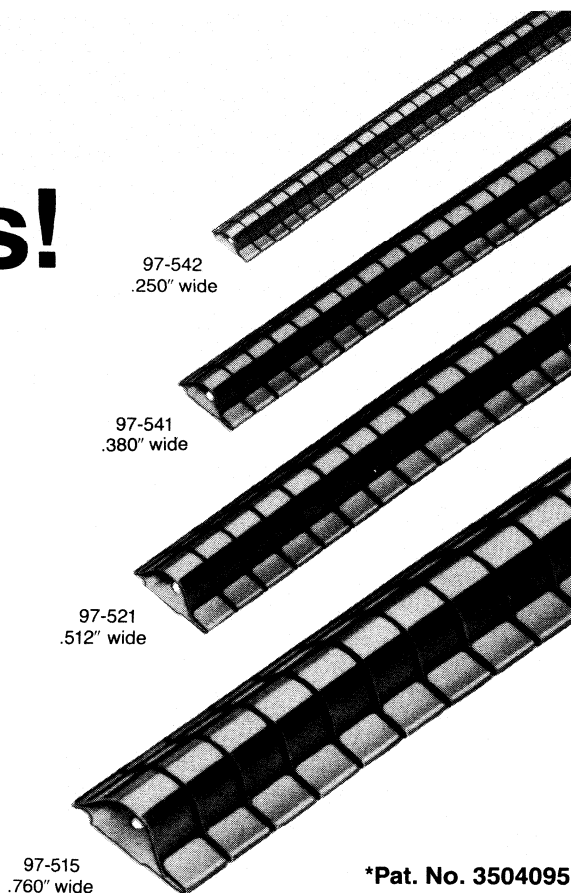
Delaware Water Gap, PA. 18327

Phone: 717-424-8510 • TWX: 510-671-4526

Specialists in beryllium copper since 1938



INFO/CARD 34



*Pat. No. 3504095

The filter method employs analog interpolation after D/A conversion. The 2, 3, or 4 point linear interpolation method is done via a computer and the output is still in a digital format. It is interesting to note how the sample rate approaches the theoretical rate of 2F as the order of the filter increases. It is also worth noting how the sample rate increases drastically as one tries to follow the input signal more closely with a minimum of error.

For communications applications, however, one is dealing primarily with input filters whose order does approach infinity. The output filters are also optimized, or of Butterworth types. For these reasons a sample rate in the range of 2 to 5 times F should prove satisfactory.

Another error that appears during sampling is known as aperture error. This error is caused by the sample pulses taking a small amount of time to capture the analog signal. During this time, the input voltage can change drastically as the signal goes through zero. This is indicated in Figure 1 by the triangular shapes of some of the sampled data pulses. The aperture error can be expressed mathematically [2] for a sinusoidal input by:

$$\epsilon = \frac{\Delta V}{V_{FS}} = 2\pi\tau$$

Table 1. Systems Resulting in a 5% Interpolation Error [1]

Normalized sample frequency (F_s/f_1)

Interpolation Method	m = 1	m = 2	m = 3	m = 4	m = 5	m = 6
Wiener Optimum Filter	640	11	5.1	3.8	2.6	2.0
Butterworth n = 4	—	16	8.3	5.5	5.5	5.5
n = 3	—	18	9.2	6.7	6.7	6.7
n = 2	1.2×10^3	29	17.0	11	11	11
RC Filter n = 1	1.2×10^4	220	130	91	91	91
2 Point and Linear Interpolation	640	13	8.3	5.9	5.9	5.9
3 Point Linear Interp.	640	12	6.2	5.2	—	4.0
4 Point Linear Interp.	640	12	5.7	4.3	—	3.3

where V_{FS} is the full scale voltage and τ is the duration of the pulse.

Expressed another way, the acceptable pulse duration can be calculated as

$$\tau = (2\pi \times F \times 2^n)^{-1}$$

where n is the number of bits of resolution of the A/D converter for an A/D converter with a 1LSB error. For instance, if the input frequency is 10 kHz and eight bits or resolution are used, the allowable pulse duration = 63.5 ns.

To alleviate aperture error, a track and hold amplifier can be inserted before the

A/D converter. This device's output will follow the input signal while its track digital level is active. When the track input switches, the output is held at its current level and will not vary over the duration of the pulse.

Quantization

After the discrete time, continuous amplitude signal is obtained, it must then be converted to a discrete time, discrete amplitude signal for the digital processor. This process is formally called quantization, but it is more commonly known as analog to digital (A/D) conversion. A quantizer takes a specific amplitude

range and divides it into a series of discrete steps, Q . A digital number is then assigned to each Q .

The number of bits in the digital word determines the number of steps that can be achieved. For n bits, the number of steps would be 2^n . Each step Q , or each change of 1LSB, would be

$$Q = V_{FS}/2^n$$

where V_{FS} is the full scale magnitude of the allowable input voltage.

If the input signal falls between steps then the digital number assigned to it depends on whether the quantizer rounds the samples or truncates them.

As its name implies, the quantizer rounds off the analog input to the nearest quantizer level, Q . In truncation, (Figure 3), the signal is represented by the highest Q level that is not greater than the signal. Thus, for each LSB (least significant bit) step of the digital output word, the error from the original signal would be $\pm 1/2$ LSB for rounding and a 0 or $+1$ LSB for truncation. An error of $\pm 1/2$ LSB yields a mean error of zero, whereas a 1LSB error yields a mean error of $+1/2$ LSB. For

this reason, rounding is preferred in most practical considerations.

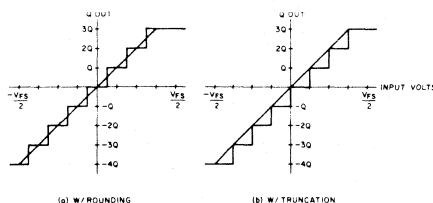



Figure 3. Quantizer Characteristics

How the digital word is represented is another area of consideration. Binary representation varies widely for positive and negative numbers. Again, for most practical considerations, two's complement representation is chosen because most processors use this type of representation. Also, for other applications only positive numbers are expected. Many A/D converters allow either; that is, a range of 0 to V_{FS} or $-V_{FS}/2$ to $+V_{FS}/2$, as well as other representations.

Finally, once the quantizer or A/D converter is chosen the number of bits of

resolution must be decided. While a large number of bits will represent an analog signal more accurately, they will not represent a cleaner analog signal. In every analog signal, there exists some inherent noise that is some small portion of that signal. The more bits of resolution, the smaller the step size in the quantizer. The smaller the step, the more the digital word is affected by noise, so that the lower significant bits only serve to give a good representation of this noise. 

References

1. L.W. Gardenhire, *Selecting Sampling Rates*, Instrumentation Society of America, April 1964.
2. Willard Bucklen, Dr. John Eldon, Louis Schirm, and Fred Williams, "Designers Guide to DSP," *EDN*, Magazine.
- Part 1, "Understanding the Fundamentals Eases Signal Processing Task," March 18, 1981.
- Part 2, "Single Chip Digital Multipliers Form Basic DSP Building Blocks," April 1, 1981.
- Part 3, "Digital Processing Facilitates Signal Analysis," April 15, 1981.
- Part 4, "DAC's and Multifunction Chips Enhance Your DSP Options," April 29, 1981.
- Part 5, "Digital Correlators Illustrate DSP Trends," May 13, 1981.
3. L.R. Rabiner and B. Gold, *Theory and Application of Digital Signal Processing*, Prentice Hall, 1975.
4. A.V. Oppenheim and R. Shafer, *Digital Signal Processing*, Prentice Hall, 1975.

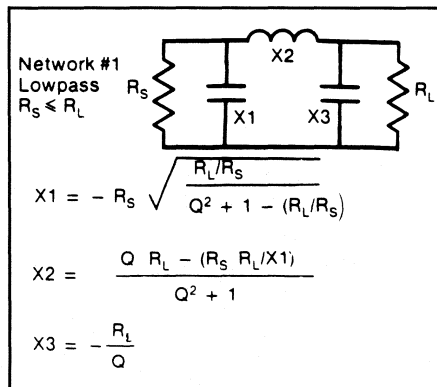
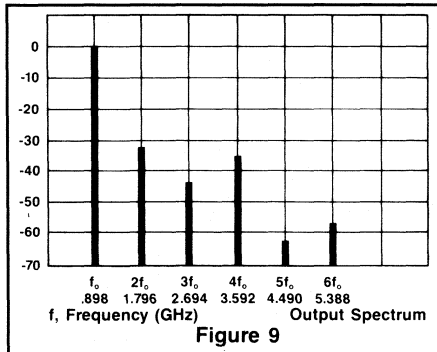
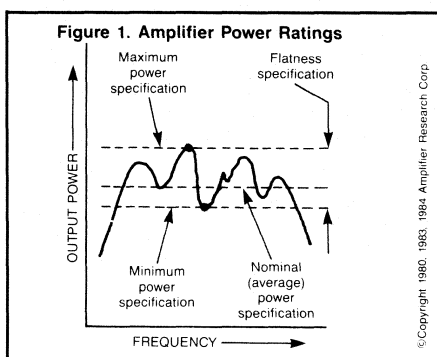


Cover

This month's cover features Microwave Modules and Devices' new 500-watt wideband power amplifier, the AC-0003-500W. This modular HF Class AB linear amplifier features wideband, high power 90 degree quadrature combiners on the input and output impedance and 1.5:1 input and output VSWR. It is a "drop-in" 50-ohm building block suitable for multi-kilowatt transmitters.

Features

- 21 Special Report: Broadband, High Power RF Amplifiers**
This month's Special Report covers the increasing use of HF communications. Because of the vulnerability of satellites, military and civilian communications experts are taking another look at the advantages of HF. New developments, such as better amplifier design, have improved HF communication capability. — James N. MacDonald.
- 28 A 14 Watt, 900-950 MHz, Low Cost Amplifier Design**
This article describes the design, construction and performance of a two stage amplifier using two inexpensive Motorola parts. The MRF839, a 3 watt device, drives the MRF843, a 15 watt, 870 MHz transistor. — David R. Miller
- 44 BASIC Program Computes Values for 14 Matching Networks**
For our readers who prefer computers to calculators for programming, this article provides a BASIC program that performs the same calculations as those described in the November/December 1983 issue for the TI-59 by Alex Burwasser. — Alan J. LaPenn
- 48 Determining Receiver Performance with a Computer Spreadsheet**
Computer spreadsheets, such as VisiCalc and SuperCalc, can be useful for design work involving tedious, repetitious calculations. The author shows how a spreadsheet can be used for calculating receiver performance. An example of a completed analysis is included. — Gregory R. Quinn



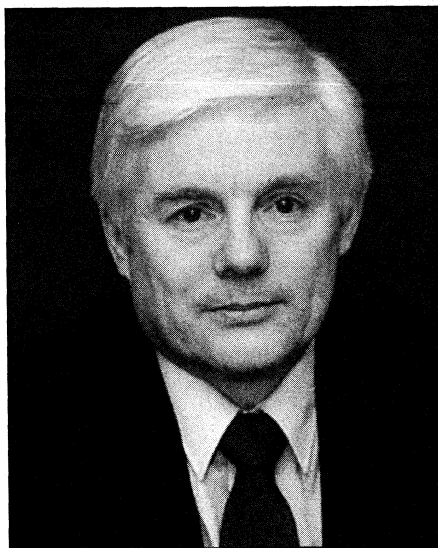
Departments

- 6 Editorial
- 8 Publisher's Notes
- 12 Letters
- 14 Calendar
- 16 News
- 37 Info/Card
- 52 The Digital Connection
- 54 RFI/EMI Corner
- 58 Product of the Month
- 59 New Products
- 69 New Literature
- 74 Advertisers Index

R.F. DESIGN (ISSN: 0163-321X USPS: 453-490) is published monthly plus one extra issue in June. April 1985, Volume 8, No. 4. Copyright 1985 by Cardiff Publishing Company, a subsidiary of Argus Press Holdings, Inc., 6530 S. Yosemite Street, Englewood, CO 80111 (303) 694-1522. Contents may not be reproduced in any form without written permission. Second-Class Postage paid at Englewood, CO and at additional mailing offices. Subscription office: 1 East First Street, Duluth, MN 55802, (1-800-346-0085). Subscriptions are sent free to qualified individuals responsible for the design and development of communications equipment. Other subscriptions are: \$15 per year in the United States; \$25 per year in Canada and Mexico; \$25 per year for foreign countries. Additional cost for first class mailing. Payment must be made in U.S. funds and accompany request. If available, single copies and back issues are \$5.00 each (in the U.S.). This publication is available on microfilm/fiche from University Microfilms International, 300 N. Zeeb Road, Ann Arbor, MI 48106 USA (313) 761-4700.

POSTMASTER & SUBSCRIBERS: Please send address changes to: R.F. Design, P.O. Box 6317, Duluth, MN 55806.

About That \$600 Toilet Seat . . .



Every once in a while a story breaks in the press about some common item purchased by the military at exorbitant cost. The best stories are about items that could be purchased at a fraction of the cost at the local hardware store. Columnists scream and congressmen investigate until some new scandal forces the old one out of the newspapers. The story fades, leaving readers with a memory of military purchasing officers approving bills from conniving businessmen and probably receiving a kickback. Unfortunately, the truth is far less exciting.

Many *RF Design* readers produce and sell components and equipment to the military. To them it is no surprise that a coffee pot for a military aircraft can cost \$400 or a toilet seat can cost \$600. They know about the incredibly expensive and time-consuming process of meeting military contract requirements.

Let us look at how the process works.

Suppose an engineer develops a superior op amp and sets up a company to manufacture it. After testing the op amp a contractor decides to include it in a computer it is building for a Navy aircraft. The engineer thinks his future is secure with a government contract. Then he learns about the Specification Control Drawing (SCD) and the volumes of related paperwork the Navy requires on every phase of the manufacture and testing of that op amp.

The SCD describes in painstaking detail every step of the manufacturing process, every test that must be performed and even the materials that must be used to make that op amp. It does not matter that this component is already being manufactured and has been on the market for some time, or that it was chosen in the first place because it was so good. The engineer now must hire people to study the paperwork and respond to the requests for documentation, in addition to those building the op amps.

Next come the government inspectors to look at his operation and discuss the steps he needs to take to conform to military specifications. Whenever they come, he must postpone his other activities and spend the time with them. This calls for more staff to carry on the regular business while he negotiates with the inspectors.

The process of establishing procedures to meet military specifications and documenting his progress with paper might take a year or longer. During this time he receives no money and is probably borrowing to keep his business going. Eventually, he will have to pay that interest.

Finally, he is approved. Now he can begin to make op amps for the Navy contractor, but every unit must be tested according to specifications and test records kept. If the Navy aircraft falls out of the sky 10 years from now, the government can demand to see the test record for the particular op amp in the computer in that plane.

If the order is a small one, as it often is, the engineer must charge many times the normal cost of that op amp. He has incurred enormous expense to manufacture the military units, and it is a fact of life that businessmen who do not recover their costs do not stay in business.

Most *RF Design* readers are not shocked by high prices for common items sold to the military. They have seen the military procurement process in action.

James H. MacDonald

A 14 Watt, 900-950 MHz Low Cost Amplifier Design

By David Miller
RF Land Mobile, Motorola Inc.

Two high performance 800 MHz parts (MRF839, MRF843) are used to produce a 14 watt, 900-950 MHz amplifier. The MRF839 is an inexpensive, 3 watt device that serves as an excellent driver for the MRF843. Its double emitter bonding, fine line (2 micron) die geometry and isolated collector construction make it superior to other similar devices. The MRF843 is a new 800 MHz 15 watt transistor. Like the MRF839, it is inexpensive, yet possesses excellent performance. Strong points of the MRF843 include good gain, high efficiency and internal input matching for broadband capabilities. This article de-

scribes the design, construction and performance of a two stage amplifier constructed with these devices.

To be considered viable an amplifier must be capable of meeting certain design criteria, regardless of the application. First, the amplifier must possess good RF performance; i.e. good gain, high efficiency and stability. Next, it must be rugged under a variety of adverse operating conditions. Third, it should be easily constructed, tuned and reproduced. Finally, in today's world of "smaller

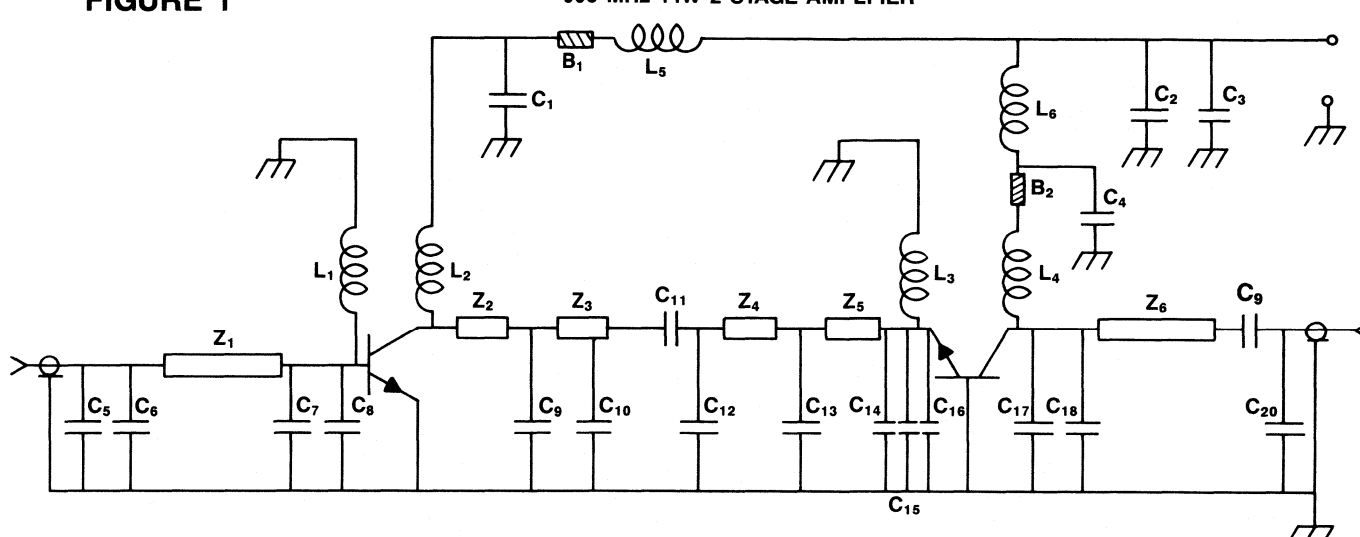
is better" it must be compact. This amplifier has been designed and developed based upon the above described design criteria (see Table 1).

Table 1
Design Criteria

Power Out	14 Watts (Typ.)
Gain	14.5 dB (Typ.)
Efficiency	≥45% 50% (Typ.)
Ruggedness 20:1 VSWR	$V_{cc} = 15.5$ Vds
	$P_{in} = 750$ mW
Stability 3:1	$V_{cc} = 6-15.5$ Vdc
	VSWR Freq. = 900-950 MHz
	$P_{in} = 300-750$ mW

FIGURE 1

900 MHz 14W 2 STAGE AMPLIFIER



C₅, C₂₀ 1.0 pF, ATC, Chip cap, 50 Mil
C₆, C₁₅ 2.2 pF ATC, Chip Cap, 50 Mil
C₁₂ 4.7 pF ATC, Chip cap, 50 Mil
C₁₀ 7.5 pF ATC, Chip cap, 50 Mil
C₁₃ 10.0 pF ATC, Chip cap, 50 Mil
C₇, C₉, C₁₆, C₁₈ 12.0 pF ATC, Chip cap, 50 Mil
C₈, C₁₄, C₁₈ 15.0 pF ATC, Chip cap, 50 Mil
C₁₇ 18.0 pF ATC, Chip cap, 50 Mil
C₁₁ 39.0 pF ATC, Chip cap, 50 Mil
C₁₉ 39 pF ATC, Chip cap, 50 Mil

C₁, C₄, 68 pF Miniunderwood mica
C₂ 2 x 470 pF ATC, Chip cap, 250 Mil
C₃ 10 μ F Tantalum Electrolytic
L₁ 4 Turns on 10 ohm 1/2W Resistor
L₅, L₆ 10 Turns on 10 ohm 1/2W Resistor
L₂, L₃, L₄ 4 Turns 0.20" I.D. 24 AWG
B₁, B₂ Bead, Ferroxcube 56-590-65/313
Z₁-Z₆ Refer to circuit photomask*
PCB 1/32" G-10 Er = 4.1

*Photomask copies available from Motorola Inc.

Circuit Design

Although two stages of amplification comprise a single amplifier, each stage is designed to stand alone. Such a design scheme allows the designer to independently tune and test each stage. This provides the necessary feedback to ascertain how well each stage is functioning. This ability is particularly important when one considers the number of variables introduced by the matching and biasing of the circuit.

The independent amplifier approach is accomplished by splitting the inter-stage matching network midway and establishing a 50 ohm intermediate impedance level. At the 50 ohm location the two stages are combined via a series coupling capacitor. Independent testing of the stages is accomplished simply by breaking the circuit in two at this point.

A more direct matching scheme might produce a simpler inter-stage match. The added flexibility of the independent amplifier approach is, however, of great advantage to the initial tuning and testing of the circuit. The circuit is shown schematically in Figure 1.

Considering the two stages as independent amplifiers allows one to identify the desirable attributes of each stage. The driver stage has primarily three responsibilities: to contribute to the overall gain, to present a minimal input VSWR and to level the frequency response of the second stage. The output stage has two major responsibilities. It must be matched to provide good gain across the operating band while maintaining a high collector efficiency.

The First Stage. The currents and voltages of the driver stage are relatively low, and parasitic losses, i.e. I^2R losses, are generally considered negligible. Performance in the low power driver stage thus becomes for the most part a function of correct impedance matching (impedance matching will be covered in a later section of this article).

The input VSWR of the amplifier is determined by how well the input impedance of the first stage device is matched. Enough internal transistor feedback exists in all RF power transistors that changes to the transistor's output operating conditions will have an effect on the input impedance of the device. Therefore, attention must be given to both the input and output impedance matching of the transistor when attempting to minimize the input VSWR.

To level the frequency response of the amplifier the first stage is used to compensate for the gain slope of the second

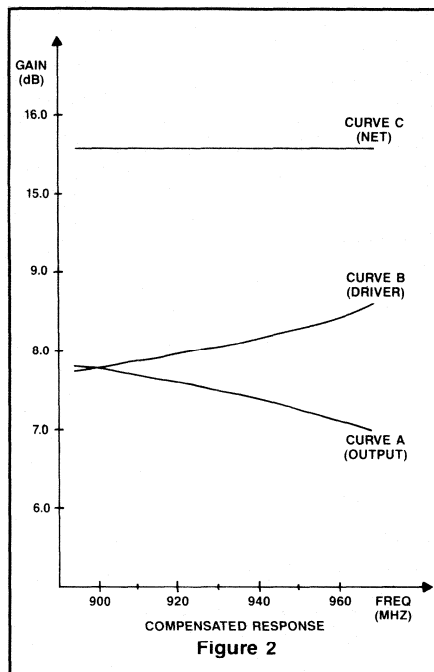


Figure 2

stage. This is accomplished as shown in Figure 2. In the figure, curve A shows the typical frequency response of the output stage. Curve B shows an intentionally mismatched (skewed) response for the driver stage. The net idealized gain slope of the amplifier is shown as curve C and is simply the composite sum of the two stages (curves A & B). The intentional skewing of the driver stage is realized by designing the output match to be optimum at 950 MHz instead of at the mid-band frequency. The device thus sees its maximum mismatch at the high gain 900 MHz band edge. The degree of required band edge mismatching can be determined empirically and depends entirely on the gain slope of the output stage. The greater the roll off, the greater the mismatch that will be required to level the amplifier.

The Second Stage. The second stage, although it does not necessarily provide the majority of the gain, does exhibit the highest current and power levels associated with the amplifier. For this reason the design must not only provide good impedance matching to achieve optimum power transfer, it must also insure low loss conduction paths to minimize parasitic losses. Minimizing the transmission line lengths is the most effective way to reduce losses associated with both the resistance of the conductor and the dielectric substrate.

The output stage of the amplifier is the major determiner of overall efficiency. Equation (1) shows the total collector effi-

ciency of the amplifier to be dependent upon the collector currents drawn by both stages, as well as V_{cc} and P_{out} .

$$\text{Eff total} = P_{out}/V_{cc} (I_c \text{ first} + I_c \text{ second})(1)$$

The second stage draws over 80% of the total supply current. For example, with both stages operating independently at about 60% efficiency the collector currents are 373 mA and 2.0 amp, respectively. Thus, with $V_{cc} = 13.8$ Vdc and $P_{out} = 14$ watts the net efficiency is about 50%.

To insure good collector efficiency (whether it be the driver stage or the output stage) it is not only important to have proper impedance matching and to minimize the transmission line losses; losses due to low Q chip capacitors must also be considered. Due to the physical construction of chip capacitors there is a parasitic series resistance and inductance. The inductance reduces the reactance of the capacitor, increasing the effective capacitance. The series resistance may be determined from the equation $R_s = X_s/Q_s$ and manifests itself as a power loss.

Impedance Matching. Low pass filter design techniques are employed throughout the circuit to achieve impedance matching. Chip capacitors and microstrip transmission lines are used to generate the matching sections. Selecting a suitable length transmission line creates the inductive reactance needed to generate the matching sections and eliminates the need for discrete inductors. This not only helps simplify the circuit design but also adds to the reproducibility of the circuit.

The first step in synthesizing a matching network is to determine the number and configuration of the matching sections necessary to achieve the desired response. Strictly speaking, the bandwidth of a ladder network is only limited by the number of sections used. It follows that the overall bandwidth of the amplifier, without feedback, is theoretically limited by the Q_s of the transistor devices. However, because of the lossy nature of the elements used to formulate each matching section, i.e. transmission lines and chip capacitors, the insertion losses limit the maximum number of usable sections. The design consideration at this juncture becomes one of optimizing the bandwidth of the amplifier while minimizing the losses of circuit. A graphical Smith chart design method is used to accomplish this optimization.

As an example of this method, the impedance matching design for the input of

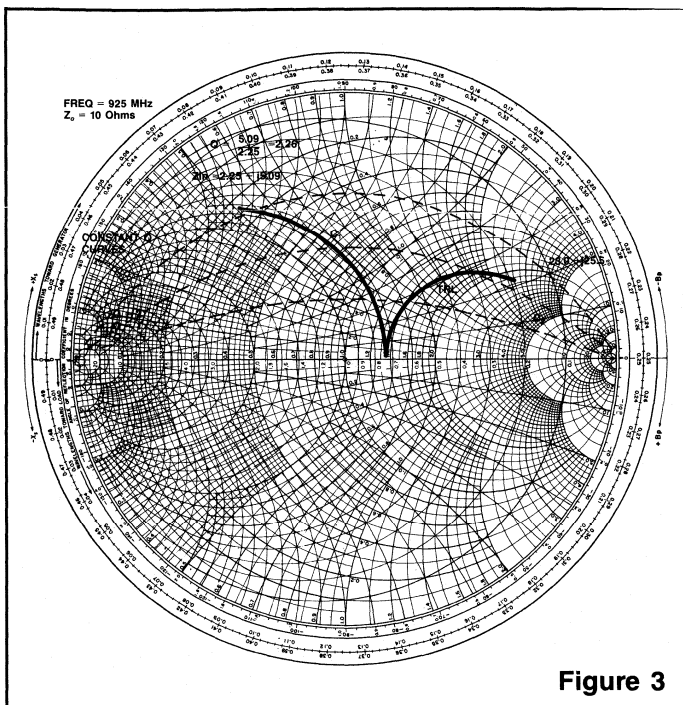


Figure 3

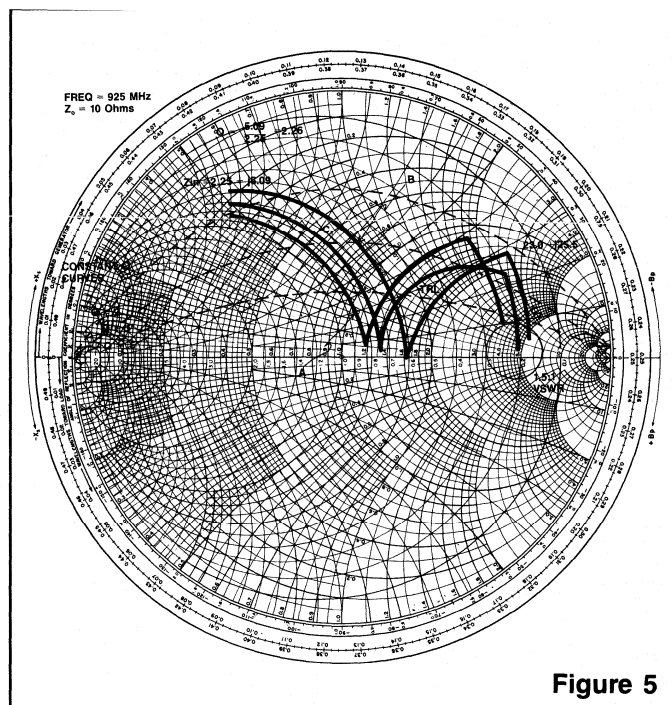


Figure 5

the MRF839 is shown in Figure 3. The midband (925 MHz) input impedance of the device is first plotted on the Smith chart, establishing a starting point (the manufacturer's impedance data for the MRF839 and MRF843 are reproduced in Table 2). The Q_s of the device is computed to be 2.26. To maintain a maximum bandwidth, no portion of the matching network should exceed this Q_s . Shunt capacitance is next used to rotate the impedance along a constant admittance circle to achieve a maximum impedance of 13 ohms. The value of this shunt capacitance (C_1) is computed in Figure 4a to be 28.39 pF. Care should be taken when selecting the actual capacitors to account for the parasitic inductance of the capacitors.¹

Table 2
Device Impedance Data

MFR 839		
Freq.	Z_{in}	Z_{ol}^*
806 MHz	$3.1 + j4.0$	$9.6 - j6.5$
870 MHz	$2.8 + j4.6$	$8.5 - j5.6$
960 MHz	$1.9 + j5.4$	$8.1 - j4.8$
$P_{out} = 3$ Watts		
$V_{cc} = 12.5$ Vdc		
$*Z_{ol}$ = Conjugate of Optimum Load Impedance.		
MRF 843		
Series Equivalent Input and Output Impedance		
Freq. MHz	Z_{in} Ohms	Z_{ol} Ohms
800	$1.23 + j6.14$	$1.98 + j2.62$
870	$2.09 + j5.91$	$2.24 + j3.49$
960	$2.58 + j5.46$	$2.51 + j3.92$

NOTE: Circuit tuning and input power adjusted to maintain output power of 15W and 65% efficiency.

a.) $b_{c1} = 1.65$ $X_{c1} = \frac{1}{b_{c1}} = .6061$ $W = 2\pi f_o = 5.8119 \times 10^9$ rad/sec
 $F_o = 925$ MHz
 $Z_o = 10$ Ohms

$X_{c1} = x \cdot Z = 6.061$ Ohm
 $X_{c1} = \frac{1}{WC_1}$ $C_1 = \frac{1}{WX_{c1}} = 28.39$ pF

b.) $b_{c2} = 0.215$ $X_{c2} = \frac{1}{b_{c2}} = 4.65$ $W = 2\pi f_o = 5.8119 \times 10^9$ rad/sec
 $F_o = 925$ MHz
 $Z_o = 10$ ohms

$X_{c2} = x \cdot Z = 45.5$ Ohm
 $X_{c2} = \frac{1}{WC_2}$ $C_2 = \frac{1}{WXC_2} = 3.69$ pF

c.) $Z_{in} = Z_o \left[\frac{Z_L + j Z_o \tan \theta}{Z_o + j Z_L \tan \theta} \right]$
 $Z_o = \sqrt{(Z_{in} R)1 - \frac{(X)^2}{R(Z_{in} - R1)}}$
 $\theta = \tan^{-1} \frac{(Z_{in} Z_o - Z_o R)}{X Z_{in}}$
 For $Z_{in} = 13$ Ohm $Z_L = 23.0 + j 25.5$
 $Z_o = 33.8$ Ohm $\theta = 45.6^\circ$
 Characteristic Impedance
 Electrical length

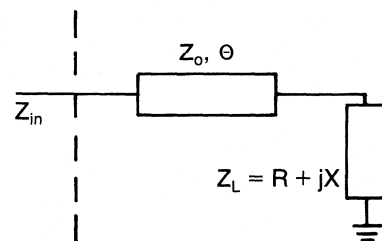


Figure 4

In an effort to hold the physical length of the transmission line to a minimum, a second shunt capacitance is next computed. This second shunt capacitance is located on the high impedance end of the transmission line. The actual value of this capacitance may vary within limits, since it is within the capacity of the transmission line to match a range of impedances. The larger the shunt capacitance the shorter the required transmission line. The maximum value of this capacitance is limited by the region of physically realizable transmission lines (1).

To maintain the bandwidth and performance of this circuit, the capacitance should rotate from a value of impedance with Q_s less than the device Q_s , to the load impedance.² For the example shown in Figure 3 the shunt capacitance (C_2) rotates from an impedance of $23.0 + j25.5$ ohms along a constant admittance circle to 50 ohms. To accomplish this rotation a capacitance value of 3.69 pF is computed in Figure 4b (3.69 pF may seem like an odd capacitance until one computes the low frequency capacitance value to be 3 pF).

The transmission line used to match from 13 ohms to $23.0 + j25.5$ ohms is next determined. The characteristic impedance and electrical length of the transmission line can readily be calculated. (1) As is shown in Figure 4c, to match between the two impedances a transmission line of characteristic impedance $Z_o = 33.8$ ohms and electrical length $\theta = 45.6^\circ$ is used.

This Smith chart method is used to establish a midband impedance match that will maintain good performance at the band edges. Curves A and B in Figure 5 show the band edge mismatch to be less than 1.6:1 VSWR. The example shown only requires a single section of matching. If, however, a lower Q matching filter had been required, additional transmission line/shunt capacitor sections may have been needed.

The initial design of the amplifier described in this article was generated at a midband frequency of 925 MHz using the Smith chart design techniques described. This design was later computer analyzed and optimized. The final design presented in this article is the Smith chart design with only minor computer aided optimizations.

Circuit Construction

Care must be taken to properly prepare the printed circuit board before any components are mounted or soldered in place. Whenever transmission lines are mean-

dered there exists a real danger that coupling between the lines and other components will lead to a potentially unstable circuit that will be difficult to tune. For this reason a good ground plane must be maintained to insure proper performance. The ground plane integrity is enhanced by two separate but related mechanisms. First, all the edges of the board are wrapped and soldered with copper foil. This edge wrapping eliminates the electrical separation between the topside ground surfaces and the bottom ground plane. The result is a unified ground plane throughout the circuit.

Second, after wrapping eyelets are installed at strategic points on the board to provide short ground paths for the shunt capacitors. This too serves to electrically connect the top and bottom ground surfaces³ (see component placement diagram for eyelet placement). A final step to board preparation is to use copper foil to wrap the ground edges of the transistor mounting holes. This must be done to minimize the parasitic common lead inductance of the device and optimize the performance of the transistor.

After the printed circuit board has been prepared circuit components are soldered in place. The component placement diagram shows the proper placement of all components. Slight lateral movement of the shunt capacitors, especially the shunt capacitors associated with the collector of the MRF843, is generally necessary to tune the circuit.

The final step to circuit construction is to provide a good heat sink for the transistor. The heat sink must be capable of maintaining a worst case junction temperature ($T_{junc.}$) of less than 200°C (refer to the manufacturer's data sheets for specific thermal specifications on the individual transistors).

Circuit Performance

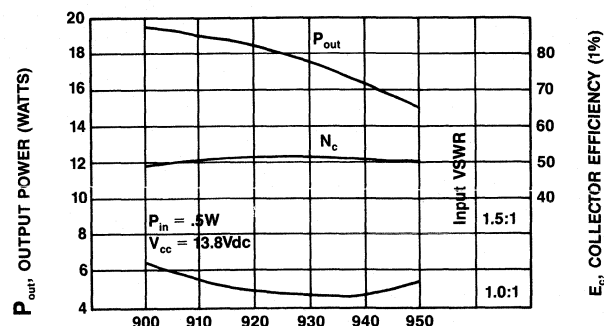
The circuit performance is shown in Figures 6-9. A comparison of this performance data to the design criteria given in Table 1 shows the amplifier to meet or exceed the desired specifications.

Figure 6 shows the efficiency across the band to be quite flat at about 50%. Also shown in Figure 6 is the input VSWR which is better than 1.3:1 across the band.

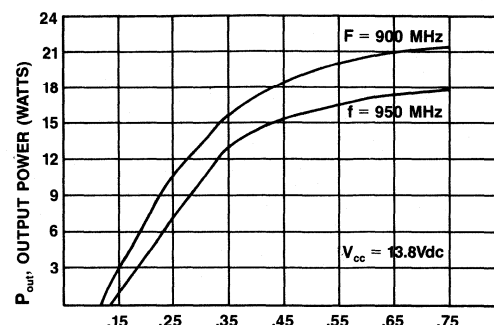
Footnotes

¹ For a detailed explanation of effective capacitance see "Designing Transistor Test Fixtures For the 800 MHz Frequency Spectrum" by Dan Moline, *R.F. Design*, March/April issue, 1984.

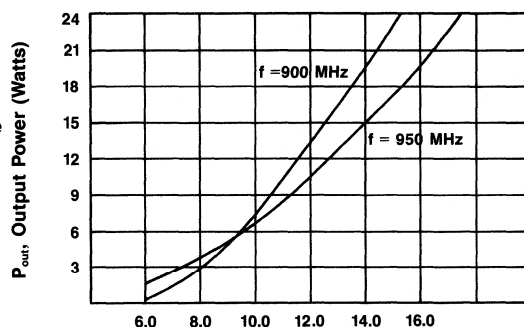
f, FREQUENCY (MHz)
TYPICAL PERFORMANCE
Figure 6



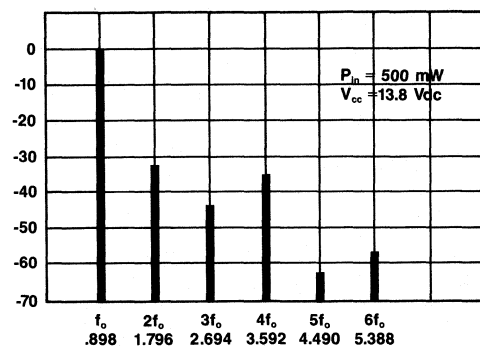
P_{in} , INPUT POWER (WATTS)
OUTPUT POWER VERSUS INPUT POWER
Figure 7



V_{cc} , Supply Voltage (Vdc)
Output Power Versus Supply Voltage
Figure 8



f, Frequency (GHz)
Output Spectrum
Figure 9



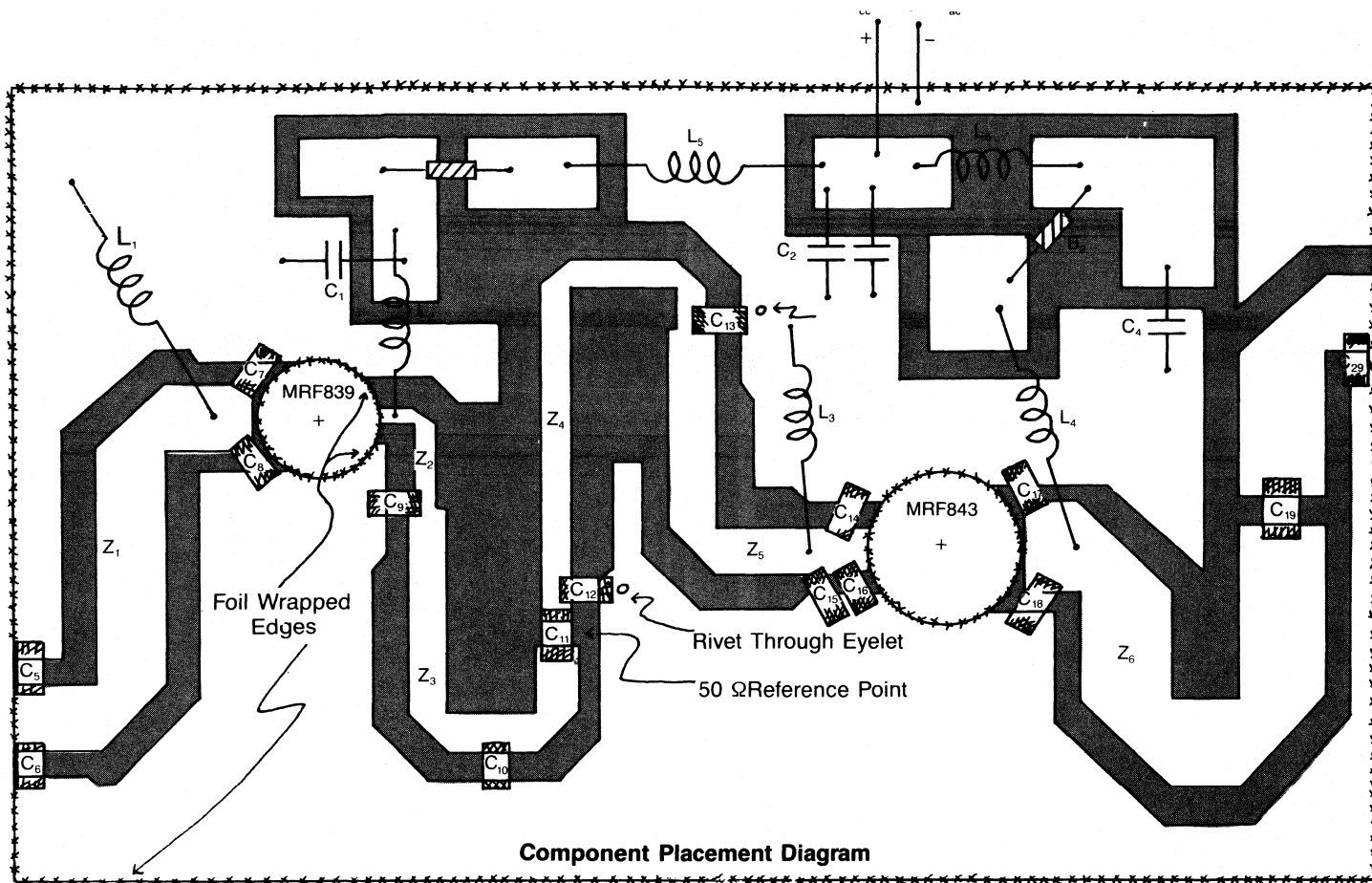
² The design example presented herein is for maximum bandwidth ($Q_{transistor} = Q_{maximum}$). It should be noted however, that maximum bandwidth design is not always desirable and may be limited by other system requirements.

³ If available, edge plating and plated through holes are a preferred alternative to edge wrapping and eyelets.

References

1. Kurt P. Schwan, "Matching: When Is A Single Line Sufficient?", *Microwaves* December 1975.

David Miller is Applications Engineer for Land Mobile Products. He can be reached at Motorola, Inc., P.O. Box 2953, Phoenix, AZ 85062.



Component Placement Diagram

BASIC Program Computes Values For 14 Matching Networks

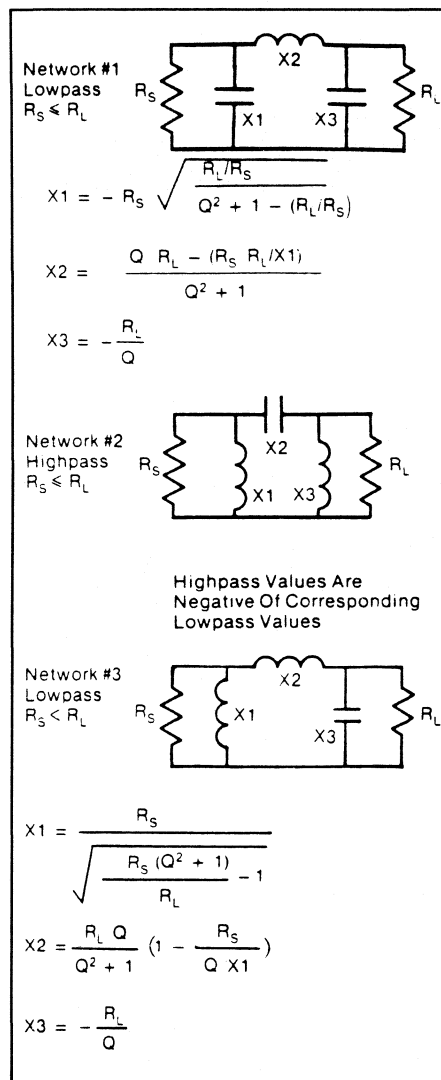
By Alan J. LaPenn

The ever increasing number of personal computers and their relatively low cost and portability makes them excellent tools for scientific calculations and model evaluations. The program that follows was intentionally kept simple and should run on any computer running the BASIC programming language. No special graphic routines have been used and all display formatting is implemented as standard BASIC print statements. There are no multiple statement lines and input prompting is provided by the use of print statements, since some BASIC interpreters do not support prompt strings imbedded in an input statement. All output is directed to the standard output device (video display). No facility has been provided to redirect output to a line printer or mass storage device such as a disk drive or cassette, since such techniques tend to be machine dependent and cause a loss of program portability.

The program has been run on the following computers without modification: Commodore Vic-20, Commodore 64, Texas Instruments TI99/4A, TRS80, Atari 400 and 800.

The program consists of 122 lines of code, including remark statements for documentation purposes. The 14 network values are calculated in eight separate subroutines. Seven of the subroutines calculate networks one, three, five seven, nine, 11, and 13. The eighth subroutine calculates the inverse values of the above mentioned networks, providing the remaining seven networks two, four, six, eight, 10, 12 and 14.

Program output is provided by a print subroutine located at line number 1200 and ending at line number 1470. User input is provided at the beginning of the program. After the network design is completed the user has the option of exiting the program or designing a new network.



There are two reasons for the use of subroutines to calculate network values and provide output. The use of subroutines reduces the number of lines of code significantly and allows the user to make personal modifications easily. Subroutines for mass storage, output to a line

printer and graphics can be added to the print subroutine without having to change the rest of the program.

Use of the software is extremely simple, as the program prompts the user for all the input data required, performs the required calculations and displays the output data values. To run the program simply type "run" from the keyboard and press the enter or return key. The user will then be prompted to enter the following information:

Enter source resistance in ohms:

Enter load resistance in ohms:

Be sure to observe the restrictions concerning the size of the source resistance (R_S) compared to the load resistance (R_L). R_S may be smaller than R_L or equal to R_L for some of the networks, but never larger than R_L . If the user enters a value for R_S that is greater than R_L , the program will issue the following error message and the user will be prompted to enter R_S and R_L again:

R_S must be less than or equal to R_L .

At this point Q_{min} will be calculated by the program. Next, the user will be prompted for the desired frequency of operation.

Enter frequency in hertz for results in henries and farads or 0 for results in reactance values.

The user is then prompted for the network number to be designed.

Enter desired network (1-14):

Note that for some networks R_S only can be less than R_L and for other networks R_S can be less than or equal to R_L . If the user attempts to design a network that fails the above conditions the program will issue one of the following error messages.

R_S must be less than or equal to R_L for network XX

R_S must be less than R_L for network XX

where XX is the network number the user wished to design. The user then will be

prompted to enter a new network number.

The program next displays the computed value of Q_{min} . If the network to be designed is not network 13 or 14, the user is given the option of specifying another value of Q . The following prompt will appear:

Enter desired value of Q ($Q \geq Q_{min}$):

Note that the range of Q must be greater than or equal to the computed value of Q_{min} , but not less than Q_{min} . If the user enters a value of Q that is less than Q_{min} the program will issue the following error message and the user will be prompted for another value of Q .

Q must be greater than or equal to XX where XX is the current value of Q_{min} .

At this point the program will compute the required network elements and display them in the following format:

Source resistance = XX ohms

Load resistance = XX ohms

$Q_{min} = XX$

If Q_{min} is not equal to the value of Q the following will also be printed:

$Q = XX$

The network number that was designed will be displayed next.

Network number XX

If zero was entered for the frequency, the following will be printed:

For two element networks:

$X1 = XX$ ohms

$X2 = XX$ ohms

For three element networks:

$X1 = XX$ ohms

$X2 = XX$ ohms

$X3 = XX$ ohms

(Note positive values are for inductive reactance and negative values are for capacitive reactance.)

Examples

Design a matching network to transform a 50 ohm antenna output to 200 ohms to match an amplifier input at 75 MHz, with a required Q of 10.

(Note: user input is underlined and <cr> is the enter or return key on the computer.)

Enter source resistance in ohms:

? 50 <cr>

Enter load resistance in ohms:

? 200 <cr>

Enter frequency in hertz for results in henries and farads or 0 for results in reactance values:

? 75000000 <cr>

Enter desired network (1-14):

? 12 <cr>

$Q_{min} = 1.732050808$

Enter desired value of Q ($Q \geq Q_{min}$):

? 10 <cr>

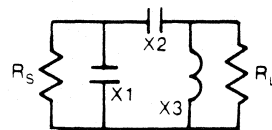
Source resistance = 50 ohms

Load resistance = 200 ohms

Network #4

Highpass

$R_S < R_L$

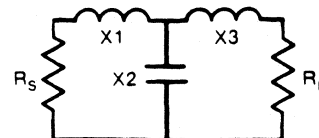


Highpass Values Are Negative Of Corresponding Lowpass Values

Network #5

Lowpass

$R_S < R_L$



$$X1 = R_S Q$$

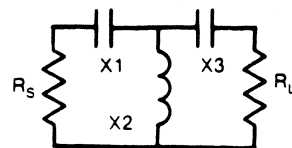
$$X2 = \frac{-R_S (1 + Q^2)}{Q + \sqrt{\frac{R_S (1 + Q^2)}{R_L} - 1}}$$

$$X3 = R_L \sqrt{\frac{R_S (1 + Q^2)}{R_L} - 1}$$

Network #6

Highpass

$R_S < R_L$



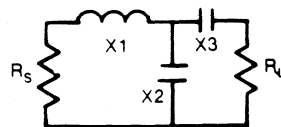
Highpass Values Are Negative Of Corresponding Lowpass Values

Standard Tee Networks.

Network #7

Lowpass

$R_S < R_L$



$$X1 = R_S \times Q$$

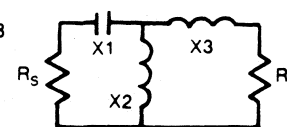
$$X2 = \frac{-R_S (1 + Q^2)}{Q - \sqrt{\frac{R_S (1 + Q^2)}{R_L} - 1}}$$

$$X3 = -R_L \sqrt{\frac{R_S (1 + Q^2)}{R_L} - 1}$$

Network #8

Highpass

$R_S < R_L$

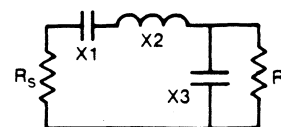


Highpass Values Are Negative Of Corresponding Lowpass Values

Network #9

Lowpass

$R_S < R_L$



$$X1 = \sqrt{R_S R_L - R_S^2 - Q R_S}$$

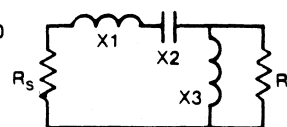
$$X2 = Q R_S$$

$$X3 = \frac{-R_S R_L}{X1 + X2}$$

Network #10

Highpass

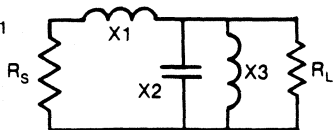
$R_S < R_L$



Highpass Values Are Negative Of Corresponding Lowpass Values

Series Enhanced -Q L Networks.

Network #11
Lowpass
 $R_s < R_L$

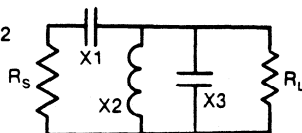


$$X1 = R_s \sqrt{\frac{R_L}{R_s} - 1}$$

$$X2 = -\frac{R_L}{Q}$$

$$X3 = \frac{X_2}{\frac{X_1}{Q R_s} - 1}$$

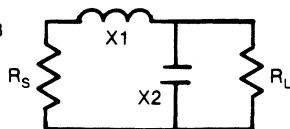
Network #12
Highpass
 $R_s < R_L$



Highpass Values Are
Negative Of Corresponding
Lowpass Values

Shunt Enhanced - QL Networks

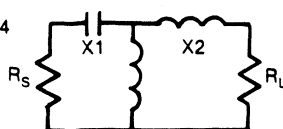
Network #13
Lowpass
 $R_s < R_L$



$$X1 = \sqrt{R_s R_L - R_s^2}$$

$$X2 = \frac{-R_s R_L}{X1}$$

Network #14
Highpass
 $R_s < R_L$



Highpass Values Are
Negative Of Corresponding
Lowpass Values

Simple L Networks.

$$Q_{min} = 1.732050808$$

$$Q = 10$$

Network number 12

Frequency = 7500000
hertz

C1 = 2.4503506E-11 Farads

L2 = 4.2441318E-8 Henries

C3 = 8.7725667E-11 Farads

Enter 1 to run program again 0 to end:

? 0 <cr>

The following example is the same as the previous except that the frequency is set equal to zero and output values are in units of reactance.

Enter source resistance in ohms:

? 50 <cr>

Enter load resistance in ohms:

? 200 <cr>

Enter frequency in hertz for results in henries and farads or 0 for results in reactance values:

? 0 <cr>

Enter desired network (1-14):

? 12 <cr>

$Q_{min} = 1.732050808$

Enter desired value of Q ($Q \geq Q_{min}$):

? 10 <cr>

Source resistance = 50 ohms

Load resistance = 200 ohms

$Q_{min} = 1.732050808$

Q = 10

Network number 12

X1 = -86.60254038 ohms

X2 = 20 ohms

X3 = -24.18979548 ohms

Positive values for inductive reactance and negative values for capacitive reactance.

Enter 1 to run program again, 0 to end:

? 0 <cr>

Alan LaPenn can be contacted at 157
Saunders Hill Rd., New Boston, NH
03070.

```

10 rem Main program
20 print "Enter source resistance in ohms:"
30 input rs
40 print "Enter load resistance in ohms:"
50 input rl
52 if rs <= rl then 60
54 print "RS must be less than or equal to RL"
56 goto 20
60 qm = sqr (rl/rs-1)
70 print "Enter frequency in hertz for results in henries and
  farads or 0 for results in reactance values:"
80 input fo
90 print "Enter desired network (1-14):"
100 input net
105 print
110 print "Qmin="; qm

```

```

112 print
115 q = qm
120 if net > 12 then 150
130 print "Enter desired value of Q (Q >= Qmin):"
140 input q
142 if q >= qm then 150
144 print "Q must be greater than or equal to "; qm
146 goto 130
150 on net gosub
  400,400,500,500,600,600,700,700,800,800,900,900,1000,1000
160 if fo = 0 then 300
170 on sgn (x1) + 1 goto 190,200
180 f1 = (1/(6.28*fo*x1))^-1
190 goto 210
200 f1 = x1/(6.28*fo)
210 on sgn(x2)+ 1 goto 230,240

```

```

220 f2 = (1/(6.28*fo*x2) )^1
230 goto 250
240 f2 = x2/(6.28*fo)
250 if net > 12 then 300
260 on sgn (x3) + 1 goto 280,290
270 f3 = (1/(6.28*fo*x2) )^1
280 goto 300
290 f3 = x3/(6.28*fo)
300 gosub 1200
305 print
310 print "Enter 1 to run program again 0 to end:"
320 input d
330 if d = 1 then 20
340 end
400 rem net1 rs<rl
410 x1 = rs*(sqr ( (rl/rs)/(q^2 + 1-(rl/rs) ) ) )^ -1
420 x2 = (q*rl-(rs*rl/x1) ) / (q^2 + 1)
430 x3 = (rl/q)^1
440 if net = 1 then 460
450 gosub 1100
460 return
500 rem net3 rs<rl
510 x1 = rs/(sqr( (rs*(q^2 + 1) ) / rl-1) )
520 x2 = ( (rl*q) / (q^2 + 1) ) * (1-(rs / (q*x1) ) )
530 x3 = (rl / q)^1
540 if net = 3 then 560
550 gosub 1100
560 return
600 rem net5 rs <= rl
610 x1 = rs*q
620 x2 = (rs* (1 + q^2) * -1) / (q + sqr( (rs* (1 + q^2) ) / rl-1) )
630 x3 = rl*sqr ( (rs* (1 + q^2) ) / rl-1)
640 if net = 5 then 660
650 gosub 1100
660 return
700 rem net7 rs < rl
710 x1 = rs*q
720 x2 = (rs* (1 + q^2) ^1) / (q-sqr ( (rs*(1 + q^2) ) / rl-1) )
730 x3 = rl*sqr ( (rs* (1 + q^2) ) / rl-1) ^1
740 if net = 7 then 760
750 gosub 1100
760 return
800 rem net9 rs < rl
810 x1 = sqr (rs*rl - rs^2-q*rs)
820 x2 = q*rs
830 x3 = (rs*rl^1) / (x1 + x2)
840 if net = 9 then 860
850 gosub 1100
860 return
900 rem net11 rs < rl
910 x1 = rs*sqr (rl / rs-1)
920 x2 = rl / q^1
930 x3 = x2 / (x1 / (q*rs)-1)
940 if net = 11 then 960
950 gosub 1100
960 return
1000 rem net13
1010 x1 = sqr (rs*rl-rs^2)
1020 x2 = (rs*rl^1) / x1
1030 if net = 13 then 1050
1040 gosub 1100
1050 return
1100 rem inverse subroutine
1110 x1 = x1^1
1120 x2 = x2^1
1130 if net = 14 then 1150
1140 x3 = x3^1
1150 return
1200 rem print routine
1204 print
1206 print
1210 print "Source resistance = "; rs; "ohms"

```

```

1220 print "Load resistance = "; rl; "ohms"
1230 Print "Qmin = "; qm
1240 if qm = q then 1270
1250 print "Q = "; q
1270 print "Network number"; net
1280 if fo <> 0 then 1340
1300 print "X1 = "; x1; "ohms"
1310 print "X2 = "; x2; "ohms"
1315 if net > 12 then 1330
1320 print "X3 = "; x3; "ohms"
1324 print
1326 print "Positive values for inductive reactance and negative
values for capacitive reactance."
1330 return
1340 print "Frequency = "; fo; "hertz"
1345 on sgn (x1) + 1 goto 1360,1370
1350 print "C1 = "; f1; "farads"
1360 goto 1380
1370 print "L1 = "; f1; "henries"
1380 on sgn (x2) + 1 goto 1400,1410
1390 print "C2 = "; f2; "farads"
1400 goto 1420
1410 print "L2 = "; f2; "henries"
1420 if net > 12 then 1470
1430 on sgn (x3) + 1 goto 1450,1460
1440 print "C3 = "; f3; "farads"
1450 goto 1470
1460 print "L3 = "; f3; "henries"
1470 return

```



Errata:

The article, "The Phase/Frequency Detector," in the February 1985 issue contained several important typographical errors. The following equations are correct:

$$(1) f^*(t) = \sum_{n=0}^{n=\infty} f(t) \delta(t-nT)$$

$$(4) F(s) = \sum_{n=0}^{n=\infty} \int_0^{\infty} f(t) \delta(t-nT) \exp(-sT) dt$$

$$(5) F^*(s) = \sum_{n=0}^{n=\infty} f(nT) \exp(-nsT)$$

$$(12) E^*(s) = \frac{\sum_{n=-\infty}^{n=\infty} \Phi r(s - j n W_s) / T}{1 + HG^*(s)}$$

(16)-(20) R1 should be RL

Determining Receiver Performance With a Computer Spreadsheet

By Gregory R. Quinn
HRB Singer

Spreadsheets are software programs that transform a computer's memory into a large worksheet made up of columns and rows. Each separate location on this worksheet is called a cell. Into these cells the user can insert values, labels or formulas instructing the computer to perform calculations. According to the user's commands, the program will recalculate any results based on new or modified data entered.

The main advantage with such a program is the ability to alter data or formulas to explore the possibilities of a particular set-up. All spreadsheets available have commands similar to those in BASIC that allow the cells to be programmed in a variety of ways to calculate answers from data found on the spreadsheet. The user can program a cell in much the same way that he or she can write out the formulas by hand.

Logical decisions within the cells are controlled by IF statements. These commands are supplemented by math functions which will operate on specified ranges of numbers, such a SUM, MAX, MIN and AVERAGE. In this application, the most complicated structures used are IF and SUM.

Two programs are mentioned: VisiCalc and SuperCalc. The information presented for the spreadsheet cells should work without alteration in either program. In fact, the set-up shown should not need any changes to work on the majority of spreadsheets available for different computers.

Electronic worksheets or spreadsheets are ingenious software tools for personal computers. These packages allow the user to make redundant calculations and "what if?" speculations very quickly once a model has been formulated. Because of their flexibility electronic spreadsheets have applications in fields other

A1 P = "NAME	A12 P = "T GAIN
A2 P = "IIP2	A13 P = "BW (MHz)
A3 P = "IIP3	A14 P = "DR2
A4 P = "COMP PT	A15 P = "DR3
A5 P = "GAIN	A16 P = "IN N FLR
A6 P = "NF	A17 P = "OUT N FLR
A7 P = "CIIP2	B1 P = "INITIAL
A8 P = "CIIP3	B6 P = 0
A9 P = "CCMP PT	B7 P = 100
A10 P = "CNF	B8 P = 100
A11 P = "TAKEOVER	B9 P = 100

All of the cell contents listed above are in protected cells.

C1 TR

B13, C2-6 \$

These cells are for the data describing each part of the system and they are formatted for two decimal places.

C7 \$TR =IF(C2=0,NA,+C2-20*LOG10 (1+SQRT (10^(.1*(C2+C5-B7))))
 C8 \$TR=IF(COUNT(C3)=0,NA,+C3-10*LOG10 (1+(10^(.1*(C3+C5-B8))))
 C9 \$TR=IF(COUNT(C4)=0, NA, +C4-10*LOG10 (1+(10^(.1*(C4+C5-B9))))
 C10 \$TR=IF(COUNT(C6)=0, NA, +C6+10*LOG10 (1+(((10^(B10/10))-1)/((10^(C6/10))*(10^(C5/10)))))
 C11 \$TR =IF(AND(COUNT (C2:C6)>0, COUNT(D2:D6)=0), +C10-B10+C5, NA)

The variables in all of the above formulas are relative.

C12 \$TR=IF(AND(COUNT(C2:C6) >0,COUNT(D2:D6)=0), SUM (B5:C5), NA)
 C14 \$TR =IF(AND(COUNT (C2:C6) >0, COUNT(D2:D6)=0), .5*(C7 +114-10*LOG10 (B13)-C10), NA)
 C15 \$TR =IF(AND(COUNT (C2:C6) >0, COUNT(D2:D6)=0),.67*(C8 + 114-10*LOG10 (B13)-C10), NA)
 C16 \$TR =IF(AND(COUNT(C2:C6) >0, COUNT(D2:D6)=0),-114 +10*LOG10 (B13), NA)

In these formulas, all the variables are relative except for B5 and B13, which are constant.

C17 \$TR =IF (AND (COUNT (C2:C6) >0, COUNT (D2:D6) =0), C16+C10+C12, NA)

All the variables in this formula are relative.

Table 1

than business and finance. For example, they can be used to calculate receiver performance, one of the most tedious chores in designing receivers.

A worksheet set-up for this purpose was designed with SuperCalc (version 1.12) on an Osborne 1. Differences between SuperCalc and other worksheet packages are so minor that the contents of this worksheet could be adapted easily to the others. This article assumes that the prospective user has a working knowledge of computer worksheets and of basic receiver design.

This worksheet accepts the following data about each module of the string:

- 1) A short label to identify each module
- 2) The second order input intercept point of the module
- 3) The third order input intercept point of the module
- 4) The 1 dB compression point of the module
- 5) The module gain
- 6) The module noise figure
- 7) The system operating bandwidth.

Given these inputs, the following system characteristics are calculated:

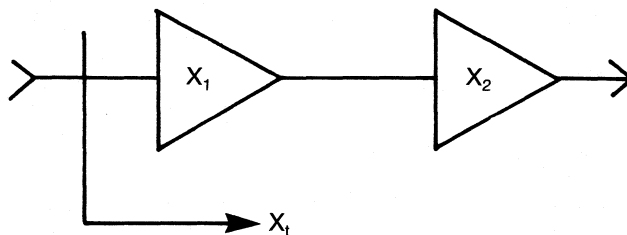
- 1) Cascaded second-order input intercept point
- 2) Cascaded third-order input intercept point
- 3) Cascaded 1 dB compression point
- 4) Cascaded noise figure
- 5) The noise takeover factor of the first element of the string
- 6) Total gain
- 7) Second order spurious-free dynamic range
- 8) Third order spurious-free dynamic range
- 9) Input noise floor
- 10) Output noise floor.

In the first six rows of the worksheet are cells that hold the necessary information to make receiver system calculations. A specific characteristic may be omitted, e.g. the second-order input intercept point, but if a characteristic is unused, all modules must have a nil ("blank" but not zero) value in that cell. Otherwise, an error in recalculation will occur. Where certain calculations are either meaningless or not possible an "N/A" appears. The worksheet also detects the first element of the string (last column of the worksheet) and stops calculating values at that point.

Worksheets generally calculate from left to right and from top to bottom. Therefore, the string of the receiver modules must be entered in reverse order on the worksheet, so the last module will appear first as one reads the worksheet from left to right.

A	B	C	D	E	F	G
1:NAME	INITIAL	Spltr	Pad	Mixer	Fltr	Amp
2:IIP2		100.00	100.00	8.00	100.00	28.00
3:IIP3		100.00	100.00	10.00	100.00	15.00
4:COMP PT		100.00	100.00	.00	100.00	15.00
5:GAIN		-3.00	-9.00	-6.00	-.50	15.00
6:Nf	0	3.00	9.00	6.00	.50	
7:CIIP2	100	95.35	95.89	8.00	8.50	-6.66
8:CIIP3	100	98.24	99.25	10.00	10.50	-4.55
9:CCMP PT	100	98.24	99.25	.00	.50	-14.50
10:CNF		3.00	12.00	18.00	18.50	8.24
11:Takeover		N/A	N/A	N/A	N/A	4.74
12:T GAIN		N/A	N/A	N/A	N/A	-3.50
13:BW (MHz)	100.00					
14:DR2		N/A	N/A	N/A	N/A	39.55
15:DR3		N/A	N/A	N/A	N/A	54.41
16:IN N FLR		N/A	N/A	N/A	N/A	-94.00
17:OUT NFLR		N/A	N/A	N/A	N/A	-89.26

Table 2 — Sample Spreadsheet



$$I_i = I_1 - 20 \log[1 + \sqrt{i_1 g_1 / i_2}]$$

Cascaded Second Order Input Intercept Point

$$I_i = I_1 - 10 \log[1 + i_1 g_1 / i_2]$$

Cascaded Third Order Input Intercept Point

$$CP_i = CP_1 - 10 \log[1 + g_1 cp_1 / cp_2]$$

Cascaded Compression Points

$$F_i = F_1 + 10 \log[1 + (f_2 - 1) / (f_1 g_1)]$$

Cascaded Noise Figure

$$DR_2 = .5[IIP_2 + 174 - 10 \log BW - NF]$$

Second Order Spurious Free Dynamic Range (Bandwidth in Hz)

$$DR_3 = .67[IIP_3 + 174 - 10 \log BW - NF]$$

Third Order Spurious Free Dynamic Range (Bandwidth in Hz)

$$\text{Takeover} = NF_i - NF_{\text{system less 1st stage}} + G_1$$

Noise Figure Takeover

("g" is the numeric ratio for gain. All other lower case variables are expressed in units of milliwatts and all upper case variables are expressed in units of dB or dBm.)

Table 3

Certain conditions must exist to initialize the calculations. An ideal noise figure, intercept point and compression point must appear at the receiver output. Column B holds these initializing conditions. A system performance bandwidth must be supplied by the user. This value is inserted into cell B13. Errors will occur if the system bandwidth is not supplied.

Because of the Osborne 1's screen size limitations, abbreviations are used here for each row name. These abbreviations are: IIP2: Second-order input intercept point in dBm; IIP3: Third-order input intercept point in dBm; COMPT PT: 1 dB compression point in dBm; GAIN: Module gain in dB; NF: Noise figure in dB; CIIP2: Cascaded second-order input intercept point in dBm; CIIP3: Cascaded third-order input intercept point in dBm; CCMP PT: Cascaded 1 dB compression point in dBm; CNF: Cascaded noise figure in dB; TAKEOVER: A dimensionless factor by which the first element of the string determines noise figure. (Values of 7 or more mean that the first element greatly determines system noise figure); T GAIN: The total gain of the system in dB; BW (MHz): The second system operating bandwidth in MHz; DR2: The second-order dynamic range in dB; DR3: The third-order dynamic range in dB; IN N FLR: Input noise floor of the system in dBm; OUT N FLR: Output noise floor of the system in dBm.

When devices such as attenuators, isolators or other passive elements appear in the string, their high intercept and compression points are approximated best by the value 100, unless it has been determined that the characteristic is not infinitely high and that there is some real limit less than 100 dB. Values higher than 100 in this application seem to cause software problems and inaccuracies.

The cascaded intercept points, noise figure and compression points are displayed on the worksheet for every module. This way modules contributing to poor system performance can be identified quickly.


Formulas and cell formats are given in Table 1. The formulas and formats in column C, once entered, are replicated to as many columns as the user needs. Whether variables in the formulas are relative or constant is shown in Table 1. A boiler plate file of 25 elements was made to eliminate replicating each formula in a new spreadsheet whenever a receiver is to be analyzed.

An example of a completed analysis is given for the user to check his setup (Table 2). A format that has only two places past the decimal was used. For

those desiring greater accuracy, the format can be changed to suit particular applications.

The advantage of worksheets is that they permit data and values to be changed simply and quickly. Although calculators relieve some of the burden in analyzing receivers, worksheets greatly speed up the iterative process that is invariably required in receiver analysis.

In SuperCalc the default format is left justification for text and right justification for numerics.

Gregory Quinn is an RF engineer at HRB Singer, a defense electronic contractor, in State College, Pennsylvania. Address correspondence to Mr. Quinn at HRB Singer, Dept. 118, P.O. Box 60, State College, PA 16804. 

Digital Signal Processing: The Digital Processor

By Thomas Callaghan
Watkins-Johnson Company

A digital processor refers to any form of hardware and/or software that has been built and/or programmed to perform signal processing algorithms on the data output from the sampler/quantizer. This definition encompasses a broad range of computing power. For the purposes of this article, we will concentrate on those processor architectures that lend themselves to signal processing and on the basic structures used in determining the processor(s) configuration.

Basically a digital processor should be modular in design; i.e., the processor, by itself, is capable of such rudimentary tasks as addition, subtraction, multiplication, memory transfers, and I/O transfers. Additional support, such as direct interface to A/D and D/A converters and the capability of working with blocks of data, would also be helpful. Although it is not expected to have all of these capabilities, the processor should still perform whatever capabilities it does have without outside support. In this way, when a simple task needs to be executed, only one module is used. As the task becomes more complicated, processor modules can be added to handle the extra load. Indeed, most applications in signal processing lend themselves readily to this modularity. Each application can be broken down into several smaller algorithms that can be further decomposed into simpler tasks.

Multiple processors can be implemented using two basic approaches, a parallel structure or a sequential structure. A parallel structure is defined by Tewksbury, et al.,¹ as being the concurrent execution

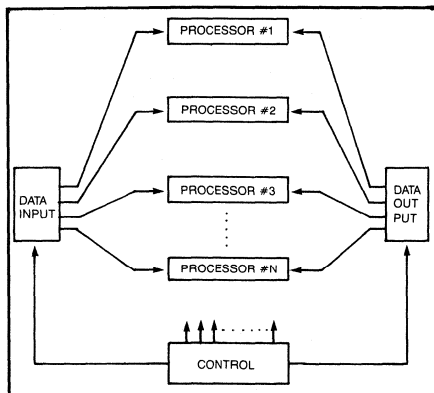


Figure 1. Parallel Processor Structure

of several functional operations using a number of distinct functional modules under the coordination of a common control structure. A sequential structure, on the other hand, sequentially executes all the functional operations of the algorithm in a single functional module. One could go on to say that a sequential structure could have several modules, but one module cannot begin processing until the one preceding it is finished.

Parallel Structures

A parallel structure is shown in Figure 1. Each processor receives its data from a shared input source. Each processor then sends its processed data to a shared output. Using this type of structure, the functional operation speed can be increased by dividing the data processing over a greater number of processing modules. However, there is a point of diminishing returns for additional pro-

cessors due to the increased complexity of the control structure.

Another advantage of a parallel structure is that each processor module can be composed of an efficient functional unit with limited capabilities. This does, however, deviate from the strict definition of modularity and allows fewer common tasks, such as multiplication, to be handled by processors especially designed for the functional task. Other general purpose processors can then handle some of the more common tasks; i.e., overflow detection, or be reprogrammed to handle different tasks. In this way overall data processing speed can be increased for the structure by allowing each processor to handle the tasks for which it is best suited.

One of the disadvantages of parallel structures is that their control structures can be quite complex. Since each module is operating at a different throughput, timing of all the functions becomes another critical area. For both of these reasons, hardware design and, consequently, programming become difficult.

Sequential Structures

A sequential processor is shown in Figure 2. The first processor in the sequence receives the incoming data. The first processor performs its assigned tasks on the data and passes along this new data to the next stage. The process continues as each processor performs its specific tasks until the final data output is reached. It is not necessary that each processor work on all the incoming data. It could just pass some of the data through to the next stage. The next stage's

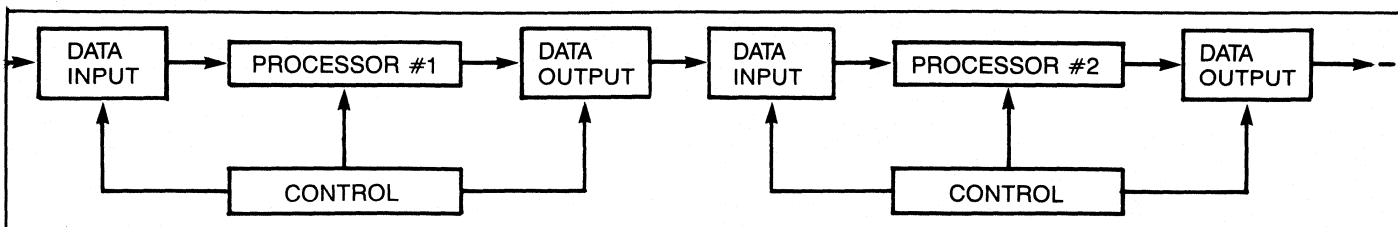


Figure 2. Sequential Processor Structure

data until it reaches the processor. The delay caused by each stage produces one of the sequential structure's disadvantages. This same delay produces one of the advantages; it simplifies controller design. The controller does not have to keep track of data that is earmarked for a particular stage. At each stage, all of the data is passed along at once. A simpler controller allows more efficient, more straightforward hardware designs. Consequently, sequential structures are easier to program.

Parallel vs Sequential

Ultimately, the choice between parallel or sequential structuring depends greatly on how well a particular signal processing algorithm lends itself to one or the other. Indeed, some algorithms may incorporate both. Another design consideration would involve a trade-off of hardware/software cost and complexity to that of speed. If speed is not a prime consideration, the less expensive, easier hardware designs of the sequential processor would be preferred.

Information Extraction

The final end product of any form of signal processing, analog or digital, is the extraction of information from the input signal. The information can be a breakdown of the signal into its frequency com-

ponents for signal analysis. The information could also be the altering of the signal's spectrum, as in filtering. It can be the intelligence content of the signal, as in detection. Whatever the reason for signal processing, the end product is as varied as the system designers who try to make use of it.

Why Use DSP

The number one force driving the push into DSP is cost. Using Fast Fourier Transform (FFT), signal analysis can now be performed at a substantially lower cost than that encountered using swept banks of analog filters. Once digitized, the power of analysis begins. Algorithms are being developed that can determine the type of modulation being used, phase detection, direction finding and digital demodulation.

The number one force preventing the acceptance of DSP is also cost. The cost of a couple of op-amps, some resistors and capacitors for a simple two pole active analog filter is only a few dollars, compared to a few hundred dollars for digital multipliers, memories and support processing for a digital filter. Of course, if the processor can be time-shared among many modules, the cost factor depreciates. For one two-pole filter, there is a big difference in cost; for a hundred two-pole filters, the analog version increases one hundred fold, whereas the digital increase is negligible. The digital version uses the same hardware plus a few other com-

ponents to multiplex the data and processor.

Another consideration in DSP is the stability of digital parts. Once coefficients are computed for a filter, they will not drift over time nor change with temperature. This allows sharp cutoffs in filters to be realized using digital processing. Furthermore, provided the hardware is set up properly, a simple change in software will turn an FFT unit into a bandpass IIR filter. Another change will result in a lowpass filter. Thus, digital components are very versatile.

Perhaps the greatest advantage of DSP is performance. A digital signal monitor can achieve a much finer resolution at a faster scan rate than an analog version. The cutoff frequency of filters can be more precisely tuned and show a steeper roll-off than analog filters.

Finally, many communications are being done in a digital format, for example, T1 standards of the Bell system. With this digital format, analog signal processing becomes the expensive option.

References

1. S.K. Tewksbury, R.B., Kiebertz, J.S. Thompson, and S.P. Verma, "Tutorials on Signal Processing for Communications, Part II, Digital Signal Processing Architecture," *IEEE Communications Society Magazine*, January 1978.

Tom Callaghan is Head of Digital Processing at Watkins-Johnson Company, 700 Quince Orchard Road, Gaithersburg, MD 20878.

Line Impedance Stabilization Networks: Theory and Use

By Mark Nave

The use of Line Impedance Stabilization Networks (LISNs) to measure the effects of filters on conducted emissions (CE) is specified in most major specs, including FCC, VDE, CISPR, MIL-STD-461 and others. While real-life conducted emissions measurements and filter performance may vary considerably from test conditions, some common reference and testing standard is necessary. LISNs allow test facilities to obtain results with greater consistency and repeatability. This article discusses methods for analyzing common-mode and differential-mode noise and examines the effects of the LISN on CE measurements.

Conducted emissions are an important, but often misconceived electromagnetic interference (EMI) phenomenon. In addition to conducted interference, power leads can act as unintentional antennas, radiating due to CE or receiving noise from the electrical ambient. Proper filtering of the leads to and from the equipment is essential to control this phenomenon. A filter's effectiveness is dependent on an impedance mismatch to both the power source (power mains) and load impedances. Figure 1 shows the statistical distribution of mains impedance with its approximate 40 dB variation. Also depicted is the variation of impedance with frequency and the $\sim 50 \Omega$ centroid behavior of the mean.

Noise Types

There are three basic noise types present on power buses: Differential Mode (DM) and Common Mode (CM) Types I and II. Differential-mode noise is the simplest kind of noise. It occurs between the leads of the intentional current path (phase-neutral or phase-phase).

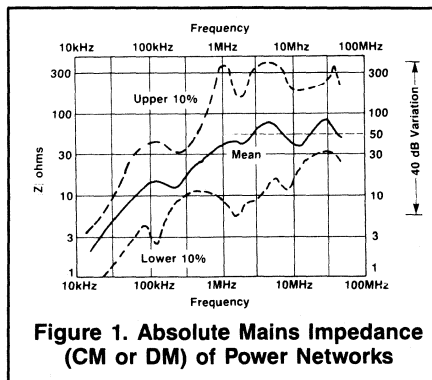


Figure 1. Absolute Mains Impedance (CM or DM) of Power Networks

Reproduced with permission of Interference Control Technologies, Inc., Gainesville, Va.

Typical sources of differential-mode noise are switching transients and motors.

Common-mode Type I noise occurs when the noise source is between safety ground and the phases, including neutral. Common-mode Type II noise occurs when the noise source is between earth ground and all phases, including neutral, and safety ground wire.

Measurement Variation

Figure 1 illustrates the approximate 40 dB variation of the mains impedance, which can result in up to a 40 dB variation in the measured value of the CE. This effect can be understood by analyzing the interaction of the bus and the source under the assumption that the noise frequency is in the constant (50Ω) region. Let the bus impedance (Z_b) vary by a ratio, χ , $0.1 < \chi < 10$, so that $Z_b = \chi 50 \Omega$. The measured voltage, V_m , is the result of voltage division across the internal impedance of the source, Z' , and the bus impedance, Z_b . The expected measured voltage ($\chi=1$) is:

$$V_m = \frac{50}{50 + Z'}$$

The voltage measured under varying bus impedance ($\chi \neq 1$) is:

$$V'_m = \frac{\chi 50}{\chi 50 + Z'}$$

The normalized variation of the measured voltage then becomes:

$$\frac{V'_m}{V_m} = \frac{\chi 50 + \chi Z'}{\chi 50 + Z'}$$

For a low impedance noise source, as Z' becomes small with respect to 50Ω , the normalized variation approaches unity. This means that the varying bus impedance has little effect on the measured voltage. However, for a high impedance source, as Z' becomes large with respect

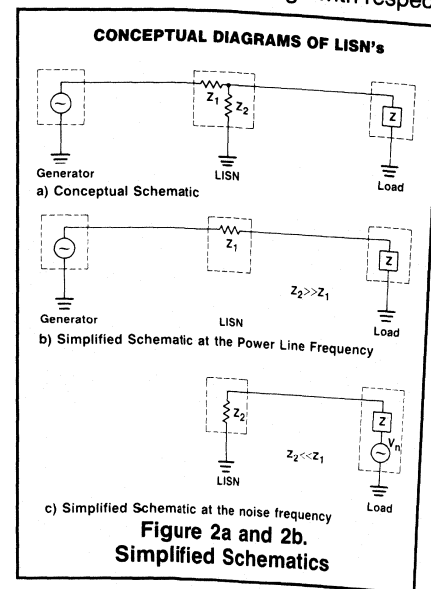
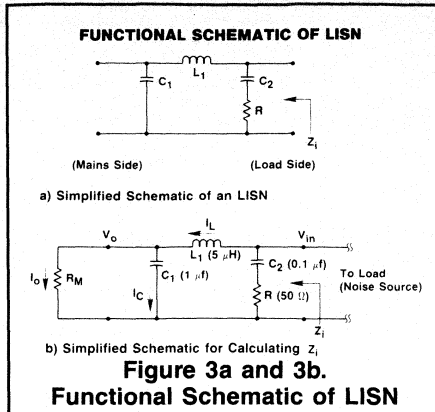


Figure 2a and 2b. Simplified Schematics

Reproduced with permission of Interference Control Technologies, Inc., Gainesville, Va.



Reproduced with permission of Interference Control Technologies, Inc., Gainesville, Va.

to 50 Ω , the normalized variation approaches χ . The worst case variation, then, is:

$$\frac{\chi_h}{\chi_l} = \frac{10}{0.1} = 100, \text{ or } 40 \text{ dB.}$$

Such a wide variation in measurements renders the data virtually useless! For this very reason, the LISN for AC mains was developed.

Schematic Concept

A LISN's purpose is to provide a stabilized impedance to conducted emissions without interfering with the normal power flow required by the Equipment Under Test (EUT). A conceptual schematic of the generator, LISN and load is shown in Figure 2.

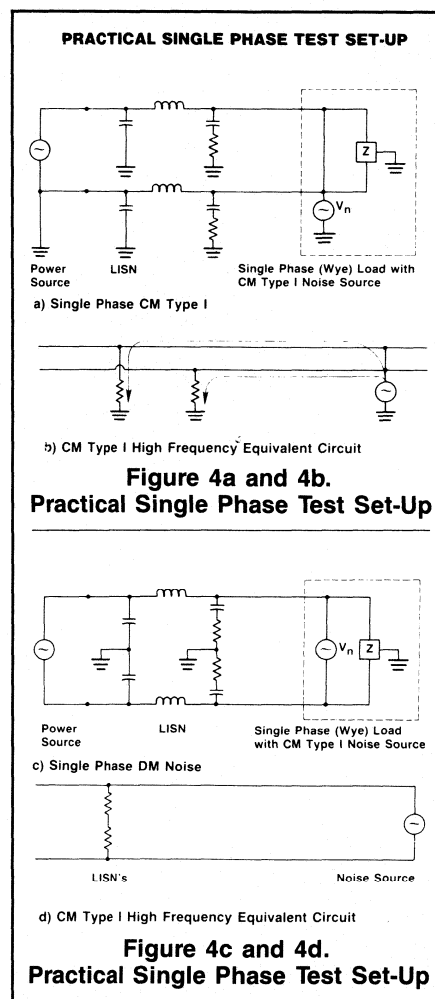
At the power line frequency f_p , the LISN shown in Figure 2 provides a low impedance path from the power source to the load impedance Z , and a high impedance path (virtual open circuit) from the load to the ground. At the noise frequency, f_n ($f_n \gg f_p$), the LISN provides a high impedance path from the power source to the load, and it provides an impedance approaching 50 ohms at high frequencies from the load to ground. The high impedance, low frequency impedance is provided by a capacitor to ground. The 50 Ω impedance to ground ("R" in Figure 3) is actually the input impedance of the spectrum analyzer or EMI meter used to measure the noise. All LISN output ports must be terminated in a 50 Ω impedance, either by meter input impedance or by a 50 Ω dummy load. Figure 2c shows this, whereby the LISN provides a stable impedance to the load and eliminates the effects of the varying mains impedance at noise frequencies.

Single Phase Test Set Up

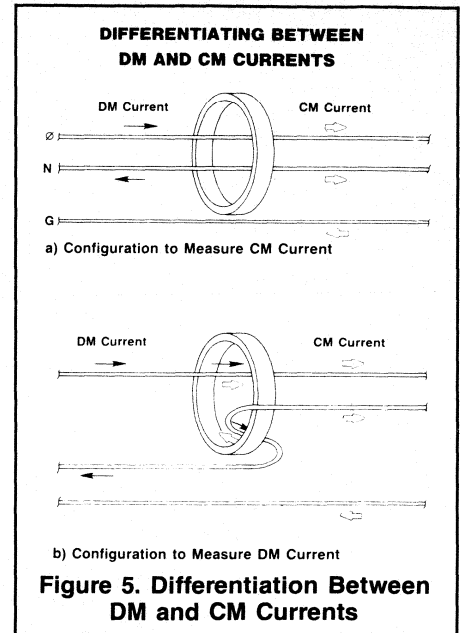
In order to provide impedance stabilization for both DM and CM, the LISN is con-

nected between phase to ground and neutral to ground. Figure 4 shows a practical single phase test set-up. Figure 4a is drawn to emphasize the effects of a LISN on CM Type I noise. At high frequencies the inductor is a virtual open circuit while the capacitor is a virtual short circuit. The high frequency equivalent circuit is shown in Figure 4b. The impedance of the two LISNs combine in parallel to present a 25 Ω impedance to the noise source.

With DM noise, the situation is altogether different. Figure 4c shows the single phase set-up redrawn to emphasize the effects of a LISN on DM noise. Under the high frequency assumptions, the equivalent circuit shown in Figure 4d results. For DM noise, the LISNs combine in series to present a 100 Ω impedance to the noise source. Use of the 50 Ω LISN has caused an unexpected impedance when used in a practical circuit, and the situation becomes worse with a three phase circuit.



Reproduced with permission of Interference Control Technologies, Inc., Gainesville, Va.



Reproduced with permission of Interference Control Technologies, Inc., Gainesville, Va.

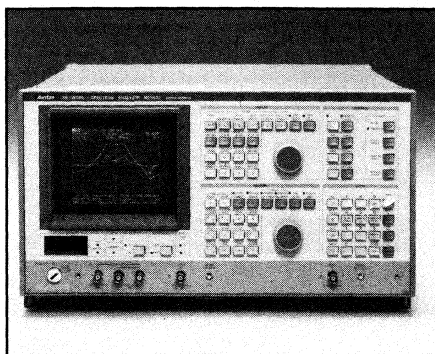
Measurement Techniques

The most common method of measuring the value of the conducted emissions with a LISN is with an EMI meter or a spectrum analyzer. Either of these will give the sum of the CM and DM emissions. Although this is usually the method called for in specifications, it provides no information as to whether the emissions are CM or DM!

The current probe makes it possible to differentiate between CM and DM. The theory is that the sum of the instantaneous currents at a point on a transmission line equals zero. Proper selection of the lines to sum (to put inside the current probe) will allow use of this principle. The application is to cancel out the DM currents to determine CM currents, and vice versa. Figure 5a shows how to use the probe so that the DM currents sum to zero and twice the CM current is measured. Figure 5b shows how the CM currents cancel and the DM currents are measured.

The LISN may also be used for susceptibility testing. If the impedance of the power mains is too low, injecting a signal of a given level may prove difficult because of the loading effect on the signal generator. This condition may be alleviated by using the LISN in the same configuration as that used for testing, except that the signal is *injected* into the LISN "output" port (now used as an input).

Mark Nave can be reached at 8270 Ver-non St., Manassas, VA 22110.



Cover

This month's cover features Anritsu's new spectrum analyzer, Model MS560J. This network/spectrum analyzer has an optional, built-in computer, called the Personal Test Automation, that uses an interpreter to execute programs written in Personal Test Language for a wide range of applications. It is designed for IF measurements.

Features

21 Special Report: Spectrum Analyzers — Higher Performance, Lower Cost

The May Special Report describes some of the features common to recently-developed spectrum analyzers. Microprocessor control and digital storage are two advances seen in most new spectrum analyzers. With the IEEE-488 interface, these instruments can be computer-controlled and set up for automatic performance of repetitive tests. The trend is toward lower costs, but since it is difficult to compare instruments with different features, actual costs are not discussed. — James N. MacDonald.

35 Predict PLL Transient Response with Computer Simulation

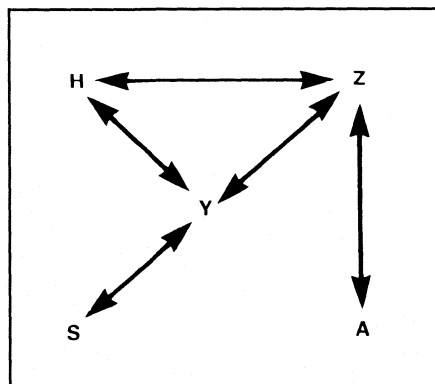
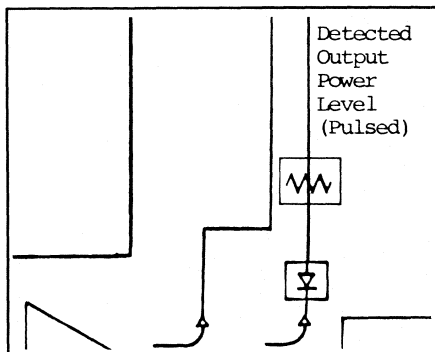
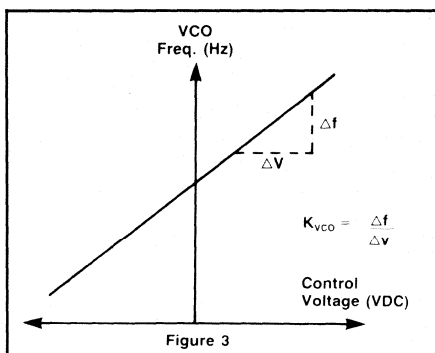
This computer program simulates a second-order phase-lock loop. With the program the instantaneous values of such parameters as VCO frequency and phase detector output voltage can be predicted easily without an engineering breadboard evaluation to verify predicted response. Many engineering hours can be saved in assessing the effects of various conditions by letting the software do the work. — Stan Zubiel

40 Broadband Leveling in Pulsed Operation

A method of evaluating a circuit designed outside the intended operating band of a transistor is to deliver a fixed power level to the circuit while sweeping across a band of frequencies, making adjustments to achieve a flat power response. Input power is held constant with a feedback loop detecting the RF for a DC reference. Pulsed amplifiers do not usually provide a constant enough DC level for reference. The pulsed broadband leveler uses a sample/hold op amp to obtain a steady DC reference. — Joseph J. D'Agostino

49 Transistor Parameter Conversion

The computer program described in this article uses certain universal transistor parameter conversion formulas as subroutines. The program avoids the tedious task of converting from one set of parameters to another when the available parameters do not coincide with those given in a design description. — Stanley Novak

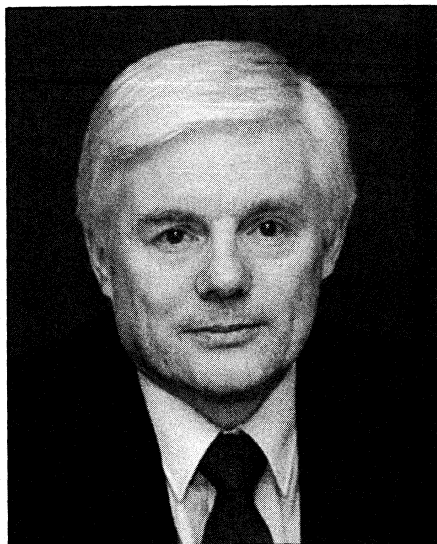


Departments

6	Editorial	43	Info/Card
8	Publisher's Notes	52	Designer's Notebook
13	Letters	57	New Products
16	News	70	New Literature
29	RFI/EMI Corner	78	Advertisers Index
32	Calendar		

R.F. DESIGN (ISSN: 0163-321X USPS: 453-490) is published monthly plus one extra issue in August. May 1985, Volume 8, No. 5. Copyright 1985 by Cardiff Publishing Company, a subsidiary of Argus Press Holdings, Inc., 6530 S. Yosemite Street, Englewood, CO 80111 (303) 694-1522. Contents may not be reproduced in any form without written permission. Second-Class Postage paid at Englewood, CO and at additional mailing offices. Subscription office: 1 East First Street, Duluth, MN 55802, (1-800-346-0085). Subscriptions are sent free to qualified individuals responsible for the design and development of communications equipment. Other subscriptions are: \$15 per year in the United States; \$25 per year in Canada and Mexico; \$25 per year for foreign countries. Additional cost for first class mailing. Payment must be made in U.S. funds and accompany request. If available, single copies and back issues are \$5.00 each (in the U.S.). This publication is available on microfilm/fiche from University Microfilms International, 300 N. Zeeb Road, Ann Arbor, MI 48106 USA (313) 761-4700. POSTMASTER & SUBSCRIBERS: Please send address changes to: R.F. Design, P.O. Box 6317, Duluth, MN 55806.

Looking at the Trends in RF Design



James MacDonald
Editor

For the final six months of 1985 the monthly Special Reports will be about current and anticipated changes in RF circuit components and designs. Topics are grouped into two themes: The New Look in RF Circuits and New Uses of RF Energy.

July, August and September will be devoted to the new look in RF circuits. In July, we will report on new materials being used in components and assemblies, including substrates; conductors, semiconductors and nonconductors; platings and coatings; and encasements. In August, the subject will be miniaturization, and we will examine the ways designers are reducing the size and weight of circuits to meet stricter requirements and the problems they must overcome. In September, the subject is packaging. In this report we will describe new ways of mounting and connecting components and printed circuits for miniaturization and reliability under physical and thermal stress.

Of course, it is not possible to separate completely materials, minaturization and packaging. For example, new materials have helped make minaturization possible, which has made new packaging and mounting techniques necessary.

While each Special Report will concentrate on one subject, these three months will indeed feature a series of articles about what is happening to RF circuits.

In October, November and December we will look at the relatively unknown ways RF energy is being used in three important fields. The subject for October is medical use of RF, such as magnetic resonance imaging, biosonics and thermal treatments. In November, we will look at the rapidly expanding field of EMI measurement, including measurement equipment, antennas, enclosures, open field sites and the major EMI standards. Finally, we will take a general look, in December, at little-known commercial and military uses of RF, such as device controls, near field communications and some surprising applications.

It is an ambitious undertaking — one which could occupy a large staff of investigative writers. A large staff we do not have, but we have the advantage of a large readership of engineers working in all these areas and marketing specialists who know about the latest products, and we are counting on our readers to help us uncover some of the material for these Special Reports.

This is an invitation to write or phone us about anything you think is new or little-known in RF circuit design or application. Call or write soon. Information received far ahead of publication will be kept on file and used as needed.

These Special Reports are topical. We do not attempt in-depth research into the subjects. We try to assemble as much information as possible to learn the latest developments in an area of interest and to discover trends. Our goal is to keep our readers aware of changes that might relate to their work. We leave it up to our contributing authors to explain design ideas and applications in depth.

We welcome such articles, for which we pay \$50 per printed page. Technical articles should be no more than six pages, although exceptions can be made. Normally, one magazine page equates to three double-spaced typewritten pages.

James M. MacDonald

The Design of EMI Hardened Connectors

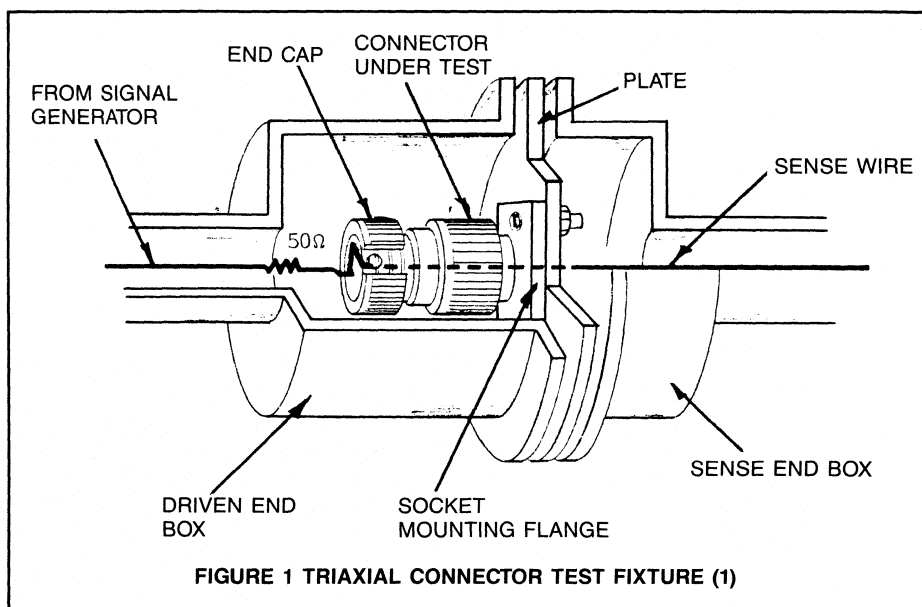
By Mike Van Brunt, Manager
G & H Technology, Inc.

In an interconnecting subsystem composed of the cable, connector and backshell accessories, the connector has been the most susceptible to the effects of electromagnetic interference. The following discussion will consider the high-density circular version, the easiest to which to apply good shielding techniques. Shapes such as rectangular or D-forms pose greater shielding difficulties, causing designers to be creative to seal off energy leakage paths.

The connector can be visualized as a region in the cable shield containing various sizes and shapes of apertures through which radiated or conducted electromagnetic fields may penetrate. It is the design group's objective to minimize the leakage of these apertures, thus increasing the performance of the connector.

The basic circular connector design is two telescoping cylinders. The initial task of the designer will be to tolerance these cylinders to fit as closely as possible in mass production and still maintain reasonable mechanical clearance. Under these conditions a continuous metal-to-metal contact around the circumference is extremely unlikely. When an electromagnetic field impinges on the surface of the cylinders, a current is driven from one cylinder to the other. This current will constrict at the points of contact causing an undesired voltage drop proportional to the specific contact resistances.

It is common practice for connector designers to minimize this problem by using uniformly designed contact fingers properly joined to one of the mating cylinders. These fingers are designed to replace the partial contact between cylinders with a uniform 360° contact, broken only by the necessary gaps between fingers. It is imperative that the design group understand the importance of



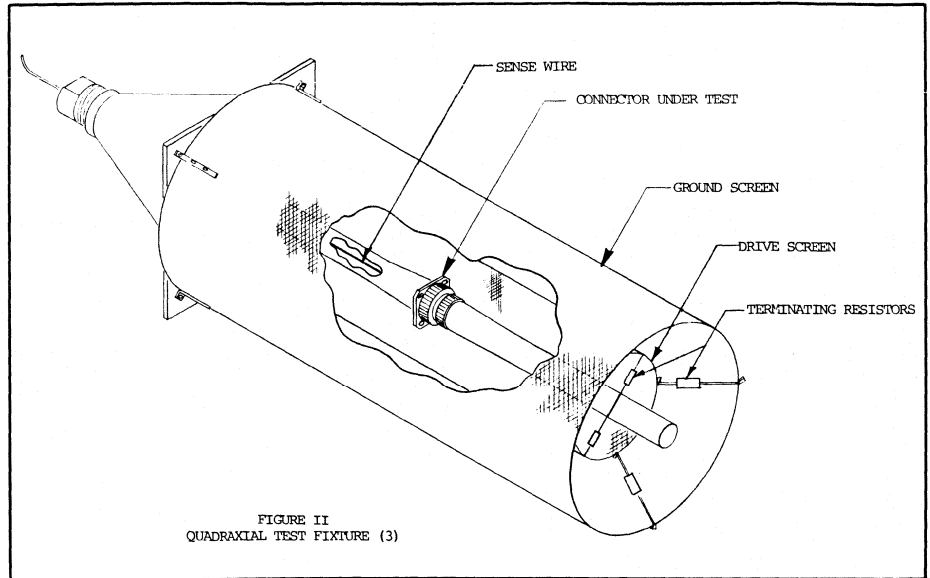
bonding the fingers properly to one of the mating cylinders. A metal-to-metal bond, if practical, will give the best results.

The importance of obtaining a uniform bond between the contact fingers and mating cylinder cannot be overstressed. If this bond is not uniform, we again experience constriction of the current flow resulting in poor connector performance. In the final analysis, the designer must understand and manage the current distribution over his sample, using such tools as geometric shapes, materials and platings.

We need to digress for a moment to discuss methods for determining the shielding performance of connectors. For convenience, we will limit the discussion to the frequency range of 10 kHz to 100 MHz. This frequency range is of interest

when designing electrical connectors that provide some degree of protection against such transient phenomena as lightning and EMP. By limiting the frequency we are able to use well known and proven test methods that incorporate transmission line theory and produce data related to surface transfer impedance. Examples of these test devices include the triaxial fixture (Figure 1) and a quadraxial (Figure 2).

The connector can be viewed as a type of shielded enclosure. A shielded enclosure is intended to isolate elements inside the enclosure from electromagnetic fields outside the enclosure. In the case of the connector, the contacts are isolated from the external electromagnetic environment. Shelkunoff (2) and others have analyzed the mechanisms by which electromagnetic energy penetrates a cable



shield. This energy penetrates by diffusion at low frequency through the thickness of the metal shield and by electric and magnetic coupling through apertures and other shield imperfections. It has been shown that diffusion and magnetic field coupling can be combined into an ex-

pression for transfer impedance as follows:

$$Z_{tr} = \frac{V}{I_o} = R \frac{\gamma d}{\sinh \gamma d} + j\omega M_l$$

where:

I_o = total current flowing on the shield
 V = open circuit voltage generated by skin current

R = DC resistance of the shield

d = thickness of the shield

M_l = mutual inductance of the shield between internal and external surfaces

$\gamma = (1 + j) / \sigma$

$S = (\pi f \mu \sigma)^{-1/2}$ = skin depth in the shield material

$\omega = 2\pi f$

The transfer impedance can be measured using fixtures that incorporate transmission line theory, such as the triax (Figure 1) and the quadraxial (Figure 2).

In recent years the term "shielding effectiveness" has been commonly used as a measure of the quality of the shield. Many military specifications have adopted this term in relation to qualifying hardware. The problem arises in relating the test data, which yields transfer impedance numbers, and the specification, which dictates shielding effectiveness numbers.

The contractor should be aware of this problem and during the formulation of the EMC control plan take the necessary precautions to avoid contract disputes.

References

1) Madle, P.J. Test Procedure to Measure the Transfer Impedance of Shielded Connectors, Tubular Cable Shield and Assemblies.

2) Shelkunoff, S.A. "The Electromagnetic Theory of Coaxial Transmission Lines and Cylindrical Shields." Bell System Tech Journal.

3) Miller, J.S., Calibrated Quadraxial System for Measuring Shielding Transfer Impedance.

Mike Van Brunt is manager of the Electromagnetics Laboratory, G & H Technology, Inc., 750 West Venture Blvd., Camarillo, CA 93010.



Predict PLL Transient Response With Computer Simulation

By Stan Zubiel
Resdel Engineering Corporation

In phase-locked loop design it is often necessary to determine the loop's response to an instantaneous step change of frequency. Data recovery loops and frequency hopping synthesizers are usually required to settle to within a small frequency offset in a predictable length of time. Calculation of the total loop acquisition time is difficult and often misleading because of the approximations and linear assumptions used.

This article presents a BASIC computer program that simulates the popular second-order PLL and produces its closed-loop transient response. Unlike the analytical method, it does not require a determination of the loop's pull-in, hold-in or lock-in ranges. The initial frequency conditions, gain constants and loop filter

component values are all that are needed to perform the simulation. Errors related to the time delay introduced by the digital divider (1) and by the non-linearity of the phase/frequency detector are eliminated because the software simulation accurately models each component of the loop.

As a result, the instantaneous values of parameters such as VCO frequency and phase detector output voltage can be predicted easily without the necessity of an engineering breadboard evaluation to verify the predicted response.

PLL Model

The computer program simulates the schematic diagram of the type two second-order PLL(2) described in Figure 1, which typifies the basic configuration used in many indirect frequency synthesizers.

A differential amplifier (A_1) operating on the digital outputs of the phase/fre-

quency detector produces the DC transfer function shown in Figure 2. It compares the phase of the divided VCO frequency with the phase of the reference frequency to provide a corrective DC voltage to the VCO. At phase offsets greater than $\pm 2\pi$ the detector output limits at $\pm V_{max}$.

During the time that the phase detector is in limiting, cycle slipping occurs and the loop filter output voltage ramps toward its final value. This frequency discrimination property is most readily observed when the offset of the VCO is large compared to the loop natural frequency, f_n .

The active second-order loop filter (A_2) is configured with the non-inverting input connected to ground. Because the filter acts as a perfect integrator its output will stabilize at the VCO control voltage necessary to reduce the phase detector output (V_1) to zero volts. Closed-loop dynamic performance is determined by the filter component values and the scale

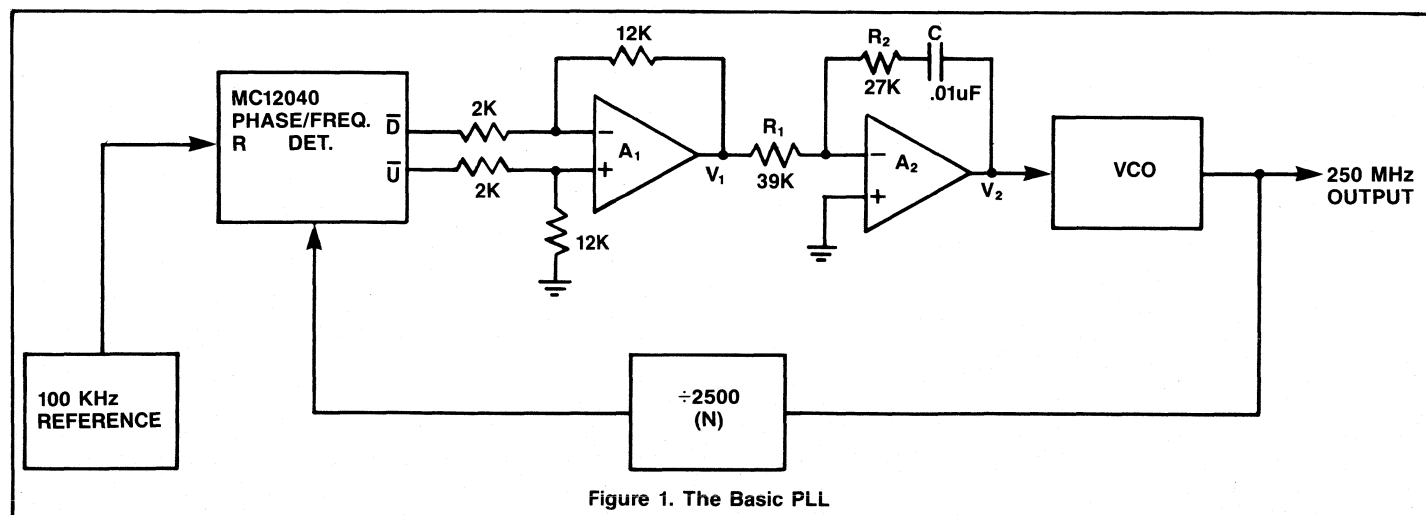


Figure 1. The Basic PLL

factors of the other loop gain elements according to the following relations:

$$\text{Natural frequency, } f_n = \sqrt{\frac{K_{PD} K_{VCO}}{2\pi N R_1 C}}$$

where: K_{PD} =Phase Detector Gain (v/rad)
 K_{VCO} =VCO Gain (Hz/v)
 N =Feedback Frequency Divider Ratio

Damping Factor, $\xi = \pi f_n R_2 C$.

The VCO produces an output frequency proportional to its control voltage input:

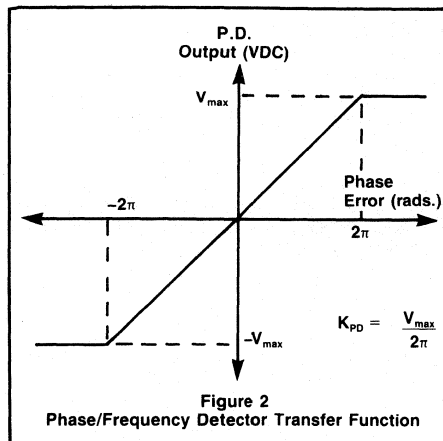
$$f_{VCO}(V_2) = f(0) + K_{VCO} V_2$$

where: V_2 =VCO control voltage, and
 $f(0)$ =VCO frequency at zero volts input.

Figure 3 illustrates the linear VCO tuning curve operating with a bipolar control voltage. The digital divider in the feedback path reduces the VCO frequency by the factor N , which is any positive integer value.

Computer Simulation Model

The second-order PLL just described can be modeled using accumulator registers to perform the integrator functions associated with the loop filter and VCO. The simulation accuracy depends on how often the accumulator values can be updated. However, in phase-locked loops involving digital frequency dividers and phase detectors, changes to the phase error voltage cannot occur at a rate

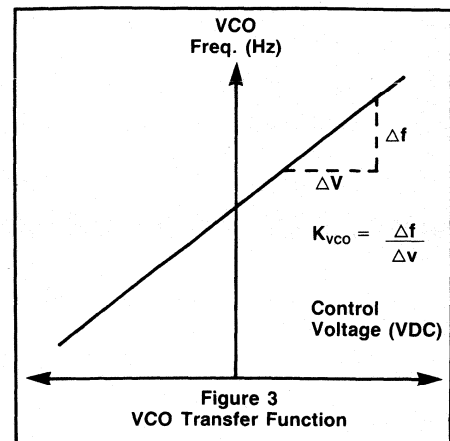


greater than the reference frequency. This permits an accurate closed-loop simulation to be implemented in BASIC using an iteration period T equal to the reciprocal of the reference frequency. The transfer functions described in Figures 2 and 3 are modeled mathematically using the specific loop constants to produce the simulation model of Figure 4. The phase detector so modeled will produce a DC output voltage (at $t=nT$ and phase offsets less than $\pm 2\pi$):

$$V_1(nT) = 2\pi T K_{pd} \left[\frac{1}{N} \sum_{i=0}^{n-1} f_{VCO}(iT) - n \cdot f_{REF} \right]$$

Applying the same modeling technique to the loop filter, the VCO control voltage is produced:

$$V_2(nT) = -\frac{1}{R_1} \left[R_2 \cdot V_1(nT) + \frac{T}{C} \sum_{i=1}^n V_1(iT) \right]$$



The minus sign in the equation is due to the phase inversion produced by the active filter.

The PLL Program

The 51 line simulation program is shown in Figure 5. Although it is written for the HP-9836 it is compatible with most other versions of BASIC, with minor modifications. Loop constants and initial frequency conditions are entered into the program from the keyboard in response to prompt commands. The loop's natural frequency and damping factor are then computed from the constants entered. Next, the user is asked whether to continue or terminate execution of the program. If continuation is selected, the values of VCO frequency and control voltage along with phase detector angle and output voltage are printed each time an iteration cycle is completed.

Computation begins with the VCO frequency at the specified initial value.

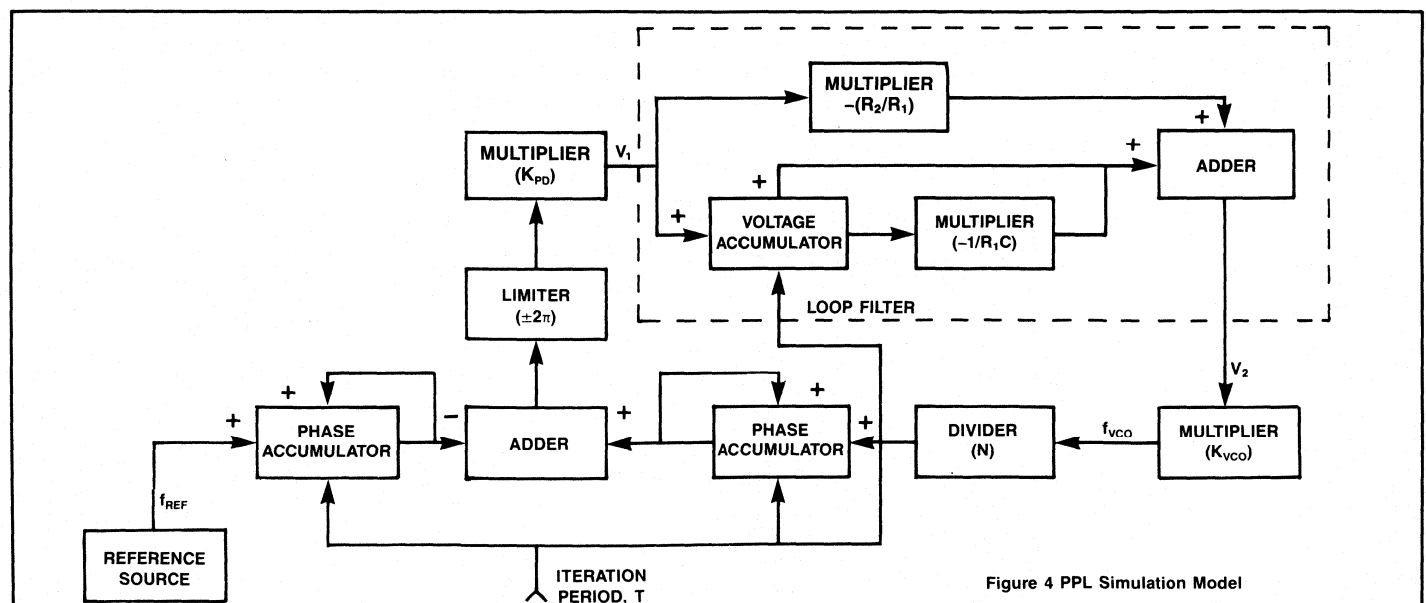


Figure 4 PLL Simulation Model

```

10 PRINT CHR$(12)
20 INPUT "Ref. Freq.(Hz)=",Fr
30 INPUT "Initial VCO Freq.(Hz)=",F1
40 INPUT "Desired VCO Freq.(Hz)=",F2
50 INPUT "Phase Det. Gain(V/rad)=",Kp
60 INPUT "V.C.D. Gain(Hz/v)=",Kv
70 INPUT "R1(Ohms)=",R1
80 INPUT "R2(Ohms)=",R2
90 INPUT "C(F)=",C
100 PRINT TAB(18);"Ref. freq.(Hz)=",Fr;TAB(11);"Initial VCO Freq.(Hz)=",F1;TAB
(11);"Desired VCO Freq.(Hz)=",F2;TAB(10);"Phase Det. Gain(V/rad)=",Kp
110 PRINT TAB(18);"VCO Gain(Hz/v)=",Kv;TAB(24);"R1(Ohms)=",R1;TAB(24);"R2(Ohms)
=",R2;TAB(28);"C(F)=",C
120 PRINT
130 Twopi=6.283185308
140 K1=-1/R2/R1
150 Fv=F1
160 N=F2/Fr
170 Wn=SQR(Kp*Twopi)=Kv/N/R1/C
180 Dp=Wn/R2=C/2
190 Fm=Wn/Twopi
200 Tr=1/Fr
210 K2=-1/Tr/R1/C
220 PRINT TAB(19);"Natural freq.=";Fm;"Hz";TAB(18);"Damping Factor=";Dp
230 PRINT
240 PRINT "CONTINUE? (Y/N)"
250 INPUT Z$
260 IF Z$="Y" THEN 510
270 PRINT CHR$(12)
280 PRINT "-----"
290 PRINT "      T(msec)      ";CHR$(124);"      Fvco(MHz)      ";CHR$(124);"VCO CONT.(v
dc)";CHR$(124);"PD Output (vdc)";CHR$(124);"PD Angle (dgs)"
300 PRINT "-----"
310 PRINT "      ";CHR$(124);"-----"
320 IF I=0 THEN 380
330 Pw=Fv/N;Fv=Fv+Pw
340 Pr=Fv-Pr;Tr=1
350 IF ABS(Y3)<360 THEN 380
360 Pw=Pr+SGN(Y3)*360
370 Y3=SGN(Y3)*360
380 Y2=Y3+Kp*Twopi/360
390 A1=A1-Y2-K2
400 Y1=A1-Y2-K1
410 Fv=F1+Y1*Kv
420 Xt=INT(Tr*I+1.E-9)
430 X0=INT(Fv*10)=1.E-7
440 X1=INT(Y1*1.E+6)+1.E-6
450 X2=INT(Y2*1.E+6)+1.E-6
460 X3=INT(Y3*1.E+4)+1.E-4
470 PRINT TAB(2);Xt;TAB(16);CHR$(124);X0;TAB(32);CHR$(124);TAB(35);X1;TAB(48);
CHR$(124);TAB(51);X2;TAB(64);CHR$(124);TAB(67);X3
480 I=I+1
490 IF INT(I/50)-I/50 THEN 230
500 GOTO 320
510 END

```

FIGURE 5 PROGRAM LISTING

```

Ref. freq.(Hz)= 100000
Initial VCO Freq.(Hz)= 1.75E+8
Desired VCO Freq.(Hz)= 2.5E+8
Phase Det. Gain(V/rad)= .8
VCO Gain(Hz/v)= 1.E+7
R1(Ohms)= 39000
R2(Ohms)= 27000
C(F)= 1.E-8

```

```

Natural freq.= 1142.75400344 Hz
Damping Factor=.969318247285

```

CONTINUE? (Y/N)

T(msec)	Fvco(MHz)	VCO CONT.(vdc)	PD Output (vdc)	PD Angle (dgs)
0	175	0	0	0
.01	185.8264116	1.082641	-1.507965	-108.0001
.02	195.4766649	2.047666	-2.798252	-200.41
.03	204.064726	2.906472	-3.894508	-278.9236
.04	211.6941735	3.694173	-4.818052	-345.0704
.05	218.4261962	3.942619	-5.026549	-360
.06	215.7150547	4.071505	-5.026549	-360
.07	211.0039132	4.200391	-5.026549	-360
.08	218.2927718	4.329277	-5.026549	-360
.09	219.5816303	4.458163	-5.026549	-360
.1	220.8704888	4.587048	-5.026549	-360
.11	221.1593473	4.715934	-5.026549	-360
.12	223.4482059	4.844820	-5.026549	-360
.13	224.7370644	4.973706	-5.026549	-360
.14	226.0259229	5.102592	-5.026549	-360
.15	227.3147814	5.231478	-5.026549	-360
.16	228.60364	5.360364	-5.026549	-360
.17	229.8924985	5.489249	-5.026549	-360
.18	231.181357	5.618135	-5.026549	-360
.19	232.4702155	5.747021	-5.026549	-360
.2	233.7590741	5.875907	-5.026549	-360
.21	235.0479326	6.004793	-5.026549	-360
.22	236.3367911	6.133679	-5.026549	-360
.23	237.6256496	6.262564	-5.026549	-360
.24	238.9145082	6.391450	-5.026549	-360
.25	240.2033667	6.520336	-5.026549	-360
.26	241.4922252	6.649222	-5.026549	-360
.27	242.7810837	6.778108	-5.026549	-360
.28	244.0699423	6.906994	-5.026549	-360
.29	245.3588008	7.035880	-5.026549	-360
.3	246.6476593	7.164765	-5.026549	-360
.31	247.9365178	7.293651	-5.026549	-360
.32	249.2253764	7.422537	-5.026549	-360
.33	250.5142349	7.551423	-5.026549	-360
.34	251.7288525	7.672885	-5.016209	-359.2596
.35	252.7655349	7.776553	-4.981443	-358.77
.36	253.6435927	7.864359	-4.925845	-352.7877
.37	254.3806652	7.938066	-4.852586	-347.5409
.38	254.9925629	7.999256	-4.764507	-341.2327
.39	255.4935441	8.049354	-4.664126	-334.0434
.4	255.8964688	8.089646	-4.553672	-326.1327
.41	256.2129088	8.12129	-4.435116	-317.6418
.42	256.4532712	8.145327	-4.310198	-308.6952
.43	256.6269065	8.16269	-4.180448	-299.4025
.44	256.7422078	8.17422	-4.047206	-289.8598
.45	256.8067005	8.18067	-3.911646	-280.151
.46	256.8271245	8.182712	-3.774789	-270.3493
.47	256.8095088	8.18095	-3.637521	-260.5189
.48	256.7592391	8.175923	-3.500608	-250.7126
.49	256.68112	8.168112	-3.364705	-240.9793

CONTINUE? (Y/N)

FIGURE 6 SAMPLE PROGRAM PRINTOUT

This can be interpreted as the steady state output frequency of a synthesizer just prior to being commanded to a new channel by a change in the value of N. In the case of a PLL being used as an FSK demodulator, the initial VCO frequency corresponds instead to a Mark or Space immediately before the next logic transition.

As the program advances, the peak overshoot and undershoot values of the output parameters can be readily observed. After every 50 lines of output data the program pauses and interrogates the user whether to continue or end the simulation.

Simulation Example

The results of the PLL simulator are demonstrated using the frequency synthesizer of Figure 1. The loop component values are entered into the program in

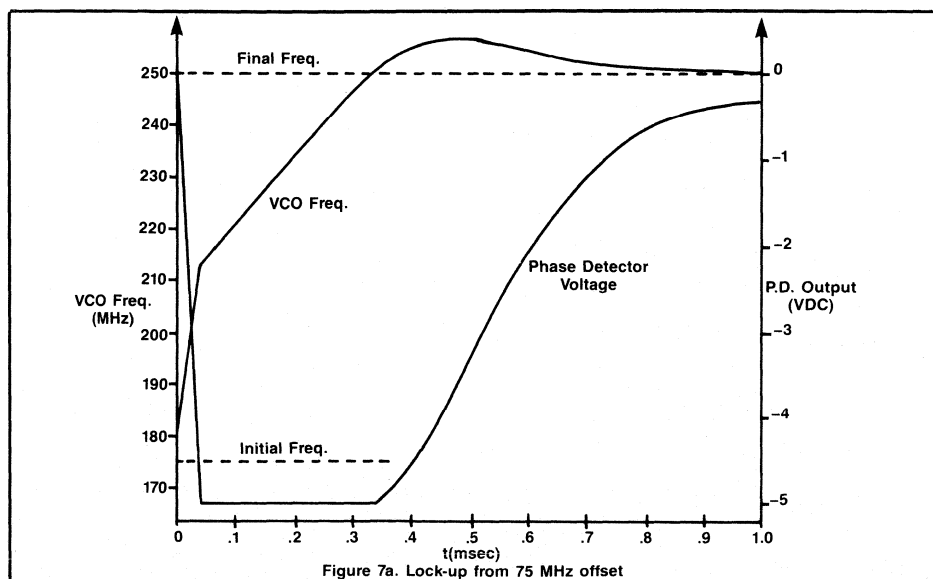
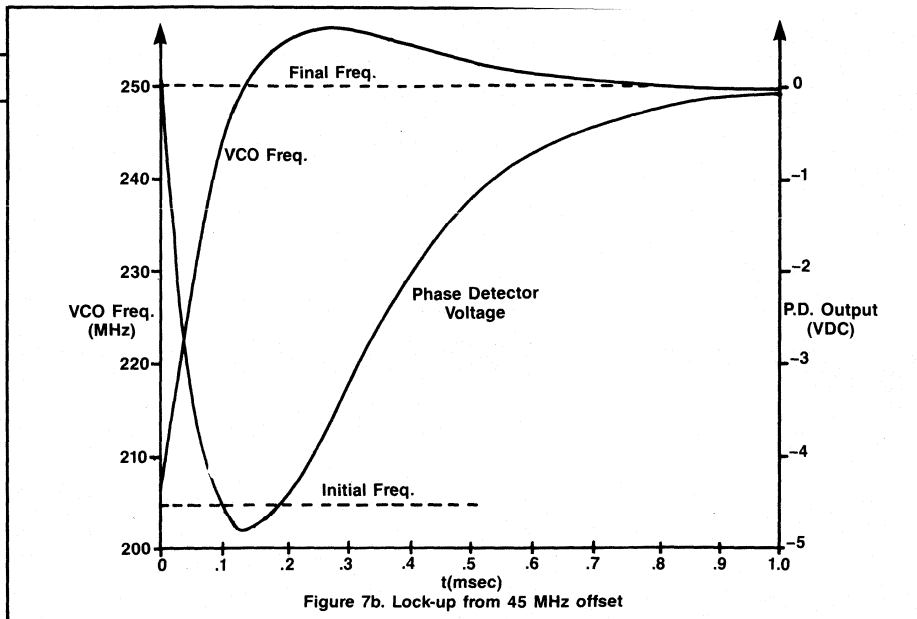


Figure 7a. Lock-up from 75 MHz offset

response to INPUT statements. The initial VCO frequency is set at 175 MHz and will settle to its final value of 250 MHz. Before the simulation begins all the loop constants are printed along with the computed natural frequency and damping factor, as shown in Figure 6.

In this example, output data is printed for every 10 microseconds, the reference frequency period. Because the initial frequency offset of the VCO is large (75 MHz) the phase detector output reaches limiting almost immediately. This is indicated by the constant -360 degree PD Angle shown in the sample printout. During the period that the phase detector output is limiting it acts as a frequency discriminator and causes the VCO to ramp linearly towards its final value. At 460 microseconds, peak frequency overshoot occurs, verifying the critically-damped second-order loop response (3).

The tabulated values of VCO frequency and phase detector output voltage are plotted in Figure 7a. This plot dramatically illustrates the unusual behavior of the loop due to its large initial frequency offset. Figure 7b is the transient response of the same loop as it pulls in from a 45



MHz offset.

Once the program is loaded, many engineering hours can be saved in assessing the effects of various conditions by letting the software do the work.

References

1. A.B. Przedpelski, "PLL Primer, Part III", *RF Design*, July/August 1983.
2. Floyd M. Gardner, "Phaselock Tech-

niques", 2nd Edition, John Wiley and Sons, N.Y., 1979.

3. Garth Nash, "Phase-Locked Loop Design Fundamentals", Motorola Application Note AN-535.

Stan Zubieli is manager of the RF Technology Group, Resdel Engineering Corp., 300 East Live Oak Avenue, Arcadia, CA 91006.



Broadband Leveling in Pulsed Operation

By Joseph J. D'Agostino
Thomson-CSF Components Corp.

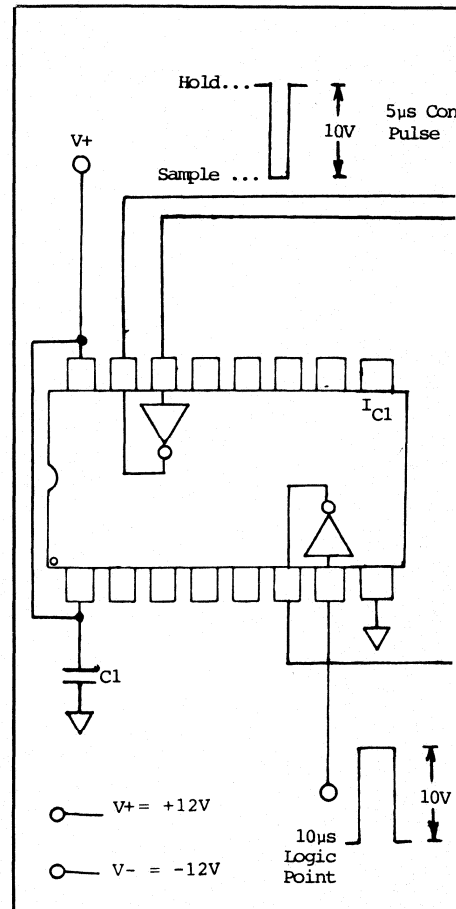
RF power amplifier circuit design has been described many times as magic or black art. This is due primarily to the discrepancies encountered between the circuit designed on paper and the finished product. Most of the time, the two resemble each other, but once in a while it is hard to find a similarity between theory and reality. Nevertheless, a large degree of bench work may be necessary to achieve the desired performance from a given amplifier. Typically, the effort required for a broadband amplifier (>10% bandwidth) is greater than for a narrow-band amplifier (1% bandwidth). This is true because the impedance of a transistor can change with frequency and it can be difficult to design circuitry to track a changing impedance.

Most semiconductor manufacturers try to hold a transistor's input and output impedance constant across the intended operating frequency band, but sometimes it is necessary to design outside this band. In this situation the "Q" of the internal matching section of a transistor may not allow a constant impedance across the frequency window. The typical solution to this design effort is to design around a nominal value of impedance and then fine tune the circuit by evaluating it in a "swept" setup.

The idea behind a swept setup is to

"sweep" across a band of frequencies in some time interval while delivering a fixed power level to the circuit under test. As long as the input power to the circuit is constant, adjustments can be made to achieve a "flat" output power response as a function of frequency. The input power level is held constant by a feedback loop which corrects the level of the sweeping generator by detecting the RF to obtain a DC reference. This DC reference allows the generator to compensate for changes in attenuation in post amps and couplers with frequency. Any change in power level is immediately seen as an increase or decrease in DC reference which will correct the generator accordingly.

The swept setup works very nicely to build CW broadband amplifiers; however, a problem develops when trying to sweep a pulsed amplifier. Most radar amplifiers are pulsed with RF for some short time period and then left idle for the remainder of the cycle. The typical test setup consists of a CW generator driving a post amp that is being pulsed (Figure 1). The problem arises when a pulsed feedback is used to level the generator. Instead of a continuous DC reference, as in the case of a CW setup, the pulsing of RF results in an intermittent DC reference. The duration of this intermittent DC is normally not long enough for the generator to use it as a reference because typical correction circuitry response time is usually slow.



As an example, when RF is pulsed, DC is present in the feedback loop and, given enough time, automatic leveling can occur. However, during the off time there is no reference and the power level can "wander." The long recovery from off time to on time prevents the pulsing DC from being used for a correction voltage.

The following circuit cures this problem and allows a pulsed setup to be swept while delivering a fixed power level to the circuit under test. The problem of intermittent feedback is taken care of by a sample/hold op amp. The rectified pulsing RF is tracked by sample/hold circuitry in the following manner:

Upon detection of the pulse leading edge, the op amp is in a sampling mode. The "sample" command changes to a "hold" command midway through the pulse. The DC level at the midway point is then held until the next leading edge. This continuous DC level is used as an error correction voltage to correct the generator. Because the DC is always present, there exist no response or recovery time problems.

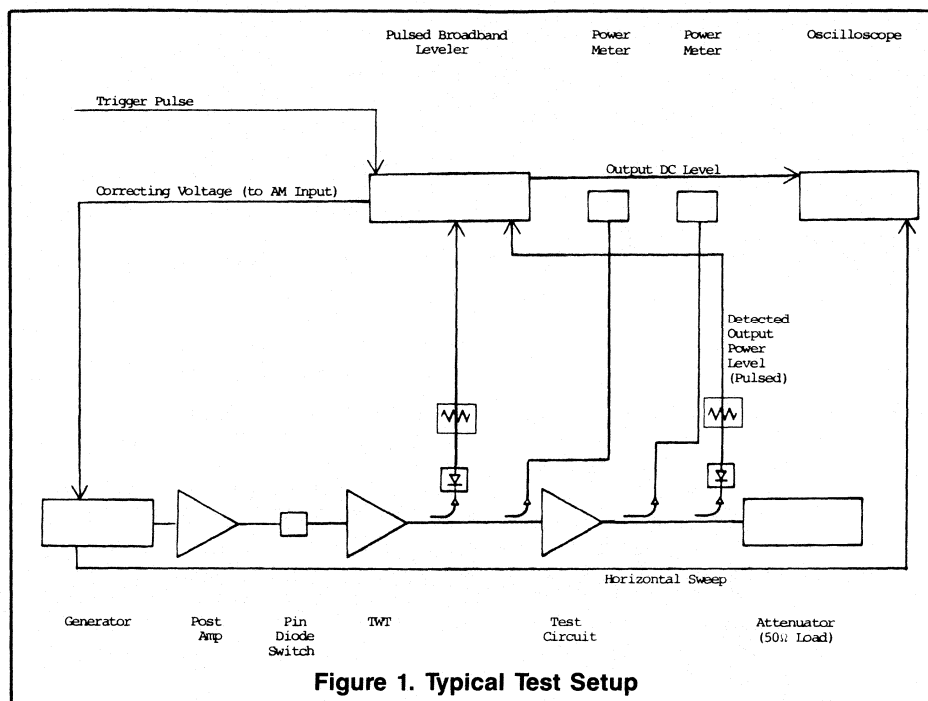
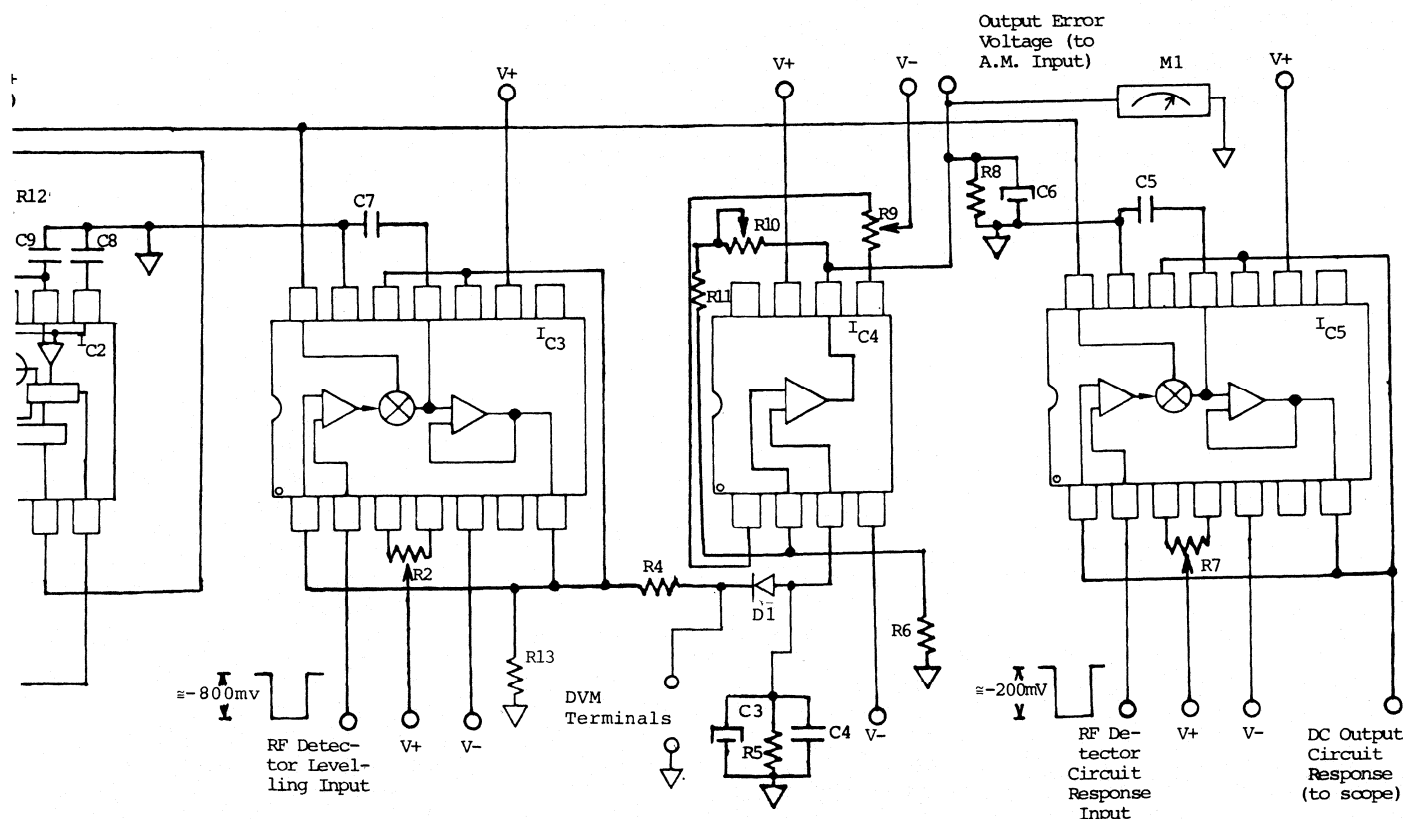


Figure 1. Typical Test Setup

Figure 2. Pulsed Broadband Leveler



Parts List

IC1 = 4009 Inverting Hex Buffer
 IC2 = NE 555
 IC3, 5 = AD583 (Analog Devices)
 IC4 = 741 OP AMP
 C1 = .001 μ F
 C2 = .001 μ F
 C3 = 4.7 μ F
 C4 = 500PF
 C5, 7 = .01 μ F (Polystyrene, Teflon or Mica)
 C6 = 2.2 μ F
 C8 = .01 μ F
 C9 = 100 PF
 C10 = .001 μ F

R1 = 1000 Ω
 R2, 7 = 100K Ω Potentiometer
 R4 = 1500 Ω
 R5 = 10K Ω
 R6 = 120 Ω
 R8 = 470 Ω
 R9, 10 = 10K Ω Potentiometer
 R11, 12 = 1500 Ω
 D1 = 2A, 100V P.I.V. Silicon Diode
 M1 = Modutec Panel Meter
 = (0-15V, ME-6062, DVV015)

plication as long as there is some way for its output power to be varied proportionately to an input voltage. The Wavetek 2002A is an excellent candidate since its AM input port provides this feature. Upon connection of an external DC power supply to the AM input, it can be verified that the output power of the Wavetek 2002A can be decreased with an increase in negative DC. The external a.l.c. port does not work this way, and it is recommended that this generator be kept in the internal a.l.c. mode in this application.

Figure 1 shows a typical setup. The first coupler in the line has a negative detector (Wilttron 73N50) which supplies the pulsing negative DC to the broadband leveler. This leveler converts the pulsing DC to a continuous DC supplied to the AM input jack on the generator. Any increase in power delivered to the test circuit due to changes in attenuation or gain of the post amps results in more negative pulsing DC which in turn results in more negative continuous DC in the feedback to reduce the generator's output power. This provides the necessary feedback, to maintain constant input power to the circuit under test.

Once the input power to the circuit under test is leveled across some frequency band, the ability to determine output power or response of that circuit must be attainable. This is accomplished by a second sample/hold op amp which will supply continuous DC level to the oscilloscope. This DC level then is proportional to the circuit's pulsed output power level.

The pulsed broadband leveler schematic is shown in Figure 2. The pulses shown are from a DME application of 10 μ s pulse width with 1% duty cycle; however, the circuit's ability to operate is independent of pulse format. The whole process starts with a 10 volt logic input supplied from the waveform generator. This logic input must be in perfect sync with the pulse supplied to the PIN diode switch for

RF control (Figure 1). IC1 inverts this logic which is then shaped by the high pass R1C2 to trigger the one shot (IC2). R1C2 differentiates the square wave to an impulse whose duration is governed by the relationship $\tau = RC$. The impulse triggers the NE 555 timer to put out a 5 μ s square wave which will become the sample hold command control pulse after inversion by IC1. The sample command is given as 0 volts and the hold command given at +10 volts. The pulse width of the control pulse can be varied by adjusting the values of R12C9 or R1C2.

IC3 is the sample hold op amp that will be used for leveling the input power to the test circuit. The rectified RF is processed through the AD583. The rise time of this pulse is affected by the impedance termination of the detector. Because the input impedance of the op amp is so high, it is necessary to insert a 1 or a 3 dB pad between the detector and the input to maintain a 50 ohm impedance.

During the sample command the output of the op amp is connected to its input and is tracking the pulse; however, during the hold command C7 is switched in and holds the voltage level last seen by the sample mode. The resulting output continuous DC voltage is amplified by the anti-log op amp IC4. The anti-log or exponential amplification is achieved via the nonlinear voltage to current relationship of D1.

DVM terminals are brought out from the circuit so that the input voltage to D1 can be monitored. Typical values range from -.65 to -1 volts. This voltage level can be achieved regardless of the amount of power being delivered to the test circuit simply by changing the attenuation between the line coupler and the detector. The DVM is only necessary during initial setup of some particular power level and can be removed during operation.

The gain of IC4 is adjustable via R10. IC4 is in the non-inverting mode so that

increased negative DC from IC3 results in more negative DC feedback. The DC level being delivered to the Wavetek 2002A works best around -2.0 volts.

The final part of the circuit is IC5. This chip receives the rectified RF from the output of the test circuit and delivers continuous DC to the vertical input of an oscilloscope. The horizontal sweep of the oscilloscope is controlled by the horizontal ramp output of the sweep generator. This permits a view of test circuit output level with respect to frequency.


Some Tips

Before building the circuit it would be wise to determine the generator's response to the correction voltage (if other than Wavetek 2002A). This can be checked by applying a DC source to the correction input of the generator. For the example given in this article, an increase in negative correction voltage to the AM input port caused less output power from the generator; however, any combination is possible. Keep in mind that the polarity of the op amp is not sacred as long as diode D1 is forward biased.

For example, if a positive pulse is to be sampled and held, D1 would be reversed, but at the same time a negative voltage could still be supplied as a feedback by hooking up IC4 in the inverting mode.

Another point worth checking is the open loop (no feedback) power deviation of the test setup with respect to frequency. Typically, if this deviation is less than 2 dB, the anti-log mode of operation for IC4 is not necessary, meaning that D1 can be bypassed with a short. This provides a linear feedback which is adequate for small corrections. The overall correction limiting factor for this pulsed broadband leveler (whether linear or non-linear) is dependent upon the frequency response of the feedback loop. The coupler providing a sample of RF to the detector should be as flat as possible. It is also important to choose a detector whose output voltage is consistent with frequency so the only change in correction voltage comes from a true change in power level.

The broadband leveler costs less than \$100 to build and can cut the design time in half. It is a worthwhile addition to all pulsed setups.

Joe D'Agostino is an applications engineer at Thomson-CSF, responsible for application circuitry work for high power push-pull and single-ended pulsed VHF, DME and IFF applications. Contact him for information on parts availability or PC layout artwork for this circuit. 

Transistor Parameter Conversion

By Stanley Novak
University of Wyoming

In transistor circuit analysis we use a variety of parameters to characterize transistors at operating point and, in some cases, at operating frequency. In various papers one or another set of parameters is preferred by a particular author, and if a certain design is to be used and we have available only another set of parameters it is necessary to use conversion tables and calculate a particular set of new parameters. This is a tedious and repetitive task sometimes leading to errors in evaluating one or more parameters. Therefore such manipulation is best performed by a suitable computer program, such as the one reported here.

In the engineering process we use relatively few sets of two port parameters to describe behavior of two port networks in general circuit theory. Each set of parameters has some advantage for a particular application; therefore, there is sometimes a need to use a particular set of parameters for an application. Most frequently used in design are impedance (Z), admittance (Y), hybrid (h), ABCD and, in high frequency and microwave design, scattering (S) parameters.

For conversion between various sets of parameters we find more or less complete conversion tables in the literature, for example in (1,2). To make conversion between all five types of parameters we need, theoretically, twenty different conversion equations. By careful inspection of complete tables (which have some errors in the above mentioned sources), we may discover that in certain cases the conversion formula works in both directions for conversion from one parameter set to another. In those cases we may use the general parameter P instead of the particular parameter being converted. For example, for conversion from Z to h parameters $P_{11} = Z_{11}$ and so on.

In this particular case we discover, comparing the resulting "P" chart, that conversion between Z and Y parameters operates both ways. Further inspection of conversion tables results in the conclusion that another two way conversion is valid between Y and h, Z and ABCD, Z and h and Y and S parameters. Therefore, from the original twenty conversion formulas we have five sets

of universal formulas which operate both ways. These may be used as alternative steps for conversion between all parameters if we use these universal relations as subroutines in a computer program for parameter conversion.

The situation may be graphically shown as in Fig. 1. From the graph we could see that the worst case results from conversion between A and S parameters, where we require three conversions (A to Z to Y to S and vice versa). In all other cases we need one or two conversions. We must also be careful about conversion to or from S parameters, which usually are measured and specified for a particular transmission line characteristic impedance, Z_0 . This slightly complicates the situation in this particular conversion but could be taken care of by introducing required formula manipulation in the computer program.

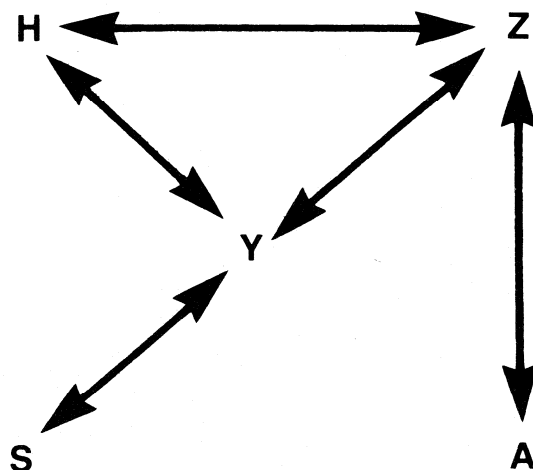


Figure 1. Chart indicating both directions conversion between various two port parameters.

```

READY.
0 REM ***S,NOVAK,OCT,84 *****
10 REM"PARAM.CONV."/8
20 POKE53281,1:POKE53280,1:PRINTCHR$(144)
30 PRINT"PARAM.CONVERSION PROGRAM"
40 DIM R(4),I(4),M(4),A(4),H$(4)
50 A$(1)="INPUT PARAM.(11)="
60 A$(2)="REVERSE PARAM.(12)="
70 A$(3)="FORWARD PARAM.(21)="
80 A$(4)="OUTPUT PARAM.(22)="
90 INPUT"PARAMETERS SUPPLIED?(Z,Y,H,S,A)";P$
100 INPUT"POLAR FORH(P) OR RE,AND IM,PARS(R)";R$
110 INPUT"PARAMETER REQUIRED(Z,Y,H,S,A)";S$
120 IF P$="S"OR S$="S" THEN GOSUB1800
130 IF R$="P" THEN PRINT"ENTER MAGNITUDE AND ANGLE IN DEGREES"
140 IF R$="R" THEN PRINT"ENTER REAL AND IMAG.PART"
150 FORK=1TO4
160 PRINTA$(K),
170 INPUTR(K),I(K)
180 IFR$="P" THEN GOSUB1800
190 NEXTK
200 REM MULTIPLY BY Z0 *****
210 IF P$="Y"AND S$="S" THEN GOSUB1950
220 REM CALC.P12*P21 AND DP*****
230 R1=R(2)
240 I1=I(2)
250 R2=R(3)
260 I2=I(3)
270 GOSUB1700
280 P=RE
290 Q=IM
300 R1=R(1)
310 I1=I(1)
320 R2=R(4)
330 I2=I(4)
340 GOSUB1700
350 R=RE-P
360 I=IM-Q
370 R1=R(1)
380 REM SELECT PARAM.*****
390 IF P$="Z"AND S$="Y"OR P$="Y"AND S$="Z" THEN GOSUB740
400 IF P$="R"AND S$="Z"OR P$="Z"AND S$="R" THEN GOSUB950
410 IF P$="H"AND S$="Z"OR P$="Z"AND S$="H" THEN GOSUB1160
420 IF P$="Y"AND S$="S"OR P$="S"AND S$="Y" THEN GOSUB1360
430 IF P$="H"AND S$="Y"OR P$="Y"AND S$="H" THEN GOSUB540
440 REM DUAL CONVERSIONS *****
450 IF P$="Y"AND S$="R" THEN 460
460 IF P$="R"AND S$="Y" THEN 510
470 GOTO2100
480 P$="Z"
490 GOSUB740
500 GOTO200
510 P$="Z"
520 GOSUB950
530 GOTO200
540 REM CONV.Y TO H OR H TO Y *****
550 R2=R(1)
560 I2=I(1)
570 R1=1
580 I1=0
590 K=1
600 GOSUB2000
610 R1=-R(2)
620 I1=-I(2)
630 K=2
640 GOSUB2000
650 R1=R(3)
660 I1=I(3)
670 K=3
680 GOSUB2000
690 R1=R
700 I1=I
710 K=4
720 GOSUB2000
730 RETURN
740 REM CONV.Y TO Z OR Z TO Y *****
750 R3=R(1)
760 I3=I(1)
770 R1=R(4)
780 I1=I(4)
790 R2=R
800 I2=I
810 K=1
820 GOSUB2000
830 R1=-R(2)
840 I1=-I(2)
850 K=2
860 GOSUB2000
870 R1=-R(3)
880 I1=-I(3)
890 K=3
900 GOSUB2000
910 R1=R3
920 I1=I3
930 K=4
940 GOSUB2000
950 RETURN
960 REM CONV.A TO Z OR Z TO A *****
970 R2=R(3)
980 I2=I(3)
990 R1=R(1)
1000 I1=I(1)
1010 K=1
1020 GOSUB2000
1030 R1=R
1040 I1=I
1050 K=2
1060 GOSUB2000
1070 R1=1
1080 I1=0
1090 K=3
1100 GOSUB2000
1110 R1=R(4)
1120 I1=I(4)
1130 K=4
1140 GOSUB2000
1150 RETURN
1160 REM CONV. H TO Z OR Z TO H *****
1170 R2=R(4)
1180 I2=I(4)
1190 R1=R
1200 I1=I
1210 K=1
1220 GOSUB2000
1230 R1=-R(2)
1240 I2=I(2)
1250 K=2
1260 GOSUB2000
1270 R1=-R(3)
1280 I1=-I(3)
1290 K=3
1300 GOSUB2000
1310 R1=1
1320 I1=0
1330 K=4
1340 GOSUB2000
1350 RETURN
1360 REM CONV.Y TO S OR S TO Y *****
1370 R3=R(1)
1380 I3=I(1)
1390 R1=1+R(4)-R(1)-R
1400 I1=I(4)-I(1)-I
1410 R2=1+R(4)+R(1)+R
1420 I2=I(4)+I(1)+I
1430 IF P$="S"AND S$="Y" THEN R2=R2*Z0
1440 IF P$="S"AND S$="Y" THEN I2=I2*Z0
1450 K=1
1460 GOSUB2000
1470 R1=-2*R(2)
1480 I1=-2*I(2)
1490 K=2
1500 GOSUB2000
1510 R1=-2*R(3)
1520 I1=-2*I(3)
1530 K=3
1540 GOSUB2000
1550 R1=1+R3-R(4)-R
1560 I1=I3-I(4)-I
1570 K=4
1580 GOSUB2000
1590 RETURN
1600 INPUT"CHAR.IMP.OF THE LINE(Z0)=",Z0
1610 RETURN
1700 REM COMPL.NO.MULT.SUB *****
1710 RE=R1*R2-I1*I2
1720 IM=I1*R2+R1*I2
1730 RETURN
1750 REM COMPL.NO.DIV.SUB *****
1760 D=R2*R2+I2*I2
1770 RE=(R1*R2+I1*I2)/D
1780 IM=(I1*R2-R1*I2)/D
1790 RETURN
1800 REM POLAR TO RECT. *****
1810 A=I(K)
1820 M=R(K)
1830 A=A*PI/180
1840 RE=M*COS(A)
1850 IM=M*SIN(A)
1860 R(K)=RE
1870 I(K)=IM
1880 RETURN
1900 REM RECT.TO POLAR *****
1910 M=SQR(RE*RE+IM*IM)
1920 A=90*(SGN(IM)+(IM=0))
1930 IF RE=0 THEN 1950
1940 A=ATN(IM/RE)*180/PI+A*(1-SGN(RE))
1950 RETURN
1960 FORK=1TO4
1970 R(K)=R(K)*Z0:I(K)=I(K)*Z0
1980 NEXTK
1990 RETURN
2000 REM SUB.STORE RESULTS *****
2010 GOSUB1750
2020 R(K)=RE
2030 I(K)=IM
2040 GOSUB1900
2050 M(K)=M
2060 A(K)=A
2070 RETURN
2100 REM SUB.PRINT *****
2110 PRINT"CALCULATED PARAMETER="S$
2120 E=1E4
2130 FORK=1TO4
2140 PRINTA$(K),
2150 PRINT"RE","IM","MAG","ANGLE"
2160 PRINTINT(R(K)*E)/ETAB(10),INT(I(K)*E)/E,INT(M(K)*E)
ETAB(30)=INT(R(K)*E)/E
2170 NEXTK
2180 INPUT"ANOTHER CALCULATION(Y OR N)";C$
2190 IF C$<>"Y" THEN END
2200 GOTO30
READY.

```


The relevant conversions operating both ways may be summarized by using universal P parameters as follows:

$$\begin{aligned} (Z \text{ or } h)_{11} &= \frac{\Delta P}{P_{22}} & (Z \text{ or } h)_{12} &= \frac{P_{12}}{P_{22}} \\ & & & (1) \end{aligned}$$

$$(Z \text{ or } h)_{21} = \frac{P_{21}}{P_{22}} \quad (Z \text{ or } h)_{22} = \frac{1}{P_{22}}$$

$$\begin{aligned} (Z \text{ or } Y)_{11} &= \frac{P_{22}}{\Delta P} & (Z \text{ or } Y)_{12} &= \frac{-P_{12}}{\Delta P} \\ & & & (2) \end{aligned}$$

$$(Z \text{ or } Y)_{21} = \frac{-P_{21}}{\Delta P} \quad (Z \text{ or } Y)_{22} = \frac{P_{11}}{\Delta P}$$

$$\begin{aligned} (Z \text{ or } A)_{11} &= \frac{P_{11}}{P_{21}} & (Z \text{ or } A)_{12} &= \frac{\Delta P}{P_{21}} \\ & & & (3) \end{aligned}$$

$$(Z \text{ or } A)_{21} = \frac{1}{P_{21}} \quad (Z \text{ or } A)_{22} = \frac{P_{22}}{P_{21}}$$

$$\begin{aligned} (Y \text{ or } h)_{11} &= \frac{1}{P_{11}} & (Y \text{ or } h)_{12} &= \frac{-P_{12}}{P_{11}} \\ & & & (4) \end{aligned}$$

$$(Y \text{ or } h)_{21} = \frac{P_{21}}{P_{11}} \quad (Y \text{ or } h)_{22} = \frac{\Delta P}{P_{11}}$$

$$\begin{aligned} (Y \text{ or } S)_{11} &= \frac{1 - P_{11} + P_{22} - \Delta P}{1 + P_{11} + P_{22} + \Delta P} \\ & & & (5) \end{aligned}$$

$$(Y \text{ or } S)_{12} = \frac{-2P_{12}}{1 + P_{11} + P_{22} + \Delta P}$$

$$(Y \text{ or } S)_{21} = \frac{-2P_{21}}{1 + P_{11} + P_{22} + \Delta P}$$

$$(Y \text{ or } S)_{22} = \frac{1 + P_{11} - P_{22} - \Delta P}{1 + P_{11} + P_{22} + \Delta P}$$

$$\Delta P = P_{11} P_{22} - P_{12} P_{21}$$

In the case of conversion from Y to S in the last set of equations (5) we must multiply each Y parameter by characteristic impedance Z_0 before substituting it into the conversion formula. In the case of inverse conversion S to Y, we must divide the resulting parameter by Z_0 .

The Computer Program

The program can be divided into a few significant sections. In the input part the operator must supply information about parameters and whether the input is to be in polar or rectangular form. In the case of S parameters, characteristic impedance of the transmission line must be supplied.

Next the program calculates product ($P_{12} \cdot P_{21}$) and ΔP , which are variables used in all subroutines. It then stores the real and imaginary parts as variables P, Q and R, I, respectively. The next segment deals exclusively with selection of ap-

Fig. 1 Chart indicating both direction conversion between various two port parameters.

Transistor MRF 966 @ 200 MHz ($V_{DS} = 3V$, $I_{DS} = 5mA$)

$S_{11} = 0.99 \angle -4^\circ$; $S_{12} = 0.002 \angle 94^\circ$

$S_{21} = 1.1 \angle 171^\circ$; $S_{22} = 0.96 \angle -3^\circ$

Resulting Y-parameters

$Y_{11} = 1E - 4 + j6E - 4$; $6E - 4 \angle 81.66^\circ$

$Y_{12} = 0 - j1E - 4$; $0 \angle -82.5731^\circ$

$Y_{21} = 0.0112 - j1.1E - 3$; $0.0112 \angle -5.5731^\circ$

$Y_{22} = 4E - 4 + j5E - 4$; $6E - 4 \angle 51.41^\circ$

Transistor 2N5222 @ 200 MHz ($V_{CB} = 10V$, $I_C = 4mA$)

$g_{ib} = 70 \text{ mmho}$; $b_{ib} = 50 \text{ m mho}$

$g_{rb} = 0$; $b_{rb} = -0.7 \text{ mmho}$

$g_{fb} = -53 \text{ mmho}$; $b_{fb} = 58 \text{ m mho}$

$g_{ob} = 0$; $b_{ob} = 2.1 \text{ mmho}$

Resulting S-parameters

$S_{11} = -0.6506 - j0.1926$; $0.6784 \angle -163.51^\circ$

$S_{12} = 7.9E - 3 + j0.0133$; $0.138 \angle 55.15^\circ$

$S_{21} = 0.2054 - j1.5454$; $1.5589 \angle -82.42^\circ$

$S_{22} = 1.0324 - j0.2063$; $1.0528 \angle -11.29^\circ$

Transistor 2N3905 @ 1KHz ($V_{CE} = 10V$, $I_C = 1mA$)

$h_{ie} = 4k$; $h_{re} = 2 \times 10^{-4}$; $h_{fe} = 100$; $h_{oe} = 20 \text{ m mho}$

Resulting 4 parameters

$Y_{11} = 2.5E - 4$; $2.5E - 4 \angle 0^\circ$

$Y_{12} = -1E - 6$; $1.E - 6 \angle -180^\circ$

$Y_{21} = 0.025$; $0.025 \angle 0^\circ$

$Y_{22} = 1.5E - 5$; $1.4E - 5 \angle 0^\circ$

Fig. 2 Examples of conversions

propriate subroutines. Included, with the exception of five direct conversion subroutines are conversions between Y and A and A and Y. The last two subroutines require two conversions, and the reader could add any other conversion needed, according to the outlined process.

The next part of the program is occupied by five direct subroutines, identified in appropriate REM statements. Those subroutines start at lines 540, 740, 960, 1160 and 1360.

The last part of the program is occupied by subroutines for multiplication and division of complex numbers and conversion from polar to rectangular form, and vice versa. Further, this part includes a subroutine for storing results and printing calculated parameters, which are displayed in both rectangular and polar forms.

With little additional effort it would be possible to include an additional loop for converting complete sets of parameters specified for various frequencies or currents, but this is left for an interested reader to do.

The program was written in Microsoft BASIC, which is used in many microcomputers. In this particular case the computer used was the Commodore 64, but the code may be adapted easily to other types of microcomputers. Also, the chosen display of final results was limited by available space on the Commodore 64 screen and limitations of this relatively simple machine.

Figure 2 shows a few examples of conversions between various parameters that could be used for testing the program. The program also will operate with real numbers only, in which case the imaginary part should be entered as zero.

References

- (1). G.D. Vendelin, Design of Amplifiers and Oscillators by the S-parameter Method, John Wiley, 1982, pp. 12-13.
- (2). H.L. Krauss, C.W. Bostian, F.H. Raab, Solid State Radio Engineering, John Wiley, 1980, pp. 110-113.

Circuit Synthesis Using Desk Top Computers

By Ulrich L. Rohde
Communications Consulting Corp.

This article introduces some software approaches that deal with synthesis of circuits and optimization of systems rather than the analysis done by standard CAD packages. However, in order to come up with an initial design, it is essential to find an optimum solution for a particular performance first. It is then possible to analyze parameter sensitivity of the circuit or do other adjustments.

In our initial example, we will address the design and ultimate analysis of digital PLL synthesizers.⁽¹⁾ The reader will agree that this is a complex task, as a large number of different components are part of the system.

Figure 1 shows the block diagram of a digital PLL single loop synthesizer. The building blocks are the VCO, the programmable divider, the phase detector, the loop filter and the reference oscillator. These building blocks compose the minimum phase-locked loop.

Phase-locked loop systems are described by the number of integrators and by the number of poles of the loop filter. A PLL which uses any kind of an active filter is a Type 2 PLL, as the VCO is the first integrator and the active filter the second integrator. For fast frequency lock and the widest possible pull-in range, a tri-state phase frequency discriminator is recommended.

The phase noise outside the loop bandwidth is determined by the performance of the VCO, while the phase noise of the synthesizer inside the loop bandwidth depends mostly on the noise contributions of the frequency standard, the divider noise and the active devices used, like the one we find in the phase discriminator.

Designing the VCO

The optimum circuit configuration of a VCO depends upon the tuning range (percentage bandwidth) or absolute frequency. In practice, it turns out that there are four configurations which can be recommended: a Colpitts oscillator for less than 15% tuning range; a grounded

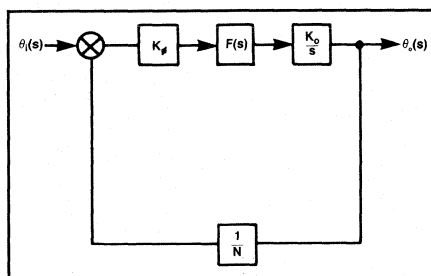


Fig. 1. Block diagram of the second-order PLL.

base oscillator for wide frequency range, like 110-210 MHz; a quarter wavelength oscillator, which sometimes has the drawback of showing "holes" in its oscillation range and at higher frequencies can cause difficulty achieving constant amplitude; or the half wavelength oscillator, which requires a few more components but provides better frequency stability and more consistent outputs as a function of frequency.

Assuming we have to design an oscillator from 470-860 MHz, the computer will determine for us the circuit configuration C and provide the design values as per Table 1.

Phase Noise Analysis

After we have "designed" a circuit, which in reality was done from a look-up table of optimized circuits, we have not answered the question of the phase noise and noise contribution of the system. We have to program the various noise contributions of the individual components. As this has to be done for many fre-

quencies and under different parameter variations, this will become tedious work best suited for a computer. There are certain minimum analysis capabilities which a design or synthesis program must have in order to make an independent choice between various configurations. The noise contributions are best expressed by the following summary:

$$L(f_m) = 10 \log_{10} \left(\text{SQR} \left(\left(\frac{1}{2} \left[1 + \frac{1}{\omega_m^2} \left(\frac{\omega_o}{2Q_{\text{load}}} \right)^2 \right] \right) \right) \right)$$

$$\frac{FkT}{P_{\text{sav}}} \left(1 + \frac{f_c}{f_m} \right)^2 + \frac{(\text{SQR}(4kT_o R_d F) K_o \sqrt{2})^4}{f_m}$$

- ω_n = $2\pi \times$ offset
- ω_o = 2π center frequency
- Q_{load} = loaded figure of merit Q of the tuned circuit
- F = noise figure
- kT = $4.2\text{E-}21$ at 300°K (room temperature)
- f_c = flicker frequency of semiconductor
- f_m = frequency offset
- R = equivalent noise resistor of tuning diode
- dF = integration bandwidth
- K_o = oscillator voltage gain

Please note that the equation determining the mean square value has to use the power 4 for the second term.

By changing the various parameters, one can do a "software-based" simulation of an actual circuit without having to build one. Simulations of this nature are beyond the capabilities and intent of analysis CAD packages. While the more

VCO Design

Calculation of VCO tuning range:

Fmin = 470 MHz Fmax = 860 MHz

Center range is 665 MHz Tuning ratio = 1.830

Cmin (at Vmax) of tuning diode = 2 pF Cmax (at Vmin) of tuning diode = 20 pF

Bipolar transistor chosen: Transistor is operated at Ic = 5 GHz at 3 mA

Output power is 1.8 mW or 2.6 dBm

Board stray capacitance = 1 pF

Strip line oscillator used

Transmission line Z = 123 ohm: Half wave circuit:

Cin = 10 pF Cout (min) = 2 pF: Center conductor is 44.1 mm; Cout (max) = 16.5 pF

Frequency compensated microstrip calculation:

Substrate epsilon = substrate thickness 6 mm width = 6.38 mm

Mechanical length is 44.1 mm

Table 1

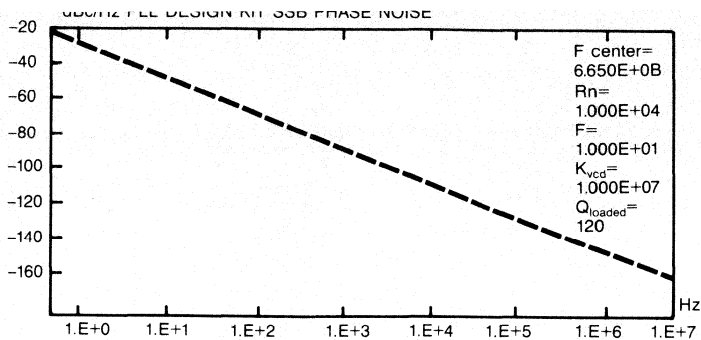


Fig. 2. SSB phase noise of the free-running VCO.

familiar CAD packages like SUPER-COMPACT, Touchstone, or CADEC and CADEC+ can only analyze linear performances, the analysis of a phase-locked loop, for instance, requires the understanding of non-linear models, including approximations for piecewise linear functions. These approximations can be programmed and called by the user.

A Complete System

Since we have designed the VCO now, we might be curious to see how the performance would be in a Type 2 third-order system which provides the best reference suppression and lock-up time with a minimum number of components. Figures 2, 3 and 4 show the phase noise of the open and closed loop system and the schematic of the integrator. Table 2 shows the lock-up function as a function of time. It would have taken about a week if not more to design such a circuit in a breadboard configuration, and maybe another one to two weeks to assemble all the test equipment and do the measurements. It is difficult to determine how long it would have taken to do corrective changes in the circuit design and recertify the performance. The fact that there are non-linear actions taking place requires the use of dedicated programs for such applications.

LOCK-IN FUNCTION :

TIME/s	PHASE DET.DEV./deg
0	3.60E+02
.0016	2.58E+02
.0032	1.16E+02
.0048	2.94E+00
.0064	-7.36E+01
.008	-1.12E+02
.0096	-1.20E+02
.0112	-1.07E+02
.0128	-8.40E+01
.0144	-5.95E+01
.016	-3.79E+01
.0176	-2.12E+01
.0192	-9.55E+00
.0208	-2.37E+00
.0224	1.45E+00
.024	2.99E+00
.0256	3.17E+00
.0272	2.67E+00
.0288	1.93E+00
.0304	1.22E+00
.032	6.45E-01
.0336	2.45E-01
.0352	3.35E-03
.0368	-1.17E-01
.0384	-1.57E-01
.04	-1.49E-01
.0416	-1.19E-01
.0432	-8.34E-02
.0448	-5.13E-02
.0464	-2.65E-02

Table 2

Other Synthesis Solutions

The design of phase-locked loops, which can be done with our PLL Design Kit software package, is only a recent use of CAD. In the last 15 years, synthesis has been primarily used for filter design and our filter design synthesis packages can handle elliptical, Chebyshev, and Butterworth filters. We are currently developing synthesis methods for linear phase filters like Gauss and Thomson/Bessel filters. In the microwave area, helix filters and interdigital filters can be built where mechanical dimensions determine the overall performance.

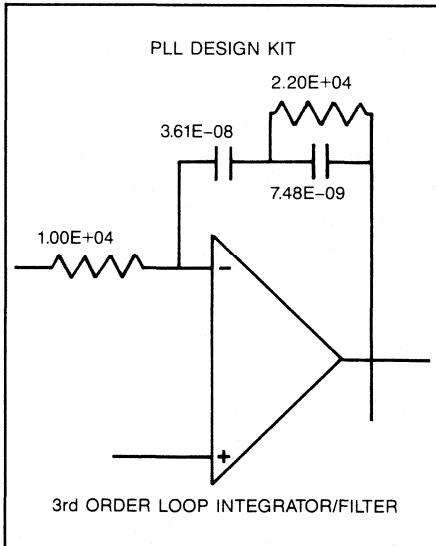


Fig. 4. Schematics of the integrator filter.

Summary

If appropriate mathematical models are developed, it can be shown that circuit and system synthesis programs can enhance productivity and provide answers to technical solutions at a fraction of the conventional design route costs. The key lies in the development of software which has enough flexibility to deal with the intricacy of the various parts of the circuit and make provision for non-linear transfer functions. In other cases, such as filter synthesis programs, where numerical accuracy is important, one has to develop software which has sufficient speed while using double precision mathematics.

1. U.L. Rohde, *Digital PPL Frequency Synthesizers, Theory and Design*, 9183, Prentice-Hall, Inc., ISBN 0-13-214239-2.

Dr. Rohde can be contacted at Communications Consulting Corp., 52 Hillcrest Drive, Upper Saddle River, NJ 07458.

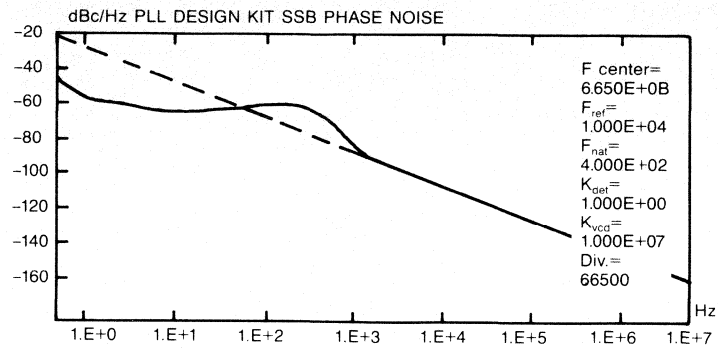
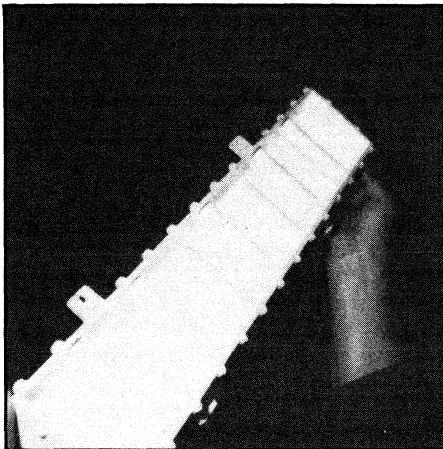


Fig. 3. Phase noise of the free-running and closed loop PLL system.



Cover

The composite cover of this month's issue denotes the theme of the Special Report. This month we take a first look at materials used in RF circuits. The photograph shows a cellular radio interdigital filter after silver plating by Cohan-Epner Company's High-Q process. A metallurgist examines the three plating layers of electroless nickel, copper and High Q silver over the aluminum casting.

Features

23 Special Report: The New Look in RF Circuits — Materials

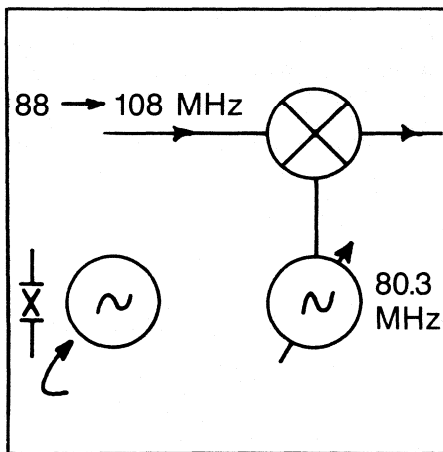
Some of the materials commonly used in RF circuits are described in this special report, along with some new materials not yet in common use. — James N. MacDonald

42 A Computer Algorithm for Mixer Spurious Analysis

The analysis and computer algorithm in this article allow prediction of various mixer spurious signals, including general harmonic analysis, cross-over spurious location, and self-quieting analysis. — Alan M. Victor.

54 Preventing Unwanted Oscillations in Crystal Oscillators Part II

Part II of this two-part article discusses non-crystal controlled oscillations and crystal spurious oscillations, concluding with a discussion of six design verification tests useful for uncovering potential unwanted oscillations — James W. Wieder



Departments

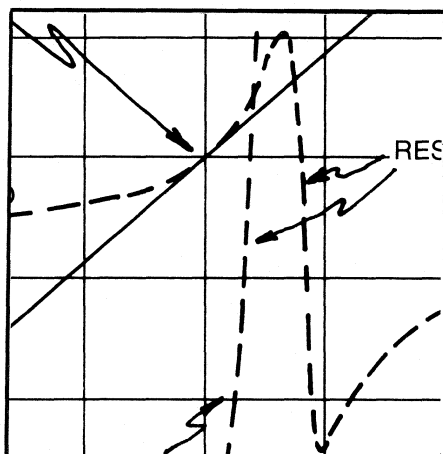
The Designer's Notebook

- 30 This month's Designer's Notebook describes the helical resonator filter and its uses. A BASIC CAD program is given to compute the physical and electrical properties of these filters. — Vincent G. Heesen

RFI/EMI Corner

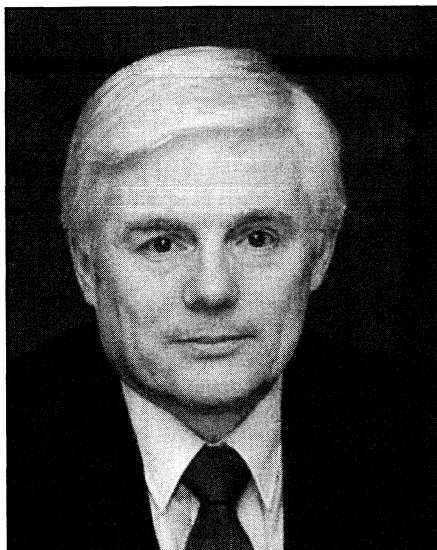
- 32 This article is a brief explanation of some of the characteristics of High altitude Electromagnetic Pulse generated by a nuclear explosion. — Kendall Childers

- 6 Editorial
- 8 Publisher's Notes
- 13 Letters
- 14 Calendar
- 14 RF Courses
- 16 News
- 35 Info/Card
- 62 New Products
- 69 New Literature
- 72 Advertisers Index



R.F. DESIGN (ISSN: 0163-321X USPS: 453-490) is published monthly plus one extra issue in August. July 1985, Volume 8, No. 7. Copyright 1985 by Cardiff Publishing Company, a subsidiary of Argus Press Holdings, Inc., 6530 S. Yosemite Street, Englewood, CO 80111 (303) 694-1522. Contents may not be reproduced in any form without written permission. Second-Class Postage paid at Englewood, CO and at additional mailing offices. Subscription office: 1 East First Street, Duluth, MN 55802, (1-800-346-0085). Domestic subscriptions are sent free to qualified individuals responsible for the design and development of communications equipment. Other subscriptions are: \$22 per year in the United States; \$29 per year in Canada and Mexico; \$33 (surface mail) per year for foreign countries. Additional cost for first class mailing. Payment must be made in U.S. funds and accompany request. If available, single copies and back issues are \$5.50 each (in the U.S.). This publication is available on microfilm/fiche from University Microfilms International, 300 N. Zeeb Road, Ann Arbor, MI 48106 USA (313) 761-4700. POSTMASTER & SUBSCRIBERS: Please send address changes to: R.F. Design, P.O. Box 6317, Duluth, MN 55806.

Helping Engineers Solve Problems



On a recent visit to a major electronics company I was asked by a marketing executive, "How is your magazine different from the others?" It was an unexpected question, but an easy one to answer.

The difference between RF Design and the other electronics trade publications is much more than the obvious — that we concern ourselves primarily with below-microwave frequency devices and designs. The important difference is the nature of our technical articles. They are not written primarily to keep readers informed about new developments. They are written by engineers to share some way the author has found to make the circuit design process easier or faster or to explain the operation of some new type of component.

My explanation to the marketing executive came down to a simple phrase, "We help engineers solve problems." We have written before about how difficult it is for RF design engineers to find the kind of information that appears every month in RF Design. Some of it simply is not available anywhere else, or it is available in such theoretical and mathematical complexity that it is of little use to the busy engineer. The technical articles in RF Design may seem mysterious to people not trained in this field, but to the engineers who read them they are direct, practical and helpful. We know this because they constantly tell us so.

RF Design has another purpose, too. We have written before about the lack of analog circuit design education in our colleges and the problems faced by electrical engineers who find themselves working in this area without sufficient knowledge. It is primarily for them that the special reports and other departments are written. In those pages we discuss more basic design principles and provide fundamental information that may be well known to the more experienced design engineers.

In this expanding and changing field, however, it is difficult for even the experienced engineer to keep up with new products and developments. So in the special reports we emphasize recent products and design ideas to keep our readers aware of trends while also mentioning some of the problems with currently available products. Last month, thinking of the trend toward interfacing analog and digital equipment, we turned the special report pages over to an expert in the digital field for an explanation of an important standard data bus configuration.

A statistical analysis of attendance at RF Technology Expo '85 convinced us that we are on the right track. We found that 45 percent of the engineers who attended that conference had been in engineering five years or less. The percentage dropped rapidly as experience increased, as might be expected for a conference emphasizing fundamentals. What is surprising, however, is that 17 percent of the attendees had been engineers more than 20 years. Statistics can be interpreted in different ways, but to us these figures represent a recognition by experienced engineers that they must keep learning to keep up with developments in their field.

That is what RF Design is for — to help engineers keep learning and solving problems.

*James M.
MacDonald*

Editor:

The article in the May, 1985 issue "Transistor Parameter Conversion" by Mr. Stanley Novak, pages 49-51, prompted me to write to inform you that Mr. Novak has "re-invented the wheel," however his wheel is less than completely circular.

Refer to the enclosed copy of an article from Electronic Design of September 17, 1974, titled "Convert two-port circuit parameters" by Mr. Robert P. Arnold which does more than Mr. Novak's. I have enclosed a copy of my adaptation (the modifications are indeed slight) of Mr. Arnold's program for use on a VAX 11/780 computer. Note that Mr. Arnold's program includes g-parameters and also can go from any parameter-form directly to any other parameter-form which is a distinct advantage. There is no need for interim stops at an unwanted parameter. Sample input data produces outputs which do agree from program to program.

Is there anything you can do to introduce Mr. Arnold's article and program to your readers? I would like to see it mentioned in "Letters to the editor" as a minimum.

Thanks for your consideration and I wish you success with your efforts to continually improve *RF Design*.

Ronald L. Wood
Principal Engineer
E.F. Johnson Co.
Waseca, MN 56093

Readers may contact Mr. Wood for information about his adaptation of Mr. Arnold's program. — editor.

Editor:

(In reference to the article in) April 1985, page 46 "BASIC Program Computes Values for 14 Matching Networks:" Line 270 X2 has to be changed to X3

Line 410 one parenthesis has to be removed

The other on statements will not run on the TI99. They were changed to IF statements. I hope that will help someone else.

170 IF (SGN(X1) = 1 THEN 200 : : IF SGN (X1) = 0 THEN 190

210 IF SGN(X2) = 1 THEN 240 : : IF SGN(X2) = 0 THEN 230

260 IF SGN(X3) = 1 THEN 290 : : IF SGN(X3) = 0 THEN 280

270 F3 = (1/(6.28*FO*X3))*-1

410 X1 = RS*(SQR(RL/RS) / (Q Λ2 + 1 - (RL/RS)))*-1

1345 IF SGN(X1) = 1 THEN 1370 : :IF SGN(X1) = 0 THEN 1360

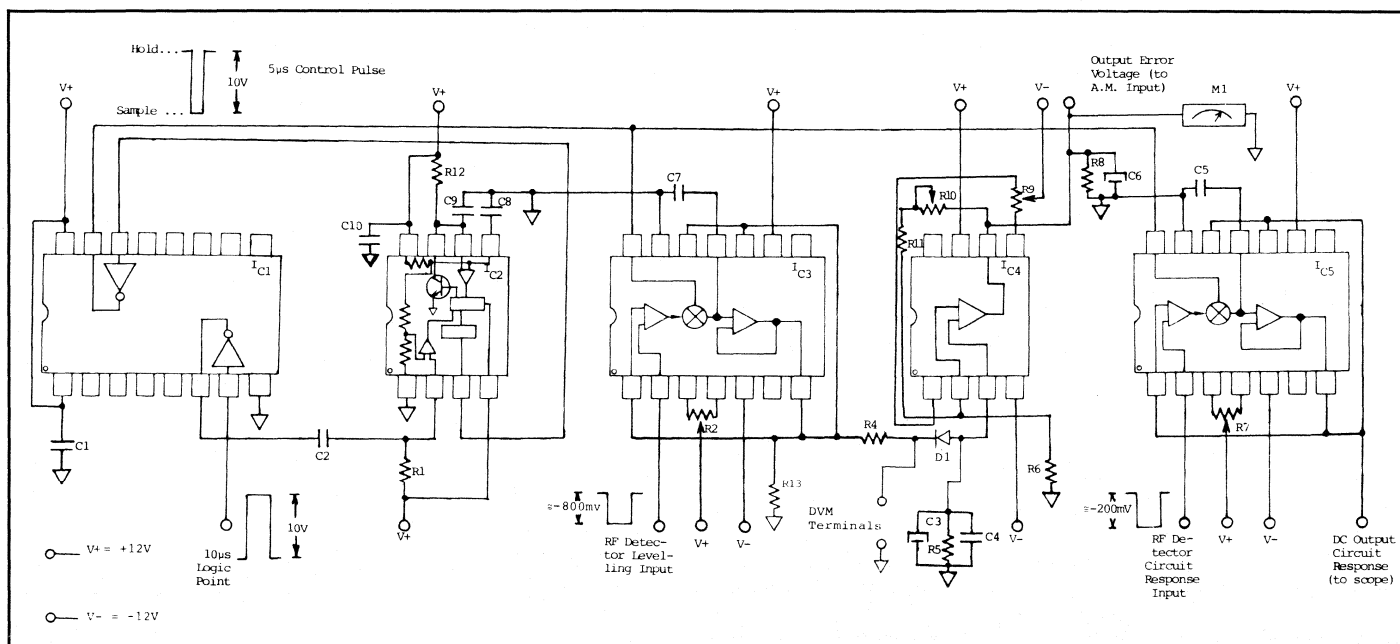
1380 IF SGN(X2) = 1 THEN 1410 : : IF SGN(X2) = 0 THEN 1400

1430 IF SGN(X3) = 1 THEN 1460 : : IF SGN(X3) = 0 THEN 1450

Kurt Bittman
Centereach, N.Y.

Author Alan LaPenn says the program should run on the TI99 as printed. That is what he wrote it on. — editor.

We have received several requests to reprint the circuit diagram from the article "Broadband Leveling in Pulsed Operation" in the May issue. Since part of the figure ended up in the binding and could not be seen, it is reprinted here, reduced to fit one page. — editor.



Helical-Resonator Filter Design

By Vincent G. Heesen
Microcom Corp.
Warminster, Penn.

Helical coil resonators fill the need for small, highly selective bandpass filters exhibiting low insertion loss in the VHF and UHF ranges. A helical resonator consists of a shielded resonant section of transmission line. The center conductor is a helically wound coil. The coil is securely affixed to the shield (outer-conductor) at one end while the other end is open-circuited. In practice, the open circuited end is often terminated in a small trimmer capacitor which serves as a frequency adjustment and mechanical support.

The shield may be cylindrical or square in shape. Shields of square cross section yield unloaded Q_s that are 20 percent higher than cylindrical shields of the same diameter to width. This program will compute the insertion loss of the more probable square shield design, which is easier to make. (An alternate approach, not factored into this program, is to reduce the square shield width by 20 percent of the computed diameter of the cylindrical shield. This will result in the same unloaded Q value; but without the reduction in insertion loss.) Many dimensional variables are found in helical resonator design; however, a number of optimum designs have been developed (1). These designs used in this program define shield/coil diameter-to-length ratio.

Butterworth filters exhibit lower insertion loss than Chebyshev filters of the same Q and bandwidth. Since reduced size and insertion loss are the desirable features of the helical resonator, the program computes the insertion loss of the preferred Butterworth designs. Consult the attenuation curves for Butterworth filters (2) to determine the number of poles (resonators) required to yield the desired rejection outside the passband. The program will accept from two to seven poles.

Coupling into or out of the resonator may be accomplished with probes or coupling loops placed in proximity of the coil or tap directly attached to the coil. In-

ductive coupling of adjacent coils is often achieved through openings in their common shield wall. Determination of the size and location of these apertures defies

```

100 CALL CLEAR
110 PRINT " ***HELICAL RESONATORS***": :
120 REM W.MACALINE, R.SCHILDKNECHT-1959;A.Zverev-1967 & V.Heesen-1985
130 PRINT "THIS PROGRAM CALCULATES THE:" "PHYSICAL and ELECTRICAL:" "PROPERTIES of
HELICAL COIL:" "RESONATORS.": :
140 FO=0 :: ZO=0 :: BW=0 :: RT=0 :: FL=0
150 PRINT :: INPUT "ENTER RESONATE FREQUENCY IN MHz :FO :: IF FO<5 OR FO>500
0 THEN 960
160 PRINT :: INPUT "ENTER RESONATOR IMPEDANCE IN ohms :ZO :: IF ZO<200 OR ZO>
5000 THEN 960
170 D=98*10^3/(FO*ZO):: IF D<1 THEN 180 ELSE DS=INT(D*100)/100 :: U$="inches" ::
GOTO 190
180 DS=INT(D*1000):: U$="mils"
190 LS=1.5*DS :: IF D>1 THEN LS=INT(LS*100)/100 ELSE LS=INT(LS)
200 DC=.55*DS :: IF D>1 THEN DC=INT(DC*100)/100 ELSE DC=INT(DC)
210 L=1.5*DC :: IF D>1 THEN L=INT(L*100)/100 ELSE L=INT(L)
220 N=1900/(FO*D):: N=INT(N*100)/100 :: IF N<3.5 OR N>100 THEN 960
230 QU=50*D*SQR(FO):: QU=INT(QU)
240 QUS=QU*1.2 :: QUS=INT(QUS)
250 SP=(FO*(D^2))/2300 :: SP=INT(SP*100000)/100
260 SD=(2.606/SQR(FO))
270 WN=.4*SP :: WN=INT(WN*100)/100
280 WX=.6*SP :: WX=INT(WX*100)/100 :: IF WX<(5*SD) THEN 960
290 CALL CLEAR :: PRINT
300 PRINT TAB(6);":-----Ds-----": :
310 PRINT TAB(6);":|-----Ds-----|": :
320 PRINT TAB(6);":| :--Dc--|":TAB(20);":| :|": :
330 PRINT TAB(6);":|":TAB(10);":|-----":TAB(17);":|/ :| :|": :
340 PRINT TAB(6);":| ( : : : : |": :
350 PRINT TAB(6);":|":TAB(10);":|-----)- :| :|": :
360 PRINT TAB(6);":| ( : : : : sp:Lc :|": :
370 PRINT TAB(6);":|":TAB(10);":|-----)- :| :|": :
380 PRINT TAB(6);":| ( : : : : |": :
390 PRINT TAB(6);":|":TAB(10);":|-----) :| :|": :
400 PRINT "TAP-----": :
410 PRINT TAB(6);":|":TAB(20);":| :|": :
420 PRINT TAB(6);":| :-----|": :
430 PRINT "Fo="FO;"MHz":TAB(16);":Zo="ZO;"ohms"
440 PRINT "SHIELD DIA. (Ds)="DS;U$
450 PRINT "SHIELD LGTH (Ls)="LS;U$
460 PRINT "COIL DIA. (Dc)="DC;U$
470 PRINT "COIL LGTH. (Lc)="L;U$
480 PRINT "WIRE SPACE. (SP)="SP;"mils"
490 PRINT "QU(round shield)="QU
500 PRINT "QU(square shield)="QUS
510 PRINT :: INPUT "ENTER BW(3DB) IN MHz :BW3 :: QL=FO/BW3 :: Q0=QUS/QL
520 PRINT "WIRE DIA. (MIN.)="WN;"mils"
530 PRINT "WIRE DIA. (MAX.)="WX;"mils"
540 PRINT "NUMBER of TURNS="N
550 PRINT :: INPUT "ENTER No. of POLES (2-7)":NP :: IF NP>7 THEN 550
560 ON NP GOTO 550,570,580,590,600,610,620
570 Q1=1.4142 :: IL=20*LOG((1.4142/Q0)+1)/LOG(10):: GOTO 630
580 Q1=1 :: IL=20*LOG((2/Q0^2)+(2/Q0)+1)/LOG(10):: GOTO 630
590 Q1=.7654 :: IL=20*LOG((2.62/Q0^3)+(3.41/Q0^2)+(2.62/Q0)+1)/LOG(10):: GOTO 630
600 Q1=.618 :: IL=20*LOG((3.24/Q0^4)+(5.23/Q0^3)+(5.23/Q0^2)+(3.24/Q0)+1)/LOG(10)
:: GOTO 630
610 Q1=.518 :: IL=20*LOG((3.84/Q0^5)+(7.42/Q0^4)+(9.11/Q0^3)+(7.42/Q0^2)+(3.84/Q0)+1)/LOG(10):: GOTO 630
620 Q1=.445 :: IL=20*LOG((4.46/Q0^6)+(10/Q0^5)+(14.5/Q0^4)+(14.5/Q0^3)+(10/Q0^2)+(4.46/Q0)+1)/LOG(10)
630 PRINT "INSERTION LOSS="INT(IL*100)/100;"dB"
640 PRINT :: INPUT "ENTER IMPEDANCE OF TAP :RT

```


Southwall Technologies, Palo Alto, Calif., makes a flexible printed circuit called Etch-A-Flex. Southwall uses sputter deposition to fix copper to the plastic substrate. The company says the process allows finer lines and denser circuit designs than systems using adhesives. They say the copper bond is stronger than that achieved with other adhesiveless systems.

Plating

Plating is an important consideration in any discussion of materials. Thin and thick film substrate plating will be discussed in the third article, emphasizing packaging. For plating entire surfaces, such as connector mating surfaces, a new material has been developed by DuPont as a substitute for gold. The company says GXT palladium nickel plating outperforms and outperforms gold. The plating consists of a 50 microinch nickel undercoat, a palladium-nickel alloy coating either 15, 30 or 50 microinches thick, depending on the application, and a thin gold overflash.

Company data indicates GXT is superior to gold in porosity test performance, environmental corrosion resistance, creep corrosion resistance, solderability, bend ductility and wear resistance. They say it is equivalent to gold in contact resistance and classical corrosion test resistance.

Photographs for this month's cover were provided by Cohan-Epner Co., Brooklyn, New York. The company has developed a process to assure uniform plating in the recessed areas of large devices with complex shapes. Shown is a newly-developed interdigital filter designed by a major telecommunications company to work in the cellular radio frequencies.

Since parts of the filter are recessed, there is a danger that the silver in the plating solution will be depleted in the corners of the recesses and not replenished by circulation of the solution. Cohan-Epner places silver mesh in these recessed areas to feed silver into the depleted solution.

Other Materials

Looking beyond the circuits, some interesting new materials have been developed for RF shielding. Southwall Technologies has developed a shielding architectural window. The company says their window provides EMI shielding while allowing visible light transmission.

Facilities which have to be shielded against EMI usually are built without windows. Floors, ceilings and walls are made

of metal and grounded. Standard glass windows pass electromagnetic waves and cannot be used in secure facilities.

Southwall says their window looks like an ordinary window but stops electromagnetic waves. The shielding comes from a conductive but highly transparent thin metal film sputtered onto an optical grade polyester. The thin film is suspended in the airspace between two panes of glass and grounded to the metal window frame, which is grounded to the building structure.

The company, a manufacturer of double insulating glass solar control windows, says the EMI shielding window also provides solar control. Each window is custom built.

This has been a brief look at some of the new materials being used in RF circuit design and related technologies. More will be said about new materials in relation to specific devices mentioned in the next two articles.

We are grateful to Roy Rice and Kevin Bennett, of W.R. Grace's, Washington Research Center, for background information on some of the new substrate materials being studied there and elsewhere, and to Ray Johnson, of Oak Mater-

ials Group, for an explanation of the fiberglass laminate manufacturing process.

The following companies produce the products mentioned in this special report. For additional information from these companies circle the corresponding number on the reader info card included with this issue.

M/A-Com Advanced Semiconductor Operations, Inc., Lowell, Mass., Please circle INFO/CARD #98

Metaramics, Sunnyvale, Calif., Please circle INFO/CARD #97

Oak Materials Group, Laminates Division, Hoosick Falls, New York, Please circle INFO/CARD #114

Rogers, Corp., Chandler, Ariz., Please circle INFO/CARD #90.

Keene Laminates Div., East Providence, R.I., INFO/CARD #96

Electronic Products Div., 3M, Austin, Tex., INFO/CARD #95

ICI Americas Inc., Wilmington, Del., Please circle INFO/CARD #94

Southwall Technologies, Palo Alto, Calif., INFO/CARD #93

DuPont Corp., Harrisburg, Penn., Please circle INFO/CARD #92

Cohan-Epner Co., Brooklyn, New York, INFO/CARD #91



A BASIC Program

mathematical analysis and they are, therefore, determined empirically. On the bright side, the location of taps can be calculated with reasonable accuracy. The

program will compute the tap location in terms of turns or degrees from the grounded end of the coil.

The application of helical resonators

has two practical limitations. One occurs when the required number of turns is less than three. Here the pitch of the helix is less than its radius and it ceases to be a helix. The other limit, encountered at low frequencies, is when the required wire diameter falls below five times the skin depth for that frequency. The program displays an error message on the screen if the design is not within these practical limits.

Dimensional relationships for helical inductors have been compiled and evaluated experimentally in a number of laboratory models (1). These equations and those for computation of insertion loss of Butterworth responses (2) and unloaded Q of resonators with copper inner and outer conductors constitute the program's design integrity.

Written in BASIC on a TI 99/4A computer, the program has been run successfully on several models of microcomputers without modification. Memory is limited to less than 5K bytes and display width need not exceed 30 columns. Conversion from radians to degrees and natural log to log base 10 has been accomplished where necessary. Those without printers or not requiring hard copies may delete lines 710 through 940.

References

1. Macalpine, W.W. and Schildknecht, R.O., Coaxial Resonators with Helical Inner Conductors, Proceedings of the IRE, Vol. 47, No. 12, p.2100, December, 1959.
2. Zverev, A.I., Handbook of Filter Synthesis, John Wiley & Sons, New York, 1967.

About the Author

Vincent Heesen is Project Engineer for Microcom Corp., 965 Thomas Drive, Warminster, PA 18974.

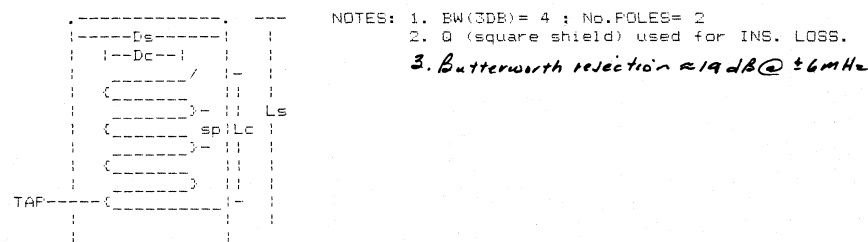
```

670 SNN=ATN(SN)/RAD
680 TLN=(N*SNN)/90 :: TLN=INT(TLN*1000)/1000
690 TLD=N*SNN/4 :: TLD=INT(TLD)
700 PRINT "TAP LOCATION=";TLN;"TURNS OR";TLD;"DEGREES FROM GROUND."
710 PRINT :: INPUT "HARD COPY REQUIRED (Y/N)";P#
720 IF P#<>"Y" THEN 950 ELSE OPEN #3:"FID"
730 PRINT #3:;TAB(25);"***HELICAL RESONATOR DESIGN***" :: IF FL=1 THEN 880
740 PRINT #3:; "PROJECT:-----":TAB(56):
"DATE:-----":
750 PRINT #3:;TAB(6);"-----". ---":TAB(30);"NOTES: 1. BW(3DB)=";BW3;";
No. POLES=";NP
760 PRINT #3:;TAB(6);"!-----Ds-----! !":TAB(37);"2. Q (square shield) used for
INS. LOSS."
770 PRINT #3:;TAB(6);"! !-----Ds-----! !":TAB(20);"! !"
780 PRINT #3:;TAB(6);"! !":TAB(10);"-----":TAB(17);"/ !- !"
790 PRINT #3:;TAB(6);"! ! {-----} ! !"
800 PRINT #3:;TAB(6);"! !":TAB(10);"-----}- ! ! Ls"
810 PRINT #3:;TAB(6);"! ! {-----} sp:Lc !"
820 PRINT #3:;TAB(6);"! !":TAB(10);"-----}- ! !"
830 PRINT #3:;TAB(6);"! ! {-----} ! !"
840 PRINT #3:;TAB(6);"! !":TAB(10);"-----} ! !"
850 PRINT #3:;TAB(6);"! !":TAB(20);"! !"
860 PRINT #3:;TAB(6);"! !":TAB(20);"! !"
870 PRINT #3:;TAB(6);"! !":TAB(20);"! !" :: FL=1
880 PRINT #3:; "RESONATE FREQUENCY=";FO;"MHz; IMPEDANCE=";ZO;"ohms; INSERTION LO
SS=";INT(IL*100)/100;"DB"
890 PRINT #3:; "SHIELD DIA. (Ds)=";DS;U#;TAB(35);"SHIELD LGTH. (Ls)~";LS;U#
900 PRINT #3:; "COIL DIA. (Dc)=";DC;U#;TAB(35);"COIL LENGTH. (Lc)=";LC;U#
910 PRINT #3:; "WIRE SPACING (SP)=";SP;"mils";TAB(35);"QU=";QU;"or";QUS;"(square s
hield)"
920 PRINT #3:; "NUMBER of TURNS=";N;TAB(35);"WIRE DIA. (MIN.) =" ;WN;"mils"
930 PRINT #3:; "TAP IMPEDANCE =" ;RT;"ohms";TAB(35);"WIRE DIA. (MAX.) =" ;WX;"mils"
940 PRINT #3:; "TAP POSITION =" ;TLN;"TURNS OR";TLD;"DEGREES FROM GROUNDED END." ::
CLOSE #3
950 PRINT :: INPUT "RERUN PROGRAM? (Y/N)";R# :: IF R#="Y" THEN 100 ELSE END
960 PRINT "THIS DESIGN IS INADVISABLE!!" :: GOTO 950
EXAMPLE:

```

HELICAL RESONATOR DESIGN

PROJECT: Channel 285 Pilot Filter DATE: 1-12-85



RESONATE FREQUENCY= 499.25 MHz; IMPEDANCE= 390 ohms; INSERTION LOSS= 2.02 DB

SHIELD DIA. (Ds)= 503 mils	SHIELD LGTH. (Ls)~ 754 mils
COIL DIA. (Dc)= 276 mils	COIL LENGTH. (Lc)= 414 mils
WIRE SPACING (SP)= 54.98 mils	QU= 562 or 674 (square shield)
NUMBER of TURNS= 7.56	WIRE DIA. (MIN.) = 21.99 mils
TAP IMPEDANCE = 75 ohms	WIRE DIA. (MAX.) = 32.98 mils

Introduction to Electromagnetic Pulse

By Kendall Childers
Senior Scientist

There are electromagnetic disturbances associated with the detonation of chemical explosives; therefore it was no surprise that there were electromagnetic disturbances associated with nuclear explosives. What was a surprise was the extent of the geographical coverage, the bandwidth of the energy spectrum and the amplitude of some of the disturbances. The nuclear induced disturbance is called Nuclear Electromagnetic Pulse (NEMP) or simply Electromagnetic Pulse (EMP).

EMP is caused by electrons ejected from materials by gamma-rays and X-rays emitted from the nuclear explosions. EMP goes by a variety of aliases; High altitude EMP (HEMP), Low altitude EMP (LEMP), Source Region EMP (SREMP), System Generated EMP (SGEMP), Internal EMP (IEMP), etc. The names identify the source of the EMP and are a "shorthand" used to indicate the characteristics of the EMP of interest. This article will deal exclusively with HEMP, the most serious threat to telecommunication systems.

Generation of HEMP

When the gamma-rays from an exo-atmospheric nuclear explosion descend to an altitude of about 40 km, the air becomes sufficiently dense that there are significant interactions. By the time the gamma-rays penetrate to an altitude of about 20 km, they are completely absorbed in the atmosphere. The primary interaction, Compton collision, results in an ejected electron and a scattered gamma-ray. The ejected electrons are turned by the earth's magnetic field (similar to the deflection [turning] of the electron beam in a TV tube by the yoke). The process of accelerating (deflecting) charged particles generates electromagnetic radiation.

The HEMP area of coverage is determined by the area of the spherical cap enclosed by the tangent drawn from the point of the explosion to the surface of the earth. An easy set of numbers to remember is: HEMP from a nuclear explosion at an altitude of 300 miles above the surface of the earth will illuminate a 3,000 mile diameter region on the surface of the earth.

The gamma-rays from a nuclear explosion are emitted in a burst with a duration of around 10 nanoseconds. Therefore, HEMP is a pulse. The risetime of the

pulse is related to the duration of the burst of gamma-rays, a few to around 10 nanoseconds. The decay of the pulse is caused by very complicated processes, which result in pulse lengths from about 1/10th to about one microsecond. The frequencies of interest when one is dealing with pulses are determined by taking the Fourier transform of the pulse. HEMP is typically "full energy rich" up to about 1 MHz and has significant energy content up to at least 100 MHz.

The degree of deflection of the ejected electrons by the earth's magnetic field depends on the direction of the electron trajectory compared to the direction of the earth's magnetic field. If the directions are perpendicular, deflection is maximized; if they are parallel, deflection is minimized. The amount of electromagnetic radiation is related to the degree of deflection, the larger the deflection the greater the radiation. The gamma-rays travel radially outward from the explosion, and the electrons are ejected "primarily in the forward direction", i.e., radially outward from the explosion. The declination of the earth's magnetic field means that (in the northern hemisphere) north of the explosion there is a region where the ejected electrons are parallel to the earth's magnetic field — in that direction there will be no HEMP. Likewise there will be a region south of the explosion where the ejected electrons are perpendicular to the earth's magnetic field — in that direction the EMP will be the maximum possible, usually characterized by a peak electric field strength of 50,000 volts/meter. In other directions HEMP will have intermediate amplitudes.

The precise characteristics of HEMP depend on the size of the nuclear explosion and the geometric relationship between the position of the explosion, the observer and the earth. Since it is not possible to specify a unique set of parameters, a composite "worst case" waveform is used. The "worst case" threat retains the nastiest characteristics of the various forms of HEMP, namely; the fastest risetime — less than 10 nanoseconds, the maximum peak electric field strength — about 50,000 volts/meter, and the longest pulse duration — about one nanosecond. The electric field strength for "worst case" HEMP is described with a double exponential (1):

$$E(t) = E_0 [e^{-t/t_1} - e^{-t/t_2}]$$

where: $E(t)$ = electric field strength as

a function of time
 E_0 : related to peak electric field strength, about 52,500 volts/meter
 t = time
 t_1 : related to pulse width, about 250 nanoseconds
 t_2 : related to rise time, about 2 nanoseconds

HEMP is a plane wave with a wave impedance of 377 ohms, therefore the corresponding magnetic field strength is given by: $H(t) = E(t)/377$

The peak "worst case" magnetic field strength is about 133 amps/meter.

The energy density in HEMP is small, about 1 joule/m² but the power density is large, about 7 megawatts/m². Whereas a significant power is incident on small (square meter) structures, significant energy is incident only on truly large (many square meter) structures.


One of the advantages of describing HEMP with a double exponential is that the Fourier transform is trivial. The transform is constant from zero hertz up to a frequency of $1/(2\pi t_1) = 640$ kHz where it starts to roll off at 20 dB/decade up to a frequency of $1/(2\pi t_2) = 76$ MHz where it starts to roll off at 40 dB/decade.

The recommended procedure for protecting modern systems is to use Faraday cage inside of Faraday cage inside Faraday case . . . until sufficient shielding is accomplished that the system survives (2). The Faraday cage inside Faraday case scenario requires single point grounding between neighboring cages, separation of signal and power cables between cages, shielding of cables between cages and "terminal protection" where the cables penetrate the cages. The key feature of this scenario is that the shielding is distributed, no single shield is required to provide an inordinate amount of shielding.

References:

1. R. Sherman et al, "EMP Engineering and Design Principles", Bell Telephone Laboratories, Inc., 1975
2. J. Mileta et al, "Defense Switched Network Design Practices for Protection Against High-Altitude Electromagnetic Pulse", HDL-SR-82-2, Harry Diamond Laboratories, Adelphi, MD, 1982

About the Author

Kendall Childers is Senior Scientist at Chomerics, Inc., 77 Dragon Court, Woburn, MA 01888. 

A Computer Algorithm for Mixer Spurious Analysis

By Alan Victor
Motorola Communications Division

The analysis and the computer algorithm which follow allow the prediction of various mixer spurious, including general harmonic analysis, cross-over spurious location and self-quieting analysis. The approach outlined is applicable to receiver designs, synthesizers and other systems that use a multitude of mixers, oscillator sources and intermediate frequencies (IFs).

A number of mixer stages, fixed sources or sweeping sources are present in the design of receivers or frequency synthesizers. In receiver design, selection of the IF is critical in minimizing unwanted responses. A similar problem exists when a multiple loop approach is used in frequency synthesizers. In this case, the IF is analogous to the synthesizer loop bandwidth. Just as in a receiver, if a spurious response is present in the IF of a frequency synthesizer, no additional selectivity will reduce the level of spurious. One could narrow the loop bandwidth or side-step around the interfering condition to reduce the level of spurious, but this is at the expense of increased lock time or VCO phase noise degradation. It is better to select the right oscillator frequency, IF and mixer type (1).

First, we shall define some of the most

prevalent types of mixer spurious as they occur in a communications receiver. The ideal mixer would behave as a perfect product multiplier, and if the input signals (local oscillator and RF source) are sinusoidal the only IF components are the sum and difference frequencies. Simple low-pass or high-pass filtering selects the desired IF frequency. Unfortunately, the sources are rarely perfect and the mixer is not a perfect product multiplier. The mixer output consists of harmonic multiples of the local oscillator source, the RF source and any other fixed or sweeping source that might couple with the mixer inputs. The harmonic multiples at the mixer output have an integer relationship with the various mixer input signals, and the IF output can be expressed as:

$$f_{IF} = N \cdot f_{RF} + M \cdot f_{LO} + K \cdot f_X \quad (1)$$

where N, M and K are integer values which are plus or minus and can be zero. The term f_X is any third frequency present and might represent a fixed source or a sweeping one.

Equation 1 can be extended to any number of sources and IFs. Proper choice of the source coefficients N, M and K permit both high and low side oscillator injection (local oscillator source is either

above or below the RF signal) into the mixer. Therefore, up conversion or down conversion can be analyzed. Consider the case in Equation 1 where f_X is absent. If $N = +1$ and $M = -1$ we have low side injection and the desired mixing term is:

$$f_{IF} = f_{RF} - f_{LO} \quad (2)$$

For $N = -1$ and $M = +1$ we have high side injection but f_{IF} remains the same. In each case Equation 1 gives the desired result and the other result is the image frequency. A particularly troublesome spurious is given by $M = N = 2$ and is referred to as the $\frac{1}{2}$ IF spurious. This spurious lies one half IF above or below the desired RF (depending on whether high or low side injection is used) and is difficult to filter if a wideband receiver is contemplated.

Troublesome spurious occurs for $M = N \pm 1$ or $N = M \pm 1$. When N and M differ by only an integer value close-in spurious can occur. These undesired signals, too, are close to the desired RF receive frequency and are difficult to filter. Proper selection of the IF as well as the mixer type helps reduce the level of this spurious.

Equation 1 can be handled graphically (2, 3) but quickly becomes a nightmare as the number of sweeping

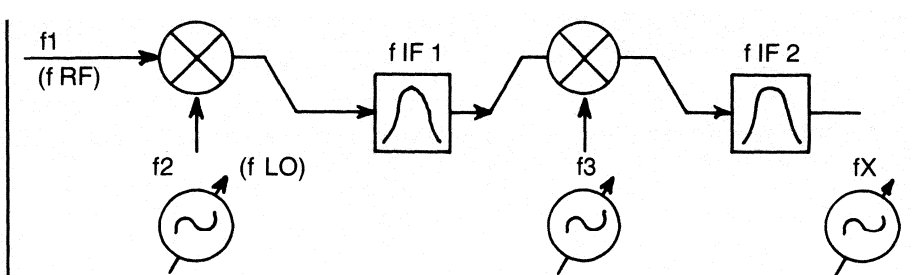


Figure 1. Three source, dual IF (dual conversion) system.

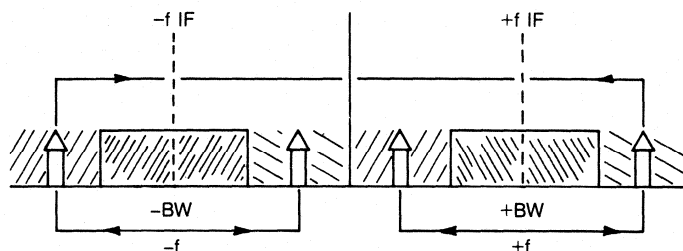


Figure 2. Movement of f IF which might constitute a crossover spurious is detected by monitoring the sign of f IF and setting and clearing flags. Arrows show possible direction of movement for generating a spurious frequency detect.

sources:	f5	f4	f3	f2	f1
	0	0	0	0	0
	0	0	0	0	1
	0	0	0	1	1
	0	0	0	1	0
	0	0	1	1	0
	0	0	1	1	0
	0	0	1	0	1
	0	0	1	0	0
3 sources:	1	1	1	0	0
combinations	1	1	1	0	1
	1	1	1	1	1
	1	1	1	1	0
	1	1	0	1	0
	1	1	0	1	1
	0	1	0	0	1
	0	1	0	0	0
4 sources:	1	1	0	0	0
combinations	1	1	0	0	1
	1	1	0	1	1
	1	1	0	1	0
	1	1	1	1	0
	1	1	1	1	1
	1	1	1	0	1
	1	1	1	0	0
	1	0	1	0	0
	1	1	1	0	1
	1	1	1	1	1
	1	1	1	1	0
	1	1	0	1	0
	1	1	1	1	1
	1	1	1	0	1
5 sources:	1	0	0	0	0
combinations					

Figure 3. Grey-Code Sequence for Multiple Signal Sources

Every zero accompanied by a one indicates that the frequency term ($f1$ through $f5$) is stepped from a minimum frequency to the maximum. If a one is accompanied by a zero then the frequency term is stepped back from f maximum to f minimum. The program routine includes three sources, but any number is handled by this technique.

sources or IFs increases. This computer program handles the above equation and allows all three sources to be swept. Two IFs are checked in the computer routine, but any number of IFs as well as any number of swept sources can be accommodated.

Figure 1 illustrates the system under consideration. To keep the number of possible spurious signals reasonable the IF bandwidth or the search range is made adjustable. Additional reduction in the number of M, N and K spurious response data points is possible if selectivity or mixer suppression is factored into the program (4). The starting and ending values for the coefficients of each source are independent and also adjustable in range.

Several problems are addressed in the program to allow all possible spurious to be detected without an undue increase in computation time. Crossover spurious, for example, can be particularly troublesome, especially if swept sources are used. These spurious signals can move through the IF and, therefore, can have zero offset from the specified IF center frequency. Instead of trying to calculate where these crossovers occur precisely, we need

only determine that a crossover spurious does exist.

Figure 2 illustrates the technique used. The program checks the sign of the calculated IF and notes whether the signal produced by the spurious lies within the IF, above it or below it. This calculation is done for the extreme end frequencies of each swept source. Clearly, if the spurious produces an IF signal within the specified search range, the spurious condition is met. If the signal lies below the IF range, a negative flag is set; otherwise, a positive flag is set. The state of the flag is checked on each calculation as the swept sources are moved to their next extreme frequency point. If any of these set flags change sign from one calculation to the next, the IF signal produced by the spurious must cross over the IF center frequency and a spurious condition exists.

Note that equation 1 is really quite general. The algorithm does not care what the signal terms are, and it is up to the individual to determine what will be identified as the RF signal, the LO and the IF.

The program will handle a multitude of signal sources and IF frequencies. The

routine being discussed will handle three sources and two IF frequencies. All of the sources can be swept or fixed. The program steps the sources in a Grey-Code sequence, given in Figure 3. Thus, each source is essentially swept one at a time and the program looks for a valid spurious condition.

Given three oscillators, 16 possible mixing conditions exist. These conditions take into account the sweeping of the three oscillators as well as the type of mixing, i.e., sum mixing or difference mixing. In addition, we need to consider both high and low side injection. Since we can take the absolute value of the result for high or low side injection and arrive at the same spurious response, only eight combinations are necessary. In addition, four combinations are needed to account for the kind of mixing, i.e. sum or difference.

To save computation time the four mixing combinations are presented in a menu and the user is asked to select the appropriate case type, one through four, or case five, which selects all combinations. The main subroutine in the program is SEARCH, which increments the coefficients of the three oscillators, f1, f2 and f3, using the alpha variables N, M and K. The mixing "type" is selected by the variables X, Y and Z and is controlled by selecting the desired case routine.

The spurious analysis does not actually sweep the three oscillators but instead makes a spurious computation at both band edges for f1, f2 and f3. The four subroutines IFRANGE, FLAGSET, FLAGTEST and SPUR compute whether a spurious response falls exactly in our specified IF bandwidth. Not only the IF bandwidth but also the mirror image of the IF is checked, since this represents a valid response. Since the IF band and the mirror image IF band are used in a calculation, we are able to check for spurious which could move through the IF from a small change in any one of the signal source frequencies. Crossover spurious are checked in this manner.

The subroutine IFRANGE checks for in-band spurious. The program requests the desired IF bandwidth or search range. The subroutines FLAGSET and FLAGTEST monitor the movement of the IF spurious as the sign of the spurious changes from one side of the IF to the other; i.e. the spurious passes through either the image IF or the IF. The last major subroutine is SPUR, which gives the final result. This routine recognizes whether a single conversion analysis is being performed or a general harmonic analysis is requested. In the latter case,

all three sources can be present and may be swept or fixed in frequency.

In single conversion analysis only one IF is allowed. A single conversion analysis is possible using a swept RF source (f1), a swept LO source using f2, and a fixed IF, f IF (2). The analysis using the IF and the image IF detects spurious at the RF image frequency, the half IF frequency and at many M and N frequencies where M and N differ by only unity. The significance of these spurious signals is that they occur close to the desired RF receive frequency, f1. Portions of the subroutine SPUR calculate the location of these spurious signals and the RF range over which they move. The designer is then presented with a good picture of how much RF filtering is required.

The computer routine is written in BASIC, and two versions are now complete. One is written for the series 200 HP desktop personal computer and the other for the APPLE II. A three-source, 30th order spur search takes less than 60 seconds on a personal computer, even faster if few spurious are found.

Examples

Equation 1 can be expanded to consider all possible mixing situations and account for the sweeping of sources one, two and three. Using variables N, M and K as the multiple coefficients for the three sources and variables X, Y and Z to account for the mixing type (sum mixing or difference mixing) we have the following:

$$f \text{ IF (1) or } f \text{ IF (2)} = N \cdot X \cdot f1 + M \cdot Y \cdot f2 + K \cdot Z \cdot f3 \quad (3)$$

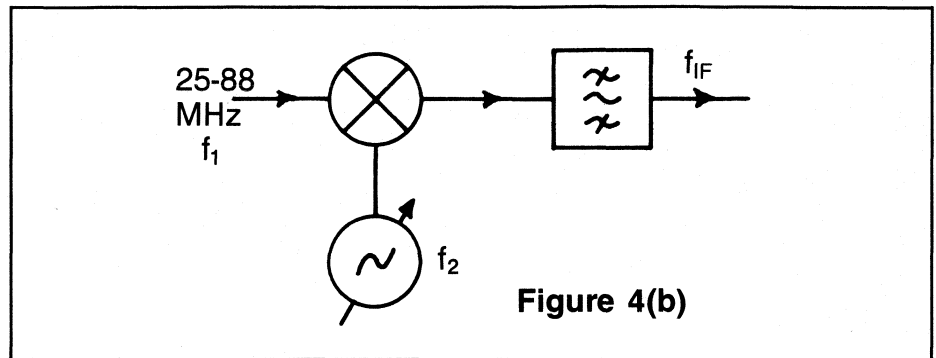
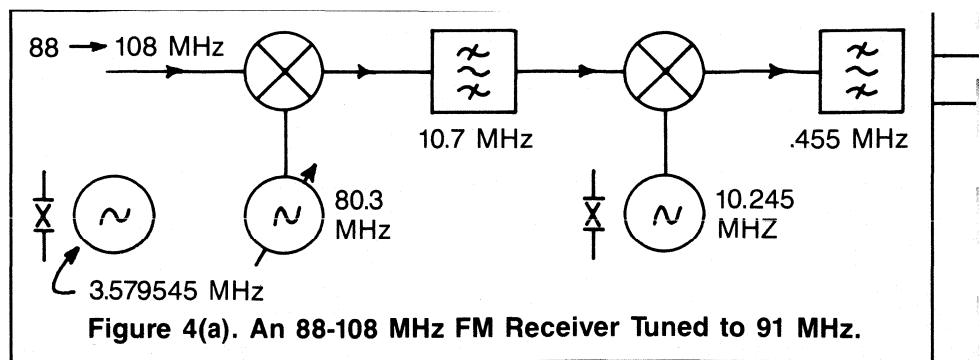
Since $f \text{ IF} = \text{ABS} (-f1 -f2 -f3) = (f1 + f2 + f3)$, only half of the 16 possible sweeping cases need to be analyzed. So, we have the following equations:

$$\begin{aligned} f \text{ IF (1) or } f \text{ IF (2)} &= N \cdot X \cdot f1 \text{ min} + M \cdot Y \cdot f2 \text{ min} + K \cdot Z \cdot f3 \text{ min} \\ &= N \cdot X \cdot f1 \text{ min} + M \cdot Y \cdot f2 \text{ min} + K \cdot Z \cdot f3 \text{ max} \\ &= N \cdot X \cdot f1 \text{ min} + M \cdot Y \cdot f2 \text{ max} + K \cdot Z \cdot f3 \text{ max} \end{aligned} \quad (4)$$

and the remaining five terms follow the Grey-Code sequence generated by Figure 3.

As an aid in understanding the spurious problem, some examples are shown in Figure 4 which illustrate the material covered.

Consider an FM receiver covering 88-108 MHz. The first IF is 10.7 MHz and the second IF is 455 kHz. A microprocessor (μP) is used to obtain a clock display function and control tuning of the receiver. The



μ P oscillator is a 3.579545 MHz (f_3) crystal. Using the program we find that the general spurious analysis points out a self-quieting condition (the receiver will essentially be quieted by its own internal oscillators) at $3 \cdot f_3$ which is 38.6 kHz below the 10.7 MHz IF. Clearly, this is a potential problem, especially with the first IF over 100 kHz wide. Other spurious are noted, including some which also effect the second IF.

Consider a communications receiver for the 25-88 MHz band (Fig. 4b). Low-side injection is used with up-conversion and the first IF is 90 MHz. A single conversion spurious analysis points up a number of harmonic related spurious, indicating the need for sub-octave band-pass filters. A low order N, M spur exists (2,1) but is at least 46 MHz away from the desired receive frequency. A (1,2) spur also exists and is more troublesome as it is within 2 MHz of the desired receive frequency. If high side injection is used, this spurious is no longer present. The (1,2) or 3rd order spurious is removed and a higher order spurious (3,2) or 5th order, becomes present. However, the increased order allows a well-designed mixer to suppress the spurious, perhaps sufficiently so that less RF filtering is necessary.

Finally, a VHF receiver is contemplated. Several IF frequencies were chosen and low- and high-side injection tried. The resultants shown in Figures 4c,d indicate the trend. An optimum IF is about $\frac{1}{2}$ the desired receive frequency when the M, N spurious differ by unity. If a wideband receiver is contemplated, the image frequency and half IF frequency could be more of a problem than the M, N spurious.

Higher IFs allow these spurious to be moved out while the M,N spurious move in closer to the desired RF frequency. High-side injection raises the order of the $M + N$ spurious and makes the filtering task easier.

These analyses can be re-evaluated as other sources become involved. Trade-offs will be required, but the computer algorithm and approach outlined for handling these conditions should make the job a bit easier.

References

1. Henderson, Bert, Mixer Design Considerations Improve Performance, *Microwave News Inc.*, October 1981, Vol. 11, No. 10, pp. 103-118.
2. Shores, M.N., Chart Pinpoints Receiver Interference Problems, *EDN*, January 15, 1969, pp. 43-46.
3. Capraro, G.T. and Perini J., A Graphical Approach to the Intermodulation and Spurious Response Problem, *IEEE Electromagnetic Compatibility*, February 1974, pp. 38-43, Vol. 16, No. 1.
4. Meixner, Raymond R., Basic Computer Algorithm Spots Spurious Responses, *Microwaves*, March 1977, pp. 42-46.

About the Author

Alan Victor is a Senior Staff Engineer at the Motorola Communications Sector, 8000 W. Sunrise Blvd., Plantation, FL 33322. He received his BSEE degree from the University of Florida in 1971 and an MSEE from Florida Atlantic University in 1980. He has been with Motorola since 1971, and is a member of the Motorola Science Advisory Board.


```

*****
*          SPURSEARCH          *
*          *                    *
* GENERAL SPURIOUS ANALYSIS *
*          *                    *
* VERSION 1.9                  *
* A.M. VICTOR B/17/84        *
*****

```

COMPUTING CASE 1 (+,-,-)

```

N=F1      M=F2      K=F3
0          0          3

DELTA IF1      DELTA IF2
-38.6 KHZ      -10300 KHZ

```

COMPUTED SPURIOUS FOR CASE 1 (+,-,-)

```

N=F1      M=F2      K=F3
1          4          8

DELTA IF1      DELTA IF2
16.4 KHZ      -10200 KHZ

```

COMPUTED SPURIOUS FOR CASE 1 (+,-,-)

```

N=F1      M=F2      K=F3
1          5          8

DELTA IF1      DELTA IF2
10300 KHZ      16.4 KHZ

```

LOW SIDE INJECTION 25-88 (90 MHz IF)

```

*****
*          SPURSEARCH          *
*          *                    *
* GENERAL SPURIOUS ANALYSIS *
*          *                    *
* VERSION 1.9                  *
* A.M. VICTOR B/17/84        *
*****

SPURIOUS RANGE FOR F1 (Using plus I.F.)
46 MHz TO 77.5 MHz
DELTA SPURIOUS F1 FROM DESIRED F1
46 MHz TO 77.5 MHz

SPURIOUS RANGE FOR F1 (Using negative I.F.)
25 MHz TO 12.5 MHz
DELTA SPURIOUS F1 FROM DESIRED F1
205 MHz TO 167.5 MHz

COMPUTED SPURIOUS FOR CASE 1 (+,-,-)
N=F1      M=F2      K=F3
1          2          0

SPURIOUS RANGE FOR F1 (Using plus I.F.)
94 MHz TO 88 MHz
DELTA SPURIOUS F1 FROM DESIRED F1
2 MHz TO 3 MHz

```

```

SPURIOUS RANGE FOR F1 (Using negative I.F.)
25 MHz TO 40 MHz
DELTA SPURIOUS F1 FROM DESIRED F1
122.5 MHz TO 115 MHz

```

COMPUTED SPURIOUS FOR CASE 1 (+,-,-)

```

N=F1      M=F2      K=F3
2          2          0

SPURIOUS RANGE FOR F1 (Using plus I.F.)
47 MHz TO 88 MHz
DELTA SPURIOUS F1 FROM DESIRED F1
45 MHz TO 45 MHz

SPURIOUS RANGE FOR F1 (Using negative I.F.)
25 MHz TO 20 MHz

```

COMPUTED SPURIOUS FOR CASE 1 (+,-,-)

```

N=F1      M=F2      K=F3
3          2          0

SPURIOUS RANGE FOR F1 (Using plus I.F.)
31.33333333 MHz TO 70.33333333 MHz
DELTA SPURIOUS F1 FROM DESIRED F1
60.66666667 MHz TO 81.66666667 MHz

SPURIOUS RANGE FOR F1 (Using negative I.F.)
25 MHz TO 12.5 MHz
DELTA SPURIOUS F1 FROM DESIRED F1
147.5 MHz TO 141.66666667 MHz

```

LOW SIDE INJECTION 25-88 (90 MHz IF)

```

*****
*          SPURSEARCH          *
*          *                    *
* GENERAL SPURIOUS ANALYSIS *
*          *                    *
* VERSION 1.9                  *
* A.M. VICTOR B/17/84        *
*****

```

COMPUTING CASE 1 (+,-,-)

```

N=F1      M=F2      K=F3
2          0          0

SPURIOUS RANGE FOR F1 (Using plus I.F.)
Crossover at infinity; M or N equals zero
Simple harmonic multiple of RF equals IF
45 MHz TO 45 MHz
DELTA SPURIOUS F1 FROM DESIRED F1
127.5 MHz TO 110 MHz
Crossover at infinity; M or N equals zero
Simple harmonic multiple of RF equals IF

SPURIOUS RANGE FOR F1 (Using negative I.F.)
25 MHz TO 45 MHz
DELTA SPURIOUS F1 FROM DESIRED F1
147.5 MHz TO 200 MHz

```

```

N=F1      M=F2      K=F3
3          0          0

SPURIOUS RANGE FOR F1 (Using plus I.F.)
Crossover at infinity; M or N equals zero
Simple harmonic multiple of RF equals IF
30 MHz TO 30 MHz
DELTA SPURIOUS F1 FROM DESIRED F1
142.5 MHz TO 125 MHz
Crossover at infinity; M or N equals zero
Simple harmonic multiple of RF equals IF

SPURIOUS RANGE FOR F1 (Using negative I.F.)
25 MHz TO 30 MHz
DELTA SPURIOUS F1 FROM DESIRED F1
147.5 MHz TO 185 MHz

```

```

N=F1      M=F2      K=F3
1          1          0

SPURIOUS RANGE FOR F1 (Using plus I.F.)
92 MHz TO 88 MHz
DELTA SPURIOUS F1 FROM DESIRED F1
0 MHz TO 4 MHz

SPURIOUS RANGE FOR F1 (Using negative I.F.)
25 MHz TO 25 MHz
DELTA SPURIOUS F1 FROM DESIRED F1
180 MHz TO 180 MHz

```

COMPUTED SPURIOUS FOR CASE 1 (+,-,-)

```

N=F1      M=F2      K=F3
3          4          0

SPURIOUS RANGE FOR F1 (Using plus I.F.)
163.43333333 MHz TO 174 MHz
DELTA SPURIOUS F1 FROM DESIRED F1
27.43333333 MHz TO 30.075 MHz

```

```

SPURIOUS RANGE FOR F1 (Using negative I.F.)
151.5 MHz TO 174 MHz
DELTA SPURIOUS F1 FROM DESIRED F1
15.5 MHz TO 21.125 MHz

```

COMPUTED SPURIOUS FOR CASE 1 (+,-,-)

```

N=F1      M=F2      K=F3
4          5          0

SPURIOUS RANGE FOR F1 (Using plus I.F.)
152.1 MHz TO 174 MHz
DELTA SPURIOUS F1 FROM DESIRED F1
16.1 MHz TO 20.48 MHz

SPURIOUS RANGE FOR F1 (Using negative I.F.)
143.15 MHz TO 174 MHz
DELTA SPURIOUS F1 FROM DESIRED F1
7.15 MHz TO 13.32 MHz

```

179 IF
LOW SIDE INJECTION

```

*****
COMPUTED SPURIOUS FOR CASE 1 (+,-,-)
N#F1      N#F2      K#F3
5          4          0
SPURIOUS RANGE FOR F1 (Using plus I.F.)
136 Mhz TO 157.1 Mhz
DELTA SPURIOUS F1 FROM DESIRED F1
11.625 Mhz TO 16.9 Mhz
SPURIOUS RANGE FOR F1 (Using negative I.F.)
136 Mhz TO 149.94 Mhz
DELTA SPURIOUS F1 FROM DESIRED F1
20.575 Mhz TO 24.04 Mhz
*****

```

```

*****
N#F1      N#F2      K#F3
6          5          0
SPURIOUS RANGE FOR F1 (Using plus I.F.)
136 Mhz TO 162.9 Mhz
DELTA SPURIOUS F1 FROM DESIRED F1
5.72 Mhz TO 11.1 Mhz
SPURIOUS RANGE FOR F1 (Using negative I.F.)
136 Mhz TO 156.933333333 Mhz
DELTA SPURIOUS F1 FROM DESIRED F1
12.88 Mhz TO 17.066666667 Mhz
*****

```

```

*****
N#F1      N#F2      K#F3
7          6          0
SPURIOUS RANGE FOR F1 (Using plus I.F.)
136 Mhz TO 167.042857143 Mhz
DELTA SPURIOUS F1 FROM DESIRED F1
1.78333333333 Mhz TO 6.95714285714 Mhz
SPURIOUS RANGE FOR F1 (Using negative I.F.)
136 Mhz TO 161.928571429 Mhz
DELTA SPURIOUS F1 FROM DESIRED F1
7.75 Mhz TO 12.0714285714 Mhz
*****

```

```

179 IF
HIGH SIDE INJECTION
+-----+
+ SPURSEARCH +
+-----+
+ GENERAL SPURIOUS ANALYSIS +
+-----+
+ VERSION 1.9 +
+-----+
+ A.M. VICTOR 8/17/84 +
+-----+
COMPUTING CASE 1 (+,-,-)
COMPUTING CASE 1 (+,-,-)

```

```

*****
N#F1      N#F2      K#F3
1          1          0
SPURIOUS RANGE FOR F1 (Using plus I.F.)
139.5 Mhz TO 174 Mhz
DELTA SPURIOUS F1 FROM DESIRED F1
0 Mhz TO 0 Mhz
SPURIOUS RANGE FOR F1 (Using negative I.F.)
136 Mhz TO 134.7 Mhz
DELTA SPURIOUS F1 FROM DESIRED F1
42.8 Mhz TO 42.8 Mhz
*****

```

```

*****
N#F1      N#F2      K#F3
2          2          0
SPURIOUS RANGE FOR F1 (Using plus I.F.)
136 Mhz TO 166.8 Mhz
DELTA SPURIOUS F1 FROM DESIRED F1
10.7 Mhz TO 10.7 Mhz
SPURIOUS RANGE FOR F1 (Using negative I.F.)
136 Mhz TO 145.4 Mhz
DELTA SPURIOUS F1 FROM DESIRED F1
32.1 Mhz TO 32.1 Mhz
*****

```

```

*****
COMPUTED SPURIOUS FOR CASE 1 (+,-,-)
N#F1      N#F2      K#F3
2          3          0
SPURIOUS RANGE FOR F1 (Using plus I.F.)
187.85 Mhz TO 174 Mhz
DELTA SPURIOUS F1 FROM DESIRED F1
48.35 Mhz TO 43.733333333 Mhz
SPURIOUS RANGE FOR F1 (Using negative I.F.)
166.45 Mhz TO 174 Mhz
DELTA SPURIOUS F1 FROM DESIRED F1
26.95 Mhz TO 29.466666667 Mhz
*****

```

```

*****
COMPUTED SPURIOUS FOR CASE 1 (+,-,-)
N#F1      N#F2      K#F3
3          4          0
SPURIOUS RANGE FOR F1 (Using plus I.F.)
164.6 Mhz TO 174 Mhz
DELTA SPURIOUS F1 FROM DESIRED F1
25.1 Mhz TO 27.45 Mhz
SPURIOUS RANGE FOR F1 (Using negative I.F.)
150.333333333 Mhz TO 174 Mhz
DELTA SPURIOUS F1 FROM DESIRED F1
10.833333333 Mhz TO 16.75 Mhz
*****

```

```

*****
21.4 IF
LOW SIDE INJECTION
+-----+
+-----+
N#F1      N#F2      K#F3
3          2          0
SPURIOUS RANGE FOR F1 (Using plus I.F.)
136 Mhz TO 137.4 Mhz
DELTA SPURIOUS F1 FROM DESIRED F1
35.9 Mhz TO 36.6 Mhz
SPURIOUS RANGE FOR F1 (Using negative I.F.)
136 Mhz TO 123.133333333 Mhz
DELTA SPURIOUS F1 FROM DESIRED F1
57.3 Mhz TO 50.866666667 Mhz
*****
N#F1      N#F2      K#F3
4          3          0
SPURIOUS RANGE FOR F1 (Using plus I.F.)

```

```

*****
N#F1      N#F2      K#F3
0          2          0
136 Mhz TO 151.9 Mhz
DELTA SPURIOUS F1 FROM DESIRED F1
16.8 Mhz TO 22.1 Mhz
SPURIOUS RANGE FOR F1 (Using negative I.F.)
136 Mhz TO 141.2 Mhz
DELTA SPURIOUS F1 FROM DESIRED F1
31.066666667 Mhz TO 32.8 Mhz
*****

```

```

*****
N#F1      N#F2      K#F3
5          4          0
SPURIOUS RANGE FOR F1 (Using plus I.F.)
136 Mhz TO 160.6 Mhz
DELTA SPURIOUS F1 FROM DESIRED F1
7.25 Mhz TO 13.4 Mhz
SPURIOUS RANGE FOR F1 (Using negative I.F.)
136 Mhz TO 152.04 Mhz
DELTA SPURIOUS F1 FROM DESIRED F1
17.95 Mhz TO 21.96 Mhz
*****

```

```

*****
N#F1      N#F2      K#F3
6          5          0
SPURIOUS RANGE FOR F1 (Using plus I.F.)
136 Mhz TO 166.4 Mhz
DELTA SPURIOUS F1 FROM DESIRED F1
1.32 Mhz TO 7.6 Mhz
SPURIOUS RANGE FOR F1 (Using negative I.F.)
136 Mhz TO 159.266666667 Mhz
DELTA SPURIOUS F1 FROM DESIRED F1
10.08 Mhz TO 14.733333333 Mhz
*****

```

21.4 IF
HIGH SIDE INJECTION

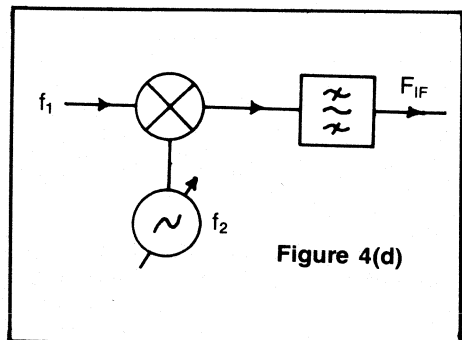


Figure 4(d)


```

      Nof1      Nof2      Kof3
      3         2         0
SPURIOUS RANGE FOR F1 (Using plus I.F.)
134 MHz TO 161 MHz
DELTA SPURIOUS F1 FROM DESIRED F1
15 MHz TO 13 MHz

SPURIOUS RANGE FOR F1 (Using negative I.F.)
134 MHz TO 131 MHz
DELTA SPURIOUS F1 FROM DESIRED F1
42.5 MHz TO 42 MHz
=====
      Nof1      Nof2      Kof3
      3         3         0
      COMPUTED SPURIOUS FOR CASE 1 (+,-,-)

      Nof1      Nof2      Kof3
      3         3         0
      Low Side Injection 136-174 (45 mhz IF)

      ----- SEARCH -----
      * GENERAL SPURIOUS ANALYSIS *
      * VERSION 1.4 *
      * A.M. VICTOR 8/17/84 *
      -----
      COMPUTING CASE 1 (+,-,-)
      COMPUTING CASE 1 (+,-,-)

      Nof1      Nof2      Kof3
      1         1         0
SPURIOUS RANGE FOR F1 (Using plus I.F.)
134 MHz TO 174 MHz
DELTA SPURIOUS F1 FROM DESIRED F1
0 MHz TO 0 MHz

SPURIOUS RANGE FOR F1 (Using negative I.F.)
134 MHz TO 84 MHz
DELTA SPURIOUS F1 FROM DESIRED F1
90 MHz TO 90 MHz
=====

```

COMPUTED SPURIOUS FOR CASE 1 (+,-,-)

```

      Nof1      Nof2      Kof3
      1         2         0
SPURIOUS RANGE FOR F1 (Using plus I.F.)
227 MHz TO 174 MHz
DELTA SPURIOUS F1 FROM DESIRED F1
91 MHz TO 44.5 MHz

SPURIOUS RANGE FOR F1 (Using negative I.F.)
137 MHz TO 174 MHz
DELTA SPURIOUS F1 FROM DESIRED F1
1 MHz TO 19.5 MHz
=====
      Nof1      Nof2      Kof3
      2         2         0
SPURIOUS RANGE FOR F1 (Using plus I.F.)
134 MHz TO 151.5 MHz
DELTA SPURIOUS F1 FROM DESIRED F1
22.5 MHz TO 22.5 MHz

SPURIOUS RANGE FOR F1 (Using negative I.F.)
134 MHz TO 104.5 MHz
DELTA SPURIOUS F1 FROM DESIRED F1
27.5 MHz TO 27.5 MHz
=====
      Nof1      Nof2      Kof3
      2         2         0
SPURIOUS RANGE FOR F1 (Using plus I.F.)
136-174 Low Side Injection (21.4 mhz IF)

      ----- SEARCH -----
      * GENERAL SPURIOUS ANALYSIS *
      * VERSION 1.4 *
      * A.M. VICTOR 8/17/84 *
      -----
      COMPUTING CASE 1 (+,-,-)
      COMPUTING CASE 1 (+,-,-)

      Nof1      Nof2      Kof3
      1         1         0
SPURIOUS RANGE FOR F1 (Using plus I.F.)
134 MHz TO 174 MHz
DELTA SPURIOUS F1 FROM DESIRED F1
0 MHz TO 0 MHz

SPURIOUS RANGE FOR F1 (Using negative I.F.)
134 MHz TO 151.2 MHz
DELTA SPURIOUS F1 FROM DESIRED F1
42.8 MHz TO 42.8 MHz
=====

```

COMPUTED SPURIOUS FOR CASE 1 (+,-,-)

```

      Nof1      Nof2      Kof3
      2         2         0
SPURIOUS RANGE FOR F1 (Using plus I.F.)
134 MHz TO 162.3 MHz
DELTA SPURIOUS F1 FROM DESIRED F1
10.7 MHz TO 10.7 MHz

SPURIOUS RANGE FOR F1 (Using negative I.F.)
134 MHz TO 141.9 MHz
DELTA SPURIOUS F1 FROM DESIRED F1
22.1 MHz TO 22.1 MHz
=====
      Nof1      Nof2      Kof3
      2         3         0
      COMPUTED SPURIOUS FOR CASE 1 (+,-,-)

      Nof1      Nof2      Kof3
      2         3         0
SPURIOUS RANGE FOR F1 (Using plus I.F.)
182.6 MHz TO 174 MHz
DELTA SPURIOUS F1 FROM DESIRED F1
46.6 MHz TO 43.70000000 MHz

SPURIOUS RANGE FOR F1 (Using negative I.F.)
161.2 MHz TO 174 MHz
DELTA SPURIOUS F1 FROM DESIRED F1
25.2 MHz TO 29.40000000 MHz
=====
      Nof1      Nof2      Kof3
      3         3         0
SPURIOUS RANGE FOR F1 (Using plus I.F.)
136-174 Low Side Injection (21.4 mhz IF)

174 MHz TO 150.70000000 MHz
DELTA SPURIOUS F1 FROM DESIRED F1
14.20000000 MHz TO 14.20000000 MHz

SPURIOUS RANGE FOR F1 (Using negative I.F.)
134 MHz TO 145.40000000 MHz
DELTA SPURIOUS F1 FROM DESIRED F1
28.50000000 MHz TO 28.50000000 MHz
=====

```

```

      Nof1      Nof2      Kof3
      3         4         0
      COMPUTED SPURIOUS FOR CASE 1 (+,-,-)

      Nof1      Nof2      Kof3
      3         4         0
SPURIOUS RANGE FOR F1 (Using plus I.F.)
159.90000000 MHz TO 174 MHz
DELTA SPURIOUS F1 FROM DESIRED F1
22.90000000 MHz TO 27.45 MHz

SPURIOUS RANGE FOR F1 (Using negative I.F.)
145.00000000 MHz TO 174 MHz
DELTA SPURIOUS F1 FROM DESIRED F1
9.00000000 MHz TO 16.75 MHz
=====
      Nof1      Nof2      Kof3
      4         4         0
      COMPUTED SPURIOUS FOR CASE 1 (+,-,-)

      Nof1      Nof2      Kof3
      4         4         0
SPURIOUS RANGE FOR F1 (Using plus I.F.)
134 MHz TO 157.95 MHz
DELTA SPURIOUS F1 FROM DESIRED F1
18.05 MHz TO 18.05 MHz

SPURIOUS RANGE FOR F1 (Using negative I.F.)
134 MHz TO 147.25 MHz
DELTA SPURIOUS F1 FROM DESIRED F1
24.75 MHz TO 24.75 MHz
=====
      Nof1      Nof2      Kof3
      4         5         0
SPURIOUS RANGE FOR F1 (Using plus I.F.)
148.6 MHz TO 174 MHz
DELTA SPURIOUS F1 FROM DESIRED F1
12.6 MHz TO 17.45 MHz

SPURIOUS RANGE FOR F1 (Using negative I.F.)
137.9 MHz TO 174 MHz
DELTA SPURIOUS F1 FROM DESIRED F1
1.9 MHz TO 9.12 MHz
=====

```

136-174 High Side Injection (21.4 mhz IF)

```

      Nof1      Nof2      Kof3
      1         1         0
SPURIOUS RANGE FOR F1 (Using plus I.F.)
178.8 MHz TO 174 MHz
DELTA SPURIOUS F1 FROM DESIRED F1
42.8 MHz TO 42.8 MHz

SPURIOUS RANGE FOR F1 (Using negative I.F.)
134 MHz TO 174 MHz
DELTA SPURIOUS F1 FROM DESIRED F1
0 MHz TO 0 MHz
=====
      Nof1      Nof2      Kof3
      2         2         0
      COMPUTED SPURIOUS FOR CASE 1 (+,-,-)

      Nof1      Nof2      Kof3
      2         2         0
SPURIOUS RANGE FOR F1 (Using plus I.F.)
168.1 MHz TO 174 MHz
DELTA SPURIOUS F1 FROM DESIRED F1
22.1 MHz TO 22.1 MHz

SPURIOUS RANGE FOR F1 (Using negative I.F.)
144.7 MHz TO 174 MHz
DELTA SPURIOUS F1 FROM DESIRED F1
10.7 MHz TO 10.7 MHz
=====
      Nof1      Nof2      Kof3
      3         3         0
SPURIOUS RANGE FOR F1 (Using plus I.F.)
134 MHz TO 137.4 MHz
DELTA SPURIOUS F1 FROM DESIRED F1
25.9 MHz TO 34.6 MHz

SPURIOUS RANGE FOR F1 (Using negative I.F.)
134 MHz TO 123.10000000 MHz
DELTA SPURIOUS F1 FROM DESIRED F1
27.3 MHz TO 50.80000000 MHz
=====
      Nof1      Nof2      Kof3
      3         3         0
      COMPUTED SPURIOUS FOR CASE 1 (+,-,-)

      Nof1      Nof2      Kof3
      3         3         0
SPURIOUS RANGE FOR F1 (Using plus I.F.)
136-174 mhz High Side Injection (21.4 mhz IF)

174.00000000 MHz TO 174 MHz
DELTA SPURIOUS F1 FROM DESIRED F1
28.50000000 MHz TO 28.50000000 MHz

SPURIOUS RANGE FOR F1 (Using negative I.F.)
150.20000000 MHz TO 174 MHz
DELTA SPURIOUS F1 FROM DESIRED F1
14.20000000 MHz TO 14.20000000 MHz
=====

```

136-174 mhz High Side Injection (21.4 mhz IF)

```

      Nof1      Nof2      Kof3
      3         3         0
SPURIOUS RANGE FOR F1 (Using plus I.F.)
134 MHz TO 151.9 MHz
DELTA SPURIOUS F1 FROM DESIRED F1
16.9 MHz TO 22.1 MHz

SPURIOUS RANGE FOR F1 (Using negative I.F.)
134 MHz TO 141.2 MHz
DELTA SPURIOUS F1 FROM DESIRED F1
21.00000000 MHz TO 22.8 MHz
=====
      Nof1      Nof2      Kof3
      4         4         0
      COMPUTED SPURIOUS FOR CASE 1 (+,-,-)

      Nof1      Nof2      Kof3
      4         4         0
SPURIOUS RANGE FOR F1 (Using plus I.F.)
162.75 MHz TO 174 MHz
DELTA SPURIOUS F1 FROM DESIRED F1
24.75 MHz TO 24.75 MHz

SPURIOUS RANGE FOR F1 (Using negative I.F.)
152.05 MHz TO 174 MHz
DELTA SPURIOUS F1 FROM DESIRED F1
14.05 MHz TO 14.05 MHz
=====

```

```

      Nof1      Nof2      Kof3
      5         5         0
SPURIOUS RANGE FOR F1 (Using plus I.F.)
134 MHz TO 160.6 MHz
DELTA SPURIOUS F1 FROM DESIRED F1
7.25 MHz TO 13.4 MHz

SPURIOUS RANGE FOR F1 (Using negative I.F.)
134 MHz TO 122.04 MHz
DELTA SPURIOUS F1 FROM DESIRED F1
17.95 MHz TO 21.94 MHz
=====
      Nof1      Nof2      Kof3
      5         5         0
      COMPUTED SPURIOUS FOR CASE 1 (+,-,-)

      Nof1      Nof2      Kof3
      5         5         0
SPURIOUS RANGE FOR F1 (Using plus I.F.)
161.65 MHz TO 174 MHz
DELTA SPURIOUS F1 FROM DESIRED F1
22.65 MHz TO 22.65 MHz

SPURIOUS RANGE FOR F1 (Using negative I.F.)
122.12 MHz TO 174 MHz
DELTA SPURIOUS F1 FROM DESIRED F1
17.12 MHz TO 17.12 MHz
=====
      Nof1      Nof2      Kof3
      6         6         0
SPURIOUS RANGE FOR F1 (Using plus I.F.)
134 MHz TO 166.4 MHz
DELTA SPURIOUS F1 FROM DESIRED F1
1.52 MHz TO 7.6 MHz

SPURIOUS RANGE FOR F1 (Using negative I.F.)
124 MHz TO 129.20000000 MHz
DELTA SPURIOUS F1 FROM DESIRED F1
10.08 MHz TO 14.70000000 MHz
=====

```

136-174 Low Side Injection (17.9 mhz IF)

```

      Nof1      Nof2      Kof3
      1         1         0
SPURIOUS RANGE FOR F1 (Using plus I.F.)
134 MHz TO 174 MHz
DELTA SPURIOUS F1 FROM DESIRED F1
0 MHz TO 0 MHz

SPURIOUS RANGE FOR F1 (Using negative I.F.)
134 MHz TO 138.2 MHz
DELTA SPURIOUS F1 FROM DESIRED F1
25.8 MHz TO 25.8 MHz
=====
      Nof1      Nof2      Kof3
      2         2         0
      COMPUTED SPURIOUS FOR CASE 1 (+,-,-)

      Nof1      Nof2      Kof3
      2         2         0
SPURIOUS RANGE FOR F1 (Using plus I.F.)
134 MHz TO 162.05 MHz
DELTA SPURIOUS F1 FROM DESIRED F1
8.95 MHz TO 8.95 MHz

SPURIOUS RANGE FOR F1 (Using negative I.F.)
134 MHz TO 147.15 MHz
DELTA SPURIOUS F1 FROM DESIRED F1
24.85 MHz TO 24.85 MHz
=====
      Nof1      Nof2      Kof3
      3         3         0
      COMPUTED SPURIOUS FOR CASE 1 (+,-,-)

      Nof1      Nof2      Kof3
      3         3         0
SPURIOUS RANGE FOR F1 (Using plus I.F.)
184.1 MHz TO 174 MHz
DELTA SPURIOUS F1 FROM DESIRED F1
20.1 MHz TO 44.00000000 MHz

SPURIOUS RANGE FOR F1 (Using negative I.F.)
148.2 MHz TO 174 MHz
DELTA SPURIOUS F1 FROM DESIRED F1
22.2 MHz TO 34.10000000 MHz
=====
      Nof1      Nof2      Kof3
      3         3         0
      COMPUTED SPURIOUS FOR CASE 1 (+,-,-)

      Nof1      Nof2      Kof3
      3         3         0
SPURIOUS RANGE FOR F1 (Using plus I.F.)
136-174 Low Side Injection (17.9 mhz IF)

174 MHz TO 142.00000000 MHz
DELTA SPURIOUS F1 FROM DESIRED F1
11.90000000 MHz TO 11.90000000 MHz

SPURIOUS RANGE FOR F1 (Using negative I.F.)
134 MHz TO 150.10000000 MHz
DELTA SPURIOUS F1 FROM DESIRED F1
22.80000000 MHz TO 27.80000000 MHz
=====

```

136-174 Low Side Injection (17.9 mhz IF)

```

      Nof1      Nof2      Kof3
      3         3         0
SPURIOUS RANGE FOR F1 (Using plus I.F.)
162.40000000 MHz TO 174 MHz
DELTA SPURIOUS F1 FROM DESIRED F1
27.40000000 MHz TO 30.075 MHz

SPURIOUS RANGE FOR F1 (Using negative I.F.)
151.5 MHz TO 174 MHz
DELTA SPURIOUS F1 FROM DESIRED F1
18.5 MHz TO 21.125 MHz
=====
      Nof1      Nof2      Kof3
      4         4         0
      COMPUTED SPURIOUS FOR CASE 1 (+,-,-)

      Nof1      Nof2      Kof3
      4         4         0
SPURIOUS RANGE FOR F1 (Using plus I.F.)
134 MHz TO 160.575 MHz
DELTA SPURIOUS F1 FROM DESIRED F1
13.425 MHz TO 13.425 MHz

SPURIOUS RANGE FOR F1 (Using negative I.F.)
134 MHz TO 151.425 MHz
DELTA SPURIOUS F1 FROM DESIRED F1
22.375 MHz TO 22.375 MHz
=====

```

```

COMPUTED SPURIOUS FOR CASE 1 (+,-,-)
  N#F1      N#F2      K#F3
    4        5        0
SPURIOUS RANGE FOR F1 (Using plus I.F.)
152.1 MHz TO 174 MHz
DELTA SPURIOUS F1 FROM DESIRED F1
16.1 MHz TO 20.48 MHz

SPURIOUS RANGE FOR F1 (Using negative I.F.)
142.15 MHz TO 174 MHz
DELTA SPURIOUS F1 FROM DESIRED F1
7.15 MHz TO 13.33 MHz
=====
  N#F1      N#F2      K#F3
    5        5        0
SPURIOUS RANGE FOR F1 (Using plus I.F.)

136-174 High Side Injection (17.9 mhz IF)
156 MHz TO 159.68 MHz
DELTA SPURIOUS F1 FROM DESIRED F1
14.32 MHz TO 14.32 MHz

SPURIOUS RANGE FOR F1 (Using negative I.F.)
156 MHz TO 152.32 MHz
DELTA SPURIOUS F1 FROM DESIRED F1
31.46 MHz TO 21.48 MHz
=====
+-----+
+ SPURSEARCH +
+-----+
+ GENERAL SPURIOUS ANALYSIS +
+ VERSION 1.9 +
+ A.M. VECTOR 8/17/84 +
+-----+
COMPUTING CASE 1 (+,-,-)
COMPUTING CASE 1 (+,-,-)
  N#F1      N#F2      K#F3
    1        1        0
SPURIOUS RANGE FOR F1 (Using plus I.F.)
171.8 MHz TO 174 MHz
DELTA SPURIOUS F1 FROM DESIRED F1
23.8 MHz TO 25.8 MHz

SPURIOUS RANGE FOR F1 (Using negative I.F.)
136 MHz TO 174 MHz
DELTA SPURIOUS F1 FROM DESIRED F1
0 MHz TO 0 MHz
=====
COMPUTED SPURIOUS FOR CASE 1 (+,-,-)
  N#F1      N#F2      K#F3
    2        2        0
SPURIOUS RANGE FOR F1 (Using plus I.F.)
162.85 MHz TO 174 MHz
DELTA SPURIOUS F1 FROM DESIRED F1
24.85 MHz TO 24.85 MHz

SPURIOUS RANGE FOR F1 (Using negative I.F.)
144.95 MHz TO 174 MHz
DELTA SPURIOUS F1 FROM DESIRED F1
8.95 MHz TO 8.95 MHz
=====

```

```

  N#F1      N#F2      K#F3
    3        3        0
SPURIOUS RANGE FOR F1 (Using plus I.F.)
159.8666667 MHz TO 174 MHz
DELTA SPURIOUS F1 FROM DESIRED F1
23.8666667 MHz TO 23.8666667 MHz

SPURIOUS RANGE FOR F1 (Using negative I.F.)
147.9333333 MHz TO 174 MHz
=====
136-174 High Side Injection (17.9 mhz IF)
DELTA SPURIOUS F1 FROM DESIRED F1
11.93333333 MHz TO 11.93333333 MHz
=====
COMPUTED SPURIOUS FOR CASE 1 (+,-,-)
  N#F1      N#F2      K#F3
    4        3        0
SPURIOUS RANGE FOR F1 (Using plus I.F.)
156 MHz TO 148.4 MHz
DELTA SPURIOUS F1 FROM DESIRED F1
21.4666667 MHz TO 22.6 MHz

SPURIOUS RANGE FOR F1 (Using negative I.F.)
156 MHz TO 159.45 MHz
DELTA SPURIOUS F1 FROM DESIRED F1
33.4 MHz TO 34.55 MHz
=====
  N#F1      N#F2      K#F3
    4        4        0
SPURIOUS RANGE FOR F1 (Using plus I.F.)
158.375 MHz TO 174 MHz
DELTA SPURIOUS F1 FROM DESIRED F1
22.375 MHz TO 22.375 MHz

SPURIOUS RANGE FOR F1 (Using negative I.F.)
149.425 MHz TO 174 MHz
DELTA SPURIOUS F1 FROM DESIRED F1
13.425 MHz TO 13.425 MHz
=====
COMPUTED SPURIOUS FOR CASE 1 (+,-,-)
  N#F1      N#F2      K#F3
    5        4        0
SPURIOUS RANGE FOR F1 (Using plus I.F.)
136 MHz TO 157.1 MHz
DELTA SPURIOUS F1 FROM DESIRED F1
11.625 MHz TO 16.9 MHz

SPURIOUS RANGE FOR F1 (Using negative I.F.)
136 MHz TO 149.94 MHz
DELTA SPURIOUS F1 FROM DESIRED F1
20.575 MHz TO 24.06 MHz
=====
COMPUTED SPURIOUS FOR CASE 1 (+,-,-)
  N#F1      N#F2      K#F3
    5        5        0
SPURIOUS RANGE FOR F1 (Using plus I.F.)
157.48 MHz TO 174 MHz
DELTA SPURIOUS F1 FROM DESIRED F1
21.48 MHz TO 21.48 MHz
=====

```

```

136-174 High Side Injection (17.9 mhz IF)
SPURIOUS RANGE FOR F1 (Using negative I.F.)
150.32 MHz TO 174 MHz
DELTA SPURIOUS F1 FROM DESIRED F1
14.32 MHz TO 14.32 MHz
=====
  N#F1      N#F2      K#F3
    6        5        0
SPURIOUS RANGE FOR F1 (Using plus I.F.)
136 MHz TO 162.9 MHz
DELTA SPURIOUS F1 FROM DESIRED F1
5.72 MHz TO 11.1 MHz

SPURIOUS RANGE FOR F1 (Using negative I.F.)
156 MHz TO 156.9333333 MHz
DELTA SPURIOUS F1 FROM DESIRED F1
12.88 MHz TO 17.0666667 MHz
=====
COMPUTED SPURIOUS FOR CASE 1 (+,-,-)
  N#F1      N#F2      K#F3
    7        5        0
SPURIOUS RANGE FOR F1 (Using plus I.F.)
136 MHz TO 139.428571429 MHz
DELTA SPURIOUS F1 FROM DESIRED F1
32.92 MHz TO 34.3714285714 MHz

SPURIOUS RANGE FOR F1 (Using negative I.F.)
136 MHz TO 134.514285714 MHz
DELTA SPURIOUS F1 FROM DESIRED F1
40.08 MHz TO 39.4857142857 MHz
=====
COMPUTED SPURIOUS FOR CASE 1 (+,-,-)
  N#F1      N#F2      K#F3
    6        6        0
SPURIOUS RANGE FOR F1 (Using plus I.F.)
156.863333333 MHz TO 174 MHz
DELTA SPURIOUS F1 FROM DESIRED F1
20.863333333 MHz TO 20.863333333 MHz

SPURIOUS RANGE FOR F1 (Using negative I.F.)
150.9166667 MHz TO 174 MHz
DELTA SPURIOUS F1 FROM DESIRED F1
14.9166667 MHz TO 14.916666667 MHz
=====
  N#F1      N#F2      K#F3
    7        6        0
SPURIOUS RANGE FOR F1 (Using plus I.F.)
136 MHz TO 167.042857143 MHz
DELTA SPURIOUS F1 FROM DESIRED F1
1.783333333 MHz TO 1.9714285714 MHz

SPURIOUS RANGE FOR F1 (Using negative I.F.)
136 MHz TO 161.928571429 MHz
DELTA SPURIOUS F1 FROM DESIRED F1
7.75 MHz TO 12.0714285714 MHz
=====

```

Preventing Unwanted Oscillations in Crystal Oscillators

Part II

By James W. Wieder
Westinghouse Defense &
Electronics Center

Part II discusses non-crystal controlled oscillations and crystal spurious oscillations. It then concludes with a discussion of six design verification tests useful in uncovering potential unwanted oscillations.

A non-crystal controlled oscillation does not rely on the quartz blank for the requirements of oscillation. The unwanted oscillation is unrelated to the desired oscillation and will have poor frequency stability. There are several possible causes of non-crystal controlled oscillation.

a) The oscillation may occur via a reactance which shunts the quartz blank. The shunting reactance may be the crystal's CO. Oscillation via CO usually occurs at a frequency well above the desired oscillation. In series resonant oscillators where an inductor (LO) is used to parallel resonate out CO (at the desired frequency of oscillation), the LO may shunt the quartz blank at frequencies well below the desired oscillation.

b) A larger portion of the oscillator may be shunted by a stray impedance. The

shunting path generally occurs from a low impedance point in the circuit to a high impedance point. The high impedance point is generally due to a parallel LC resonance (possibly due to stray reactance).

c) Oscillation may occur due to a sustaining stage instability. The transistor or amplifier becomes unstable due to certain combinations of impedances loading the amplifier input and/or output.

Unwanted Oscillation Via CO or LO

A typical value of CO for AT-cut crystals above 1 MHz is 2 to 6 pF. Figure 1 compares the reactance of CO with the crystal motional resistance. Above about 60 MHz, the reactance of CO is no longer very large compared with the crystal motional resistance. At 150 MHz, for example, the reactance of 5 pF (around 210 ohms) is only about twice the motional resistance (R₁₇) of a seventh overtone AT-cut crystal. At higher frequencies (say 500 MHz), the reactance of CO may be less than the motional resistance of the crystal's desired overtone.

Unwanted oscillation via the crystal CO

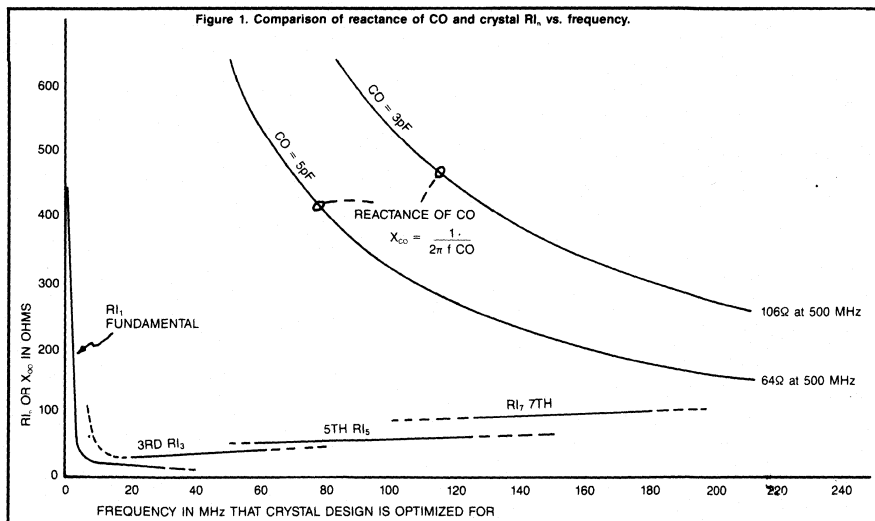
may occur at an unintended peak of the overtone select filter or for oscillators above 60 MHz within the overtone select bandpass. Oscillation via CO within the overtone select passband can be prevented by parallel resonating an inductor (LO) with CO at the desired overtone frequency. Depending on CO, this is usually done for oscillators above 60 to 120 MHz. The effect of LO on a seventh overtone 175 MHz AT-cut crystal is shown in Figure 2.

It is important that the sharpness (Q) of the CO-LO parallel resonance be significantly lower than that of the overtone select filter. This assures that the impedance of the CO-LO parallel combination remains large over the overtone select passband. In some cases, the CO-LO Q must be deliberately lowered by using resistance in series with the inductor.

Note that the CO-LO resonance is only useful in preventing oscillation via CO from occurring within the overtone select bandpass. At frequencies well above the CO-LO resonance, the CO-LO combination will still appear as CO and hence a low impedance. At frequencies well below the CO-LO resonance, the CO-LO combination will appear as LO and a low impedance. If an unintended peak exists, non-crystal controlled oscillation may occur via CO or LO above or below (respectively) the desired overtone.

A second reason for parallel resonating out CO is to increase an oscillator's trim range. As shown in Figure 3, CO has a significant effect on the 175 MHz crystal's effective reactance and resistance near series resonance. The increasing effective resistance limits the frequency adjustment range to 4 or 5 KHz above series resonance. As shown in Figure 3, parallel resonating out CO with LO dramatically increases the possible trim range by maintaining a constant effective resistance over a wider frequency range.

To determine if a non-crystal controlled

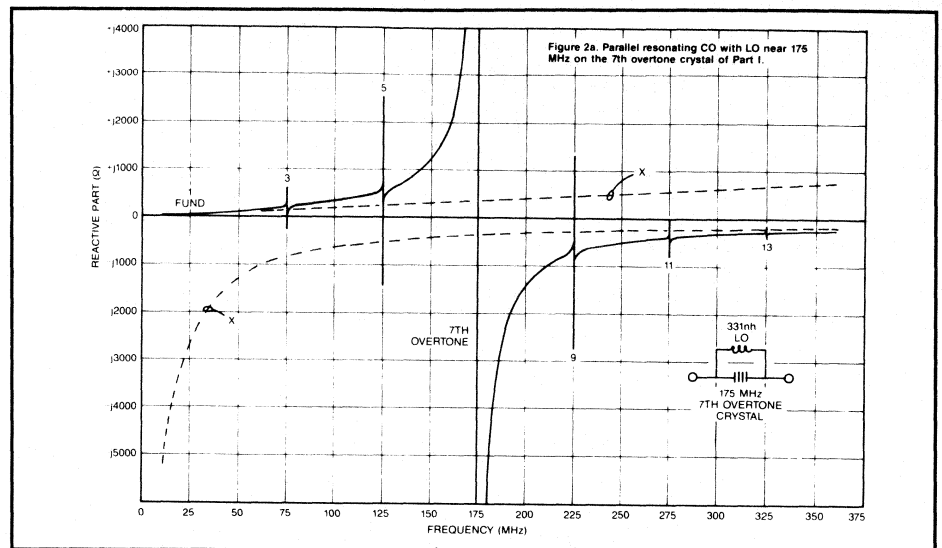


oscillation is due to either CO or LO shunting of the crystal blank, remove the crystal from the circuit and replace it with a capacitance equal to CO (while keeping LO in the circuit). In a properly designed circuit, no oscillation should occur.

Unwanted Oscillation due to Sustaining Stage Instability.

All transistors and amplifiers in addition to their forward gain also exhibit an internal reverse gain (loss). It is this internal reverse gain that can lead to a sustaining stage instability. For certain combinations of transistor (or amplifier) source and load impedances, the transistor may become unstable at a frequency which is unrelated to the desired frequency of oscillation. The oscillation is independent of the transfer function $H(f)$ of the feedback stage. The oscillation, however, is influenced by the input impedance of the feedback stage since this represents the transistor load impedance. The oscillation is also influenced by the output impedance of the feedback stage since this represents the transistor source impedance. This type oscillation will occur when the circuit is reconfigured as shown in Figure 4. No signal source needs to be applied in Figure 4 for the unwanted oscillation to occur.

The reverse gain characteristics differ with the transistor type. Even if two transistors are biased to the same forward gain, one type may be unstable while another type works fine. References 2 and 3 discuss a method of determining if any



linear 2-port is unconditionally stable at each frequency (stable for any combination of source and load impedances). This method is based on S-parameter (scattering parameter) device characterization. A method of determining the source and load impedances where the linear 2 port is stable at a given frequency (referred to as conditionally stable) is also shown.

The transistor can generally be stabilized by modifying the input or output impedance of $H(f)$. When the frequency of the transistor instability is away from the desired crystal frequency, it may be pos-

sible to modify the input and output impedances of $H(f)$ at the unstable frequency without affecting the desired $H(f)$ transfer function. If the circuit can be accurately modeled, both the SPICE and COMPACT simulation programs can provide insight into a sustaining stage instability.

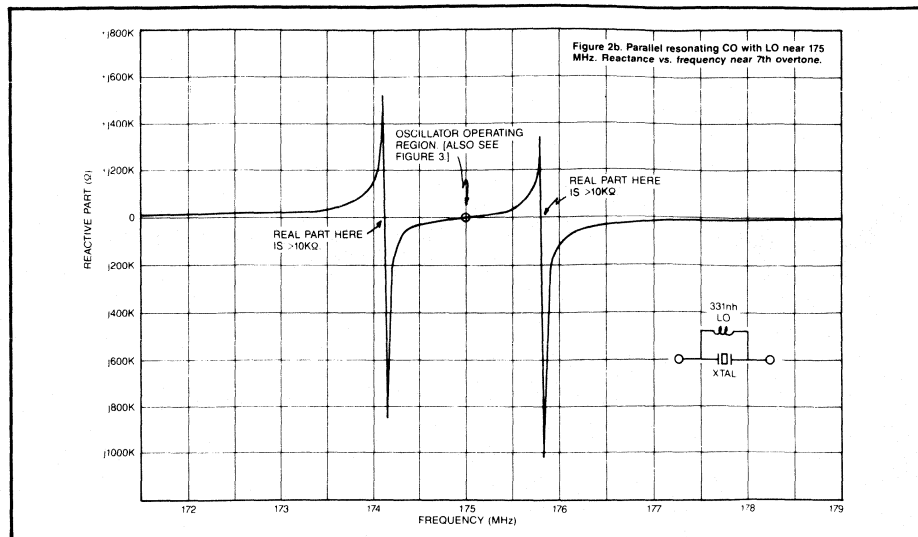
Oscillation at a Crystal Spurious Response

In addition to the fundamental and the odd overtone responses, quartz crystals exhibit spurious responses unrelated to

the desired response. This is because the quartz blank is capable of vibrating in many different modes and directions. The number of spurious responses and their frequency locations are unique for each crystal. The model for a spurious response is the same as the crystal fundamental responses, with the following differences:

- a) R_{1s} of the spurious is higher
- b) Q of the spurious is higher (L_1 larger, C_1 smaller)
- c) Temperature stability of the spurious is generally poor

The quartz crystal is designed and screened so the R_{1s} values of all spurious in the vicinity of the desired response are larger than R_{1d} . (R_{1d} is the R_{1n} value for the desired response.) A crystal specification normally lists a minimum allowed value for the ratio of R_{1s} over R_{1d} . This ratio is often referred to as the spurious resistance ratio. For fundamental and third overtone AT-cut crystals (where R_{1d} is small), a spurious resistance ratio of 4:1 or larger is obtainable. At higher overtones, R_{1d} is larger and the spurious resistance ratio will be lower. For the seventh overtone,



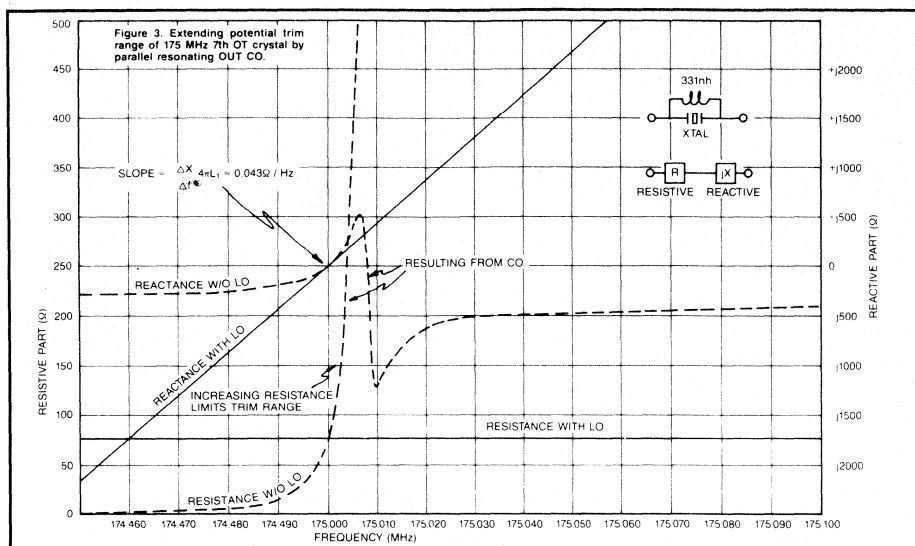
a ratio of only 2:1 may be feasible. A low spurious resistance ratio is one of the factors that limits the production use of crystals to the fifth or seventh overtone.

Oscillation at a crystal spurious might occur in one of two ways.

- a) Oscillation may occur at a spurious located within the overtone select band-

pass (near the desired response).

- b) Oscillation may occur at a spurious which happens to be located at an unintended peak. In this case, the spurious will be located well away from the desired response. The crystal manufacturer normally screens only for spurious that are near the desired response. To prevent



oscillation at a spurious located outside the screen range you must verify that unintended peaking does not occur.

For spurious located near the desired response, oscillation can be prevented by assuring that oscillation will not occur with the minimum R_{1s} value the crystal specification would allow. This can be

checked by adding resistance in series with the crystal to determine the R_1 value where the desired oscillation will not start up. The minimum value of R_{1s} should be larger than this R_1 value.

Note that specifying a minimum allowed spurious resistance ratio may not adequately specify the minimum allowed

spurious resistance (R_{1s}). If a particular crystal in a batch has a low value of R_{1d} , the spurious resistance ratio allows the spurious R_{1s} to also have a low value — low enough that the requirements of oscillation might also be met by the spurious. For this reason, a minimum allowable value of R_{1s} should also be specified where practical. For the higher overtone crystals, a minimum R_{1s} value significantly larger than the maximum value of R_{1d} can only be obtained at a very low crystal yield. For these crystals the specification of a minimum allowed R_{1s} value may not be practical.

The higher the overtone used, the more likely oscillation may occur at a crystal spurious. This is because:

a) The close R_{1d} and R_{1s} values make it difficult to prevent the requirements of oscillation from being satisfied at a spurious, and

b) A sharper overtone bandpass must be used. This makes it more likely that this bandpass may discriminate against the desired overtone in favor of a spurious. It is important that the overtone bandpass not be made any sharper than is necessary. The effect of tuning on

possible bandpass discrimination should also be considered.

Many VHF oscillators end up employing a design where the requirements for oscillation may also be satisfied at a spurious but start-up domination by the desired response is used. For a random noise start-up, domination by the desired frequency is aided by two factors.

a) The lower $R1_d$ value of the desired response results in a larger gain at the desired frequency. This helps the desired oscillation to build up faster than a spurious.

b) The higher Q of the spurious means the closed loop spurious bandwidth is narrower. The resulting spurious group phase delay will be larger. This causes the spurious oscillation to build up slower than the desired oscillation.

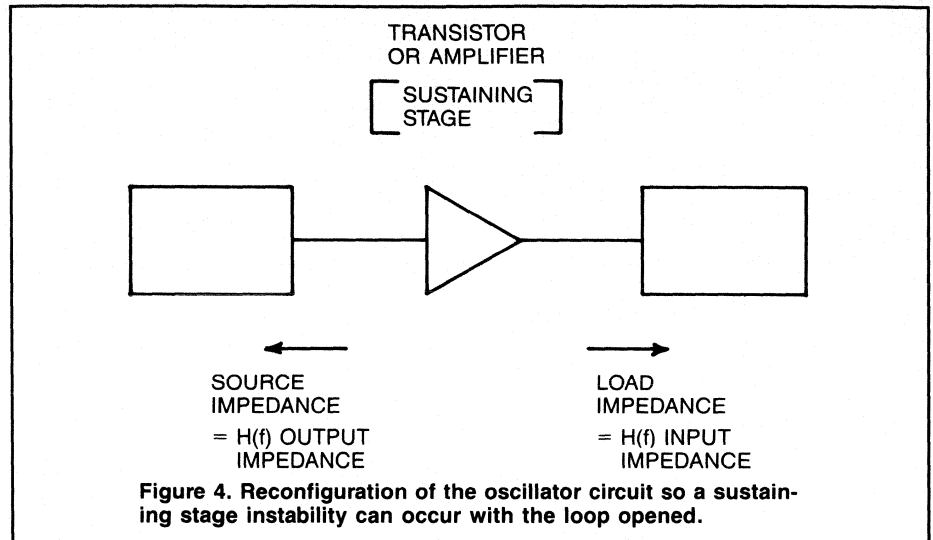
When relying on start-up dominance, the following should be considered.

a) Another frequency source (with frequency near a spurious) might leak into an oscillator during start-up and allow the spurious to build up faster than the desired response. The isolation between oscillators should be maximized. When crystal switching or oscillator switching is used, the first oscillation should be allowed to die out before the next oscillation is allowed to start up.

b) An oscillator could have a non-crystal controlled oscillation near a crystal spurious. The non-crystal controlled oscillation may start up more quickly than the desired oscillation. The non-crystal controlled oscillation may then run synchronously with the crystal spurious oscillation.

Testing to Uncover the Problems

The causes of unwanted oscillations are numerous. Experience in selecting the oscillator type, its design and layout can minimize potential problems, but due to the complex interaction of oscillator components, design oversight is possible. The ability of a computer simulation to reveal potential unwanted oscillations is limited by the extent to which stray reactances are accounted for and by the sophistication of the transistor (amplifier) model. Testing the oscillator in its normal oscillating configuration is of limited use in determining if the requirements of oscillation are met at more than one frequency. The desired oscillation may dominate the unwanted oscillation for the particular oscillator and unit being tested. Variations in either the test conditions or oscillator components could result in an unwanted oscillation becoming a problem. The following tests are useful in uncovering potential unwanted oscillations.



Test 1. Open Loop Amplitude Response

A reliable method of detecting many potential unwanted oscillations is to open the loop and examine the gain (and in some cases the phase) response. Since the layout can be significant, the open loop response should be performed on the actual production layout. Conducting this test during the development phase may prove useful in establishing the suitability of the oscillator circuit type and may provide insight into the desired final layout.

A frequency synthesizer can be used along with a vector voltmeter, spectrum analyzer or network analyzer.

The following guidelines should be considered.

a) To see the crystal response, the frequency synthesizer should be swept in 100 Hz or finer steps in the vicinity of each crystal overtone.

b) The cause of any circuit peaking should be determined. As was previously shown, a minor circuit modification may turn a small peak into a significantly larger peak. In some situations the phase variation of a small peak may be more observable than the amplitude variation.

c) Open loop response should be examined at several trim capacitor values across the trim range.

d) Measuring the open loop response over temperature and voltage helps verify the needed excess gain at the desired oscillator frequency.

e) Use signal levels representative of oscillation start-up. Typical excess gain at start-up should be 2 to 6 dB.

f) Final oscillation level can be checked by increasing the signal level to the point

where unity gain at the desired frequency is reached.

g) Carefully choose the point where the loop is to be broken.

h) Load the input and output of the open loop with the same (powered) circuit it will normally be seeing. Portions of two other oscillator boards can be interconnected using short leads.

i) To minimize standing waves on the cable, use a 10 dB attenuator at the point where the frequency synthesizer is applied to the circuit.

j) Use probes to observe the loop input and output. The probe input impedance should be large enough to prevent significant loading of the circuit being tested.

k) The impedance loading the input and output of the transistor (or amplifier) should be the same as for the closed loop.

The open loop response measurements can be used to improve the computer modeling of the various stray reactances. In the ideal, the measured response would closely match that of the open loop computer model.

Test 2. Closed Loop Amplitude Response

In this test the overtone select filter is deliberately detuned so oscillation at the desired overtone does not occur. No other oscillation should be observed. A frequency synthesizer is used to apply a signal to the loop, perhaps via what is normally the oscillator output. A probe is placed at various points in the closed loop to detect amplitude peaking as the frequency synthesizer is swept. The circuit should be detuned both above and below the desired overtone. The amount of de-

tuning necessary to prevent the desired oscillation provides a feel for the amount of excess gain. The advantages of this method over the previous are:

- a) It is easier to configure the test, and
- b) If probe loading is not too great the transistor input and output load impedance may be closer to the actual circuit, making it easier to observe a sustaining stage instability.

The disadvantages of this test method are:

- a) Amplitude peaking which might occur at the trim values in the normal trim range will be missed,
- b) Check of excess gain at the desired overtone is limited, and
- c) Limited information is obtained to improve the computer model.

Test 3. Determine Resistance Where Desired Oscillation Ceases

This should be done with either or both of the previous two tests; it provides a feel for the circuit's excess gain. Basically, resistance (RA) is added in series with the crystal until the desired oscillation will no longer start up. This test can be done over temperature, voltage and

trim range. If the resistance where oscillation stops ($R1 + RA$) is more than two or three times the maximum crystal motional resistance, the circuit gain is probably too high and should be decreased. Additionally, to assure that oscillation at a crystal spurious is not possible, $R1 + RA$ should be less than the minimum crystal spurious resistance. This test is not as useful as the previous two tests but is commonly done because it is so easy to do.

Test 4. Replace Crystal with CO (Max)

The crystal is removed from the circuit and replaced with CO (MAX). If the circuit has an inductor (LO) to parallel resonate with CO, leave LO in the circuit. With the crystal removed, the desired oscillation does not occur and will not dominate the non-crystal controlled oscillations. If the circuit is properly designed, no oscillation should occur over the full trim range with temperature and voltage variations. As a minimum, this test should be run at the conditions where the active device(s) have their maximum gain. To check for margin, use a capacitor larger than CO (MAX) and also use LO values

on either side of the design LO value. Since the crystal is removed, unwanted oscillations at adjacent overtones or spurious are not addressed with this test.

Test 5. Place Additional Capacitance Across the Crystal

A capacitor is placed in parallel with the crystal to simulate the maximum value of crystal CO (plus additional margin). This test provides a feel for the circuit's susceptibility to oscillation (non-crystal controlled) via the crystal shunt capacitance (CO). The oscillator should be started up several times for each trim condition. No oscillation other than the desired one should be observed. No scope edge jitter or spectrum analyzer modulation sidebands should be observed. This test is easy to do but is of limited usefulness, since the desired oscillation may be suppressing all other oscillation.

Test 6. Replace Crystal with Resistor (Series Resonant Oscillator Only)

In series resonant crystal oscillators (tuned on series resonance), the crystal is essentially resistive (of value R1). If the crystal is replaced by a resistor between

the minimum and maximum value of R_1 , an oscillation should be seen within several MHz of the crystal series resonant frequency. This provides an indication of the overtone select filter peak location. Since oscillation is not stabilized by the crystal's large $\Delta X/\Delta f$, the frequency counter will only have around four digits of short term stability.

With the resistor in place of the crystal no other oscillation frequency should be observed over the full trim range. This test, too, is of limited usefulness since the unwanted oscillations may be suppressed.

Conclusion

The choice of the start-up excess gain at the desired frequency of oscillation is critical. If the gain is too low, some oscillators will not start-up due to amplifier, crystal or reactive component variations. In some cases oscillation may stop or not start-up at certain temperatures or voltages. When the gain is made too large, unwanted oscillations are more likely. In addition, the resulting severe non-linear operation of the active device allows low frequency flicker noise to modulate onto

the oscillation frequency, increasing phase noise. An oscillator design that minimizes the variation in the closed loop gain at the desired frequency is advantageous since a low gain can be used while still assuring start-up will always occur.

Even if oscillator gain at the desired frequency is optimum an unwanted oscillation may still occur due to one or more of the causes discussed in this article. In general, the higher the oscillator frequency and the higher the amplifier high frequency cut-off, the greater the chance of having an unwanted oscillation. The possibility of an unwanted oscillation in a given design or layout cannot always be seen in advance. Performing verification tests on the final circuit configuration and layout that can uncover these specific problems is an important part of the design process.

References

- 1) M.E. Frerking, "Crystal Oscillator Design and Temperature Compensation," Van Nostrand Reinhold Company, 1978.
- 2) Hewlett Packard Application Note

154, "S-Parameter Design," 1973

3) Avantek, "High-Frequency Transistor Primer" Parts I & II, 1975

4) T.T. Ha, "Solid-State Microwave Amplifier Design," John Wiley & Sons, 1981

5) National Bureau of Standards Monograph 140, "Time and Frequency," 1974.

6) D.K. Belcher, "Designing a High Stability VHF Oscillator," *RF Design*, Jan./Feb. 1983.

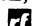
7) R.J. Matthys, "Crystal Oscillator Circuits for VHF" *RF Design*, May/June 1983.

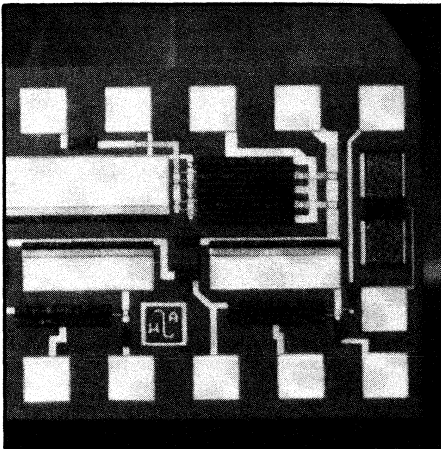
8) Mil-C-3098 General Specification for Quartz Crystal Units.

9) SPICE Version 2F.1 User's Guide, University of California, Berkeley

10) SUPER-COMPACT User's Manual (1.6), CGIS, Inc. Palo Alto, California.

About the Author

Jim Wieder is a design engineer at Westinghouse Defense and Electronics Center, P.O. Box 1521, M.S. 3642, Baltimore, MD 21203. 



Cover

This month's cover features a GaAs monolithic VHF/UHF amplifier currently being developed by M/A-Com Advanced Semiconductor Operations, Lowell, Mass. This feedbacked, three-staged amplifier outperforms conventional silicon monolithic amplifiers in terms of gain and noise. It is one of a series of broadband and narrowband GaAs MMIC circuits currently under development at M/A-Com.

Features

29 Special Report: The New Look in RF Circuits — Miniaturization

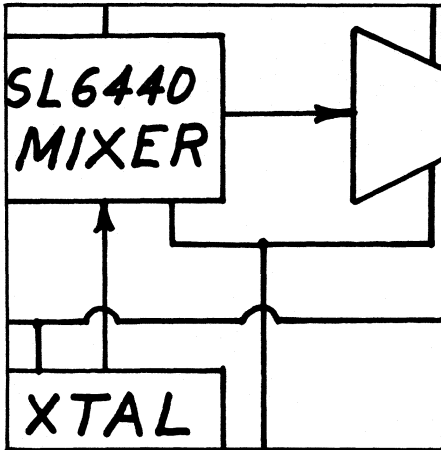
The trend is to smaller and lighter circuits in RF as it has been in microwave. Because of the greater volume of RF manufacturing, it is automated surface mounting that is making miniaturization practical. This month we look at surface mounted RF devices and other aspects of circuit miniaturization. — James N. MacDonald.

46 An Ultra-Lightweight HF Transmitter Using High Voltage MOSFETs

Here is an RF amplifier with a transformerless power supply driven by a one-pound heterodyne VFO. The complete transmitter weighs four pounds and can be carried in an attache case. This article examines several myths about MOSFETs. — Robert W. Vreeland.

52 The Surface Acoustic Wave Filter

Because of the interest generated by previous articles on SAW design, the author has begun a series on one of the primary uses of this technology. The first article deals with specifying SAW filters and explains some of the terminology in common use. — Jeff Schoenwald.

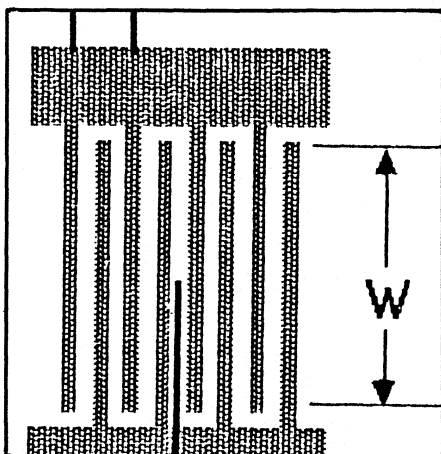


Departments

RFI/EMI Corner

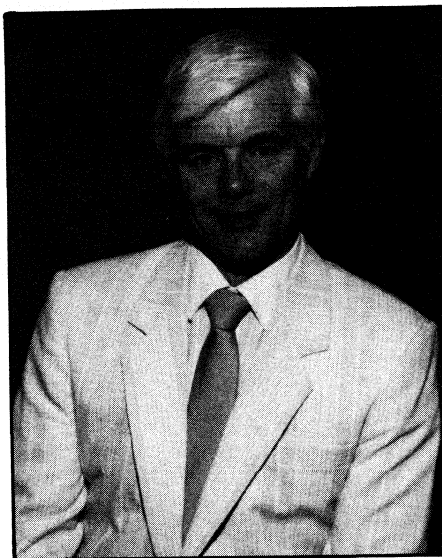
- 61 Protection circuits designed to prevent equipment overload can radiate signals. These unintentional "jammers" are difficult to identify and deal with. — Kenneth Grymala.

- 6 Editorial
- 8 Publisher's Notes
- 12 Letters
- 16 Calendar
- 22 News
- 39 Info/Card
- 63 New Products
- 68 New Literature
- 71 Classified Advertising
- 74 Advertisers Index



R.F. DESIGN (ISSN: 0163-321X USPS: 453-490) is published monthly plus one extra issue in August. August 1985, Volume 8, No. 8. Copyright 1985 by Cardiff Publishing Company, a subsidiary of Argus Press Holdings, Inc., 6530 S. Yosemite Street, Englewood, CO 80111 (303) 694-1522. Contents may not be reproduced in any form without written permission. Second-Class Postage paid at Englewood, CO and at additional mailing offices. Subscription office: 1 East First Street, Duluth, MN 55802, (1-800-346-0085). Domestic subscriptions are sent free to qualified individuals responsible for the design and development of communications equipment. Other subscriptions are: \$22 per year in the United States; \$29 per year in Canada and Mexico; \$33 (surface mail) per year for foreign countries. Additional cost for first class mailing. Payment must be made in U.S. funds and accompany request. If available, single copies and back issues are \$5.50 each (in the U.S.). This publication is available on microfilm/fiche from University Microfilms International, 300 N. Zeeb Road, Ann Arbor, MI 48106 USA (313) 761-4700. POSTMASTER & SUBSCRIBERS: Please send address changes to: R.F. Design, P.O. Box 6317, Duluth, MN 55806.

A Technology Whose Time Has Come



James N. MacDonald
Editor

In this month's Special Report we mention a company with a vision of incredibly tiny electronic devices for consumer use. This is just one of many companies we have visited with amazing R&D projects for components and devices. Project managers will only talk in the vaguest terms, of course, since much of the work is experimental, but the excitement and optimism are apparent.

Also apparent is a healthy caution about raising public expectations for advances that might not occur. As one executive put it, "We try to avoid the 'magic dust' syndrome — the new development that is supposed to solve everybody's problems but turns out to be another five years down the road."

With this realistic attitude, RF designers and manufacturers will avoid the situation the computer industry finds itself in. The home computer market that showed such great promise is now floundering. There are many theories for this slump, but the underlying problem is that the mass market has not materialized. Although small computers are a big help in small

businesses, they have not proved very useful in the home. Ordinary people with an interest in technology and those who like to be among the first to have new gadgets have bought them. Those without the time and inclination to learn how they work have avoided purchasing them.

It seems likely that home computers are a technology ahead of their time. Carried along by rapid advances in miniaturization and reductions in cost, manufacturers began producing home computers as soon as they were able. They knew the amazing power and capability of these little machines and, apparently, expected the average consumer to see quickly how useful they could be. What they did not study thoroughly enough was whether the average consumer needed a computer.

Some critics saw this problem. One columnist wrote sarcastically that soon there would be a computer in every closet. "Necessity is the mother of invention," but in the case of computers for the mass market the invention came before there was a need for it. The RF industry could make the same mistake.

The major companies we have talked to lately seem to be determined to avoid producing for markets that are not there. We hope all RF companies will learn from the experience of the home computer industry and avoid a competitive rush to bring electronic devices on the market just because they have learned how to make them.

Two important points can be learned from the experience of the computer manufacturers: there has to be a need for the new technology and it has to be easy to use. Thanks to the cumulative experience of RF design engineers, new consumer devices are easy to use. Let's also be sure the consumer wants them.

*James N.
MacDonald*

Editor:

Thanks for publishing my article "Smith Chart Calculations on Your Microcomputer" in your June issue. I've had my magazine only one day and already have received three inquiries about copies of the program. To save unnecessary phone calls, please inform other readers who may be interested in the program but do *not* have Simons' BASIC that I have a version which will run on a standard Commodore 64 (stated in my manuscript but edited out).

Thank you.

L.A. Gerig

Editor:

In addition to comments I sent on a recent issue of *R.F. Design*, there are two additional comments I wish to offer on the May issue.

The first is that amateurs in the 1920s learned the importance of use of BFOs as a consequence of the use of regenerative and super-regenerative detectors. But the spectrum analyzer engineers *still* don't understand the importance of BFOs. I tried to get the message across to the Hewlett-Packard design engineer on the design of their first spectrum analyzer in the 1960s, but was unsuccessful. Needless to say, deep-space probes would be useless without the product detectors that are vital to the basic BFO principle.

The second is that the central location of the "Y" parameters in the drawing on page 49 in the May issue is not accidental. Only Y parameters are basic with bipolar transistors, as well as FET devices and electron tubes, as was shown on page 287, Lo et al, "TRANSISTOR ELECTRONICS," published in 1955. The

H parameters, both h_f and h_i , depend on the small difference in emitter and collector currents, whereas device transconductance is a direct function of either the collector current (common-emitter configuration), or the emitter current (common-base configuration). One almost always can discard H parameters, Z parameters, and A parameters. The small-difference of large currents is endemic in the H parameters, and has caused continuing difficulties in circuit design over the years. My books point this out clearly, and they also present the basics for the parameter relations given by this author.

All active device conductances take the form:

$$y = K \cdot (q/kT) \cdot I$$

Where the $\kappa(K)$ has the value unity with bipolars under low-current conditions (this is also true with FET devices at very small currents, and also for electron tubes under similar conditions), and may have a value as high as 1.6 for NPN transistors and 0.6 for PNP transistors under high-injection conditions.

I published the conversion formulae for all but the S parameters in my Handbook of Transistor Circuit Design (1962, Prentice-Hall) and in Reliable Military Electronics. The former was published before the S parameters were developed, but I didn't add them to the latter. It is evident from the chart that the Y parameters, if used properly, usually will meet one's needs in RF applications. The principal point is that for stability, voltage gain must be limited, typically to less than 10, and the only way it can be assured is through the use of the Y parameters.

Keats A. Pullen, Jr.
2807 Jerusalem Road
Kingsville, MD 21087

Editor:

As per our telephone conversation, may I point to a misprint in the Transistor Parameter Conversion Program.

Line 2160 should read:

```
2160 PRINT INT (R(K)*E)/ETAB(10)INT(I(K)*E)/E,INT(M(K)*E)/
ETAB(30)INT(A(K)*E)/E
```

Keep these beautiful RF programs coming for the Commodore 64. We enjoy them very much.

Al Goldberg
Circuit Designer
Spectrum Enterprises, Miami, Fla.

Editor:

Two subjects here: first, in response to Keith Aldrich's note regarding advertising — I agree that "... advertising is one of the most useful aspects of a magazine. . ." *However*, there is one aspect of your advertisements that I find both frustrating and indefensible — the omission of PRICE information in both the advertising and New Products areas.

Second, I would really like to see an in-depth (or a series) article on *practical* spread-spectrum pulse techniques using SAW devices. I would like such an article to:

- 1) be written in practical, working level terms
- 2) discuss (with figures and photos) both time and frequency domain signal characteristics
- 3) give examples of pulse compression, expansion
- 4) use *simple* math (save the triple-integrals and the exponentials of the exponentials for the IEEE transactions)
- 5) discuss trade-offs in choosing a SAW device
- 6) present a complete design example for a simple compression, expansion.

Thank you for listening.

Sid G. Knox
Pacific Missile Test Center
Code 3421
Point Mugu, CA 93042

ERRATUM:

Lines 650 and 660 were accidentally left out of the article "Helical-Resonator Filter Design — A BASIC Program" in the July issue. They are:

```
650 QD=.5*Q1*(FO/BW3)::RZ=(PI/4)*((1/QD)-(1/QU))
```

```
660 SN=SQR((RZ/2)*(RT/ZO))::RAD=180/PI
```

RF Design regrets the omission.

An Ultra-Lightweight HF Transmitter Using High Voltage MOSFETs

By Robert W. Vreeland
University of California
Research and Development Laboratory

Modern solid state transceivers are ideal for battery powered applications. However, the extremely heavy power supplies required make them unsuitable for lightweight, portable AC powered use.

We have taken a lesson from the AC-DC vacuum tube radios of the World War II era and have utilized high voltage MOSFETs in a two pound RF amplifier for the 3.5, 7.0 and 14.0 MHz amateur bands. The transformerless power supply weighs an additional pound and runs on either 220 volts or 117 volts AC. The amplifier is driven by a one pound dry battery powered heterodyne VFO. By using tuned push-pull operation we have reduced all harmonics sufficiently that no low pass output filters are needed. We have used this transmitter to work Japan from San Francisco. The complete station can be carried in an attache case or in a camera gadget bag.

Traditionally, AC-DC receivers have used a half wave rectifier in a transformerless unregulated power supply. The supply bridge is usually in the 150 to 170 volt range. By using a bridge rec-

tifier on 220 volts or a voltage doubler from 117 volts it is possible to develop sufficient voltage to run a simple linear voltage regulator with an output of 200 volts. This is an ideal power supply for an RF amplifier using a pair of 450 volt MOSFETs. The allowable drain to source voltage swing is zero to 400 volts leaving a 50 volt margin of safety.

Some of the older vertical power MOSFETs have a rise time as short as five nanoseconds, making them suitable for use in the 14 MHz amateur band. Unfortunately, the present design trend is toward higher power, lower frequency MOSFETs.

There are obvious safety problems resulting from transformerless design. The amplifier must have RF link coupling in and out. All circuits must be insulated from the metal panel and the panel must be grounded. Since the amplifier cannot be safely keyed, we must key the VFO. The VFO must be dry battery powered because a safe isolated power supply would add unnecessary weight.

These safety requirements were easily satisfied by building the RF power amplifier into a 2 x 4-1/2 x 6-1/2 inch plastic box with a grounded aluminum panel.

The box has a plastic cover which closes to form a neat, easily carried two-pound package. Separate 2 x 3-3/8 x 5-1/2 inch plastic boxes contain the power supply and the VFO, which weigh a pound each. The VFO is powered by a pair of 9 volt MN1604 alkaline batteries. This three-package configuration makes the transmitter easy to carry in a variety of containers.

The transmitter is designed to operate in the 7 and 14 MHz amateur bands using 14 foot long inductively loaded dipoles. For 3.5 MHz operation we use a tuned loop antenna formed from a 14 foot length of RG-8/U coaxial cable.

The foregoing looks like a fairly straightforward design problem. Let us now look at the real world of power MOSFETs. They are marvelous devices when properly used but they do present a number of unusual problems. Unfortunately, their true identity has been shrouded in a certain amount of mythology.

Myth Number One:

"Due to the absence of second breakdown and thermal runaway, MOSFETs are virtually indestructable."

This may be true if one adheres strict-

ly to the manufacturer's ratings. However, they will blow in microseconds if the peak current rating or the gate-to-source voltage rating is exceeded. To illustrate, look at the simple series regulator shown in Figure 1. This is a good regulator with one percent regulation from no load to a full load of several hundred milliamperes. However, the pass transistor will blow when the switch is moved from "R" to "S."

The charging current of a bypass capacitor as small as $0.02 \mu\text{F}$ exceeds the MOSFET's peak current rating. Since the source is momentarily grounded through the capacitor, the gate-to-source voltage rating is also exceeded, resulting in a punctured gate. Obviously some form of very high speed current limiting is required. This is most easily done by the use of series limiting resistors, as shown in Figure 2.

Excessive limiting will defeat the regulation for which the power supply was designed. It is usually possible, however, to divide the load so that the high current position, which does not require much regulation, does not interfere with the low current, well regulated loads. One must remember that the total peak charging current for all bypass capacitors must not exceed the MOSFET's peak rating. The reverse diode (D_o) is built into the MOSFET and need not concern us for normal drain-to-source voltage excursions.

Myth Number Two:

"Due to their insulated gate construction, MOSFETS require virtually no driving power."

While this is true for DC operation, it certainly does not apply to RF amplifiers. In Figure 3 the MOSFET is represented by a resistive channel. Current from source to drain through this channel is controlled by an electric field set up by the gate capacitor plate. As the driving generator frequency is increased, the capacitive reactance of the gate structure goes down, resulting in an increase in driving current into the lossy structure of the MOSFET. Our amplifier is noticeably harder to drive at 14 MHz than on the lower frequency bands. The drive requirements are moderate, however, when compared to a bipolar transistor amplifier.

Myth Number Three:

"Due to their self compensating thermal characteristics, MOSFETs will automatically adjust to share the load equally when connected in parallel."

This is true only when the MOSFETs

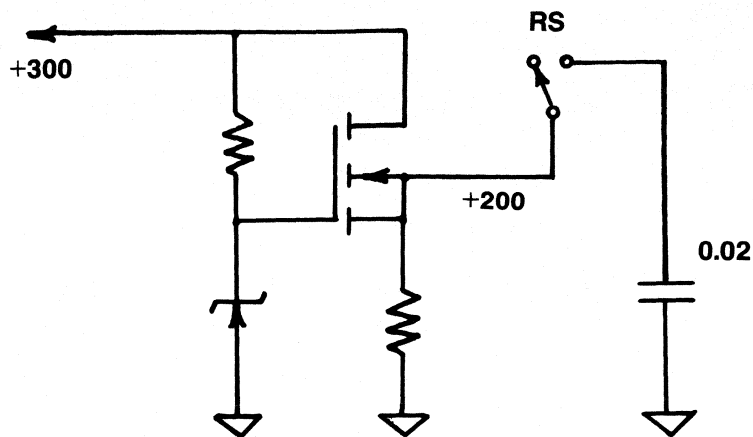


Figure 1.

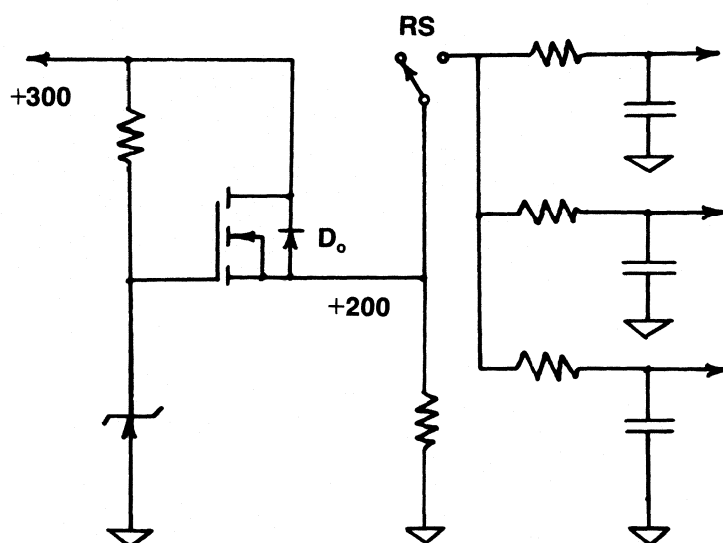


Figure 2.

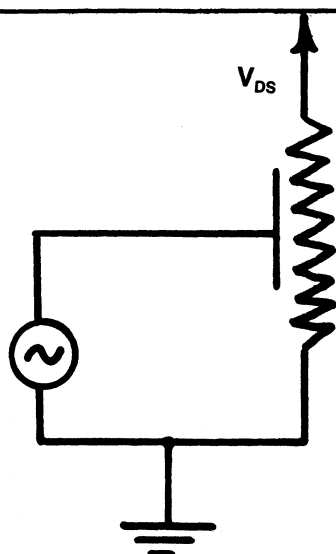


Figure 3.

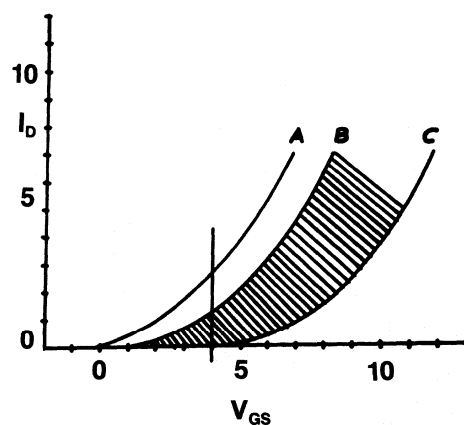


Figure 4.

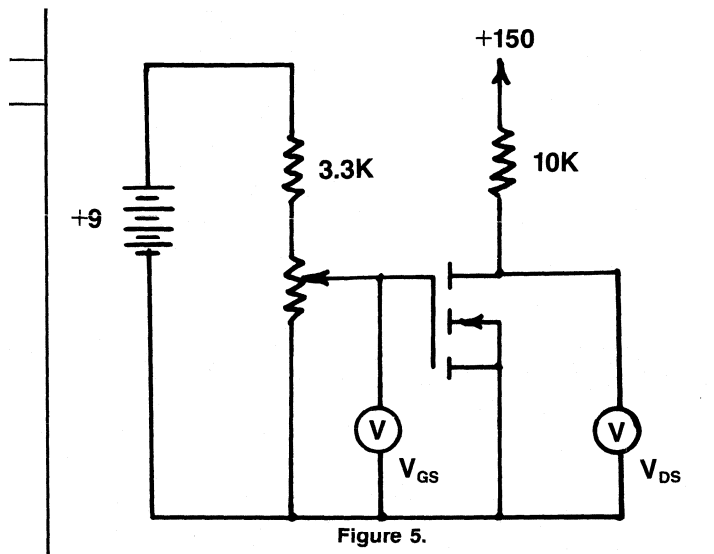


Figure 5.

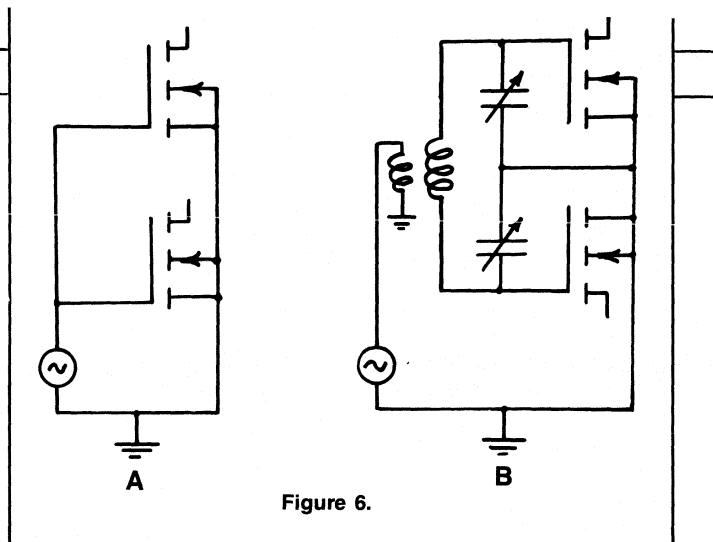


Figure 6.

are selected in matched pairs. Actually the gate threshold voltage may vary from 1.5 to 5 volts from transistor to transistor. For this reason manufacturers print normalized rather than actual transfer characteristic curves. In Figure 4, curve A is the normalized transfer curve. The actual curve may fall anywhere in the shaded region between curve B and curve C. Let us connect a curve B MOSFET in parallel with a curve C MOSFET. If we bias the parallel combination at +4 volts, the curve B MOSFET will carry a current of about 1-1/3 amperes, whereas the curve C MOSFET will not even turn on. Actually, the manufacturer is probably overly conservative in specifying such a wide range of gate threshold voltage. Inspection of Table I will show that the majority of IVN6000KNTs fall within the 2-3 volt region.

In our power supply we use a parallel pair of MOSFETs as pass transistors. The parallel pair was selected using the circuit shown in Figure 5. The gate-to-source voltage (V_{GS}) is gradually increased until the drain-to source voltage (V_{DS}) drops from 150 volts to 100 volts. The V_{GS} meter is then read. This is then the gate threshold voltage; $V_{GS} (th)$.

We did not select matched MOSFETs for our RF amplifier because individual bias voltage controls were provided. The amplifier was designed so that 10,000 ohm load resistors could be plugged into the output transformer jacks. The bias controls could then be used to determine the gate threshold voltages of the transistor pair using the previously described technique.

Drain-to-source voltage, drain current, rise time and input capacitance are perhaps the most important factors to be considered when selecting MOSFETs for RF use. The drain-to-source voltage rating must be high enough to allow the drain to swing up to double the power supply voltage with 50 volts or so to spare. The

drain current rating should be sufficient for the desired power level. Also, don't overlook the peak drain current rating, as exceeding this value will instantly destroy the MOSFET. Manufacturers provide safe operating area curves that are helpful for selecting the DC drain current operating point.

Rise time is perhaps the most critical factor affecting high frequency operation. It must be less than 10 nanoseconds for 14 MHz operation. Input capacitance is also extremely important. It can range anywhere from about 200 to 300 pF for a good RF MOSFET, such as the IVN6000KNT, to more than 10 times that value for the low frequency switching MOSFETs.

How to drive an input capacitance even as low as a couple of hundred pFs can be a real problem if two or more MOSFETs are connected in parallel. In parallel operation the input capacitances add as shown in Figure 6A. If, however, we use a tuned push-pull circuit, as shown in Figure 6B, the input capacitances appear in series across the tuning capacitor. This effectively cuts the input capacitance in half. Furthermore, the series combination becomes part of the input tuning capacitor, thereby serving a useful purpose. Push-pull operation effectively reduces the input capacitance by a factor of four over parallel operation.

The gate-to-drain feedback capacitance (C_{gd}) is important because it introduces positive feedback that can lead to oscillation and transistor destruction. In a tuned push-pull circuit conventional crossed capacitor neutralization can be used as in the case of vacuum tubes. Neutralization must be done with the full operating supply voltage applied because the gate-to-drain capacitance is a function of drain to source voltage. Neutralization is done with an oscilloscope connected across a dummy load on the amplifier output. The gate-to-source voltages are reduced so

that no drain current flows. A small amount of RF excitation is then applied and the neutralizing capacitors are adjusted for a null on the oscilloscope. This adjustment is only approximate and must be touched up for stable operation at full output.

Our power supply is packaged in a small covered plastic box (Figure 7, left). Note the cooling fins and the miniature meter, which is shunted for one ampere full scale. The regulated output and the transmitter safety ground are on the four pin connector. Separate grounded three wire power cords are used for 117 volt and 220 to 240 volt operation. Connecting the appropriate power cord to the six pin connector makes the necessary circuit changes.

TABLE I
Measured IVN6000KNT
Gate Threshold Voltages (Volts)

4.538	3.897	2.981
4.478	3.815	2.964
4.219	3.804	2.898
	3.243	2.801
	3.199	2.748
	3.129	2.699
	3.079	2.677
		2.666
		2.578
		2.406
		2.403
		2.376
		2.069

A simplified circuit diagram of the power supply appears in Figure 8. Diodes D_1 and D_2 form a voltage doubler with C_1 and C_2 for 117 volt operation. For 220 volt operation, the power cord completes the bridge circuit via jumper J_1 . The triangular symbols represent a floating common (not ground). The safety ground is not shown. A pair of Intersil IVN6000KNT MOSFETs serve as pass transistors and the Zener is a 1N5388. The regulation is one percent from no load to a full load of 500 mA.

Selecting diodes that would handle the inrush current into the 160 μF capacitors (C_1 and C_2) turned out to be a bit of a problem. We finally chose RCA SK3051s. It was necessary to limit the AC inrush current with a series 5 ohm, 5 watt resistor in order to prevent the on-off switch from burning out. Changing the power cord selects a 1-1/2 ampere fuse F_1 for 117 volts or a 3/4-ampere fuse (F_2) for 220 volt operation. Output current limiting is provided in the transmitter package.

For stability we chose a heterodyne VFO (Fig. 7, right). It is powered by two 9 volt alkaline transistor radio batteries (Fig. 9). The signal from the variable oscillator is mixed with one from a crystal oscillator to produce an output in the desired amateur band. The mixer is followed by a tuned output amplifier. Also included is an audio side tone oscillator.

The ground returns for all VFO circuits except the variable oscillator are keyed. An R-C circuit was inserted in the positive 9 volt lead to slow the rise of the keyed signal in order to reduce key clicks. By not keying the variable oscillator we have avoided any chirp problems. Since none of the harmonics from this oscillator fall within the bands used it is left on while receiving. It is, however, very important to keep the harmonics low while transmitting as they will mix with the crystal oscillator to produce spurious outputs.

A simplified circuit of the final amplifier is shown in Figure 10. Since the power supply is transformerless, toroidal isolation transformers T_1 and T_3 are used for the amplifier input and the output. The triangular symbols represent a hot floating common (not ground).

The driver transistor (Q_1 is an RCA SK3044. It is coupled via T_2 to a push-pull pair of IVN6000KNTs (Q_2 and Q_3). Both the primary and the secondary of T_2 are tuned. A separate transformer (T_2) is used for each amateur band. The transformers are wound on toroidal cores and are selected by a band switch (not shown). The positive bias on Q_1 is increased slightly for 14 MHz operation in order to

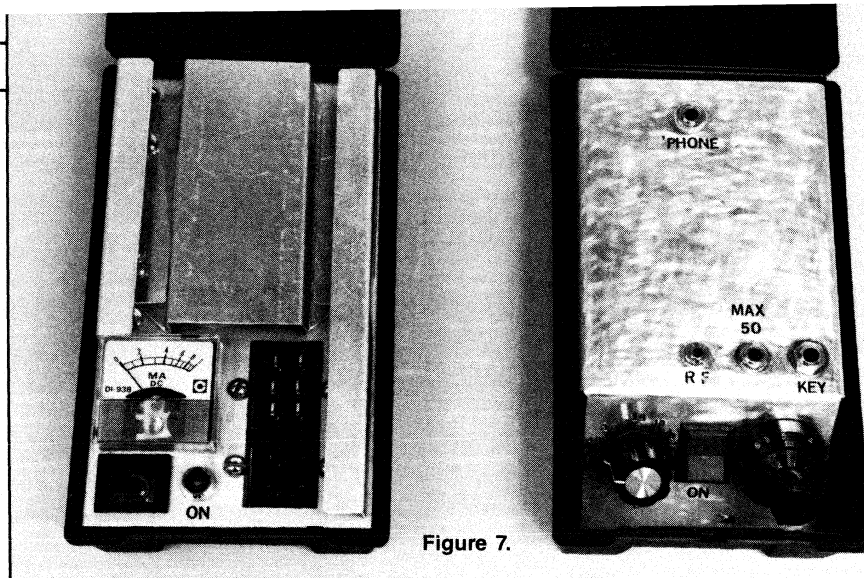


Figure 7.

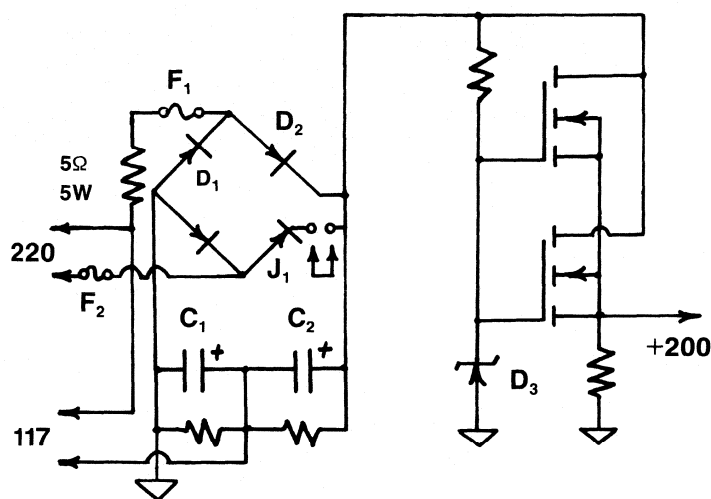


Figure 8.

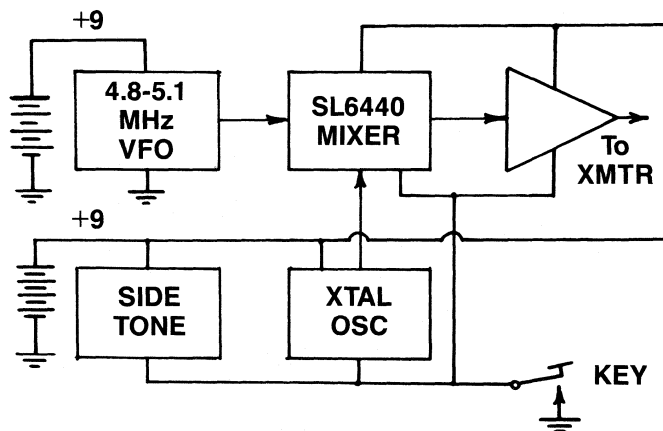


Figure 9.

The Surface Acoustic Wave Filter

Or, how to get

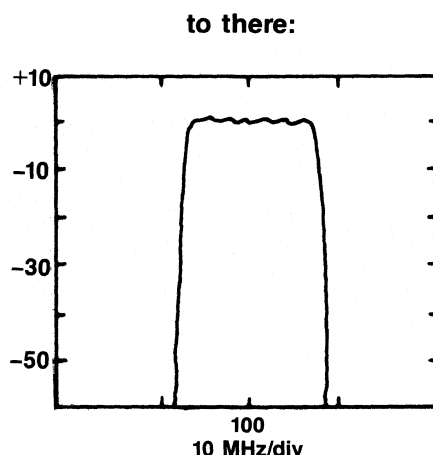
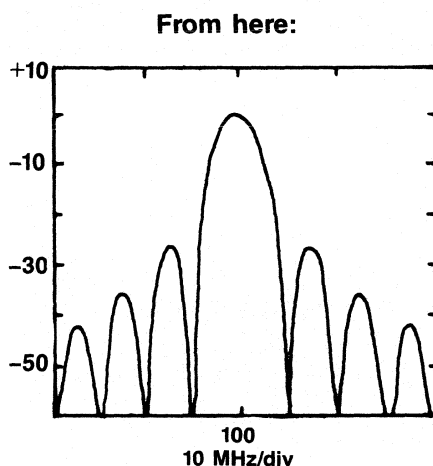
By Jeff Schoenwald
Contributing Editor

While several books, tutorial collections and journal special issues have been published to treat this topic, these works have mainly targeted audiences of narrower and more specialized interest than the readership of this magazine. In keeping with the editorial goal of serving the needs of a very broad and varied readership, this series will strive to take a balanced approach to the subject. We will make an effort to provide the relevant mathematics, philosophy upon which design rules are based, rules and procedures from which the design algorithms follow, equivalent circuit properties and how they are treated and fabrication and packaging techniques that must be regarded as integral elements in the successful design and execution of a satisfactory SAW bandpass filter.

The major portion of the discussion will be given to the interdigital transversal filter, although we expect to cover more sophisticated topics such as the unidirectional low loss bandpass filter and the SAW resonator multi-pole narrow bandpass filter, so the reader can develop enough familiarity to recognize which type of device is suitable, and when. Interested readers may go further and develop computer aided design procedures for simulating filter behavior.

Figure 1 is a general description, or roadmap, of the basic elements of SAW filter engineering. It is not unique, since other approaches will become apparent, but it is workable and has proved very successful, even if only as a basis for developing more sophisticated methods required by more sophisticated devices.

Let's start from a neutral point of view. Suppose the user is a systems designer and has some idea that a SAW bandpass filter is just the thing to clean up the signal processing in an IF section. The user develops a specification, calls up several SAW fabrication houses and kicks it around with the first SAW engineer the operator can locate. Even more common these days, the user's purchasing agent is put through to the director of marketing at the SAW house. Since it is not unusual for both persons to have only second-



hand knowledge of the design options available, some formal exchange of letters, brochures, business cards and a request for quotation takes place before things get going.

The user will generate a specification for the device. This usually includes the following, (summarized in Figure 2): center frequency, bandwidth (min and max), shape factor, sidelobe level, maximum insertion loss, in-band amplitude and phase or group delay ripple, direct cross-talk, insertion delay, and temperature dependent excursion limits of all the properties just indicated, variation limits at some standard operating temperature, and, of course, the usual salt spray, shelf

life, humidity and fungus (fungus?) resistance requirements that often accompany any electronic component requirement; and quantity, naturally.

After absorbing all these details, the SAW designer and marketing director decide if a straightforward response is in order. Years ago, but not so often now, SAW designers had to invest a great deal of time in educating prospective users, since the device was a novelty. Andersen Labs, for instance, periodically issues a brochure describing performance capabilities and system applications of SAW devices in their product line. In fact, the SAW research community has provided the largest investment in time, money and effort, redesigning systems to accommodate SAW devices rather than fighting the useless argument that "one filter should be able to replace another, so let's yank out the LC Butterworth and drop in a SAW." The first generation of SAW devices had more insertion loss than conventional filters and had linear phase (fixed delay). This has become less of a constraint as SAW technology has advanced, but problems still abound.

After the specs come in, the first decisions the SAW engineer makes is whether the center frequency presents a problem (too high, too low) and how the bandwidth affects design strategy. These two issues may be easy ones about which to make decisions, but they are still quite important.

Low frequency devices tend to get large, and to not reflect well the intent of microelectronics. The purchaser certainly would like a device smaller than the more conventional ones he might otherwise have to use. Substrate area and thickness will impact the materials cost. If the frequency is uncomfortably high, such as beyond 1 GHz, the imaging capabilities of the vendor's pattern generation equipment may be hard pressed, driving yield down and production costs up.

Bandwidth requirements will dictate the choice of substrate; large bandwidth requires large coupling substrate material; narrow bandwidth indicates lower coupling efficiency is more suitable. In addi-

tion, there are two basic approaches to transducer design that are generally (though not exclusively) specific to each bandwidth domain. These two methods are referred to as apodization (or overlap) weighting and withdrawal weighting.

The interdigital transducer (idt) achieves its filtering characteristics by a weighted sampling technique. A pattern of interleaved electrodes, like two interlaced combs (Fig. 3), are formed on a piezoelectric crystal substrate. The orientation of the surface and direction of propagation determine several characteristics: (a) the electromechanical coupling coefficient which, in turn, affects the equivalent circuit properties, and (b) the velocity of the surface wave, which sets the peak response frequency. This is described in more detail in two articles that have appeared in *R.F. Design* which discussed the basic properties of the idt.

The frequency characteristics of a simple idt, i.e., in which the opposing electrodes have a constant overlap, are derived by taking the Fourier transform of the impulse response of the idt. If a very narrow voltage spike — ideally a delta function — is applied to the opposing electrodes of the idt via the bus pads shown in Figure 3, a facsimile of the electric fields produced at the substrate surface in the form of mechanical stress will be excited under and between the electrodes. A delta function is an excitation containing all frequencies, because it contains no time interval. Time and frequency have this inverse relationship — shorter time intervals imply larger frequency bandwidths and small bandwidths imply temporal signals of large extent.

Since the spike voltage is distributed

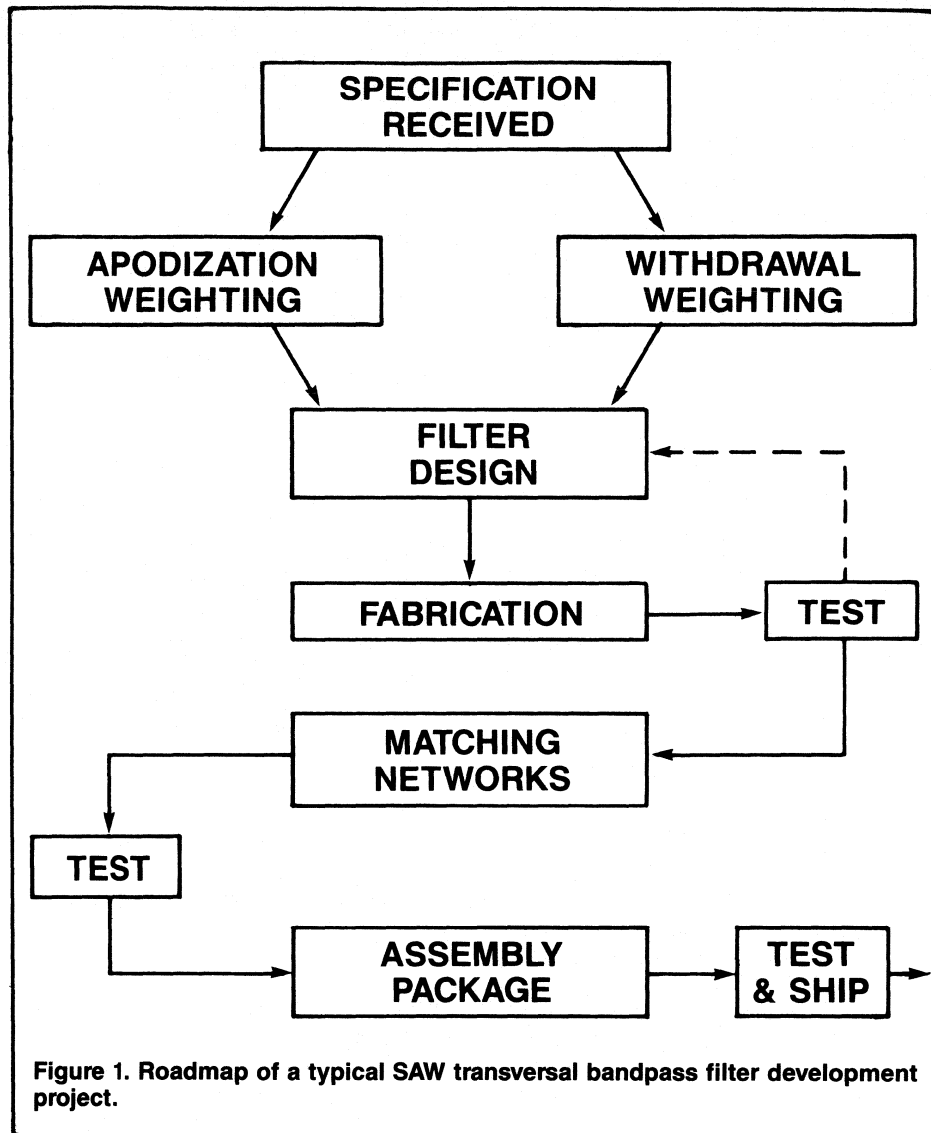


Figure 1. Roadmap of a typical SAW transversal bandpass filter development project.

CENTER FREQUENCY $F_0 \pm \Delta f_0$
3 dB BANDWIDTH, MIN/MAX
SHAPE FACTOR (40 dB/3 dB) MAX
SIDELobe LEVEL (dB), MAX
INSERTION LOSS (dB), MIN/MAX
PHASE SLOPE OR GROUP DELAY
PHASE OR GROUP DELAY
LINEARITY
OPERATING TEMPERATURE
RANGE
TEMPERATURE COEFFICIENT OF
DELAY/FREQUENCY DRIFT

Figure 2. A typical list of specifications for a SAW bandpass filter.

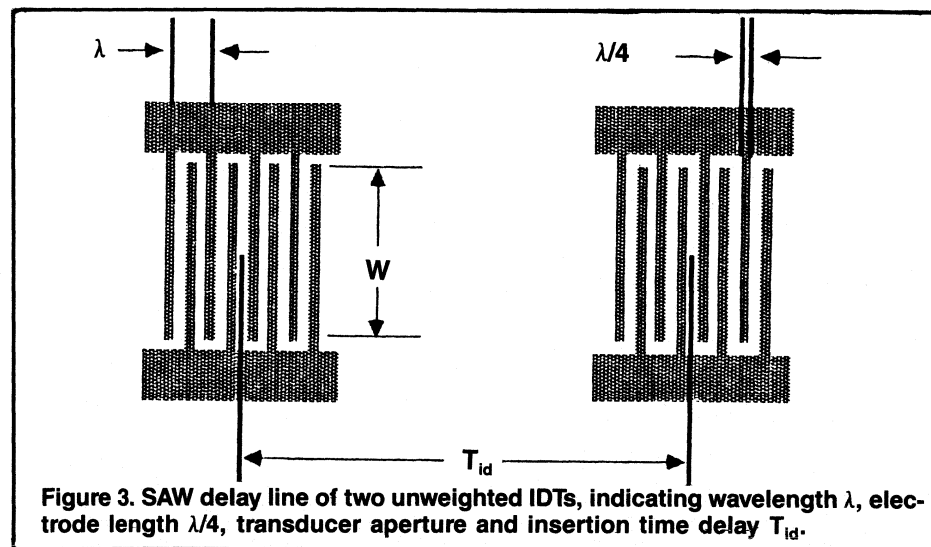


Figure 3. SAW delay line of two unweighted IDTs, indicating wavelength λ , electrode length $\lambda/4$, transducer aperture and insertion time delay T_{id} .

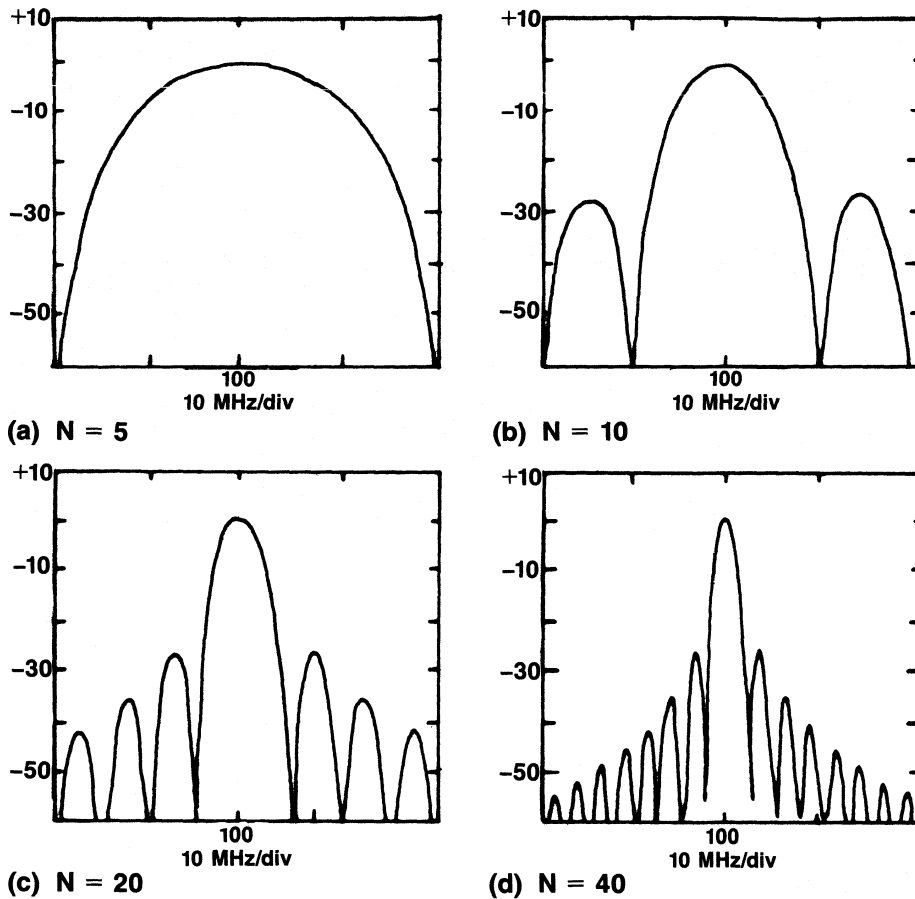


Figure 4. Filter characteristics of a SAW delay line consisting of two identical interdigital unweighted transducers consisting of N electrode pairs. (a) $N = 5$, (b) $N = 10$, (c) $N = 20$, (d) $N = 40$.

over the entire area of the idt, and therefore has a finite spatial extent along the direction of propagation (both forward and backward), the very short voltage spike is transformed into an impulse of finite time duration. The stress field induced will now propagate away from the electrode pattern and travel as two pulses of time duration (T_d) determined by the time length of the idt:

$$T_d = N \cdot L / V, \text{ where} \quad (1)$$

N is the number of electrode or finger pairs, L is the spatial period (pitch) of the electrode pattern — in effect the wavelength (λ_0), and V is the velocity of the surface acoustic wave, which for all practical situations is constant, independent of frequency. The frequency of the wave (f), is, to first order, given by the relationship $f\lambda = V$. In fact, since the transducer is finite in length, the frequency response is not a single frequency, but spread over a range. We may see this from the following mathematical development.

The Unweighted Interdigital Transducer

Each electrode in the transducer has an excitation or detection strength of magnitude unity and sign + or -, depending on which bus bar (pad) it extends from. This means that the phase of the excitation voltage flips 180 degrees from one electrode to the next. The designation of sign is arbitrary and is usually defined with respect to which pad is wire bonded to electrical ground. If we locate the origin of the X axis at the center of the first electrode, the position of each electrode is located at

$$X = \lambda_0 n / 2 \quad n = 0, 1, \dots, 2N-1 \quad (2)$$

If we define the frequency dependent wave vector, $k(f) = 2\pi/\lambda$, then the function

$$U = \exp[jkX^n] = \exp[j\pi n \lambda_0 / \lambda] \quad (3)$$

contains enough information to determine the magnitude and phase of the excita-

tion strength at each of the electrode positions. Note that $f_0 \lambda_0 = f \lambda = V$, the SAW velocity and f_0 is the frequency corresponding to the pitch, or period of the electrode pattern. Staring at equation (3) for a few moments should convince us that this excitation structure should generate a wave even when f is not quite equal to f_0 . This statement will be made explicit later.

At synchronism, when $f = f_0$,

$$U = \exp[j\pi n] = +1 \quad n = 0, 2, \dots, 2N-2 \\ = -1 \quad n = 1, 3, \dots, 2N-1 \quad (4)$$

To determine the frequency response (for both excitation and detection) it is necessary to take the inverse Fourier transform of the time domain of this structure. The time domain of the transducer is related to the spatial structure in a simple way. A crest of a stress wave (SAW) excited under one electrode will propagate to an equivalent position under the adjacent electrode (one half wavelength away) in a time t , such that

$$X^n = V_{nt} = n \lambda_0 / 2 \quad (5)$$

Taking the inverse Fourier transform of the time domain of the transducer (which extends from $t=0$ to $t=T$, the time length of the idt) will result in an expression for the frequency domain response:

$$A(f) = \frac{1}{T} \int_{t=0}^{t=T} \exp[j2\pi f_0 t] \exp[-j2\pi f t] dt \quad (6) \\ = \exp[j2\pi(f_0 - f) \frac{T}{2}] \frac{\sin[\pi(f_0 - f)T]}{\pi(f_0 - f)T}$$

Since $T = N\lambda_0/V = N/f_0$, $A(f)$ takes the simpler form

$$A(f) = \exp[j\pi \frac{(f_0 - f)N}{f_0}] \quad (7) \\ \frac{\sin[N\pi \frac{(f_0 - f)}{f_0}]}{N\pi \frac{(f_0 - f)}{f_0}}$$

$A(f)$ is the amplitude response of the idt and is complex, with the phase given by the exponential factor. The relative power (or gain) is given by the square of the magnitude:

$$A(f) = \frac{\sin^2(x)}{x^2}, \quad x = N\pi(f_0 - f)/f_0 \quad (8)$$

This is the celebrated $\sin(x)/x$ dependence of a SAW idt of uniform electrode aperture, i.e., unweighted. Figure 4 shows the frequency response predicted for a succession of transducers with increasing numbers of finger pairs.

Several features of this set of curves should be appreciated. First, whenever the argument x , as defined in equation (8), is an integer multiple of π , but not equal to zero, a null in the response occurs. The first null occurs at $f = f_0(1 \pm 1/N)$. Second, whenever x is nearly equal to an odd half-integer multiple of π , a local peak (sidelobe) occurs. The exact value of x can be found by taking the first derivative of equations (7) or (8) with respect to frequency, setting them equal to zero and solving for the value of f at which this occurs. This locates the true maxima. Using the approximation, however, is quite satisfactory. The result is that the first sidelobe is found to occur at -13.45 dB relative to the main signal. Any SAW filter consists of two transducers. The power versus frequency response is the product of the individual idt power curves:

$$P(f) \sim |A_1(f)|^2 |A_2(f)|^2 \quad (9)$$

For two identical transducers, the first sidelobe is then found at -27 dB.

The third feature is the bandwidth. The change in frequency from the band center to the first null is f_0/N . This is the number usually quoted as the 3 dB bandwidth, but is not correct, strictly speaking. For a single transducer, the frequency band centered around f_0 , of extent f_0/N falls to -3.9 dB at the band edge. For transmission between two transducers, the roll-off is -7.8 dB.

These three factors — the lack of monotonic roll-off in filter response away from the central response, the limiting of the first sidelobe to -27 dB and the lack of flatness in the response within any reasonably defined bandwidth — are the basic motivations for developing design techniques that may be applied to improve the filtering capability of SAW devices.

The Fourier transform of the unweighted (rectangular) transducer is a $\sin(x)/x$. Since the inverse transform will return the rectangular time domain (impulse) response, the Fourier transform of a time domain excitation function weighted as $\sin(x)/x$ will produce a frequency response that has a rectangular appearance, i.e., flat within a given frequency

band, dropping off sharply outside of it. (In this context, x does not refer to any spatial position. It is only the argument — in radians — of the trigonometric sine function.)

Once we accept this mathematical symmetry, a second feature must be attended to. The finite impulse response results in a frequency domain which extends to all values of frequency, albeit with decreasing strength. So a transducer that has a truly finite and rectangular frequency response — constant in some bandwidth, zero elsewhere — must be infinitely long.

This defines the fundamental art and skill of SAW transducer design: How to achieve sufficient bandwidth limited filtering with good sidelobe suppression and sharp transition skirts beyond the band edge, all within a device structure of manageable size.

When we simply weight a SAW idt with a $\sin(x)/x$ function and truncate the device to a finite length, something undesirable happens. Refer to the series of examples illustrated in Figure 5.

Column 1 of Figure 5 is a schematic of the actual SAW transducer for each specified transducer length (i.e., number of electrode finger pairs or, equivalently, number of wavelengths). Column 2 is the frequency response of the power transmission efficiency between two such identical transducers. In column 1 the horizontal scale is reduced by $2x$ between Figures 5c-1 and 5d-1 to accommodate the entire image as it grows longer. In column 2 the vertical scale is in decibels, with tick marks indicated every 10 dB. The filter response is measured relative to the response at band center (100 MHz), which is 0 dB. The scale has an upper limit of $+10$ dB to allow for an in-band response that may ripple above 0 dB. The horizontal scale shown spans 40 MHz about the center frequency and has tick marks every 10 MHz. The nominal bandwidth specified for this filter is 10 MHz.

Just how is the desired bandwidth specified mathematically so that the transducer apodization is correctly generated? The most straightforward approach is to go back and use a method parallel to that shown above for the frequency response of a rectangular (unweighted) idt time domain. This time, the frequency domain is specified as rectangular, with the bandwidth B and the center frequency f_0 as the only important parameters. Following the development above, we can obtain a function which specifies the relative overlap between adjacent electrodes spaced every half wavelength (at center frequency):

$$A(n) = \frac{\sin[(n-N)\pi B/2f_o]}{[n-N]\pi B/2f_o} \exp[j\pi n] \quad (10)$$

$$n = 0, 1, \dots, 2N$$

The function changes sign every electrode with the term $(-1)^n = \exp[j\pi n]$ to account for the 180° phase reversal every half wavelength. The entire function has the $\sin(x)/x$ behavior. The product results in a main lobe with a set of monotonically decreasing lobes that string out until arbitrarily truncated at some value $N1$ to limit the extent of the idt. A phase reversal occurs when the sine function goes through zero. This can be seen in Figure 5c-1, where two adjacent electrodes suddenly appear to emerge from the same pad. This is because two sign reversals take place simultaneously between two consecutive electrode positions — one from the term in $(-1)^n$ and one from the change in sign of the sine term (no play on words intended).

Now let's look at what happens as we let the idt get longer. Compare Figure 5a to Figure 4b. Both idts have 10 finger pairs, but now the $\sin(x)/x$ function is weighting the apodization. Both look pretty much the same, except that now the first set of sidelobes are lower by about 4 dB. By tapering off the excitation strength of the electrodes at each end of the idt, we have made some improvement in lowering their ability to generate a signal in the frequency domain beyond the first null. However, notice a small trade-off: the first pair of frequency nulls in 5a-2 have spread slightly compared to 4b. Apparently the idt is behaving as if, in this respect, it had slightly fewer electrodes.

In Figure 5b-1 the idt extends out to the first spatial nulls, or phase reversal points. Now, clearly, because there are more electrodes (i.e., finger pairs) the frequency response has narrowed considerably, both at the null points and at the 3 dB level. Even more remarkable, the first sidelobes have dropped below -50 dB, in continuation of the process noted in the last paragraph.

Extending the idt another 10 wavelengths, as shown in Figure 5c-1 results in interesting new behavior. Now that a phase reversal has occurred and there are several electrodes generating waves out of phase with those in the main lobe, in-band the transducer tends to act as if it had fewer electrodes. Indeed, the 3 dB bandwidth has broadened and the positions of the first nulls have spread out. Unfortunately, the sidelobe level has jumped

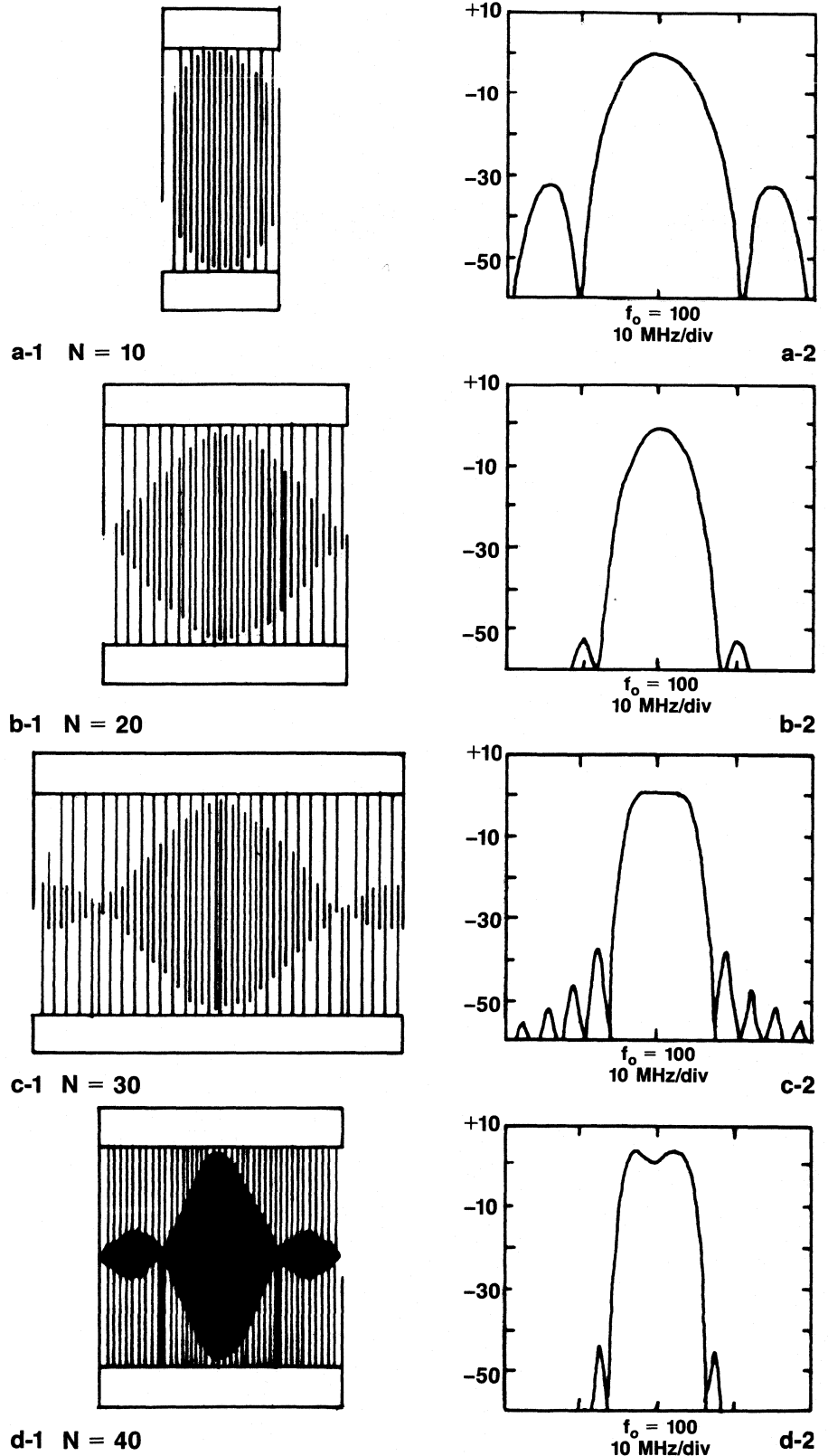


Figure 5. Progressive filtering characteristics of pairs of IDTs apodized with a $\sin(x)/x$ weighting as the number of electrodes increases from $N = 10$ to $N = 70$.

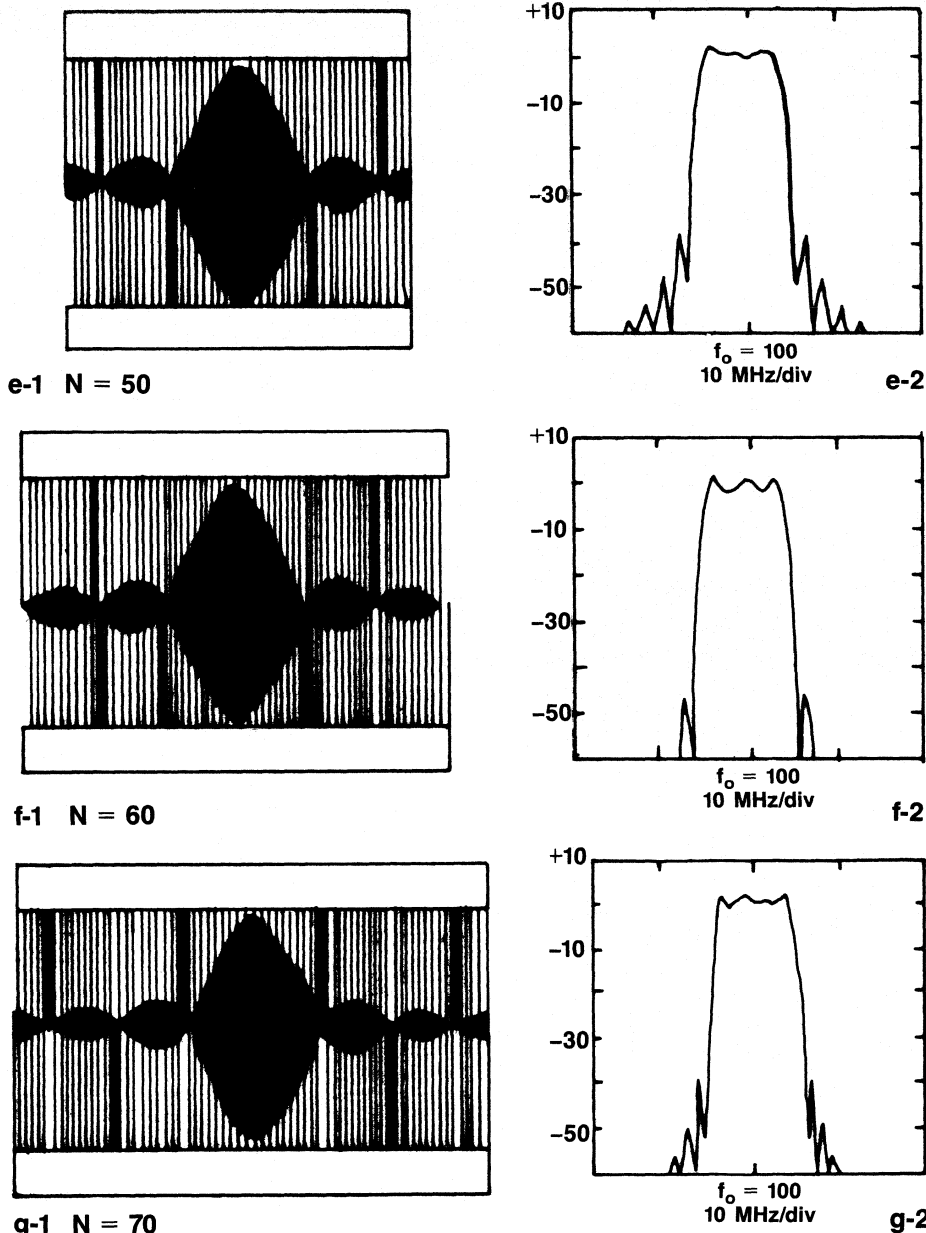


Figure 5 (continued).

back up, as if the outer electrodes, with their corresponding phase reversal, are suitably positioned to generate more acoustic energy out-of-band.

The most impressive things to happen, however, are the flattening of the response in-band and the somewhat precipitous drop-off in response outside the central frequency domain. These are features that we like, although they have occurred at the expense of undesirably degraded sidelobe levels out of band.

When the first pair of idt sidelobes are completed, a new phenomenon occurs. The sidelobe level again subsides, as in 5b-2 when the main lobe was complete,

but rather noticeable ripple is introduced in the main response. What we had accomplished in the last figure has clearly been undone here.

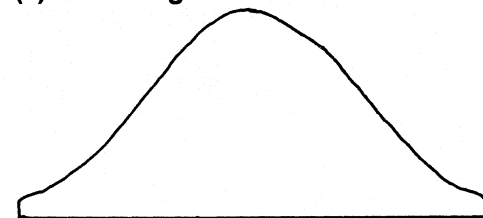
As we proceed through the remaining cases in Figure 5, it is evident that when the idt lobes are complete, the frequency sidelobes are lower, but the in-band ripple is large. When the outer idt lobes are half of a full lobe length, the in-band response is much flatter but frequency sidelobes rise. Throughout the progression, however, the transition skirts — the frequency bands on either side of the main response between the inband and out of band regions — become increas-

ingly steep, which is one of the features we want most.

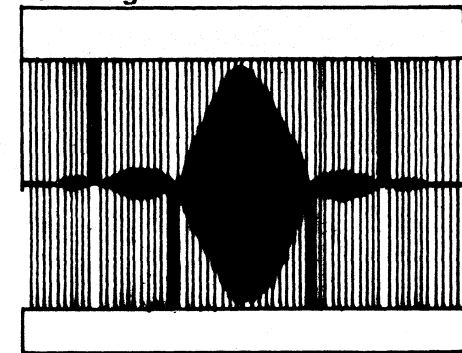
It would seem that, in principal, if we could simply let the transducer continue on to infinity, the sidelobes should drop off altogether, the passband should go flat and the transition skirts should become vertical. This will never happen. Instead, the sidelobes stay with us, the in-band ripple gets more bothersome (Gibbs phenomena) and the filter would have to get unpractically large. Why this happens is related to the discrete sampling nature of the design method. Note that the behavior of the filter is the result of a discretely sampled function, not a continuum.

To close this installment, the reader is given a taste of the technique used to op-

(a) Hamming function.



(b) IDT weighted by $\sin(x)/x$ and Hamming.



(c) Filter performance.

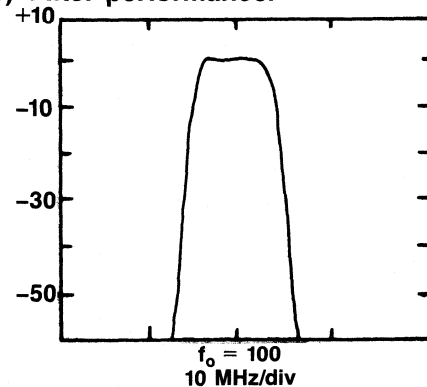


Figure 6. Influences of a Hamming function window on the filtering characteristics of a SAW device.

timize all of the features simultaneously that seem to evade us — low sidelobes, flat in-band response and steep transition skirts, within a device of practical size. Like a set of syncopated bellows, just when one undesirable characteristic appears to deflate another breathes full of life.

The method that has received much attention, and achieved much success, is

called windowing. It is a well known technique used in radar to weight the frequency spectrum in pulse compression transceivers to suppress time domain sidelobes and thus improve range accuracy. We use it the opposite way — the time domain waveform is windowed to suppress sidelobes in the frequency domain.

There are many types of window func-

tions, and we will discuss several of them in the next part of this series. Right now, an example is given of one called the Hamming function. It physically applies a scale factor that modifies the $\sin(x)/x$ function for each electrode, and is itself dependent on position along the transducer. Figure 6a is a plot of the Hamming function. It has maximum value (set at unity) in the center and tapers off at the ends. In fact, it is a cosine function on a pedestal, with one full cosine wave cycle across the length of the idt.

If we apply this window function to the transducer in Figure 5f-1, which is 60 wavelengths long, we get the transducer in Figure 6b. Notice how the transducer sidelobes are strongly attenuated. The frequency response for a pair of such idts is shown in Figure 6c. The change is dramatic. No sidelobes are observable above -60 dB, and the in-band response is devoid of ripple. We have reached a milestone; a technique is available which allows us to overcome the limitations of the (discrete) digital sampling approach used in designing a SAW transversal filter.

About the Author

Jeff Schoenfeld has been a contributing editor of *R.F. Design* for more than three years. Surface acoustic wave devices and their systems applications has been his principal specialty and interest in the field of RF. Jeff is currently program manager of research for robotic sensor systems at a major Southern California aerospace/electronics company where science gets down to business. Please contact him through *RF Design*, 6530 S. Yosemite St., Englewood, Colorado 80111.

For Further Reading . . .

L.T. Clairborne, G.S. Kino and E. Stern, Special issue on Surface Acoustic Wave Devices and Applications, Vol. 64, No. 5, May 1976.

H. Matthews, Editor, *SURFACE WAVE FILTERS*, Design, Construction and Use, John Wiley, New York, 1977.

C.S. Hartmann, D.T. Bell, Jr., and R.C. Rosenfeld, "Impulse model design of acoustic surface wave filters," *IEEE Trans. MTT-21-162* (1973).

R.H. Tancrell and M.G. Holland, "Acoustic surface wave filters," *Proc. IEEE*, Vol. 59, p.359 (1971).

R.M. Bracewell, *The Fourier Transform and its Applications*, McGraw-Hill, New York, 1965.



Designing Unintentional Jammers

By Kenneth J. Grymala
Technical Consultant
GC Technologies, Inc.

Every year it costs our military a lot of money to track down unintentional jamming systems inadvertently designed with passive components. These devices were never meant to radiate. In fact, some of them have been through full EMI/TEMPEST testing and have been proved to be non-radiating. Yet these "non-radiating passive jammers" can very seriously degrade the communications capability of an entire military platform, such as a ship or aircraft.

The circuits are radio receiving front-end components. The worst offenders are the "protection circuits" used for wideband intercept receivers and wideband receiving multicouplers. Most use some type of diode limiting, and some also use light bulbs, fuses, spark gaps, gas fired tubes or a myriad of other non-linear devices. Figures 1A through 1C show typical overload protection circuits that can cause problems.

The protection circuit in Figure 1A may be low capacitance switching diodes that act together as a conventional limiter. It also may be a hot carrier diode that acts as a detector to bias a pin diode into attenuation. In either case, levels sufficient to produce intermodulation products or broadband white noise can occur easily in a typical overload situation.

Figure 1B has a fusible link. These were originally meant to protect signal generators from accidentally being burned out during transceiver testing. However, they have frequently found their way into receiver and multicoupler circuits. They are probably the safest from the re-radiation standpoint, but they are quite non-linear. As a consequence, these fuses will lower the second and third order intercept points of most equipment they are meant to protect.

The circuit shown in Figure 1C is similar to 1B, except a light bulb is used instead of the fuse. The bulb's increasing resistance as it heats up works against the diode limiter. This allows a higher level of overvoltage protection than can be tolerated by the limiter alone. This circuit is one of the worst offenders. Frequently, the bulb and diode combination are just

Figure 1A. Coaxial diode limiter

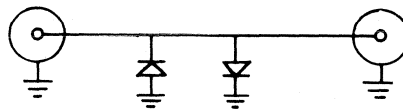


Figure 1B. Coaxial RF fuse

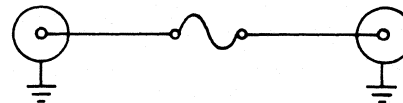


Figure 1C. Coaxial overload protector

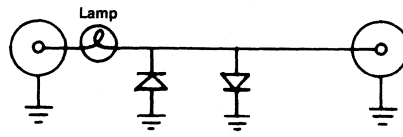


Figure 1. Protection Circuits

right to turn the limiter into a white noise generator. In this case, only one strong signal is needed to activate the circuit and cause serious re-radiation problems.

Problems begin to occur when just a few hundred milliwatts are applied to these devices. In the case of a ship or aircraft, it is common to have watts of transmitter power, from more than one transmitter, coming down a receive antenna line. In a typical military system, such as a ship or aircraft, the separation between MF/HF transmit to receive antennas will be much less than 60 dB. Receive antennas are frequently grouped together and may have as little as 10 dB of isolation from each other. Figure 2 illustrates a typical military system composed of communications and intercept equipment.

If such a protection device is hooked directly to the antenna it normally will provide the needed protection to the equipment it's supposed to protect. However, it will also generate a very strong level of broadband noise or thousands of intermodulation products that go right back out to the antenna. From here, these spurious signals are propagated to other nearby receiving systems where they cause

serious interference. Under "ideal" conditions, the generated interference can be 60 to 80 dB higher than signals of interest.

The protection devices often are external to equipment and have been added by a well meaning technician or engineer who wanted to protect sensitive equipment from burnout whenever a nearby high powered transmitter was turned on. The problems often are just brushed off as "bad atmospheric" or excellent propagation ("just listen to all those signals!").

What is really happening is re-radiation of intermodulation products caused by the mixing of two or more high powered transmit signals within the protection device. It's kind of like the old rusty bolt, but it is intentionally designed to be highly efficient. The antennas are well matched and the diodes are of the highest quality. To make matters worse, the culprits are usually impedance matched to the antenna system. They have their most detrimental effect when connected to antennas that are co-located with other receiving antennas whose systems are capable of operating within high power fields. This problem can occur from active antennas, varactor tuned preselectors, pre-amplifiers and receiver first converters.

Solutions and recommendations

In cases where LC filtering is not possible, the devices to be protected must be removed from the antenna line, or the strong transmit signal amplitudes must be attenuated to a point where they no longer cause a problem. As a minimum, a good RF overload protection circuit should have the following characteristics: non EMI-radiating during overload; low insertion loss and low VSWR; protection whether equipment power is on or off; protection against short duration, high power bursts; and protection against long term, high power overload.

Figure 3 illustrates how a typical well designed protection circuit works. When the device to be protected is not in use, a relay at the input is normally opened to protect against an RF overload. When the unit is in operation, the relay is closed. The relay should provide low insertion

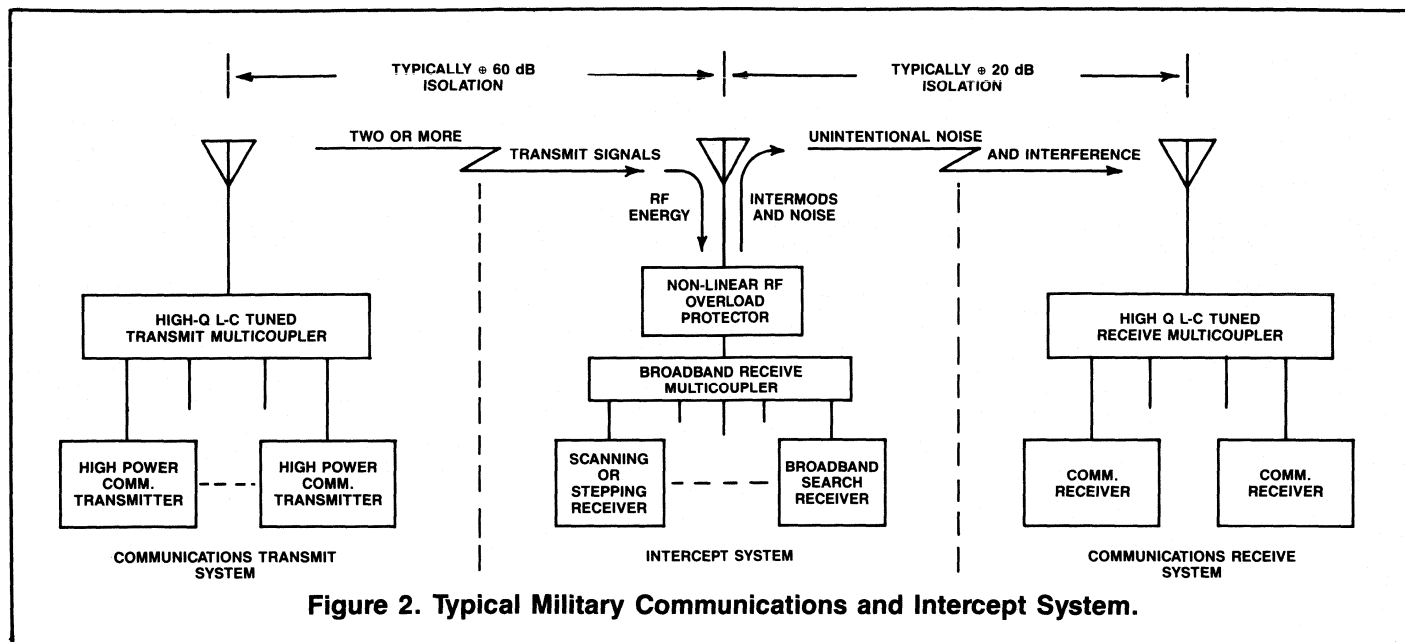


Figure 2. Typical Military Communications and Intercept System.

loss and low VSWR at the frequencies the circuit is designed for. It must also be capable of withstanding the anticipated power levels.

The protection circuit has a very high impedance detector that does not disturb the impedance characteristics of the equipment. Its output feeds a relay driver. Whenever an RF overload is sensed, the relay opens the circuit between the high incoming power and the sensitive circuitry. The relay driver usually contains a release timer circuit of 1 to 10 seconds. This circuit serves two purposes: One is to save the operators' nerves if the overload is from a non-CW signal, such as an SSB voice signal, and to hold the protection circuit on between overload dips and peaks. The other is to reduce chatter if the feedline length between the antenna and the overload protector happens to be an appropriate $\frac{1}{4}$ wavelength multiple. It is possible that the input to the protector will drop to zero when the circuit opens the line, causing the circuit to deactivate and begin chattering. With the timer circuit in place the relay will still cycle on and off but at a much lower rate. (A second alternative to the chatter problem is the addition of an external high power, matched dummy load).

Most protection circuits also employ limiters behind the relay. The purpose of the limiter is to provide protection to the sensitive circuits during the reaction time of the relay, which is typically 15-25 milliseconds. At low level signal inputs the limiter does not cause any problems, and at high overload levels the limiter is only

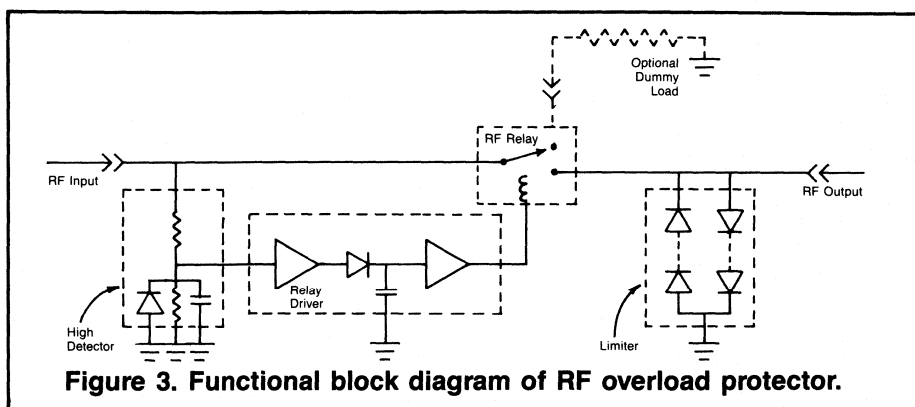


Figure 3. Functional block diagram of RF overload protector.

in the circuit for a very short time.

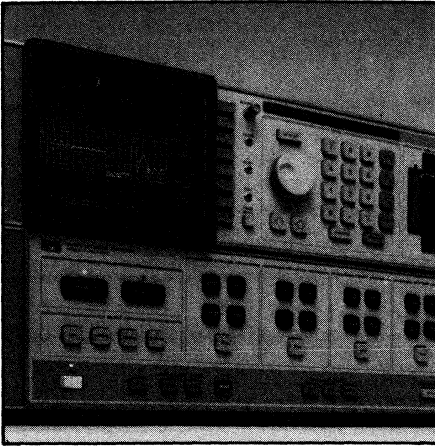
Numerous other variations can exist. For example, a multiple stage attenuation circuit can be added. With this method the receiving system is not fully disabled except under severe overload. Instead, fixed attenuators are placed in series with the line. In most MF/HF receiving systems, as much as 20 dB can be added without seriously affecting sensitivity. This is because in a well designed MF/HF system the sensitivity should be based on minimum atmospheric and galactic noise levels that are external to the antenna system.

Lightning and EMP protectors also can be designed into the circuit, but if they are used ahead of the relay they must not cause any non-linear action with typical overloads. If a lightning or EMP protection device is used ahead of the relay circuitry it should be thoroughly tested to ensure that it does not cause problems.

Since these devices are typically high impedance devices, they should be tested to levels of several hundred volts. This will simulate the effects of the unmatched impedance transformations caused when the conventional overload protection circuit opens the line.

Conclusions

When designing new equipment or systems that are likely to be subjected to multiple high level inputs, adequate attention must be paid to overload protection. The circuits must adequately protect equipment from burnout. They must also provide a high degree of compatibility with other systems. In recent years a few receiver manufacturers and most of the test equipment manufacturers have begun to install very good reverse power protectors in their equipment. The rest of us should build them into our new equipment and systems.



Cover

This month's cover features a representative sampling of Metaramics/W.R. Grace Co.'s line of advanced ceramic-metal packaging assemblies, including standard high power RF and microwave designs and custom designs for Gallium Arsenide, Indium Phosphide and specialized integrated circuit packaging.

Features

21 Special Report: The New Look in RF Circuits — Packaging

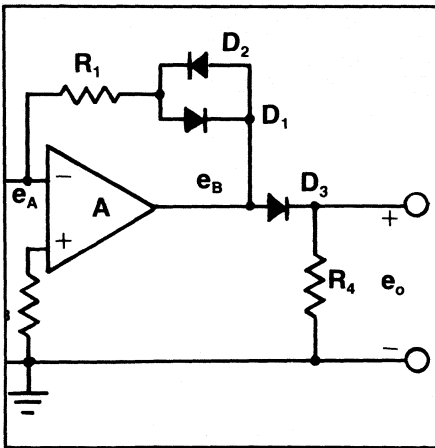
In the final article in this series we let representatives of two packaging design companies tell us about their products and operations. Current design considerations and some future trends are among the topics discussed. A general description of standard package types is included. — James N. MacDonald.

29 Wide Dynamic Range Linear Detection

This article describes a design for a wide dynamic range linear detector, with the rectifier output directly proportional to the input signal level over a wide range. The design uses an op amp with nonlinear feedback to achieve detection exceeding 60 dB of dynamic range. — William C. DeAgro

44 Measuring a Dipole Antenna Radiation Pattern Using Time Domain and Gating

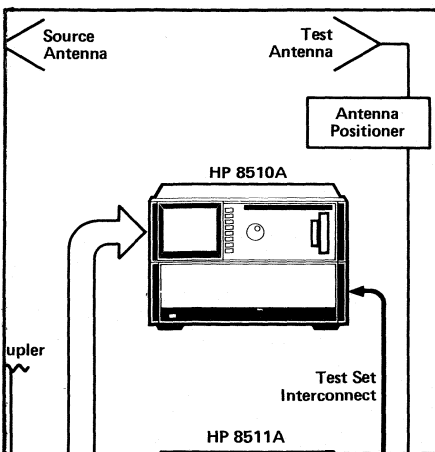
This article describes how the HP8510 network analyzer can be used to reduce the effects of reflected signal paths when measuring the far field radiation pattern of an antenna by measuring the swept frequency response of the antenna and computing the Inverse Fourier Transform to give the time domain impulse response. — John W. Boyles



Departments

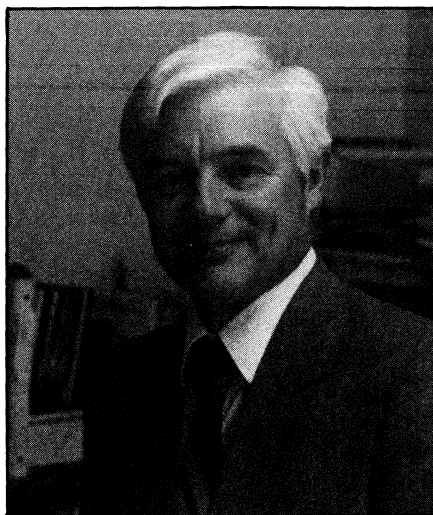
56 Designer's Notebook — A New Approach to Op Amp Design

The usefulness of conventional op amps in very high speed applications is limited. Comlinear Corporation says their new design provides better high speed performance than conventional op amps. — Scott Evans



- 6 Editorial
- 8 Publisher's Notes
- 13 Letters
- 13 News
- 16 Calendar
- 35 Info/Card
- 41 RFI/EMI Corner
- 61 New Products
- 70 New Literature
- 71 Courses
- 72 Classified Advertising
- 74 Advertisers Index

Growing With The Industry We Serve



James N. MacDonald
Editor

Gary Breed joins our staff this month as Technical Editor. He has been Chief Engineer at four radio and/or television stations during the past 10 years, and we look forward to the viewpoint he will bring to the magazine as a result of this experience. He also has published 13 articles in *Broadcast Engineering*, from which he has gained an understanding of the requirements of magazine writing. He will assist with staff written articles and will work with authors to prepare their manuscripts for publication.

The addition of a technical editor is part of a substantial increase in Cardiff Publishing Company's commitment to *RF Design* over the past year. First, the magazine went from bimonthly to monthly publication; now we have, in fact, doubled the editorial staff. The latter action is, of course, largely a consequence of the earlier decision. It is also a testimony to the correctness of that decision. There is far too much knowledge being generated in this field to be adequately exchanged every two months.

A business can grow for two reasons — in anticipation of a larger market or as a result of it. Usually both reasons are influential in the decision to expand, and this has been the case with *RF Design* magazine. Publisher Keith Aldrich's faith and understanding of the industry pro-

vided the impetus to double the publication frequency. The encouraging response of readers and advertisers has convinced us that the growth has just begun.

The growth of the magazine is not just due to the appropriateness of its content for our readers, although we take a great deal of pride in that content and know from reader comments that it is appropriate. We are part of the growth of the RF electronics industry, in general. We talk about this growth often, because there is much gloom in some parts of the general electronics industry. We want our readers to know that the slump is not industry-wide. Typical of the kind of news that crosses this desk almost every day is the following paragraph from a news release announcing that Raytheon Company's second quarter earnings were up 10.7 percent over a year ago.

"The company's improved performance for the quarter was generated principally by Electronics, Raytheon's largest business segment, which continued to be paced by defense electronics systems."

Most defense electronics systems operate in microwave frequencies, but we have mentioned before the increasing interest of the military in the lower frequencies. Other news releases tell similar success stories about commercial RF products. It is our observation that most companies are doing quite well, although some segments of their operation may be curtailed because the particular industry they serve is in a slump.

With this addition to the staff, *RF Design* will be able to expand the scope of its coverage of the electronics industry, and one expansion will be into economic news. In the near future you will see reports on economic activity in the RF sector, helping you keep up with trends.

Many of you will be receiving telephone calls and visits from Gary about technical matters. For you hams, Gary's call is K9AY. Mine, by the way, is NØFXB.

James N. MacDonald

Wide Dynamic Range Linear Detection

By William C. DeAgro,
Hazeltime Corporation

In many signal processing applications, it is desired to extract the AM of a signal accurately over a wide dynamic range. Such applications may include high fidelity audio and video systems, high accuracy direction finding systems or any signal processing application where signal amplitude is important. Ordinary series diode-resistor detectors are not very linear and can only achieve roughly a 20 dB dynamic range in the linear region; an active detector, however, using nonlinear feedback can yield linear detections exceeding 60 dB dynamic range. The following is a brief discussion and some results of a scheme using an op-amp with nonlinear feedback to achieve a linear detection exceeding 60 dB of dynamic range.

The basic AM linear detector is composed of two parts: a linear half or full wave rectifier and a low pass filter, in succession. In order to achieve wide dynamic range linear detection it is necessary for the rectification portion of the circuit to have an output directly proportional to the input signal level over a wide dynamic range. Therefore, most of this discussion will concern the rectification portion of the circuit.

The schematic in Figure 1 shows the structure of a wide dynamic range linear half wave rectifier. Its function is to produce an output (e_o) that is a linear function of the input (e_i) when the input is negative and no output when the input is positive. The ideal transfer characteristic, e_o vs. e_i , is shown in Figure 2.

The reason this circuit behaves this way is because when e_i is negative, e_B becomes positive, which places D_2 and D_3 in the forward bias region. The gain (e_B/e_i) is given by:

$$\frac{e_B}{e_i} = -\frac{R_1 + r_{D2}}{R_2}; A \rightarrow \text{LARGE} + e_i < \phi \quad (1)$$

and the gain function (e_o/e_B) is clearly given by:

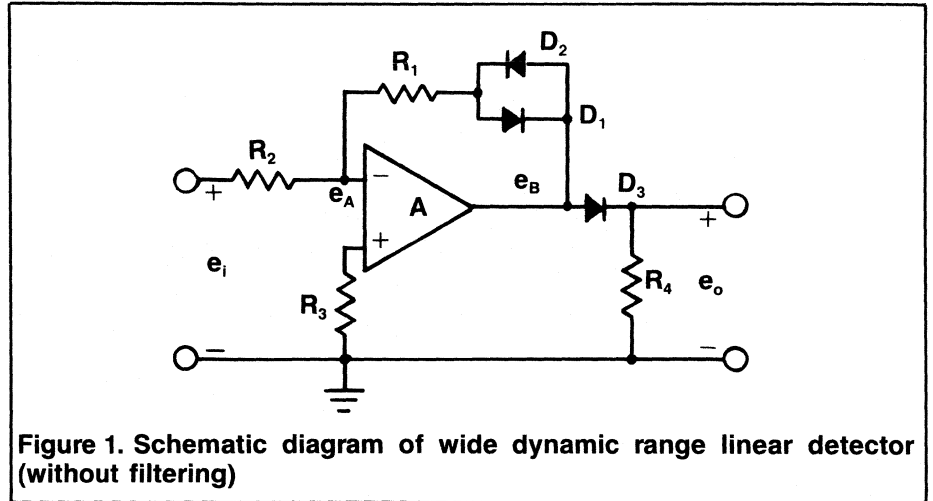


Figure 1. Schematic diagram of wide dynamic range linear detector (without filtering)

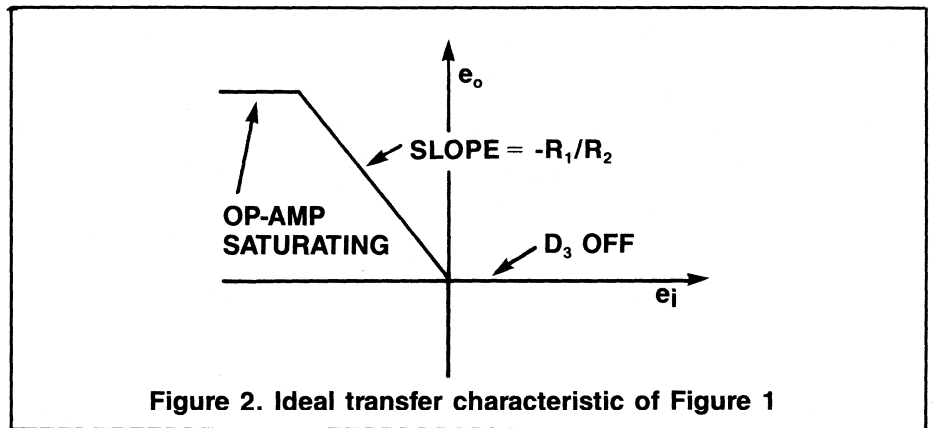


Figure 2. Ideal transfer characteristic of Figure 1

$$\frac{e_o}{e_B} = \frac{R_4}{R_4 + r_{D3}} \quad (2) \quad = -\frac{R_1}{R_2}; e_i < \phi \quad (3)$$

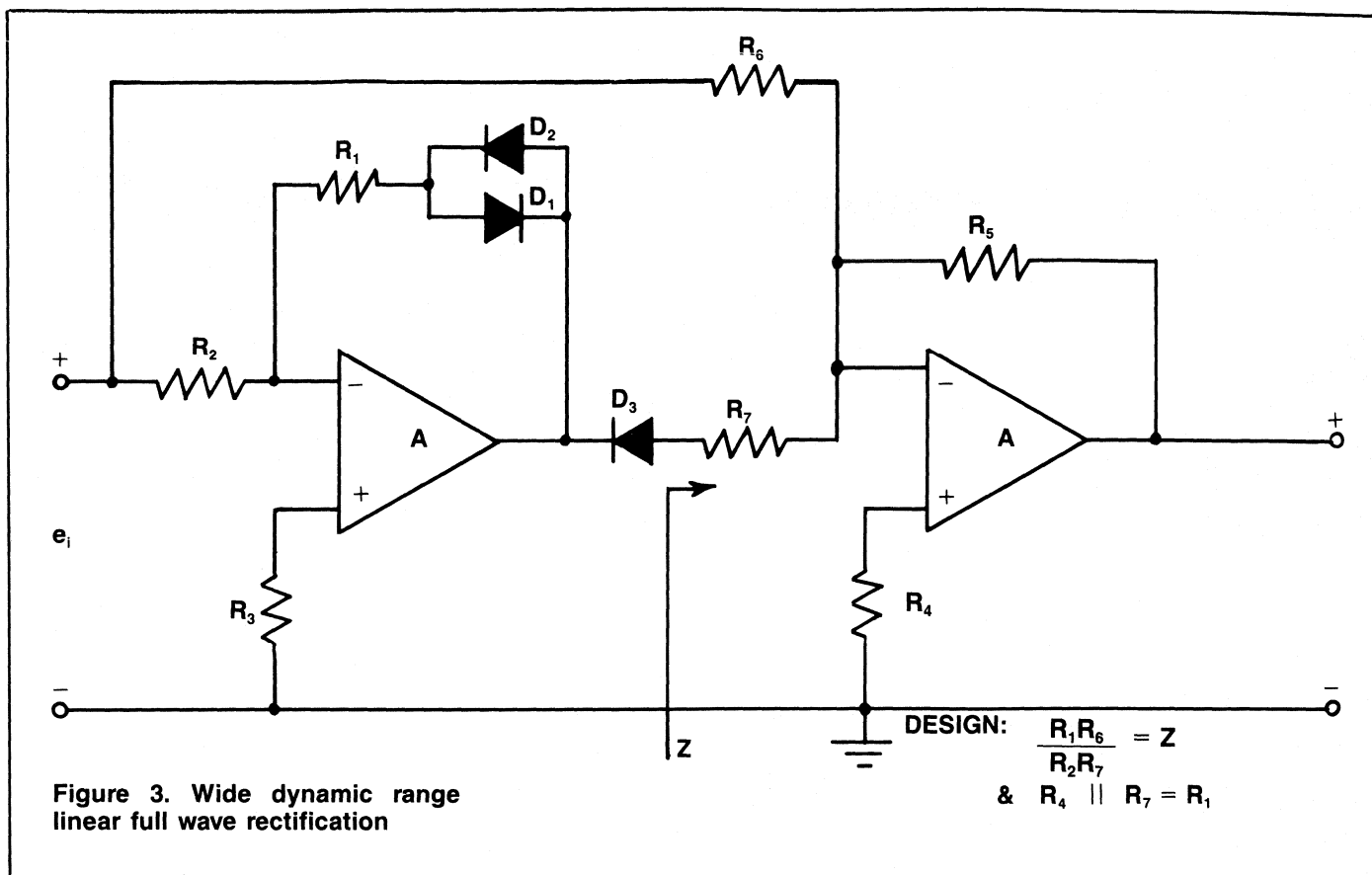
Knowing (from feedback theory) that e_A is at virtual ground and setting $R_4 = R_1$ and matching D_2 and D_3 leads to $i_{D2} = i_{D3}$ and $r_{D2} = r_{D3}$, the overall gain (e_o/e_i) when $e_i < \phi$ is given by:

$$\frac{e_o}{e_i} = \left(\frac{e_B}{e_i}\right) \left(\frac{e_o}{e_B}\right) = \left(-\frac{R_1 + r_{D2}}{R_2}\right) \left(\frac{R_4}{R_4 + r_{D3}}\right)$$

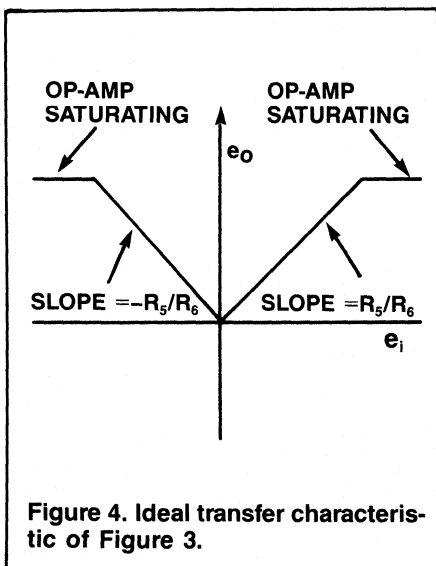
Clearly when $e_i > \phi$, e_B is less than 0, D_3 is reverse biased and the overall gain is given by:

$$\frac{e_o}{e_i} = \phi; e_i > \phi \quad (4)$$

For large fractional bandwidth type signals sometimes it is desired to use linear full wave rectification to eliminate spectral overlap (with nonbaseband compon-



ents) without reconverting to a higher center frequency prior to detection, or to reduce the rolloff constraints of the succession filter, as would be required in the half wave rectification type detector. In order to obtain a wide dynamic-range linear full-wave rectifier circuit, an exten-



sion of Figure 1 (with D_3 reversed) may be employed as shown in Figure 3. Note that the impedance Z looking into R_7 is roughly R_7 .

Therefore, the parallel combination at R_4 and R_7 should equal R_1 .

In order to perform the complete detection, filtering of either e_o or e_o is necessary. This can be done by placing a capacitor across R_4 for the half wave rectification type or placing a capacitor across R_5 for the full wave rectification type. The 3 dB radian bandwidth of the filter is the reciprocal of the RC product. If it is necessary to use a sharper rolloff filter (for the larger fractional bandwidth type signals), R_4 may be replaced by an n-pole filter with a passband impedance equal to that of R_1 or an n-pole filter may be placed at the output e_o . Note that the ideal filter would be flat in the passband, have a linear phase characteristic and have a rolloff sharp enough to degrade nonbaseband components to a specified level. Implementation of these higher order filters will not be addressed here.

The circuit of Figure 1 was designed using an NE5538 op-amp made by Signetics. The values for R_1 , R_2 and R_4 were 1.1 k Ω and the value for R_3 was 750

Ω . The diodes were all IN5712 Schottky barrier, which have a low turn-on voltage of 0.34V. The filtering was performed by placing a capacitor of 0.01 μ F in parallel with R_4 to give roughly a 15 kHz audio bandwidth. A schematic diagram of the practical circuit is shown in Figure 9. Prior to placing the filtering capacitor on the output, the transfer characteristics were plotted on an oscilloscope in X-Y mode and are shown in the oscillograms of Figures 5, 6 and 7. From these figures, it is clear that the rectifier circuit is linear over a dynamic range greater than 60 dB.

To show the performance of the complete detector circuit, a 3 MHz carrier frequency was used with a 10 kHz AM signal with modulation index greater than 1. The input waveform along with the detected waveform is shown in Figure 8.

Conclusions

It was found that the detector circuit built could detect signals in a linear region over a 60 dB dynamic range for roughly 11 kHz bandwidth signals of carrier frequencies ranging from 1 MHz to 4 MHz when using a simple RC succession filter. It is believed that much larger fractional bandwidth signals (e.g. 1/2) could be

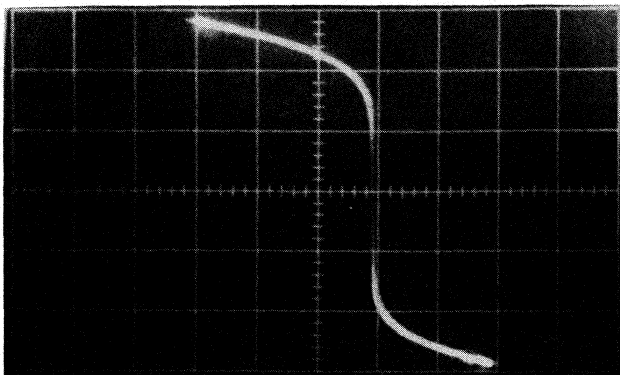


Figure 5. Non-linear characteristic

e_B vs e_i

Y: 5 mV/div

X: 100 mV/div

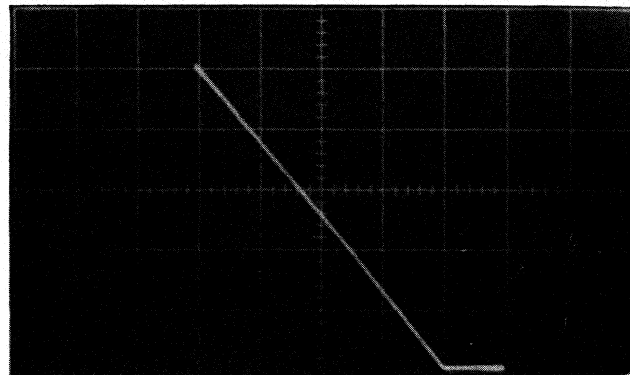


Figure 7. Linear characteristic

e_o vs e_i

Y: 2.5 mV/div

X: 2.5 mV/div

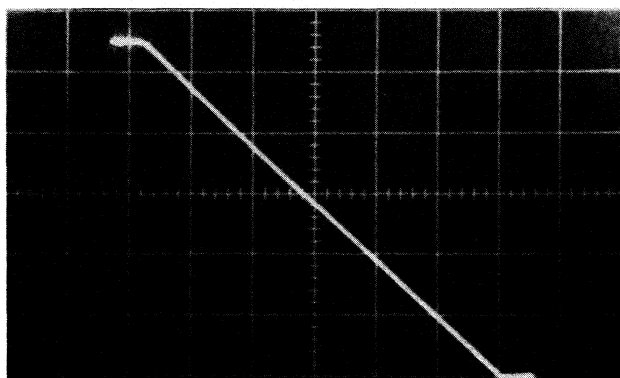


Figure 6. Linear characteristic

e_o vs e_i

Y: 5 V/div

X: 6.3 V/div

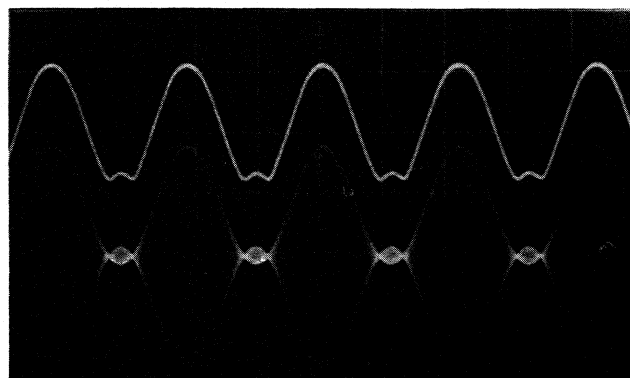


Figure 8.

Upper Trace: Detected output

Lower Trace: Input waveform (3 MHz Carrier,
10 kHz modulation, modulation
index > 1)

detected with this circuit if more exotic filtering were employed. In addition, it is believed that much higher carrier frequencies (up to 200 MHz) could be achieved when using state of the art type op-amps. Some of these op-amps may include the Comlinear CLC220AI, the OEI9914A and the Plessey SL541B.

About the Author

William DeAgro is a senior engineer in Research Labs at the Hazeltine Corporation, a defense contractor. Bill has a BSEE and a MSEE from the Polytechnic Institute of New York where he was a Cum Laude graduate and was elected Who's Who Among Students in American Universities and Colleges. Bill is a member of the Association of Old Crows, the International Society of Hybrid Microelectronics, Eta Kappa Nu Association and the Tau Beta Pi Association. Address correspondence to him at Hazeltine Corporation, Cuba Hill Road, Greenlawn, N.Y. 11740.

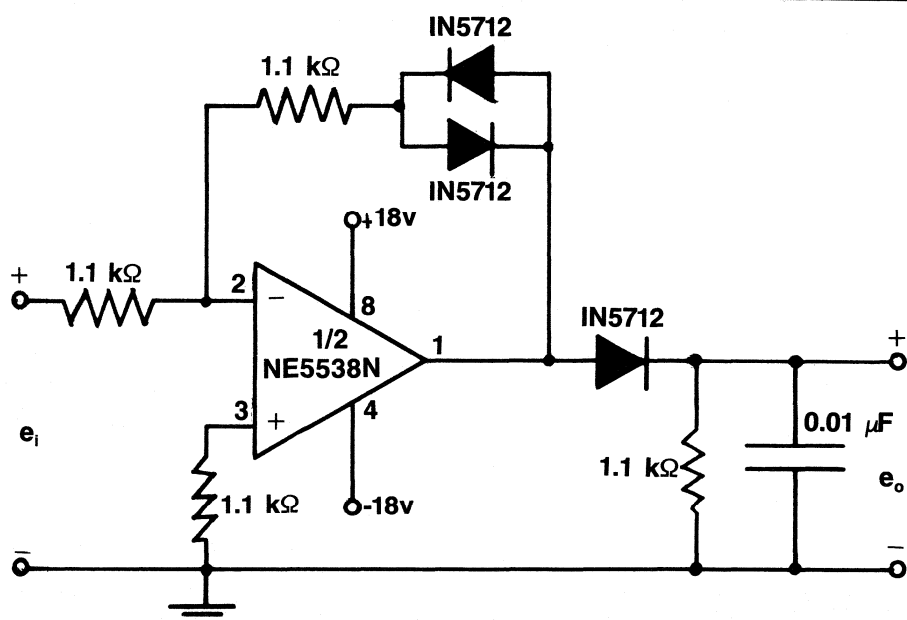


Figure 9. Practical circuit of wide dynamic range linear detector

Measuring a Dipole Antenna Radiation Pattern Using Time Domain and Gating

HP 8510 Network Analyzer Can Remove Ground Clutter Effects

By John W. Boyles
Hewlett-Packard Company
Santa Rosa, CA

A classical problem encountered when measuring the far-field radiation pattern of an antenna in a medium-distance range is the degradation that occurs when undesirable reflections (from the ground or nearby objects) are present. To reduce this problem, the source and test antennas are often installed on towers to remove them from reflective objects, RF absorptive materials are used to reduce the amplitude of the reflected signals and diffraction fences are installed in the range in order to null out the reflections and "clean up" the range. These solutions are often limited in their effectiveness and can be prohibitively expensive to implement.

The HP 8510 network analyzer can be used to reduce the effects of reflected signal paths in an antenna measurement and determine the response of the antenna to the main path signal only, without costly range modifications. This is done by using the HP 8510 to measure the swept frequency response of the antenna and compute the Inverse Fourier Transform to give the time domain impulse response. The time domain response allows the user to identify the reflected signal path responses in time and then remove them with the gating feature. In converting back to the frequency domain, the effects of the responses outside the gate are removed. This article summarizes the results of using this technique to measure the radiation pattern of a standard gain dipole antenna at RF frequencies on a medium-distance antenna range.

The HP 8510 is a microwave network analyzer designed to make S-parameter measurements in the frequency domain. It also has the optional capability to compute the Inverse Fourier Transform of the measured data to give the time domain response. When used with the HP 8511A frequency converter, the HP 8510A can be configured as a general purpose four-channel phase-locked receiver, and it can simultaneously display in real time the frequency and time domain responses of any channel or the ratio of

any two channels. One channel of the HP 8511A frequency converter must be used as a reference to achieve phase lock and therefore must have an input signal level between -10 and -50 dBm. The other three channels can be used to measure signals at the reference frequency with a dynamic range of close to 100 dB (-10 dBm max input).

A general block diagram for making antenna pattern measurements with the HP 8510 is shown in Figure 1. The required test equipment includes the HP

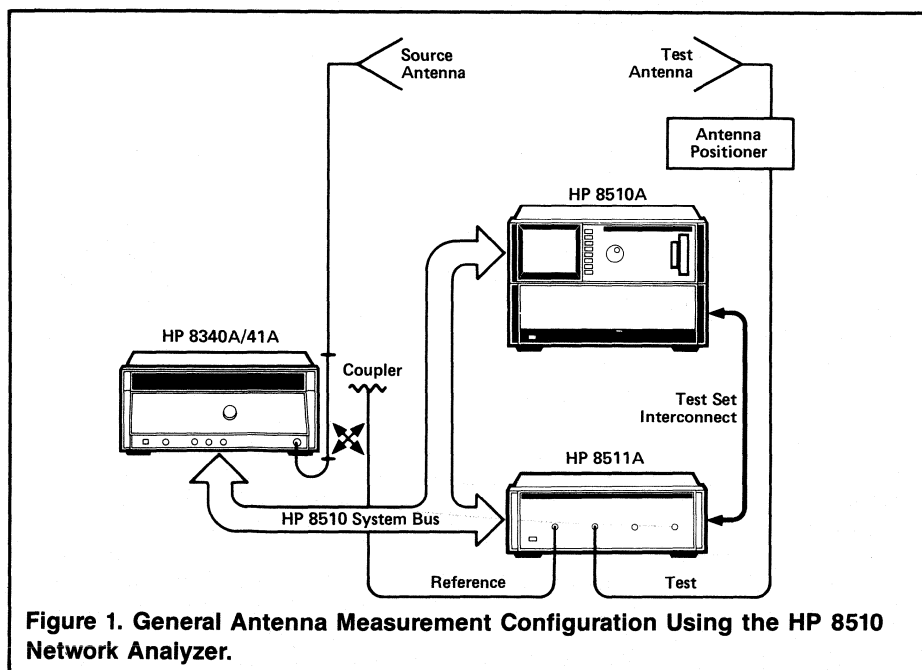
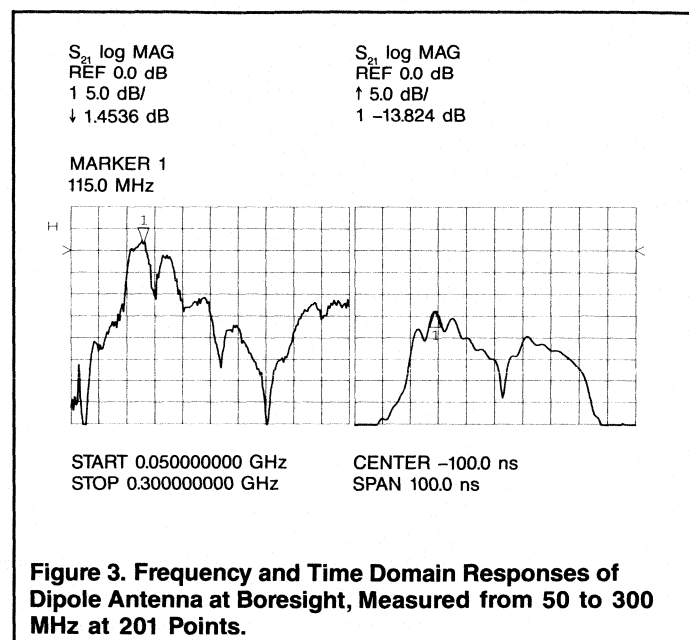
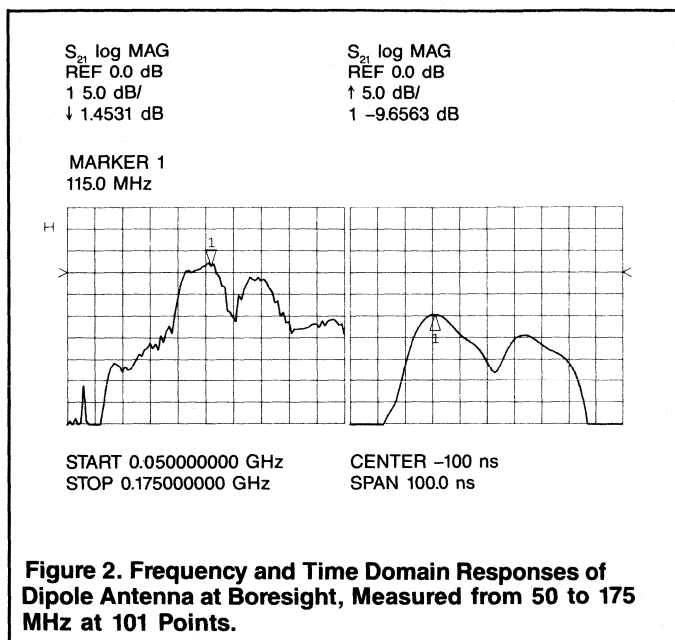


Figure 1. General Antenna Measurement Configuration Using the HP 8510 Network Analyzer.



8510A network analyzer, a synthesized source (HP 8340A or 8341A) and the HP 8511A frequency converter (test set). The source and test set are controlled by the network analyzer via the HP 8510 system bus. The output of the source is sent through a coupler to the source antenna. The secondary output of the coupler is used to provide the reference signal which is sent back via low loss cable to the HP 8511A. The signal received by the antenna under test is also input to the HP 8511A, and the HP 8510 is set up to display the ratio of the test and reference signals.

To illustrate the gating measurement technique with the HP 8510, consider measuring a dipole antenna (Scientific Atlanta model 15-115). The dipole antenna is particularly difficult to measure because its radiation pattern is only slightly directional in azimuth (with a figure-eight shape) and omnidirectional in elevation. Therefore, the dipole picks up reflections from almost every direction and is particularly sensitive to reflections from the ground. Because of its sensitivity to ground reflections and because it has a calculable (1) radiation pattern with which to compare measured results, the dipole antenna is a good device to test out the new measurement procedure.

The standard way to characterize the far-field radiation pattern of an antenna is to make the measurement at a single (CW) frequency as the positioner is rotated. However, in order to generate a time domain response, the measured data must be taken over a span of frequencies. The time domain representa-

tion of a CW signal is, by definition, a sine wave. In order to generate an impulse response, the measurement frequency span must be inversely proportional to the desired time domain impulse width.

The frequency domain response of the dipole from 50 to 175 MHz and the corresponding time domain impulse response (Band Pass mode) are shown in Figure 2. The antenna was tuned to 115 MHz. The large amount of ripple in the frequency domain response is caused by interference due to reflections from the ground and other reflective objects within the antenna range.

The time domain display shows the measured transmission response of the antenna as a function of time. Because no calibration was used in this measurement to balance out the phase difference between the test and reference signal paths, the absolute location of the time domain response is somewhat arbitrary. Because the reference signal is routed through cable and the test signal travels a shorter distance through air, the difference in electrical length causes the time domain response to arrive in negative time. However, it is the relative path difference between the time domain responses that is most useful.

Identifying the Time Domain Responses

The plot in Figure 2 shows two major time domain responses that are separated in time by 33 ns, which corresponds to a physical separation of 9.89 m. The first time response is that of the main

path signal, and the second response is that of the signal reflected from the ground plane which, because it travels a longer distance, is lower in amplitude and arrives later in time. The 6 dB difference in amplitude between the two responses represents the additional path loss of the reflected signal and also accounts for the large amount of ripple in the frequency domain response.

The required measurement bandwidth and separation between the two responses are determined by the characteristics of the antenna under test. The 50 percent (-6 dB) impulse width of the time domain stimulus is inversely proportional to the frequency span, and for a span of 125 MHz it is calculated (2) to be 9.6 ns. This represents, in the best case, the absolute minimum separation in time that the two responses can have and still be distinguished from one another. However, to use the gating feature effectively to remove the second response, the actual separation should be several times this minimum value to prevent overlapping of the responses.

A second factor to consider, which affects the required separation of the responses, is the bandwidth of the antenna under test. The dipole is a narrow band antenna that has a dispersive phase characteristic which causes its time domain impulse response to be smeared out in time. The result, observable in the time domain responses of Figure 2, is that the actual measured impulse width is more than twice the calculated width.

Figure 3 shows the response of the

same antenna measured over a frequency range of 50 to 300 MHz. Because the measurement bandwidth is doubled, the width of the time domain impulse stimulus is reduced by one half, which results in an improvement in the time domain response resolution. Notice, however, that the overall shape of the two responses is unchanged and that the amount of overlap of the responses is also unchanged. This is because the distributed shape of the response is caused by the dispersive nature of the dipole antenna. This indicates that the only way to decrease the amount of overlap between the two responses is to increase the relative travel time between them by increasing the height of the antenna under test above ground. In this example, there exists some overlap between the two responses, however (as will be demonstrated) they are adequately separated to use the gating feature to remove most of the effects of the second response.

This also indicates that the gating operation can be used to remove only the effects of reflections that are far enough out in time to be beyond the distributed main path response of the antenna. In this measurement, the effect of any signals that are picked up from reflections from the antenna positioner or other close in reflective objects will not be removed. However, the major error is due to the reflection from the ground plane, which is far enough away from the main path response to be removed using gating.

The gating feature of the HP 8510 provides a way to remove the effects of unwanted time domain responses and view in the frequency domain the effects of only those responses that are inside the gate. A gate is a time filter. In Figure 4, the center of the gate is set to the peak of the first time domain response, and the gate span is increased to include all of the distributed time domain response. With the gate turned on, the second time domain response is removed, and the resulting frequency domain response is that of only the main path signal. As expected, the gated frequency response very closely resembles the ungated response except that the ripple caused by the reflection from the ground plane has been removed.

The two major sources of error in this measurement are the tracking error between the test and reference signal paths and the interference error caused by the signal reflected from the ground. A simple model depicting these measurement errors is shown in Figure 5.

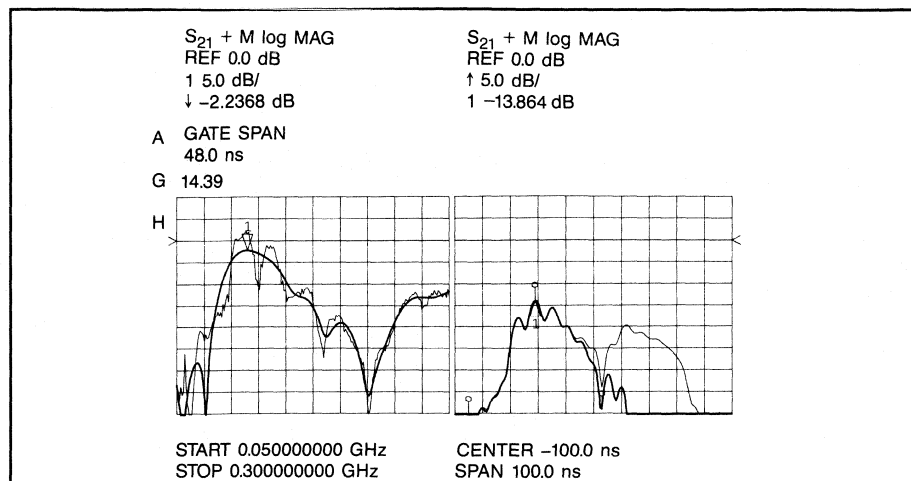


Figure 4. Gated Frequency and Time Domain Responses of Antenna Showing the Removal of the Ground Path Reflection.

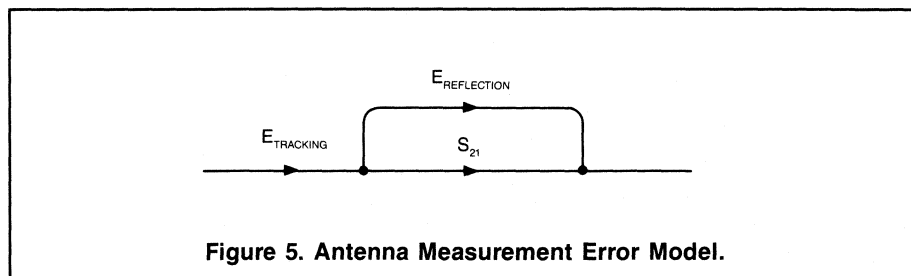


Figure 5. Antenna Measurement Error Model.

The correction for these two errors is accomplished in two steps. The first step is to remove the interference signal (E_{ref}) using gating. Then, assuming that the tracking error (E_{tr}) does not change as the antenna is rotated, it is removed using normalization. The procedure for doing this is as follows:

First, the gated response of the antenna at boresight (main beam) is saved into a memory register of the HP 8510A. Then, as the antenna is rotated, the gated response of the antenna at each angle is normalized to the boresight trace (using the data-divided-by-memory feature of the HP 8510). This gives the response of the antenna relative to the boresight response. Because the tracking error is common to both the measured and stored responses, it is normalized out in the ratio.

To take advantage of the time domain capability of the HP 8510 the measured data must be taken over a sweep of frequencies at each angle of rotation. Therefore, the time to make a pattern measurement is greater with this technique than for a comparable CW measurement. Because of the difference in test and reference path lengths involved the frequency accuracy is critical, and

therefore the source (HP 8340A or 8341A) should be operated in the stepped (synthesized) sweep mode. The sweep time for this mode is 50 ms per point, so for a 201 point measurement each sweep will take approximately 10 seconds. However, in addition to the frequency stability of a synthesizer, the stepped sweep mode has the benefit of allowing up to 128 averages without significantly changing the sweep time, which greatly reduces the effects of measurement noise.

Allowing 10 seconds per sweep, 5 seconds to increment the antenna positioner and 1 second to perform the gating operation and record the data, the measurement time is approximately 16 seconds per positioner setting. For a full 360 degree rotation at 5 degree increments, the total measurement time is approximately 19 minutes. If the frequency data is taken at 101 points (5 second sweep time), the total measurement time reduces to 13 minutes. (If the test and reference channel paths are balanced, it may be possible to use the ramp sweep mode, which would reduce the measurement time to approximately 7 seconds per positioner setting (8 minutes total).)

This longer measurement time is a

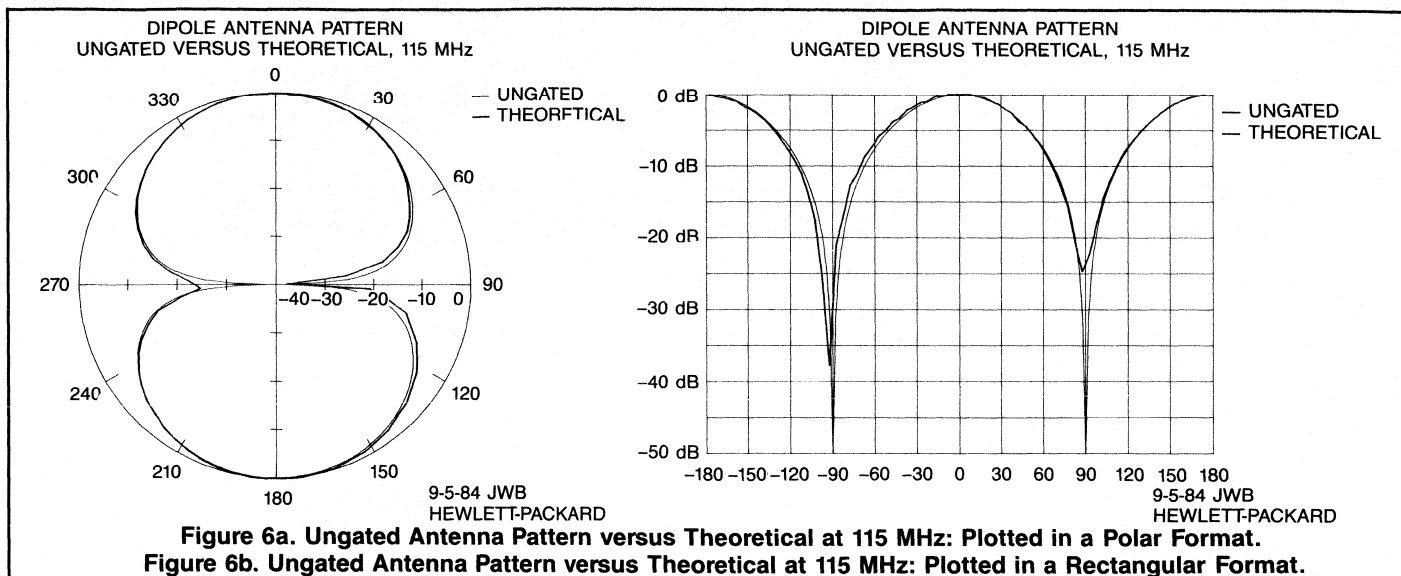


Figure 6a. Ungated Antenna Pattern versus Theoretical at 115 MHz: Plotted in a Polar Format.

Figure 6b. Ungated Antenna Pattern versus Theoretical at 115 MHz: Plotted in a Rectangular Format.

tradeoff for being able to use time domain and gating. If CW frequency testing is desired, the HP 8510 can be used as a CW receiver. However, although the swept frequency measurement technique requires additional time, the radiation pattern of the antenna at 201 frequencies of interest from 50 to 300 MHz can be plotted after only one rotation of the antenna positioner, and the improvements derived from gating more than offset the additional test time.

Measurement Results

The dipole was measured with 201 points from 50 to 300 MHz at each 5 degree increment of azimuth rotation (72 sets of 201 point data). The radiation pattern of the dipole was measured at several frequencies, and both the gated and ungated responses were compared with the theoretical response. (Because the antenna was boresighted visually, the measured antenna patterns were plotted with a small offset angle to correct for the resulting misalignment.)

Fig. 6 shows the measured radiation pattern of the dipole at 115 MHz with no gating, plotted in a log scale with the theoretical pattern. This is the CW measurement. The difference between the theoretical and the ungated pattern is due primarily to the reflected signal from the ground that causes the uneven side lobes and offset nulls.

Fig. 7 shows the same measured pattern using gating to remove the effects of the ground plane reflection, plotted together with the theoretical response in a log scale. The gated response is virtually identical to the theoretical response with an average disagreement of only 0.18

dB. This improvement in antenna pattern measurement accuracy is due only to gating. (The measured antenna pattern is plotted point to point at 5 degree increments, and because of the offset in alignment the actual nulls at 90 and 270 degrees were not measured.)

A more dramatic improvement in the antenna pattern occurred at 125 MHz. At this frequency, the effect of the ground path interference was more severe. Fig. 8 shows the ungated response. In this conventional CW plot, there is very little resemblance between the measured pattern and the theoretical pattern. Fig. 9 shows the measured antenna pattern obtained using gating. In this case, the gating technique has improved the measurement of the nulls by better than 25 dB.

Fig. 10 shows the antenna pattern measured at 100 MHz without using gating, and Fig. 11 shows the pattern obtained using the gating technique. The improvement with gating is again very dramatic, however at this frequency there is also larger disagreement between the gated and theoretical responses. The gated pattern has a symmetrical shape that is very close to that of the theoretical pattern, however, it also has a rotational offset. The cause of this offset is unknown. Because of the nearly perfect results that were obtained at the resonant frequency (115 MHz), it is assumed that the offset is the result of an imbalance in the antenna at 100 MHz. This would also account for the lack of symmetry in the original ungated (CW) pattern.

In all, the radiation pattern of the antenna at 201 frequencies can be plotted from the data taken from one rotation of the antenna positioner.

Reduced Bandwidth Antenna Pattern

The actual measurement was made with 201 points from 50 to 300 MHz. The first 101 data points (from 50 to 175 MHz) were taken and used to re-compute the antenna pattern of the dipole at 115 MHz using gating. The resulting frequency and time domain responses at boresight are those previously shown in Figure 2. As mentioned, this bandwidth reduction doubles the time domain impulse width which reduces the response resolution, but it also reduces the measurement time. Fig. 12 shows the resultant gated pattern of the antenna at 115 MHz obtained with the reduced bandwidth data. This pattern is virtually identical to the one generated with the wider bandwidth information.

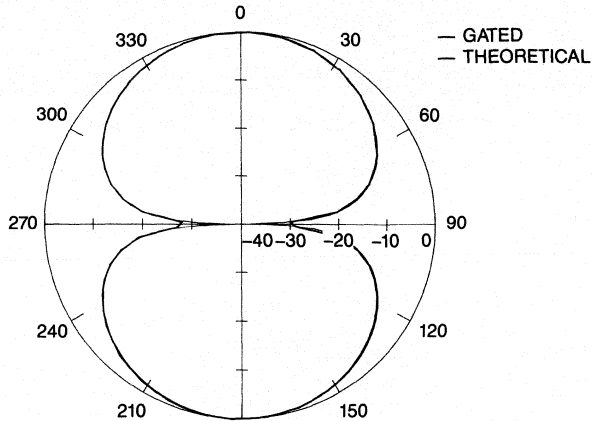
About the Author

John Boyles is an applications engineer for microwave vector network analyzers, Hewlett Packard Network Measurements Division, Santa Rosa, CA 95401. He has a BSEE from North Carolina State University and an MSEE from Georgia Institute of Technology.

References

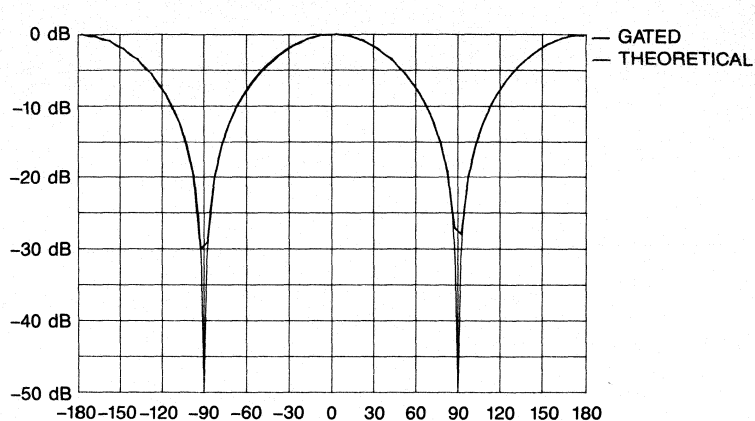
1. Jordan, E.C. and K.G. Balmain, *Electromagnetic Waves and Radiating Systems*, Prentice-Hall, Inc., Englewood Cliffs, N.J., 1968.
2. *HP 8510 Network Analyzer Operating and Service Manual*, Hewlett-Packard Company, Santa Rosa, CA, 1984, pp.127-149.

DIPOLE ANTENNA PATTERN
GATED VERSUS THEORETICAL, 115 MHz



9-5-84 JWB
HEWLETT-PACKARD

DIPOLE ANTENNA PATTERN
GATED VERSUS THEORETICAL, 115 MHz

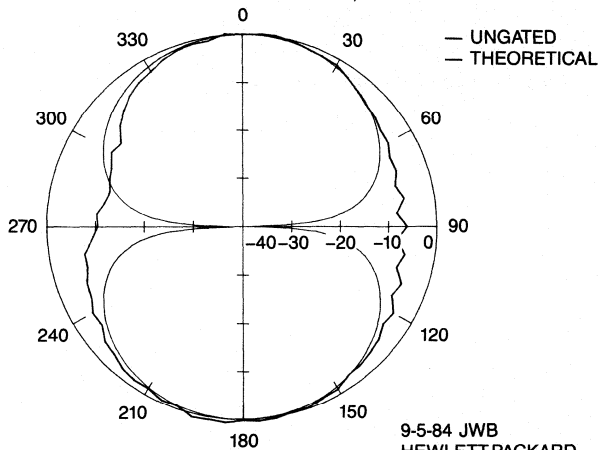


9-5-84 JWB
HEWLETT-PACKARD

Figure 7a. Gated Antenna Pattern versus Theoretical at 115 MHz: Plotted in a Polar Format.

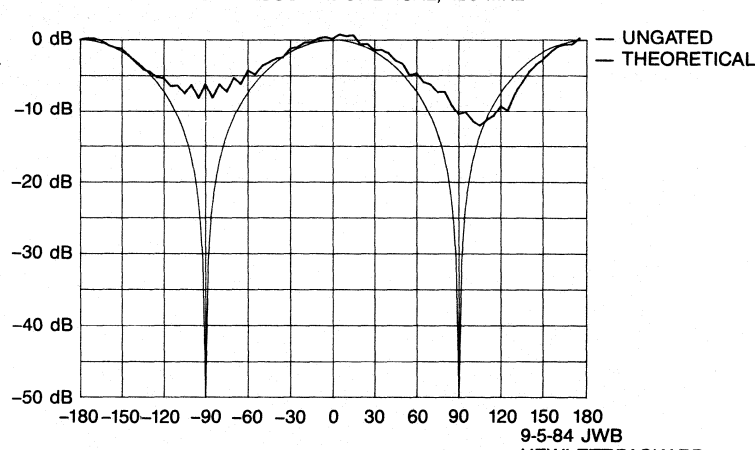
Figure 7b. Gated Antenna Pattern versus Theoretical at 115 MHz: Plotted in a Rectangular Format.

DIPOLE ANTENNA PATTERN
UNGATED VERSUS THEORETICAL, 125 MHz



9-5-84 JWB
HEWLETT-PACKARD

DIPOLE ANTENNA PATTERN
UNGATED VERSUS THEORETICAL, 125 MHz

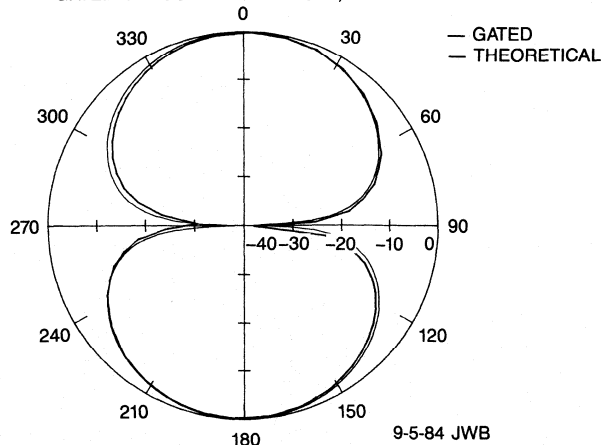


9-5-84 JWB
HEWLETT-PACKARD

Figure 8a. Ungated Antenna Pattern versus Theoretical at 125 MHz: Plotted in a Polar Format.

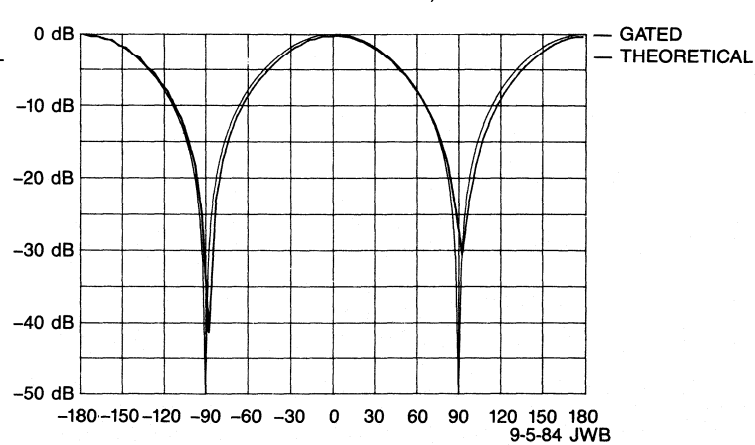
Figure 8b. Ungated Antenna Pattern versus Theoretical at 125 MHz: Plotted in a Rectangular Format.

DIPOLE ANTENNA PATTERN
GATED VERSUS THEORETICAL, 125 MHz



9-5-84 JWB
HEWLETT-PACKARD

DIPOLE ANTENNA PATTERN
GATED VERSUS THEORETICAL, 125 MHz

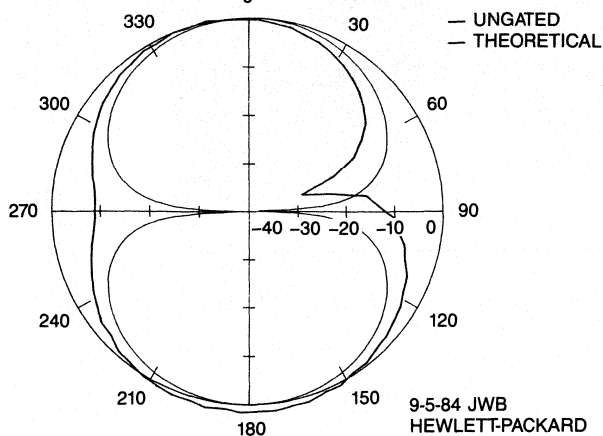


9-5-84 JWB
HEWLETT-PACKARD

Figure 9a. Gated Antenna Pattern versus Theoretical at 125 MHz: Plotted in a Polar Format.

Figure 9b. Gated Antenna Pattern versus Theoretical at 100 MHz: Plotted in a Rectangular Format.

DIPOLE ANTENNA PATTERN
UNGATED VERSUS THEORETICAL, 100 MHz



DIPOLE ANTENNA PATTERN
UNGATED VERSUS THEORETICAL, 100 MHz

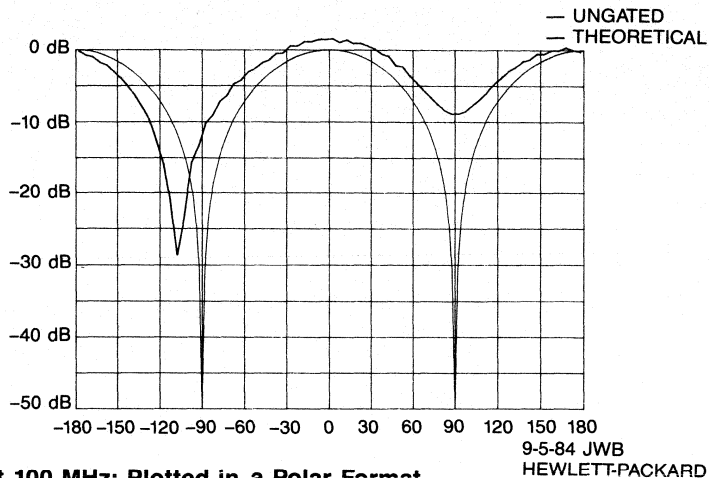
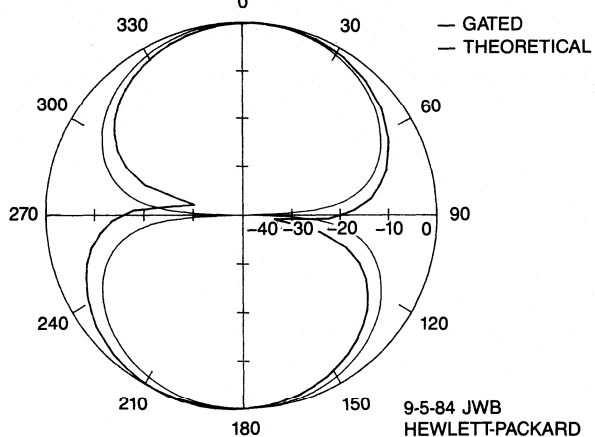


Figure 10a. Ungated Antenna Pattern versus Theoretical at 100 MHz: Plotted in a Polar Format.

Figure 10b. Ungated Antenna Pattern versus Theoretical at 100 MHz: Plotted in a Rectangular Format.

DIPOLE ANTENNA PATTERN
GATED VERSUS THEORETICAL, 100 MHz



DIPOLE ANTENNA PATTERN
GATED VERSUS THEORETICAL, 100 MHz

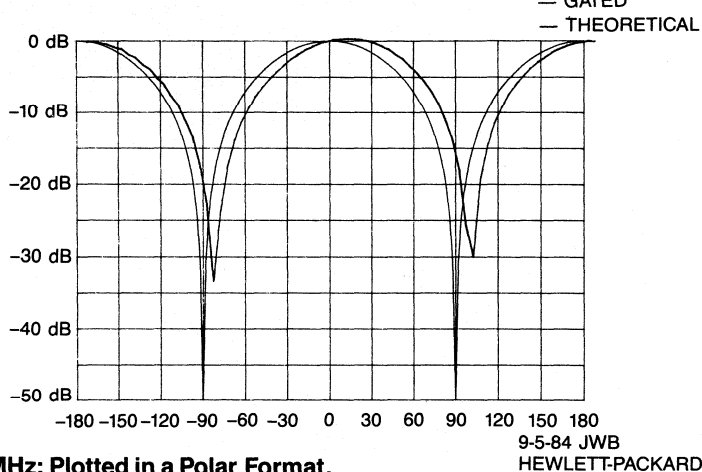
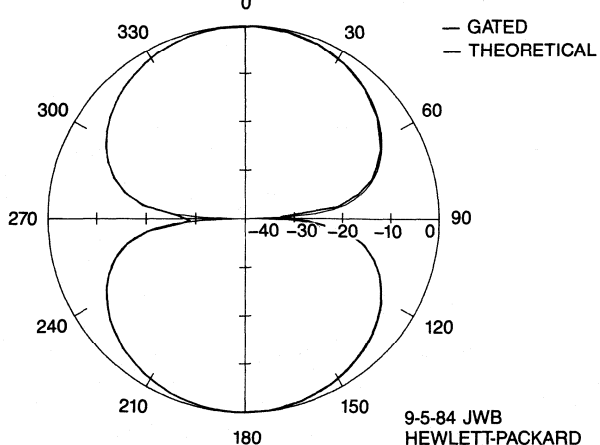


Figure 11a. Gated Antenna Pattern versus Theoretical at 100 MHz: Plotted in a Polar Format.

Figure 11b. Gated Antenna Pattern versus Theoretical at 100 MHz: Plotted in a Rectangular Format.

DIPOLE ANTENNA PATTERN
GATED VERSUS THEORETICAL, 115 MHz



DIPOLE ANTENNA PATTERN
GATED VERSUS THEORETICAL, 115 MHz

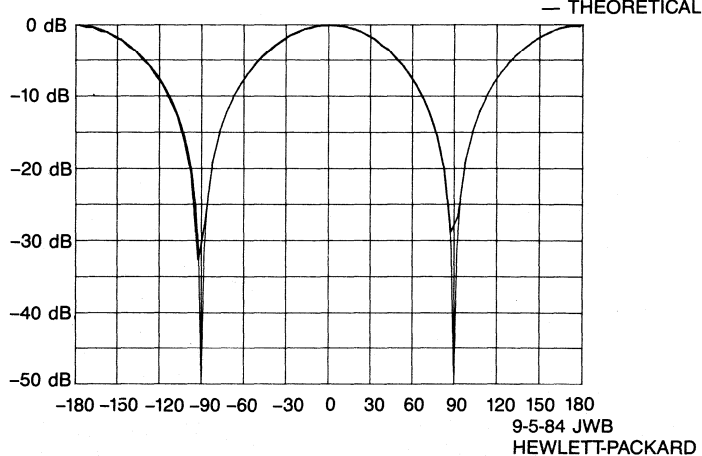


Fig. 12a. Gated Antenna Pattern vs. Theoretical at 115 MHz: From Reduced Bandwidth Data (50 to 175 MHz, 101 Points).

Fig. 12b. Gated Antenna Pattern vs. Theoretical at 115 MHz: From Reduced Bandwidth Data (50 to 175 MHz, 101 Points).

A New Approach to Op Amp Design

By Scott Evans
Comlinear Corporation

This article describes a high speed op amp topology that offers high frequency performance an order of magnitude faster than conventional op amp designs. One of the results of this design is the elimination of the gain-bandwidth product. Bandwidth remains virtually constant as the gain is changed; as a result, ease of use and predictability of performance have been greatly improved.

Conventional op amps have a differential, high input impedance stage that feeds several subsequent gain stages. The open loop output of the amplifier is $V_o = A(s) [V_1 - V_2]$. (See Figure 1.)

With the feedback connection made, feedback in the form of a voltage is applied to the inverting input. The closed loop gain becomes:

$$\frac{V_o}{V_1} = \frac{\frac{R_1}{R_1 + R_2}}{1 + \frac{R_1}{A(s)}}$$

By letting $(R_1 + R_2)/R_1 = G$:

$$\frac{V_o}{V_1} = \frac{G}{1 + \frac{G}{A(s)}}$$

To see the effect that gain setting, G , has on the frequency response it is instructive to break the open loop gain, $A(s)$, into a ratio of a numerator, $N(s)$, and a denominator, $D(s)$. $N(s)$ contains the zeros of the response and $D(s)$ contains the poles of the response.

$$A(s) = \frac{KN(s)}{D(s)}$$

where K is the DC value of the open loop gain.

Substituting this ratio into the closed loop gain and rearranging:

$$\frac{V_o}{V_1} = G \frac{KN(s)}{KN(s) + (G)D(s)}$$

G not only scales the magnitude of the gain (as desired) but also multiplies the effect of $D(s)$ on the closed loop response. The locations of the closed loop poles are now a function of G ; thus, if an application requires a large G , the poles will be at a lower frequency than for a low value of G . This is the chief failure of conventional high speed op amp designs. This is a major cause of instability problems in conventional op amps, correcting the problem leads to performance far inferior to data sheet specifications.

Figure 2 shows the closed loop frequency response of a conventional single-pole op amp for various gains. Notice that increasing the gain decreases the bandwidth.

In addition to poor high frequency performance, there are several other severe problems with conventional op amp design.

Compensation — Conventional high speed op amps are unstable at most gain settings so compensation must be used. Compensation creates a very low frequency pole that limits bandwidth so severely that the problematic high frequency poles are no longer dominant. Unfortunately, compensation does not allow complete control of the pole and zero locations, so simultaneously optimizing bandwidth, gain flatness and settling time is difficult if not impossible.

External Compensation — Compensation is usually connected external to the amplifier so the designer can tailor the response to the application. Unfortunately, conventional op amps are very sensitive to stray reactance in the PC board layout, temperature, loading and variations in the transistors of the op amp itself that make reliable compensation difficult. In addition, production can become expensive since each op amp compensation network must be individually "tweaked" to the desired response or the op amps must be individually tested and selected.

AC Feedforward — In order to achieve faster rise times and wider bandwidths, conventional op amps often use a technique called AC feedforward. This techni-

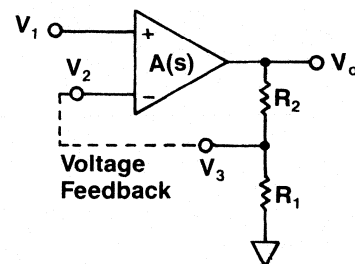


Figure 1. Open loop output

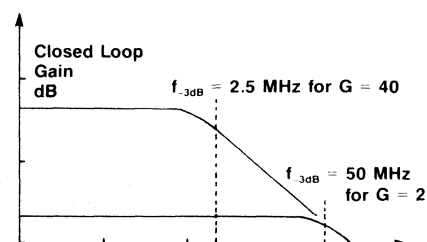


Figure 2. Closed loop frequency response of a conventional single-pole op amp.

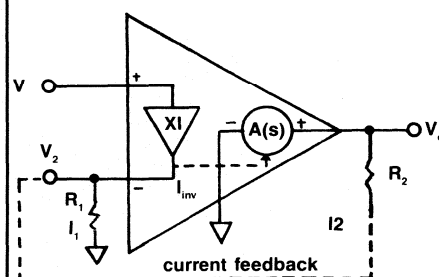


Figure 3. The Comlinear op amp

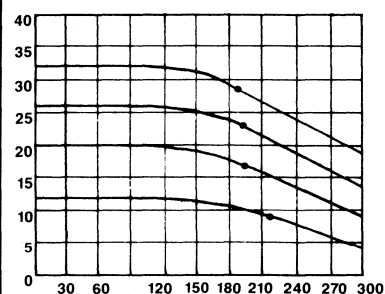


Figure 4. Gain vs. frequency response of the Comlinear op amp.

que cancels a low frequency pole by introducing a zero at the same frequency. Unfortunately, temperature, aging, loading and supply voltages affect pole locations. Pole locations also change with gain setting so the degree of cancellation depends on gain. This is part of the reason why conventional op amp performance is usually specified at a gain of -1. At this gain, the performance is optimal, but it deteriorates rapidly at other settings.

Slew Rate Limiting — In order to obtain high open loop gain, several internal gain stages must be used. As a result, transmit times through the amplifier are large. In addition to reducing the phase margin this also leads to problems when large or fast rise time signals are present at the input. These large or very fast signals can cause an internal gain stage to saturate or be cut off before feedback can propagate back to the input to reduce the error signal. To prevent this behavior the slew rates of the internal stages are simply limited so nonlinear behavior cannot occur before the signal propagates through the amplifier. Consequently, the slew rate and large signal bandwidth of the op amps are reduced severely.

The Comlinear Innovation

Most of the problems with conventional op amps shown are either directly or indirectly caused by the limitation of having G , the gain setting, affect the frequency response. If G could be removed from the denominator of the expression, performance and ease of use could be extended dramatically. This is exactly what Comlinear designers have done. The drawing of the Comlinear op amp (Fig. 3) shows an unusual (and patented) circuit configuration.

The input buffer is a unity gain voltage amplifier that is connected across the inputs of the op amp. In operation, the buffer forces V_2 to equal V_1 independent of any external feedback through R_2 . This causes the inverting input to have a very low input impedance. When feedback around the loop is applied, the impedance of this node is reduced further and V_2 becomes a "virtual ground" with respect to V_1 . This low impedance allows current to flow easily into or out of the inverting input.

The transimpedance amplifier is the gain block inside Comlinear op amps. In operation, the transimpedance amplifier senses the inverting input current (literally the current flowing into or out of the inverting input) and transforms this current into the output voltage. The transfer func-

The Fallacy of the Gain-Bandwidth Product

The gain-bandwidth product has for years been a key specification for op amps; in fact, the concept of the gain-bandwidth product is a major topic of op amp tutorials. Unfortunately, this often touted specification means little to the engineer who must work with very high speed op amps. For most high speed op amps the gain-bandwidth product is actually very misleading.

The basis for the gain-bandwidth product is the assumption that the open loop gain rolls off due to a single pole. When the assumption is valid, as is the case with some low frequency op amps, the gain-bandwidth product concept is also valid. Having frequency performance depend on gain is troublesome, but at least with a single pole rolloff the bandwidth is easily determined and stability is assured.

High speed op amps, however, have several poles before unity gain crossover is reached.

Clearly, a conventional op amp with a gain-bandwidth product of 1 GHz will not yield a bandwidth of 500 MHz at a gain of 2. This is why most manufacturers specify their gain-bandwidth products at very high gains, typically 1000.

A much more useful (and accurate) way to show frequency performances is to actually show the performance for various gains. This allows the engineer to fully characterize the amplifier without having to actually test the device. Although the performance of Comlinear amplifiers varies little with changes in gain, Comlinear provides complete specifications for at least three representative gain settings.

$$I_{inv} = I_2 - I_1$$

$$I_{inv} = \frac{V_2}{R_1} - \frac{V_o - V_2}{R_2}$$

Then, since $V_o = I_{inv} \cdot A(s)$ and $V_2 = V_1$ (because of the buffer)

$$\frac{V_o}{A(s)} = V_1 \left(\frac{1}{R_1} + \frac{1}{R_2} \right) - \frac{V_o}{R_2}$$

Then, rearranging

$$\frac{V_o}{V_1} = \frac{\frac{R_1 + R_2}{R_1 \cdot R_2}}{\frac{1}{R_2} + \frac{1}{A(s)}} = \frac{1 + \frac{R_2}{R_1}}{1 + \frac{R_2}{A(s)}}$$

$$\text{Again, letting } 1 + \frac{R_2}{R_1} = G$$

$$\frac{V_o}{V_1} = \frac{G}{1 + \frac{R_2}{A(s)}}$$

$$\text{Letting } A(s) = \frac{KN(s)}{D(s)}$$

$$\frac{V_o}{V_1} = G \frac{KN(s)}{KN(s) + R_2 D(s)}$$

Table 1. Mathematical justification of the Comlinear op amp design.

tion of this transimpedance amplifier is $A(s)$; the units are in ohms.

Feedback in the form of a current is applied through R_2 to the inverting input.

A Comparison: Conventional vs. Comlinear

Table 1 shows the mathematical justification of the Comlinear op amp design. As a result of these mathematical operations the closed loop gain equations are in the same form and can be compared directly.

For the conventional op amp:

$$\frac{V_o}{V_1} = G \frac{KN(s)}{KN(s) + (G)D(s)}$$

For the Comlinear op amp:

$$\frac{V_o}{V_1} = G \frac{KN(s)}{KN(s) + (R_2)D(s)}$$

R_2 has replaced G in the frequency-dependent portion of the transfer function. Since R_2 can be held constant, whereas G cannot, the pole locations and hence the performance can be held constant. ($G = 1 + R_2/R_1$, so the gain setting can be varied by changing R_1).

The results of this new approach to op amp design are dramatic:

Elimination of the Gain-Bandwidth Product — The frequency response of the Comlinear op amp changes very little when the gain is increased by a factor of 10, from a gain of 4 to a gain of 40. Other specifications are similarly unaffected.

ected by gain changes. A similar change in gain with a conventional op amp could reduce the bandwidth by a factor of 10, even under ideal single pole conditions. As shown in Figure 4, the -3dB bandwidth remains constant over a wide range of gains. Small second order effects explain the slight deviation in performance from that predicted by the equations.

Excellent Performance — The high speed performance of Comlinear op amps is dramatically better, usually by an order of magnitude, than conventional op amps. A typical rise time for a 5V output step can be as low as 1.6 ns, for example. With a conventional op amp rise times of 30 to more than 100 ns are common. Other outstanding specifications include settling times which can be as low as 10 ns for a 0.2 percent tolerance and slew rates that range from 3000 V/ μ s to over 7000 V/ μ s, depending on which model is chosen. (The slew rate was intentionally kept very fast so it would not limit the response of the amplifiers under large signal conditions. Bandwidth, not slew rate, controls amplifier response and keeps it linear.)

Linear Phase — Although phase linearity is a rarely mentioned specification, it is very important for signal fidelity. Comlinear op amps have excellent phase linearity, usually the deviation from linear phase is less than two degrees from DC to over 50 percent of the bandwidth. Conventional op amps, however, must use techniques like AC feedforward which increase bandwidth but degrade phase linearity; thus, signal fidelity is sacrificed.

Predictable Performances — Since most of the specifications are virtually independent of gain setting, the performance of Comlinear op amps remains consistent even with varying circuit configurations. As design requirements change, adjustments in gain usually can be achieved by a change in one resistor; with a conventional op amp a change in gain could require a redesign of the entire circuit.

Internal Compensation — With R_2 fixed and the poles of the frequency response consequently fixed, internal compensation is provided to simultaneously optimize bandwidth, settling time, linearity and distortion. Since the compensation is internal, Comlinear op amps can save time and money in production with no compensation networks to "tweak." Although Comlinear uses an internal high precision resistor for R_2 , on many models an external resistor of another value can be used. Since this

would change the pole locations, the internal compensation is made accessible to the user through one package pin. One external capacitor is then used to re-optimize the performance.

Standard Usage — Determining the gain for Comlinear op amps is the same as that for conventional op amps, where $G=1+R_2/R_1$. The same ease of use ap-

plies equally well to both inverting and differential configurations.

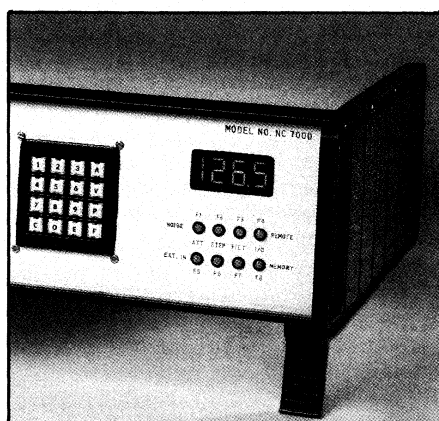
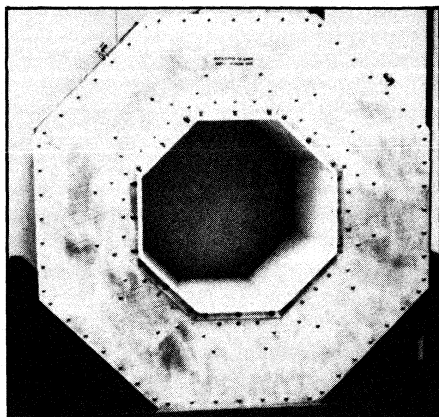
About the Author

Scott Evans is a product marketing engineer for Comlinear Corp., P.O. Box 20600, 4800 Wheaton Drive, Fort Collins, CO 80522. His telephone number is (303) 226-0500.



Cover

Our cover features the Noise Com NC7000 noise generating instrument appearing on the market this month. The instrument combines programmable controls with white Gaussian noise generators in one unit. Standard models cover the 10 Hz to 2 GHz frequency range and feature seven switchable discrete filters. The instrument can be connected to IEEE-488, RS-232, RS-422 or RS-423 interfaces for automatic testing and other external control.



Features

29 Special Report: The New Uses of RF. Part I — Noise Generating Instruments Part II — Medical Uses of RF Energy

Part I of this two-part Special Report covers the relatively new field of noise generation. The reasons for noise generation and the basics of noise are explained, along with a description of two noise generating instruments. Part II is a report on the use of RF radiation for internal imaging of the human body and for cancer treatment. — Gary A. Breed and James N. MacDonald

41 Re-Normalizing the Scattering Parameters

Network S-parameters are not independent of source and load impedances. Measurements using standard network analysis equipment may not accurately reflect device characteristics if the source and load impedances of the equipment do not match those of the system being designed. The author shows how to mathematically correct data to reflect the actual circuit configuration of a two-port network. — Daniel N. Meeks

45 Elliptic Filter Wins A Comparison Test

In a comparison of Butterworth, Chebychev and elliptic low-pass filter implementations, the author finds the elliptic filter to be the best choice for most applications in terms of insertion loss and component value sensitivity. COM-PACT is used for the analysis. — Peter Vizmuller.

59 ESD Sensitivity of a Diode Mixer

This article describes a test procedure used to measure the ESD sensitivity of mixers using the double-balanced diode-ring configuration. The mixers were tested relative to the Category B classification of MIL-STD-883 Method 3015. — David Geiser.

Departments

Designer's Notebook — Another One-Transistor FM Transmitter

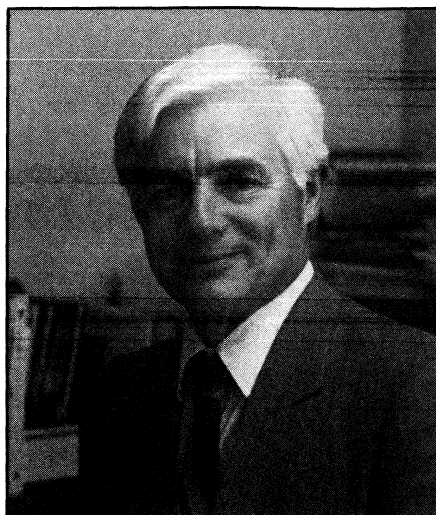
53 This article describes a variant of a similar design published in the February 1985 issue. — S. Kan

RFI/EMI Corner — Medical RF Applications Require Special Shielding

57 This article examines the special problems of shielding RF apparatus in hospitals, especially the kind of equipment mentioned in the Special Report, and describes the Lindgren modular enclosure. — Gary A. Breed

6	Editorial	52	Courses
8	Viewpoint	62	New Products
13	Letters	74	New Literature
13	Calendar	77	Classified Advertising
16	News	78	Advertisers Index
35	Info/Card		

R.F. DESIGN (ISSN: 0163-321X USPS: 453-490) is published monthly plus one extra issue in August. October 1985, Volume 8, No. 10. Copyright 1985 by Cardiff Publishing Company, a subsidiary of Argus Press Holdings, Inc., 6530 S. Yosemite Street, Englewood, CO 80111 (303) 694-1522. Contents may not be reproduced in any form without written permission. Second-Class Postage paid at Englewood, CO and at additional mailing offices. Subscription office: 1 East First Street, Duluth, MN 55802, (1-800-346-0085). Domestic subscriptions are sent free to qualified individuals responsible for the design and development of communications equipment. Other subscriptions are: \$22 per year in the United States; \$29 per year in Canada and Mexico; \$33 (surface mail) per year for foreign countries. Additional cost for first class mailing. Payment must be made in U.S. funds and accompany request. If available, single copies and back issues are \$5.50 each (in the U.S.). This publication is available on microfilm/fiche from University Microfilms International, 300 N. Zeeb Road, Ann Arbor, MI 48106 USA (313) 761-4700. POSTMASTER & SUBSCRIBERS: Please send address changes to: R.F. Design, P.O. Box 6317, Duluth, MN 55806.



James N. MacDonald
Editor

This month we begin our second three-part series of Special Reports, this series featuring the new uses of RF. Writing these reports is a learning experience for us because we are investigating areas few people know much about.

The first subject is medical uses of RF. As with the other subjects, we knew there were some interesting uses of RF in medicine, but we did not know how dramatic the uses were and what potential they have for saving lives. Included with the Special Report is an image of the inside of a rat's head made using RF radiation, showing far more detail than an X-ray. We could not include color images made by the same process that are so realistic they look like photographs made during an autopsy. Such images are made with no discomfort and no health risk for the patient because they are made with low frequency radiation. The technique described in this Special Report has been used less than five years.

Another use of RF has a longer history, but the technology has been made to work successfully only in the last few years. This is hyperthermia. Researchers, who do not like to make predictions, speak cautiously about the potential of RF induced hyperthermia to cure cancer, but investigational use on hopeless patients has demonstrated that properly directed RF radiation can kill large, inoperable tumors. Once again, the safety of RF is a significant factor, especially compared to the severe effects of massive chemotherapy, X-ray or surgery.

This month's Special Report is in two parts because we recently became aware of a relatively new use of RF that is be-

coming increasingly important. Most of us think of noise as something to keep as low as possible, swamping it with a high S/N ratio. In a world of increasing RF sources, however, it becomes necessary to factor noise into the calibration of receivers and other equipment. Two companies manufacture general purpose noise generating test instruments and many others manufacture diodes to be built into transmitters and test equipment for easy calibration. To cover this new use of RF in a timely manner we have devoted part of the Special Report to the subject of noise and featured the newest noise generator on the cover.

Another relatively new use of RF is in testing susceptibility of electronic equipment to radio frequency interference. This RFI susceptibility becomes more important almost daily as RF signal transmitting devices become more portable and more numerous. In November we will report on RFI testing and provide an update on the status of US and foreign regulations. We'll try to clear up some of the confusion caused by recent regulatory changes and the different requirements of US and foreign agencies.

Susceptibility testing is becoming more important because RF devices are proliferating rapidly. Two-way alarm systems for home or business or construction sites, shoplifting detectors, remote meter reading and personnel locating systems are a few of the unusual industrial uses of RF that will be covered in the December Special report. We are literally surrounded by RF.

Attendees at the RF Technology Expo 86, next January, will be surrounded by RF in a different way. The exhibit space, doubled from last year, will be filled by 89 companies showing their latest RF products. A two-and-a-half day program has been assembled with 75 papers to be presented, in addition to the Fundamentals of RF Design course. It will be the most comprehensive forum of RF design knowledge ever offered. Papers will be presented in five simultaneous sessions, and Proceedings will be available at the conference, so attendees will be able to read the papers they could not hear and perhaps consult with the authors.

We're looking forward to it.

*James N.
MacDonald*

Editor:

I read with great interest the article in the July 1985 issue of *RF Design*; "Helical-Resonator Filter Design — A Basic Program" by Vincent Heesen. I would like to offer the following comments:

1) The calculations, as stated by Mr. Heesen, are for cylindrical resonators. These are not as practical to build as resonators with square shields. It would be more useful to use a square shield design.

2) The coupling between the resonators is most often capacitance, not inductive as he states but either or both may be used.

3) It is true that the coupling shield height is determined empirically, but data exists that allows for accurate calculation.

4) Line 940 prints out the tap position. It appears that the publisher cut off the last line of the outputted data.

5) No mention is made as to how to determine the resonator-to-resonator coupling, without which the resonator information is useless and the filter cannot be designed. The only place the filter bandwidth is used is in the calculation of the insertion loss.

6) Insertion loss calculations are limited only to Butterworth filters (order 2-7).

7) Having been involved in filter designs for over 19 years this is the first time I have seen suggested the use of a trimmer capacitor at the resonator ends. It may work but most likely will not provide the necessary resolution required for proper tuning. As for providing support to the resonators it is useless.

In general I find this type of article worse than useless, in that it not only provides incomplete information on design, but wastes the reader's time in trying to understand what's going on. I would suggest that anyone interested in Helical Filter Design review the following article.

"Need a Helical Filter? These Design Aids Will Make it Easy," by Lee R. Watkins, *RF Design* May/June 1981.

One correction to the above article should be made. On page 46:

$$\text{eq. } \theta = \text{ARCSIN} \frac{R_b R_{\text{tap}}}{2Z_o^2}$$

Should be:

$$\theta = \text{ARCSIN} \sqrt{\frac{R_b R_{\text{tap}}}{2Z_o^2}}$$

Lee R. Watkins P.E.

Mr. Heesen's response:

Re: Item #1

Stated in the text (an alternate approach is to reduce the square shield width by 20 percent of the computed diameter of the cylindrical shield).

Re: Item #2

See text: "Coupling into or out of the resonator may be accomplished by probes, etc.," Probes, by definition, include passive capacitive networks.

Re: Item #3

Accurate calculation of the coupling window between resonators requires knowledge of the precise location of the open-ended end of the helix — a task beyond the scope of this program.

Re: Item #4

Reader Watkins is correct. Then too, the program lines 650 and 660 are also missing.

Re: Item #5

The intent of this article is to provide accurate dimensional information to facilitate fabrication and/or feasibility of design. Neither this nor reader Watkins' article are "stand-alone" design presentations. Readers are encouraged, indeed expected, to consult the references cited.

(continued on next page)

Re: Item #6

As stated in the text, Helical Resonators are employed where small, selective, low loss filters are required. Obviously, other filter designs, e.g., Chebyshev, could be used; but since the Butterworth exhibits the lowest loss it is the logical choice for this device.

Re: Item #7

Mechanical instability is one of the major draw-backs of the Helical Resonator. All core materials lower the resonator's Q and should be avoided, where possible. The use of heavy gauge wire self-supported at the grounded end and terminated in an air-variable "trimmer" capacitor at the open-circuited end is "common practice." The text refers to this practice as a practiced procedure, not as a requirement.

Frankly, I'm surprised that reader Watkins has never in all his 19 years experience seen the "trimmer" employed as a tuning and mechanical support element. Perhaps during the next 19 years, as he catches up to some of us, he will have an opportunity to peruse through a copy of the Radio Amateur's Handbook, which has illustrated this technique for years.

I have received far too many accolades from reputable RF circuit designers for this article to take this reader's views seriously.

With the addition of the missing program lines 650 and 660, this article remains, as intended, a very useful tool for the design and fabrication of Helical Resonators.

Where else can one find a "free" computer program which will yield: coil length, coil diameter, wire diameter (min. and max.), number of turns, wire spacing, shield diameter or square shield width, shield length, unloaded Q, tap location, plus insertion loss for up to seven poles — all within twenty seconds?? All this on a "Home Computer!!!" Where else, indeed, but the July 1985 issue of *RF Design* magazine.

Vincent G. Heesen P.E.

Editor:

I have found some additional difficulties with Alan J. LaPenn's article "Basic Program Computes Values for 14 Matching Networks," April 1985. Included are my formulas and changes for your consideration. The errors appear to have originated with Alex J. Burwasser's article "TI-59 Program Computes Values for 14 Matching Networks," Nov./Dec. 1983. They were also repeated in an "RF Letter" from Keats A. Pullen, Jr., June 1985.

Article: "Basic Program Computes Values for 14 Matching Networks," *RF Design*, pgs. 44-46, April 1985, Alan J. LaPenn.

Network #9, p. 45:

$$\begin{aligned} X_1 &= \sqrt{R_S R_L - R_S^2 - Q R_S} \\ X_2 &= Q R_S \\ X_3 &= \frac{-R_S R_L}{X_1 + X_2} \end{aligned}$$

Should be:

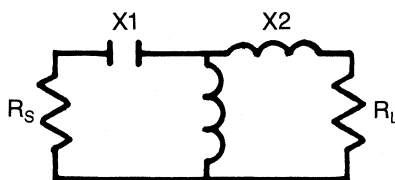
$$\begin{aligned} X_1 &= (Q \times R_S) X - 1 \\ X_3 &= \left(R_L \sqrt{R_S / (R_L - R_S)} \right) X - 1 \\ X_2 &= \left(X_1 + \frac{R_S \times R_L}{X_3} \right) X - 1 \end{aligned}$$

$$810 \quad X_1 = Q \cdot R_S^* - 1$$

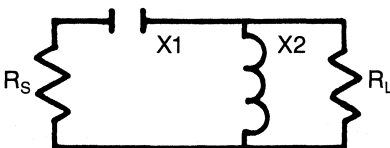
$$820 \quad X_3 = R_L \cdot \text{SQRT}((R_S / (R_L - R_S)))^* - 1$$

$$830 \quad X_2 = (X_1 + R_S \cdot R_L / X_3)^* - 1$$

Diagram on page 46 for Network #14.



Should be:



The corrected program seems to verify tabulations in the Motorola RF Data Manual and the ARRL Electronics Data Book as well as verifying the results on the "Smith Chart Program" (Lynn A. Gerig, June 85).

Thank you for providing us with a top grade magazine for the RF field.

S. Ticknor, President
Wide Band Engineering Co., Inc.

Mr. Burwasser's response:

Mr. Ticknor is quite correct in his finding that there are errors in the equations for network #9 ("TI-59 Program Computes Values for 14 Matching Networks," Nov./Dec. 83), and is to be commended on his constructive "detective" work.

The most major of these errors is a typographical one in the equation for X1, where the radical sign incorrectly extends over the quantity "-Q · R_S." In the original manuscript, the equation reads as follows:

$$X_1 = \sqrt{R_S \cdot R_L - R_S^2} - Q \cdot R_S$$

Even with this typographical correction, however, the reactance values for X1, X2 and X3 are somewhat at variance with those values obtained using Mr. Ticknor's equations. Yet, networks synthesized using either set of equations are legitimate series enhanced -Q L reactance matching networks for the source and load resistances specified. A further investigation by this author of the original TI-59 article manuscript found corrections to the equations that, regrettably, were never mailed in to *RF Design*. The corrected equations for network #9 should have been as follows:

$$X_1 = -Q \cdot R_S$$

$$X_2 = \sqrt{R_S \cdot R_L - R_S^2} - X_1$$

$$X_3 = \frac{-R_S \cdot R_L}{X_1 + X_2}$$

In the above equations, the network Q is defined in terms of X1 (rather than X2 as was done in the original equations). Thus, networks synthesized using the original equations will have Qs slightly different than the specified value (for moderate and high Q values, this difference is small). The corrected equations above yield the specified Q value. Although these equations appear different than Mr. Ticknor's, the same values for X1, X2 and X3 are obtained using either set.

A similar correction is also required for the equations of the shunt enhanced — Q L reactance matching network. The corrected equations for network #11 are as follows:

$$X_1 = R_S \cdot \sqrt{\frac{R_L}{R_S} - 1}$$

$$X_3 = \frac{R_L}{Q}$$

$$X_2 = \frac{-X_3}{\frac{X_1}{Q \cdot R_S} + 1}$$

Alex J. Burwasser
RF Products

Re-Normalizing the Scattering Parameters

By Daniel N. Meeks
Q-bit Corporation

Many component and subsystem users rely on normalized scattering parameter data (S-parameters) to determine compatibility of the component or subsystem in an overall system configuration. Fortunately, the S-parameters are easy to measure using standard network analysis equipment. In some cases, the S-parameters may even be supplied by the manufacturer of a component. However, the S-parameters of a network are not independent of the source and load impedances. In the strictest sense, the actual S-parameter data is meaningless unless the source and load impedances of the measurement system are known. It therefore follows that if the unit is to be designed into a system that provides input and output impedances other than those specified with the S-parameter data, the test data will not accurately reflect the device characteristics. Two alternatives present themselves in this situation: Test data may be obtained from a network analyzer with the desired source and load impedances, or the data on hand may be mathematically corrected to reflect the actual circuit configuration.

The first alternative has obvious practical limitations, especially for component users who may not actually have access to the required test equipment and fixtures. To utilize the second alternative, the following discussion presents a mathematical solution of the normalized scattering parameters of a two-port network operating into source and load impedances different from those used to measure the original S-parameters.

A two port terminated by Z_0 at both ports (Fig. 1) may be described by the associated normalized scattering matrix:

$$[S] = \begin{bmatrix} S_{11} & S_{12} \\ S_{21} & S_{22} \end{bmatrix}$$

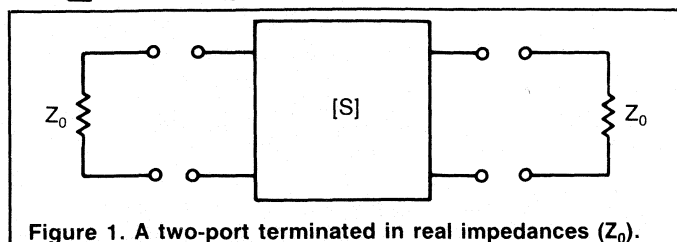


Figure 1. A two-port terminated in real impedances (Z_0).

This is the conventional model, and $[S]$ may be easily determined using standard test methods and equipment, or $[S]$ may be sup-

plied by the manufacturer of the component or subsystem. Thus, it is assumed that $[S]$ is known for the given two-port.

Using transmission line voltage-current relationships and the definition of the scattering parameters, the normalized scattering matrix $[S']$ of a two-port is given by:

$$[S'] = [R_e Z_{0n}^{-1/2}] [S] [R_e Z_{0n}^{-1/2}] \quad (1)$$

$$\text{where, } [R_e Z_{0n}^{-1/2}] = \begin{bmatrix} \sqrt{R_e Z_{01}} & 0 \\ 0 & \sqrt{R_e Z_{02}} \end{bmatrix} \quad (2a)$$

$$[R_e Z_{0n}^{-1/2}] = \begin{bmatrix} \frac{1}{\sqrt{R_e Z_{01}}} & 0 \\ 0 & \frac{1}{\sqrt{R_e Z_{02}}} \end{bmatrix} \quad (2b)$$

Z_{01} and Z_{02} are the complex source and load impedances the two-port is operating into (Fig. 2).

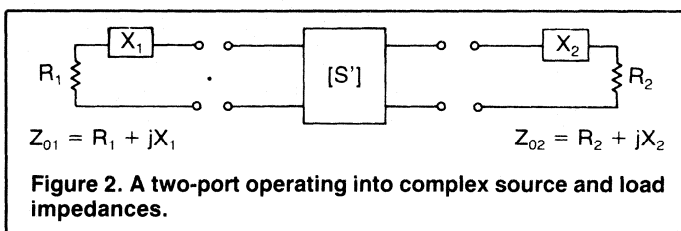


Figure 2. A two-port operating into complex source and load impedances.

$[S']$ is the current scattering matrix and is given by:

$$[S'] = ([Z] + [Z_{0n}])^{-1} ([Z] - [Z_{0n}^*]) \quad (3)$$

where $[Z]$ represents the impedance matrix of the two-port.

(1) and (2a, 2b) give $[S]$ to $[z]$ transformations. Using these transformations and noting that $[Z] = Z_0 [z]$ gives:

$$[Z] = \frac{Z_0}{D} \begin{bmatrix} (1 + S_{11})(1 - S_{22}) + S_{12} S_{21} & 2 S_{12} \\ 2 S_{21} & (1 - S_{11})(1 + S_{22}) + S_{12} S_{21} \end{bmatrix} \quad (4)$$

where $D = (1 - S_{11})(1 - S_{22}) - S_{12}S_{21}$, and Z_0 is the characteristic impedance of the system used to measure $[S]$.

Using equation 3 and noting that:

$$Z_{On} = \begin{bmatrix} Z_{01} & 0 \\ 0 & Z_{02} \end{bmatrix}$$

and,

$$Z_{On}^* = \begin{bmatrix} Z_{01}^* & 0 \\ 0 & Z_{02}^* \end{bmatrix}$$

gives:

$$[S_i] = \begin{bmatrix} Z_{11} + Z_{01} & Z_{12} \\ Z_{21} & Z_{22} + Z_{02} \end{bmatrix}^{-1} \begin{bmatrix} Z_{11} - Z_{01}^* & Z_{12} \\ Z_{21} & Z_{22} - Z_{02}^* \end{bmatrix} \quad (5)$$

Solving the inverse matrix and multiplying through gives:

$$[S_i] = \frac{1}{D'} \begin{bmatrix} (Z_{22} + Z_{02})(Z_{11} - Z_{01}^*) - Z_{12}Z_{21} & Z_{12}(Z_{02} + Z_{02}^*) \\ Z_{21}(Z_{01} + Z_{01}^*) & (Z_{11} + Z_{01})(Z_{22} - Z_{02}^*) - Z_{12}Z_{21} \end{bmatrix} \quad (5)$$

where $D' = (Z_{11} + Z_{01})(Z_{22} + Z_{02}) - Z_{12}Z_{21}$

Using (1) and combining (2a), (2b) and (5) gives:

$$[S'] = \frac{1}{D'} \begin{bmatrix} (Z_{22} + Z_{02})(Z_{11} - Z_{01}^*) - Z_{12}Z_{21} & 2Z_{12}\sqrt{(R_e Z_{01})(R_e Z_{02})} \\ 2Z_{21}\sqrt{(R_e Z_{01})(R_e Z_{02})} & (Z_{11} + Z_{01})(Z_{22} - Z_{02}^*) - Z_{12}Z_{21} \end{bmatrix} \quad (6)$$


where D' is a given, as in (5) above.

Therefore, the scattering parameters for the two-port, augmented by the complex source and load impedances of Z_{01} and Z_{02} , are given as $[S']$ by (6). The impedance parameters $[Z]$ in (6) are found using the scattering parameters $[S]$ of the original two-port configuration shown in Figure 1 and 4.

References:

1. R. Carson, "High-Frequency Amplifiers," John Wiley & Sons, N.Y., 1982, pp. 188-201.
2. Hewlett Packard Application Note 95-1, "S-Parameter Techniques for Faster, More Accurate Network Design."

About the Author

Daniel Meeks is an RF Design Engineer with Q-bit Corporation, 311 Pacific Avenue, Palm Bay, FL 32905-2699. He received his B.S.E.E.T. degree from Capitol Institute of Technology, and has worked on large automated RF test systems, as well as his current work in RF and microwave circuit design. 

Elliptic Filter Wins A Comparison Test

By Peter Vizmuller
Motorola Canada

Modern computer-aided circuit analysis and optimization programs can provide important insights into circuit operation and shorten design time. In this article, COMPACT® was used to analyze and optimize the performance of Butterworth, Chebychev and Elliptic low-pass filters for comparison purposes. Of the different low-pass filter implementations, the elliptic filter turns out to be the best choice in terms of insertion loss and component value sensitivity, for most applications.

Filter design with ideal, lossless components is quite straightforward, with component values tabulated in many sources (1). The filter designer only needs

to perform frequency and impedance scaling for his selected filter shape and decide how to realize the required components using discrete components, sections of transmission line or coupled resonators. Unfortunately, in the real world, lossless components do not yet exist and we have to design with inductors and transmission lines that are lossy and capacitors that are self-resonant.

Most reference books on filter design treat the problem of lossy components in a rather artificial manner, by assuming that capacitors and inductors contribute to the losses equally. (1, 2) By assuming equal losses, a technique called predistor-

tion is used to modify component values so that the basic filter shape is preserved. Predistortion thus maintains the desired shape (Butterworth, Chebyshev, etc.) but at the expense of increased insertion loss and degraded return loss.

For many filter designs predistortion is quite unacceptable as a realization procedure since capacitors have much lower losses (higher Qs) than inductors and, therefore, must be made lossy by placing resistors in parallel to satisfy the requirement for equal component losses. If one of the objectives of a filter is to minimize insertion loss, as it is for a majority of filters, increasing component losses ar-

Table 1. Sample of COMPACT® analysis for ideal Chebyshev filter:

Sensitivity Analysis With 7 Variables:
Initial Circuit Analysis

Polar S-Parameters in 50.0 ohm System

Freq.	S11 (Magn<Angl)		S21 (Magn<Angl)		S12 (Magn<Angl)		S22 (Magn<Angl)		S21 dB
20.00	0.15<	-152	0.99<	-62.3	0.989<	-62.3	0.15<	-152	-0.10
40.00	0.04<	144	1.00<	-126.3	0.999<	-126.3	0.04<	144	-0.01
60.00	0.15<	-105	0.99<	164.5	0.989<	164.5	0.15<	-105	-0.10
80.00	0.03<	-4	1.00<	85.9	1.000<	85.9	0.03<	-4	-0.00
100.00	0.15<	67	0.99<	-22.6	0.989<	-22.6	0.15<	67	-0.10
102.00	0.31<	51	0.95<	-39.2	0.951<	-39.2	0.31<	51	-0.43
104.00	0.48<	33	0.87<	-56.9	0.875<	-56.9	0.48<	33	-1.16
106.00	0.65<	15	0.76<	-74.5	0.761<	-74.5	0.65<	15	-2.37
108.00	0.78<	-1	0.63<	-90.7	0.631<	-90.7	0.78<	-1	-4.00
110.00	0.86<	-15	0.51<	-104.6	0.508<	-104.6	0.86<	-15	-5.89
250.00	1.00<	-139	0.00<	131.3	-72.9 dB	131.3	1.00<	-139	-72.90
260.00	1.00<	-141	0.00<	129.5	-75.5 dB	129.5	1.00<	-141	-75.49

Sensitivity Analysis With Following Variables and Gradients

VARIABLES

(1): 37.600
(2): 113.20
(3): 66.700
(4): 125.20
(5): 66.700
(6): 113.20
(7): 37.600
ERR. F. = 0.057

GRADIENTS

(1): -.43170E-01
(2): .24999E-01
(3): .55469
(4): .78824
(5): .55570
(6): .24603E-01
(7): -.43950E-01

tificially to preserve some elegant mathematical theory is simply not justified. In practical filter design, the number of lossy components should be minimized, even though having the minimum number of inductors does not always guarantee lowest insertion loss, as shown below.

In some cases, choosing a particular filter realization for minimum insertion loss can be quite easy. For example, a given elliptical filter can be realized using two inductors and five capacitors or by its dual, which uses two capacitors and five inductors (Fig. 1).

The filter using five inductors should be expected to have a higher insertion loss than the filter using only two inductors. In other cases, it is not really obvious which realization is preferable. Let us look at some representative filter designs using lossless capacitors and lossy inductors and investigate, by means of a numerical comparison, the effect of inductor losses on filter performance to see if the component values can be changed to partially compensate for inductor losses, minimizing the insertion loss.

The Basis For Comparison

The comparison was carried out by following these four steps:

1. Butterworth, Chebyshev and Elliptic low-pass filters were designed with approximately the same 3 dB bandwidth of 100 MHz and approximately the same attenuation at some out-of-band frequency, i.e. around 70 dB at 255 MHz.

2. Performance of each circuit was analyzed with infinite inductor Q and with an inductor Q of 80.

3. With inductor Q = 80, circuits were optimized using COMPACT, with the same optimization function for each circuit:

- a) insertion loss < 0.3 dB, 20 to 100 MHz

- b) insertion loss > 70 dB at 255 MHz

4. Component value sensitivities were evaluated in the optimized design.

It is perhaps surprising to some readers how small are the differences among the different realizations, which in every case differ from each other by less than 0.5 dB in the passband. On the other hand, filters of fairly low order were chosen for illustration. With higher order filters, the differences would be greater. In some applications even the small differences would be significant; for example, in miniature transmitter filters where a fraction of a dB might mean several additional watts of power that the filter would have to dissipate.

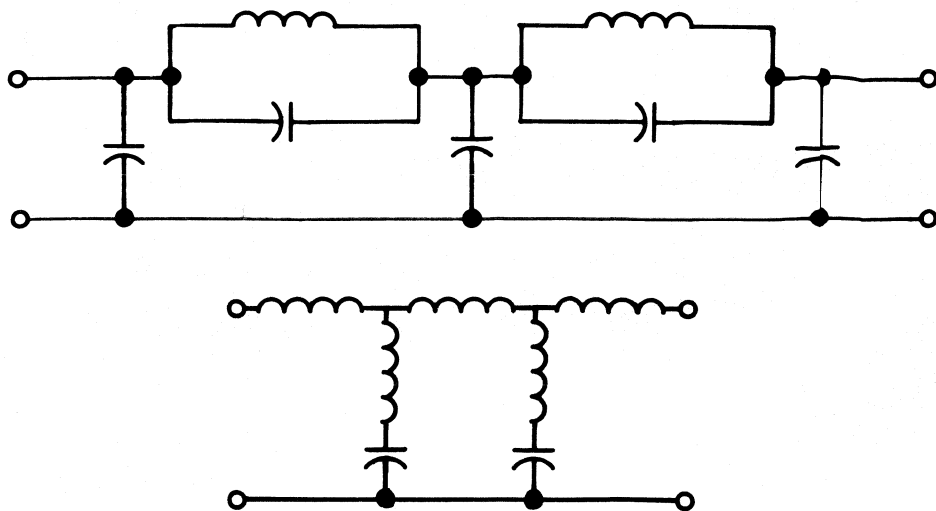
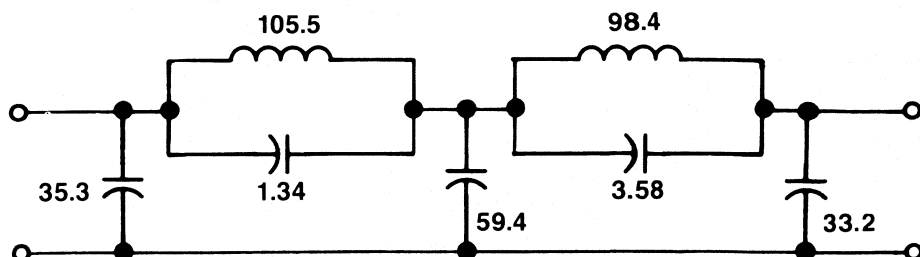
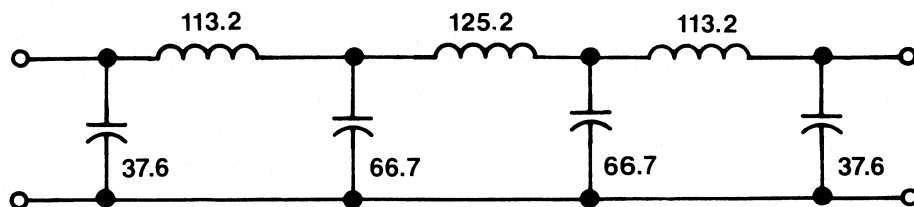


Figure 1. An elliptic low-pass and its dual, both realizing the same low-pass function



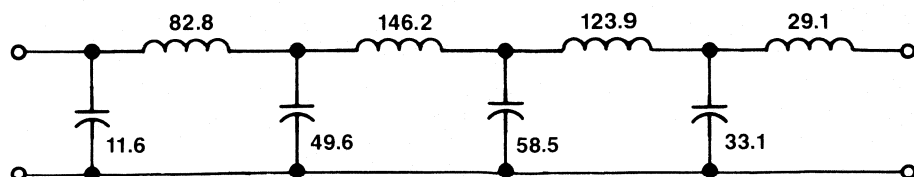
Elliptic

: 0.1 dB ripple, 100 MHz corner frequency, 70 dB at 255 MHz



Chebyshev

0.1 dB ripple, BW 3 dB = 106.8 MHz, 74 dB at 255 MHz



Butterworth

BW 3 dB = 106.8 MHz, 61 dB at 255 MHz

Figure 2. Theoretical designs (inductor Q = infinite):
(Capacitors in pF, inductors in nH, 50 ohms in/out)

Table 2. Sample computation of insertion and return loss

Insertion loss = S21 (dB) Return loss = 20 log (S11)		Freq. (MHz)	Ins. Loss (dB)	Ret. Loss (dB)
Stage	Component	50	.025	22.34
		55	.065	18.256
		60	.096	16.588
		65	.095	16.647
		70	.058	18.786
		75	.012	25.621
		80	4E-03	30.165
		85	.054	19.045
		90	.1	16.406
		95	.038	20.57
		100	.096	16.603
		101	.224	12.989
		102	.433	10.233
		103	.741	8.045
		104	1.165	6.286
		105	1.71	4.876
		106	2.373	3.758
		107	3.142	2.883
		108	3.998	2.207
		109	4.919	1.689
		110	5.886	1.295
		250	72.899	0
		255	74.211	0
		260	75.492	0

Freq (MHz)	Ins Loss (dB)	Ret Loss (dB)
5	.011	25.639
10	.041	20.183
15	.075	17.626
20	.097	16.546
25	.096	16.604
30	.071	17.862
35	.035	20.876
40	6E-03	28.15
45	1E-03	34.247

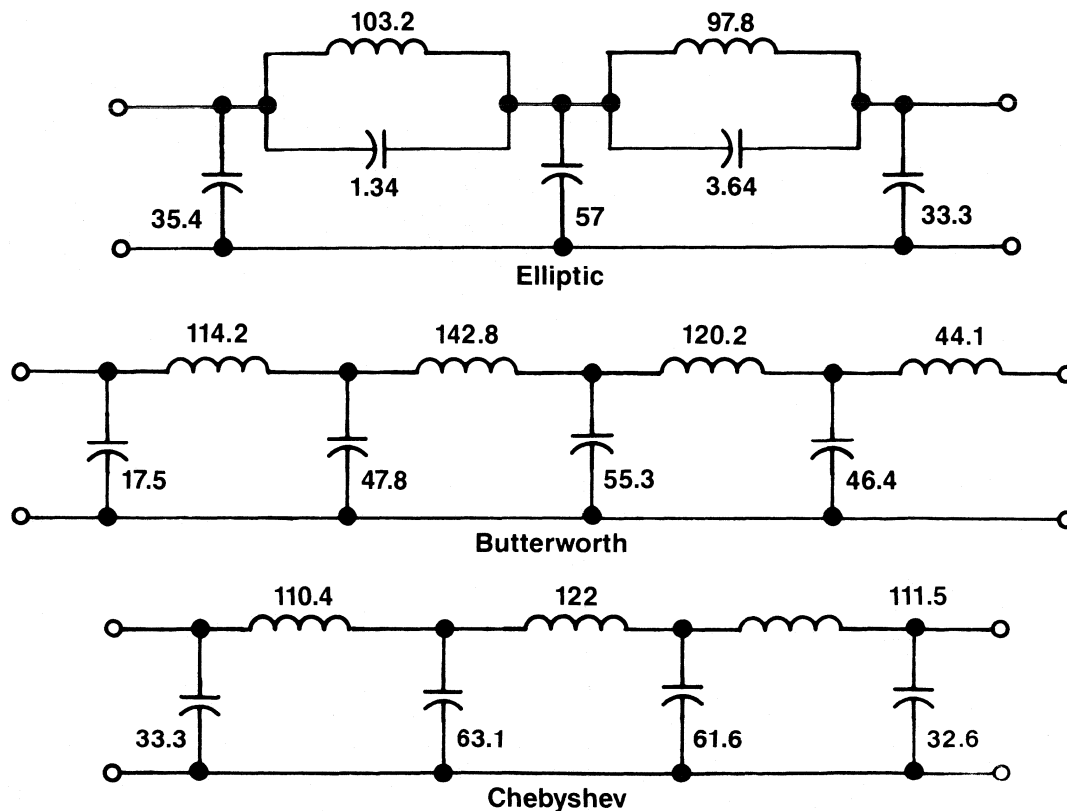


Figure 3. Schematics of the three optimized filters (Capacitors in pF, inductors in nH, 50 ohms in/out)

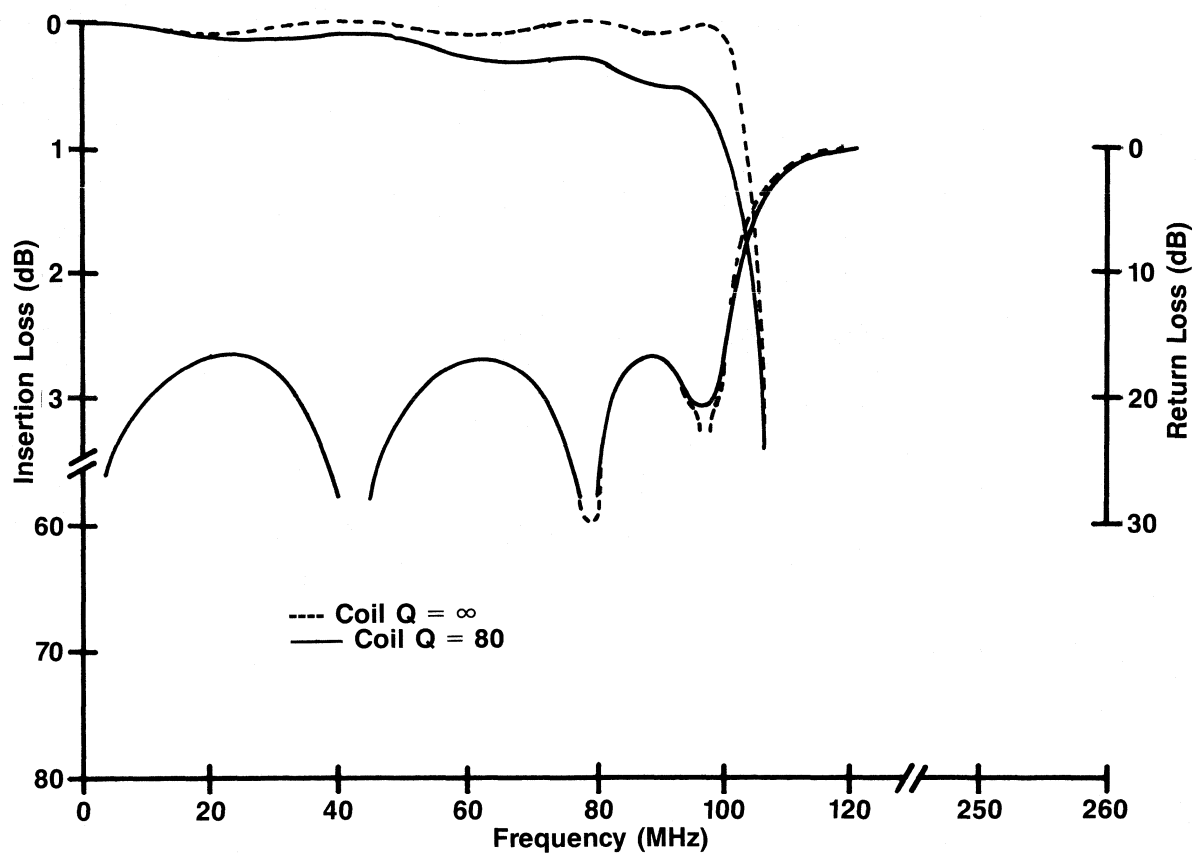
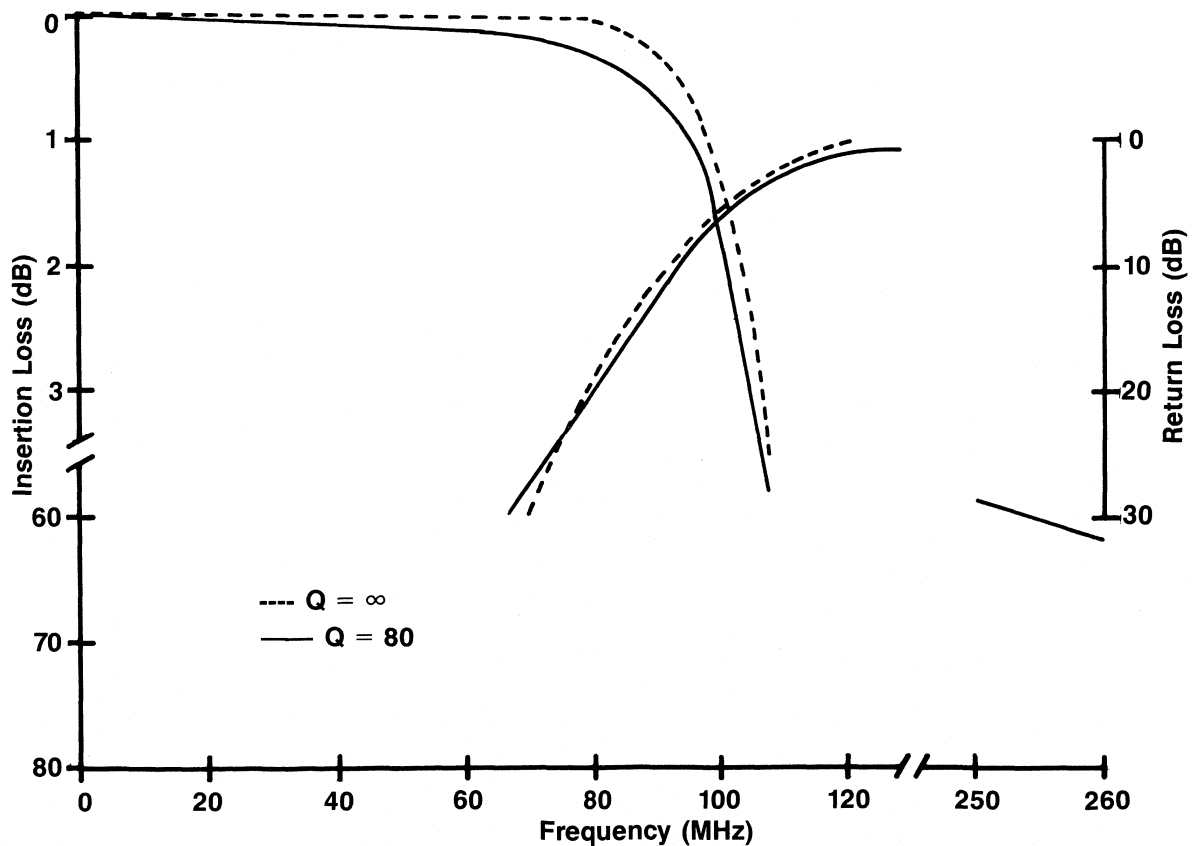


Figure 4. Comparison of filters realized using lossless and lossy inductors ($Q = 80$)

Chebyshev



Butterworth

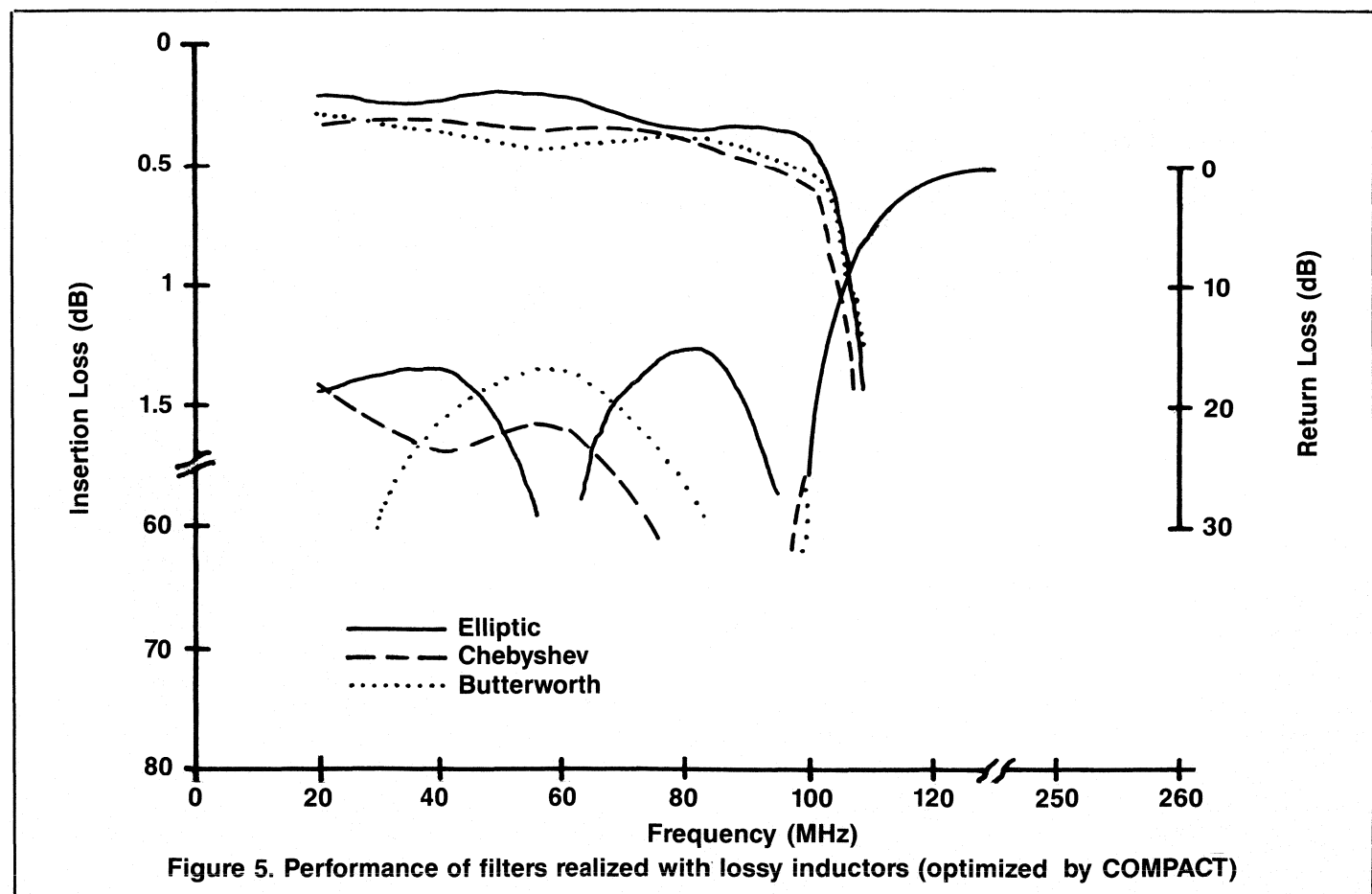
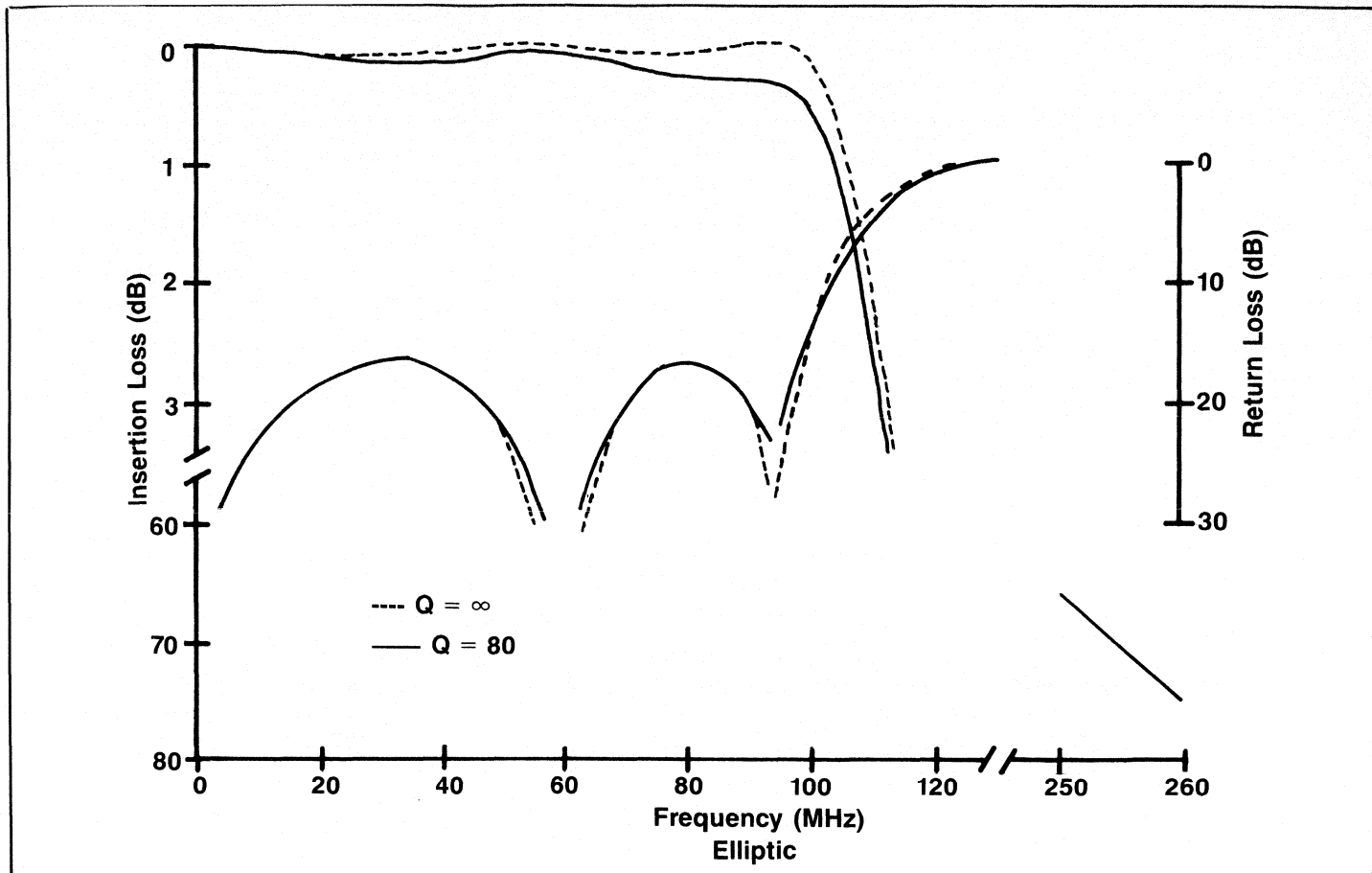


Figure 5. Performance of filters realized with lossy inductors (optimized by COMPACT)

Conclusions

1. For finite Q components (inductors) the Elliptic filter has the lowest insertion loss in the passband, whether optimized or not.

2. The Elliptic filter has the lowest sensitivity to component tolerances. Average sensitivities of the optimized filters per component are:

0.133 Elliptic
0.202 Chebyshev
0.268 Butterworth

3. The Elliptic filter required the least amount of optimization, Butterworth the most. In other words, the amount of improvement obtained by trying to change component values to compensate for inductor losses was minimal for the Elliptic filter. The Chebyshev filter lost its ripple after optimization, with some improvement in insertion loss and return loss.

4. Near the band-edge, the Chebyshev filter has the greatest insertion loss; so, in this case a filter with three lossy com-

ponents has worse insertion loss in part of its passband than one with four lossy components!

5. If the optimization function is changed slightly to minimize insertion loss from 60 to 100 MHz rather than 20 to 100 MHz (while at 255 MHz, the loss is still 70 dB), the Elliptical filter still has the lowest insertion loss, but now it is the Chebyshev filter that has the least sensitivity to component tolerances.

In summary, the Elliptic filter can be designed as if it were ideal (with lossless components) with a high degree of confidence that once it is built with lossy components it will perform close to its optimum. A low sensitivity to component value variation counts as an additional bonus, if the filter is to be used as a true low-pass.

About the Author

Peter Vizmuller is a staff engineer at Motorola Canada; 3125 Steeles Ave E.,

North York, Ontario, Canada M2H 2H6. Readers may contact him for information about a circuit analysis program he has written.


References

1. Zverev, A.I., Handbook of Filter Synthesis, John Wiley and Sons Inc., New York, 1967.

2. Humphreys, S.D., The Analysis, Design and Synthesis of Electrical Filters. Prentice-Hall, Inc., Englewood Cliffs, N.J. 1970.

3. Motorola RF Data Manual, Second edition 1980, p.17-160.

4. Close, C.M., The Analysis of Linear Circuits, Harcourt, Brace & World, Inc., New York, 1966.

5. COMPACT is a trademark of Compact Software Inc., 1131 San Antonio Rd., Palo Alto, California 94303. 

Another One-Transistor FM Transmitter

By S. Kan

*Institut d'Electronique Fondamentale
Universite Paris*

A variant of the one transistor FM transmitter published in the February issue of RF design (1) is as shown in Figure 1. It has been used to transmit an audio signal over a frequency modulated carrier at 106 MHz. Very good quality sound reproduction can be assured using an ordinary commercial portable FM radio receiver at a distance up to 50 meters.

The Clapp-Gouriet type oscillator (2, 3) using a junction FET (BF 256 L/B) was designed to operate at a gate-source voltage of about -1.5 V, thus biasing the two varicaps (BB 105 A) without extra components. Inductance L, a spiral antenna, was also printed on the same copper-clad PC board. Its value can be calculated fairly accurately by Dill's formula (4). Audio signal is fed via a potentiometer R_p in series with R_1 to modulate the RF carrier. The chosen transistor has a drain-source current of about 1 mA at the operating gate-source voltage. In spite of this low biasing voltage, the Q of the varicap is well over 200 measured with the HP 4191 A RF impedance analyzer.

(1) RF Design, "A one transistor FM transmitter," William Rynone, February 1985, p. 64.

(2) PIRE, "An inductance capacitance oscillator of unusual frequency stability," J.K. Clapp, Vol. 36, 1948, pp. 356-358.

(3) Wireless Eng., "High stability

oscillator," G.G. Gouriet, Vol. 27, 1950, pp. 105-112.

(4) Electronic Design, "Designing inductors for thin-film applications," H.G. Dill, February 17, 1964, pp. 52-59.

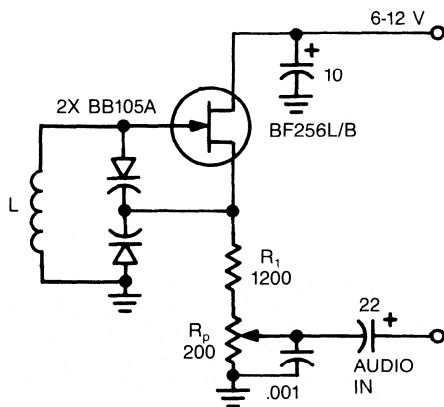


Figure 1. Schematic of the one-transistor FM transmitter with capacitance in μ F and resistance in ohms.

Medical RF Applications Require Special Shielding Techniques

By Gary A. Breed

In the past few years, hospitals and other medical facilities have been making ever-increasing investments in high-tech equipment to aid in the diagnosis and treatment of patients. From sensitive EEG equipment to powerful MRI (magnetic resonance imaging) units, the peaceful coexistence of the varied types of equipment requires electrical and magnetic shielding techniques unique to the medical environment. Lives depend on it!

Consider for a moment the radiated chaos that would occur if medical electronic shielding requirements were ignored. Can you imagine performing an EEG or EKG in the room next to an X-ray machine pulsing on and off? Could you rely on remote heart rate monitors on the floor directly above an MRI unit generating magnetic and RF fields at kilowatt levels? It does not take much imagination to recognize the problems that result from inadequate isolation between powerful generators of energy and sensitive detectors of physiological electrical currents.

The principal difficulty in shielding medical equipment is the extreme diversity of equipment types and the energy radiated and conducted during their use. For example:

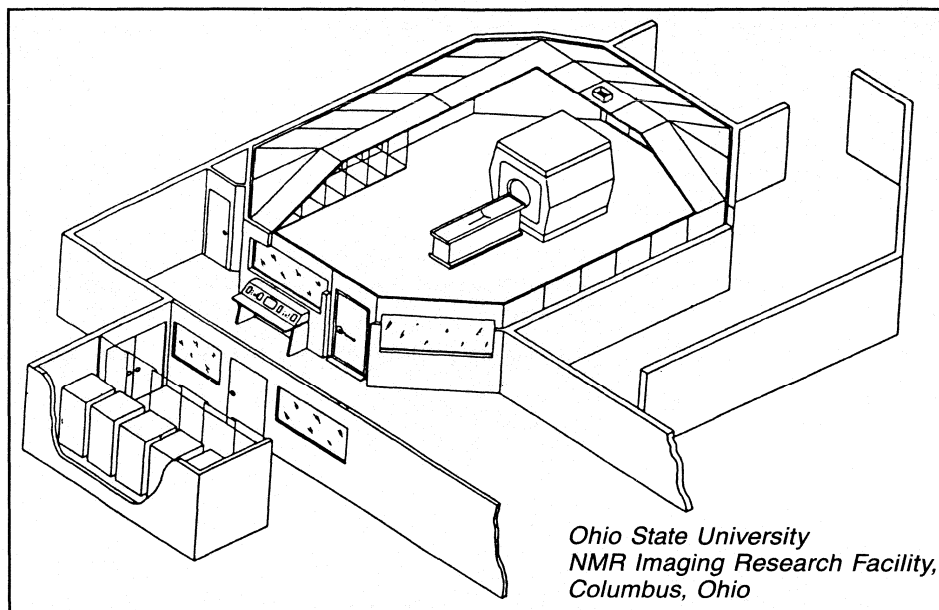
X-ray equipment is always shielded for radiation, but uses enough power to generate sizable transients that may propagate through AC power lines.

Hyperthermia equipment, the modern evolution of diathermy technology, uses RF in the MF through VHF range.

MRI systems represent a major challenge in shielding design, as they generate high magnetic fields as well as high RF fields (HF and VHF range). The sensitive detection circuitry requires protection from external fields, as well.

Lithotropy, a new technique for treatment of kidney stones, uses high power ultrasonic transducers.

Measuring equipment, as used for EKG, EEG, fetal monitors, heart monitors, nerve conduction testing, and laboratory analysis all needs to operate without interference from external sources. Most often, it is impractical to operate this equipment in a shielded environment, so



the efforts of the shielding engineer are concentrated on the design of enclosures for larger radiating equipment.

Lindgren RF Enclosures, Inc. is a major supplier of shielded enclosures for medical use, and technical information supplied by them outlines the four major shielding materials: bronze screening, copper screening, sheet copper and sheet steel. Bronze screening is very effective for RF between 1 MHz and 1 GHz. Copper screening has somewhat better microwave attenuation characteristics and better magnetic field performance than bronze. Sheet copper offers the best high microwave attenuation and outstanding durability, but like all non-ferrous metals it has limited magnetic field attenuation at lower frequencies (below 1 MHz). Sheet steel provides much better magnetic shielding than copper, and is effective for RF up to the 1 GHz range. Steel has the problem of more difficult fabrication than copper and a greater potential for degradation with time, due to oxidation at joints and seams.

In the medical realm, a hyperthermia treatment room requiring RF shielding at MF through VHF can use bronze or copper screening very effectively. However,

for an MRI system, a double electrically isolated shielding system provides the best attenuation of radiated energy, using copper screen for the inner enclosure, and sheet steel for the outer shield.

Lindgren's RF enclosures feature panelized construction, which is essential for medical shielding installations. An enclosure often must be built within an existing structure, requiring modular or knock-down construction. Special resilient fastening techniques developed by Lindgren make it possible to maintain effective shielding in a bolt-together system.

Finally, aesthetics are important in a medical environment. Hospitals are trying to make patients more comfortable by reducing their "antiseptic" appearance. Pleasant surroundings are very important to the use of new high-tech equipment, where a high level of patient cooperation is required for successful use. Shielding systems which can be made attractive are an asset to their users.

The work hasn't ended yet, as new concepts are being developed for future use. Every new device will have its own requirement for shielding, whether it is radiating energy, or protection from outside interference.

ESD Sensitivity Of A Diode Mixer

By David T. Geiser
General Electric Company

Assemblies of mixers may cost hundreds of dollars each, so the cause of occasional burn-out is important. ESD sensitivity is a frequent suspicion, particularly in light of the fact that Schottky Barrier semiconductor diodes are commonly used.

Experiencing burn-out of complex mixers using the double-balanced diode-ring configuration, the author decided to investigate the possibility of ESD damage. This article describes the test procedure and results.

The basic mixer is made up of two transformers and four diodes. Figure 1 shows how T1 and T2 are shunted (in the presence of only one signal) with two series-connected forward diodes for either polarity. The circuit also shows that DC and very low frequencies cannot reach the diodes via the radio frequency (RF) or local oscillator (LO) ports.

Direct current can reach the diodes via the intermediate frequency (IF) port (Fig. 2). The basic circuit (a) is approximated by its DC equivalent, (b). This implies that the diodes with lower forward conduction voltages will divert current from those having higher conduction voltages. Thus diode A might draw more than C, and B more than D.

However, transformers T1 and T2 cannot be ignored at high frequencies or for short pulses. The combined effect of the two transformers (Fig. 2c) shows that the result is the so-called "current-equalizer tap," raising the voltage (and therefore the current) of the diode that tended to draw the lower current.

Power applied to any port therefore tends first to be divided between two diodes, and then to have reverse voltages limited to the order of a single diode forward voltage drop. Failure mode in a diode-ring configuration is usually caused by power or excess forward-current. Other mixer configurations may experience different failure modes and be more susceptible to damage.

The test mixers were two basic Olektron model O-CDB-145, modified so the diode-

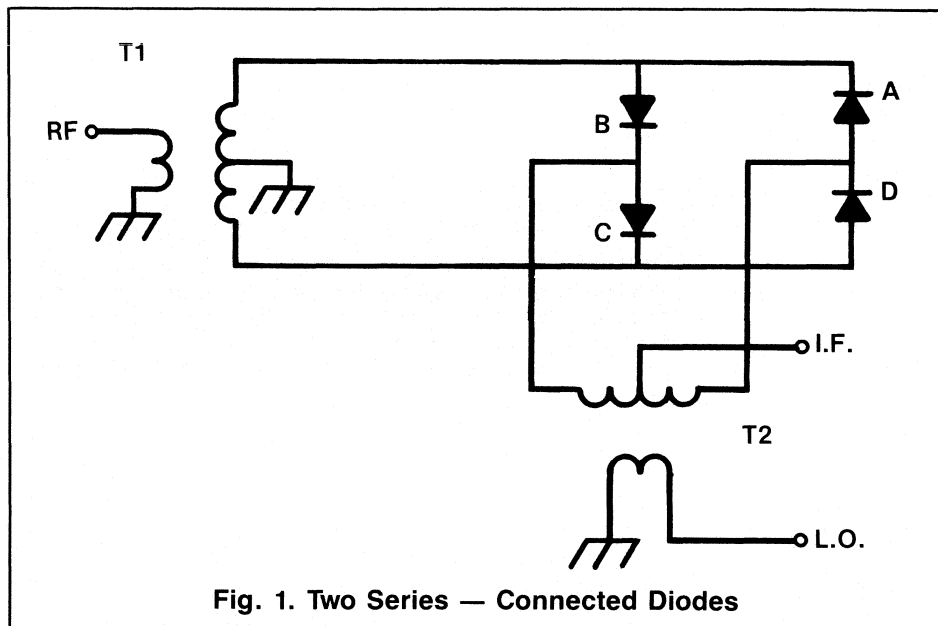


Fig. 1. Two Series — Connected Diodes

ring assembly (HP 5082-2831) could be replaced easily. Approximate ratings were:

- Diode ring: 75 mW/junction (4 junctions)
 - Mixer:
 - LO power (nominal) 5 mW
 - Input power (maximum) 300 mW
 - Conversion loss 6 dB
 - Isolation (actual) 65 dB
- Conversion loss and isolation were checked in the vicinity of 75 MHz. The diode characteristics as seen through the IF port were monitored with a Tektronix 576 Curve Tracer.

The Electrostatic Discharge Sensitivity Classification Test (MIL-STD-883 Method 3015) consists of charging of 100 pF capacitor to a stated voltage. The capacitor is then discharged by way of a 1500 ohm resistor through the terminals of the device under test, five times with forward and five times with reverse polarity. RF and diode curve characteristics are then measured, the test voltage raised, and the steps repeated (Fig. 3).

Voltage steps in this test were 20, 50,

100, 200, 500, 1000 and 2000 volts. The 2000 V discharge was repeated with a capacitance of 250 pF. Five mixer assemblies passed this last step, while one (B1) failed.

The five mixer assemblies that passed were then given a monitored 60 Hz over-stress on the Curve Tracer. They went into the thermal response precursor of failure at the levels of Table I. ("Thermal Precursor" is the tendency for the curve trace to loop rather than retrace, showing that the thermal change of diode electrical characteristics is beginning to lag the application of the 60 Hz sweep source. Experience shows that it first becomes apparent just before obvious damage at slightly higher stress levels.) Two-minute periods of lesser over-stress did not cause any apparent damage to the mixers.

It should be noted that the diode-ring assemblies in the mixers as supplied had been epoxy-attached to a fairly good thermal mass. Replacement diode-rings were attached with cyanoacrylate (Eastman 910) adhesive.

TABLE I. Damage to mixer assemblies.

Mixer	Damage at ESD Test Level	Destroyed at Swept Power
A0	None	1200 mW (pk), 2 min.
B0	None	1200 mW (pk), 2 min.
A1	None	800 mW (pk), 2 min.
B1	2000 V, 250 pF	—
A2	None	800 mW (pk), 2 min.
B2	None	800 mW (pk), 2 min.

Other tests

Passing current through the opposite corners of an individual diode-ring approximates currents caused by an input to either the RF or LO ports. A curve-tracer test of unmounted (no heat sink) diode-rings showed that the ring entered the thermal response precursor region at approximately 600 mW peak input.

Passing current through adjacent corners of an individual diode-ring also causes (no heat sink condition) the ring to enter the thermal response precursor region at approximately 600 mW peak.

Conclusions

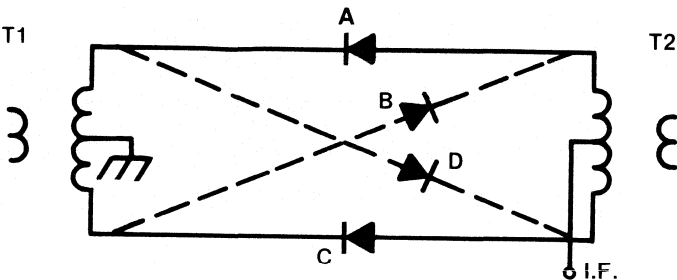
Electrostatic discharge sensitivity testing and intentional burn-out attempts support the conclusion that double-balanced diode-ring mixers of the types tested merit Category B classification of MIL-STD-883 Method 3015. According to these standards:

“Category B devices may be ESD sensitive to damage in a range above 2000 V, but normal good practice for the handling of semiconductors should suffice. Category B devices are preferred for general use in military equipment because they require no special ESD packaging or handling precautions other than normal good practice for semiconductor devices.”¹

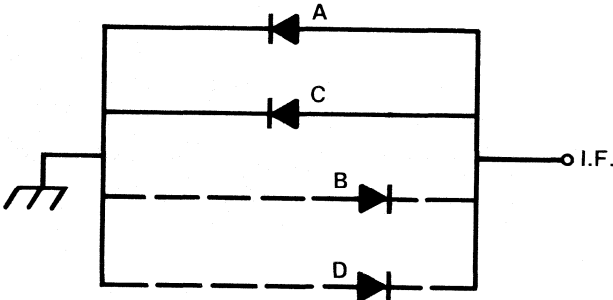
About the Author

David Geiser has overall responsibility for components at the Aerospace Electronic Systems Department of General Electric, French Road, Utica, NY 13503. A Registered Professional Engineer, Mr. Geiser has 30 years experience in the design, testing and application of mixers.

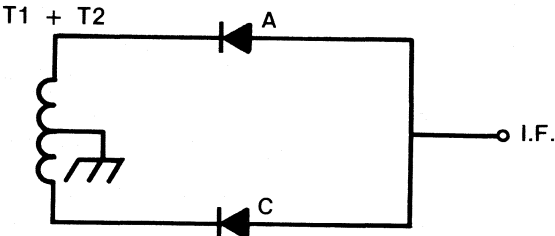
¹Method 3015.2 Figure 3015-3 Note 2, MIL-STD-883C.



(a) Basic Circuit



(b) Basic Circuit Approximated by its DC Equivalent



(c) Combined Effect of Two Transformers

Fig. 2. Direct Current to Diodes

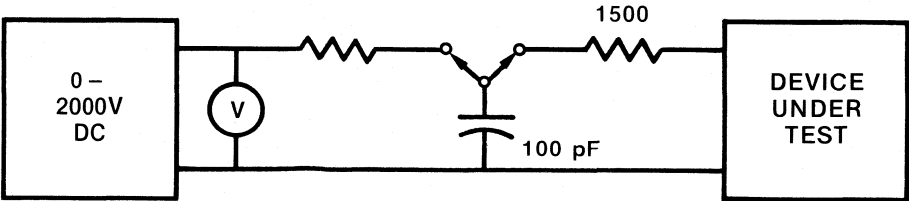
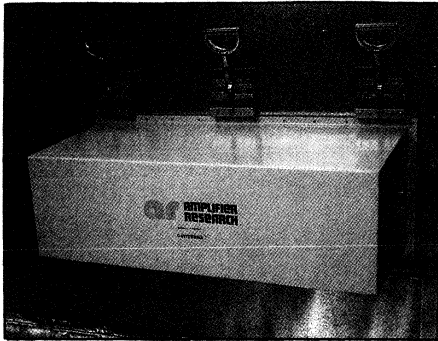
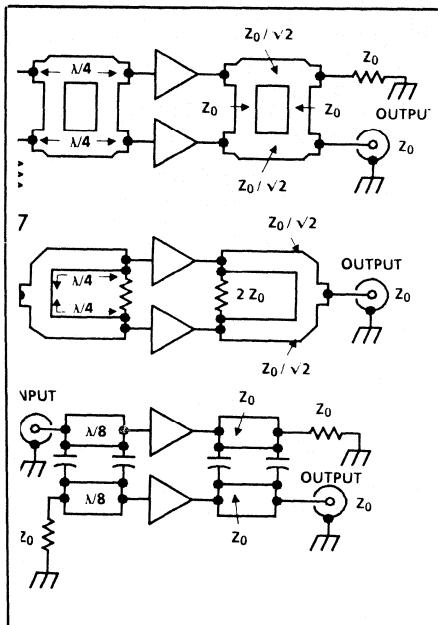


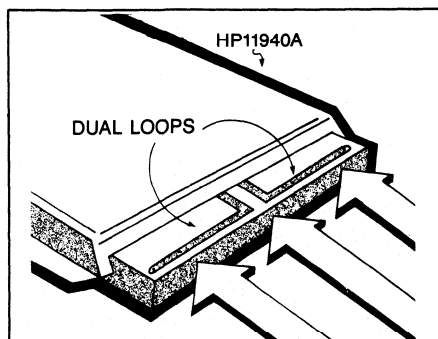
Fig. 3. Basic ESD Test Setup



The Cavitenna — p.29



Combining RF Power Hybrids — p.43



The Close Field Probe — p.50

Cover

This month's cover shows a test engineer at R&B Enterprises making final preparations for a high-power sweep frequency test of RFI susceptibility. On the lower right is a 2000 watt power amplifier manufactured by Amplifier Research, Souderton, Pennsylvania. The inset photograph shows a postage meter inside the test chamber and the Cavitenna radiator described in the Special Report.

Features

29 Special Report: The New Uses of RF EMI Susceptibility: Update on Test Methods

Government regulations and industry standards require testing of equipment for EMI susceptibility. This Special Report focuses on the techniques and equipment used in susceptibility testing and their relationship to the regulations and standards. — Gary A. Breed

43 Excess Insertion Loss at the Input Ports of a Combiner Hybrid

Combined amplifiers may exhibit losses greater than the sum of the insertion losses of each component. The author shows how imbalance in the combining circuits results in these excess losses. — Earnest A. Franke

50 The Close-Field Probe: A Powerful EMI Troubleshooting Tool

The Hewlett-Packard 11940A Close-Field Probe is analyzed, examining its construction and practical use in EMI troubleshooting of new designs.

— Mark Terrien

Departments

The Digital Connection — The Sciteq SCX-256: A 100 MHz Accumulator

33 With applications in direct-digital frequency synthesis, digital filters and fast Fourier transforms, this high-speed integrated circuit puts top performance in a small package. — Gary A. Breed

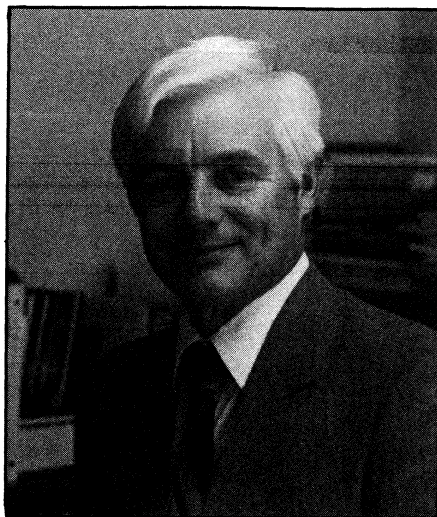
RFI/EMI Corner — ANSI Committee Studying Voluntary EMI Susceptibility Standards to Release First Report on TV/VCR Immunity

36 In response to laws establishing federal regulation of EMI susceptibility, the FCC requested that voluntary standards be developed by industry. The first of those standards is about to be released. — Gary A. Breed

6	Editorial	39	Info/Card
8	Viewpoint	54	New Products
13	Letters	67	New Literature
15	News	72	Classified Advertising
22	Calendar/Courses	74	Advertisers Index

R.F. DESIGN (ISSN: 0163-321X USPS: 453-490) is published monthly plus one extra issue in August, November 1985, Volume 8, No. 12. Copyright 1985 by Cardiff Publishing Company, a subsidiary of Argus Press Holdings, Inc., 6530 S. Yosemite Street, Englewood, CO 80111 (303) 694-1522. Contents may not be reproduced in any form without written permission. Second-Class Postage paid at Englewood, CO and at additional mailing offices. Subscription office: 1 East First Street, Duluth, MN 55802, (1-800-346-0085). Domestic subscriptions are sent free to qualified individuals responsible for the design and development of communications equipment. Other subscriptions are: \$22 per year in the United States; \$29 per year in Canada and Mexico; \$33 (surface mail) per year for foreign countries. Additional cost for first class mailing. Payment must be made in U.S. funds and accompany request. If available, single copies and back issues are \$5.50 each (in the U.S.). This publication is available on microfilm/fiche from University Microfilms International, 300 N. Zeeb Road, Ann Arbor, MI 48106 USA (313) 761-4700. POSTMASTER & SUBSCRIBERS: Please send address changes to: R.F. Design, P.O. Box 6317, Duluth, MN 55806.

The Glamour Job Of The Future



James N. MacDonald
Editor

Someone in the office wondered what the glamour job of the future would be.

For about the past decade it seems most young people have wanted to be computer programmers or systems analysts. Before that they wanted to be natural scientists and before that engineers. Of course, people respond to public attention directed at certain professions, but there is also a trend toward jobs that seem to be able to solve significant problems and contribute to the improvement of life in general.

The question assumes that computer programming is no longer a glamorous job, and this seems to be the case. It usually takes a few years for a career to lose its glamour. First, the field becomes crowded and jobs are no longer plentiful. Then come reports from new employees that the career is not what they thought it would be and advancement is slow. It is usually a simple case of supply and demand.

Recent glamour jobs have suffered in another way — the conditions that created them have changed suddenly. Engineering students were going to build a better America, then came the reaction against technology in the "back to the basics" movement. Natural scientists were going to save our forests and clean up the environment, but they came up against the reality of economics and a growing population. Computer specialists saw this amazing device as a way to reduce the

complexity of the modern world, but it has not gained the necessary wide acceptance. In fact, we may be seeing the beginnings of another anti-technology trend.

There is a pattern in these movements from one career field to another. It is like a pendulum swinging between technology and social service. After WWII a doctor was the thing to be, or a lawyer. In the mid-50s the engineering boom started. The environmental movement got underway in the mid-60s. Computer science took off in the mid-70s.

If the pattern continues, we are ready to start another social service trend. It is logical to expect the pattern to continue. Obviously, past emphasis on either technology or social service has not solved the world's problems, and as disillusionment with one emphasis has set in people have tended toward the other. Perhaps we could combine the two.

What we have needed since the beginning of the Industrial Age is a way to use the products of technology with an understanding of social needs. RF technology may be the way we will do it. Recently, as in so many similar cases, radio communications were the only contact between earthquake stricken Mexico City and the rest of the world. Ham operators passed messages diligently, for days, asking for no compensation and knowing they could not accept any if it were offered. Their actions demonstrated an outstanding combination of technology and social service.

We see many examples of such a combination. Last month we reported on medical uses of RF technology, uses with astounding possibilities for prolonging health. A news item in that issue noted that drivers with car telephones often reported road hazards, accidents and other serious incidents. Our readers probably know of a number of ways RF technology serves a social need.

RF is a mature technology with a long history of public service. As it expands beyond communications to other uses, RF probably will continue to be guided by that same motivation.

The glamour job of the future? You may be in it.

James N. MacDonald

Editor:

Mr. Aldrich's "note" in the August issue includes a very serious historical error.

The word "electronics" was coined by Dr. Orestes Caldwell who was the first editor of *Electronics*, published by McGraw-Hill. I believe publication of *Electronics* began in 1933 or 1934 — long before Emperor Franklin's War (WWII).

Dr. Caldwell later became a major publisher in the electronics field, being the Caldwell half of Caldwell-Clements through the forties and fifties.

Another point of interest: I have been a licensed radio amateur (presently under the call sign K6BH) since 1932 and never heard of a ham who used a crystal set as a portion of an amateur radio station. When I got into radio, in about 1930, the vacuum tube had completely replaced the galena crystal except as a curiosity.

Albert E. Hayes, Jr., Ph.D.
Consulting Radio Engineer

Editor:

I've been reading your editorials for quite a while and appreciate your fine efforts publicizing amateur radio. Being retired and out of the mainstream hasn't prevented me from helping, in some instances, to provide the next generation of RF engineers as indicated by the attached news release. I've also included the information about our 1984 winners.

The Foundation For Amateur Radio is pleased to announce the 1985 winners of the 19 scholarships which it administers.

John W. Gore Memorial Scholarship — \$900
James H. Baker, KI4YN — Alexandria, VA

Richard G. Chichester Memorial Scholarship — \$900
Eugene S. Reilly, KA8JIG — Cincinnati, OH

Edwin S. Van Deusen Memorial Scholarship — \$350
Richard K. Soper, KA2IKV — Syracuse, NY

QCWA Memorial Scholarships — \$600 each
Francis P. Horan, KA3CJR — Drexel Hill, PA
Hai T. Nguyen, KA0ALZ — Colorado Springs, CO
Carl E. Puckett, KA7BWC — Great Falls, MT
John E. Schnupp, N3CNL — Ephrata, PA
David J. Schmocker, KJ9I — Oconomowoc, WI
John G. Sullivan, N2DYC — Haddonfield, NJ

QCWA Robert S. Cresap
Memorial Scholarship — \$500
Douglas Swiatlowski, KA2KMT — Camillus, NY

Radio Club of America Scholarship — \$500
James W. Healy, NJ2L — West Hurley, NY

Edmund B. Redington Memorial Scholarship — \$500
David Swiatlowski, KA2KLM — Camillus, NY

Young Ladies' Radio League Scholarship — \$500
Diane E. Willemin, N8CAY — Elyria, OH

Amateur Radio News Service Scholarship — \$500
Michael Krensavage, KA3CUP — Marietta, GA

Columbia (MD) Amateur Radio
Association Scholarship — \$650
Christine L. Gray, KA3NAK — Elkton, MD

Baltimore (MD) Amateur Radio
Club Scholarship — \$500
Eric J. Smith, KA3KJO — Silver Spring, MD

Dade Radio Club Tropical
Hamboree Scholarships — \$500 each
Christopher A. Atkins, KA2QWC — Fort Pierce, FL
David R. German, N4FAD — Sarasota, FL

Lewis W. Wilkinson Memorial Scholarship — \$500
Wayne F. Poole, KC4XL, Surfside, FL

These scholarships were open to all Radio Amateurs meeting the qualifications and residence requirements of the various sponsors. The foundation is a non-profit organization representing fifty clubs in Maryland, the District of Columbia and Northern Virginia. It is devoted exclusively to the scientific, literary and educational pursuits that advance the purposes of the Amateur Radio Service.

Announcements of the 1986 awards will appear in the April or May issues of the major amateur radio publications. Additional information regarding the foundation's scholarship program can be obtained from FAR Scholarships, 6903 Rhode Island Avenue, College Park, MD 20740.

Hugh Turnbull W3ABC
Director Atlantic Division, ARRL

Editor:

Your September issue gave me a chuckle when I read every page and arrived at page 42.

On page 14 in the continuation of your "RF News" brief, you announced the surprising demise of Compact Software of Palo Alto, Calif. But, on pages 42 and 43 we are presented with a beautifully stylized advertisement from — guess who?

A telephone call to their advertised number — (415) 966-8440 — brings the interrupt operator!

I hope they gave you a current billing address!!

Another subject: When will the Expo have their speaker lineup ready and have the program ready for mailing? This time I hope to be there!

Ed Oxner
Staff Engineer
Siliconix, Inc.

Compact Software is with us again. See the News section. The Expo '86 program has been mailed and you have probably received it by now. We hope to see you there, Ed. — editor.

The Sciteq SCX-256: A 100 MHz Accumulator

By Gary A. Breed

The Digital Connection features products and techniques with direct application to the design of RF circuitry. This month, a new high-speed digital accumulator from Sciteq Electronics, Inc. is introduced. This device represents a major development in high-speed logic, with clock rates much faster than any previous single-chip device.

Sciteq designs and manufactures frequency synthesizers, specializing in direct-digital techniques. For one MIL-STAR application they developed an ultra-fast switching synthesizer using 100K ECL which met all electrical requirements but was too large. To reduce space, a custom gate array was designed for the accumulator portion of the circuit, replacing 12 ICs in the original design. The result of that design is the SCX-256.

The accumulator design required a guaranteed clock rate of at least 70 MHz, requiring meticulous attention to every path and junction. Together with Hamilton Avnet's ASIC design center and the fabrication expertise of Motorola, the process of design and prototyping took over three months of intensive work. The result is an accumulator with a typical clock rate over 100 MHz.

An accumulator is a series of adders and latches which add the input number to the previous output sum on every clock cycle, *accumulating* a larger and larger output sum. Fig. 1 shows an 8-bit accumulator with input latches to demonstrate the process. The input word (increment

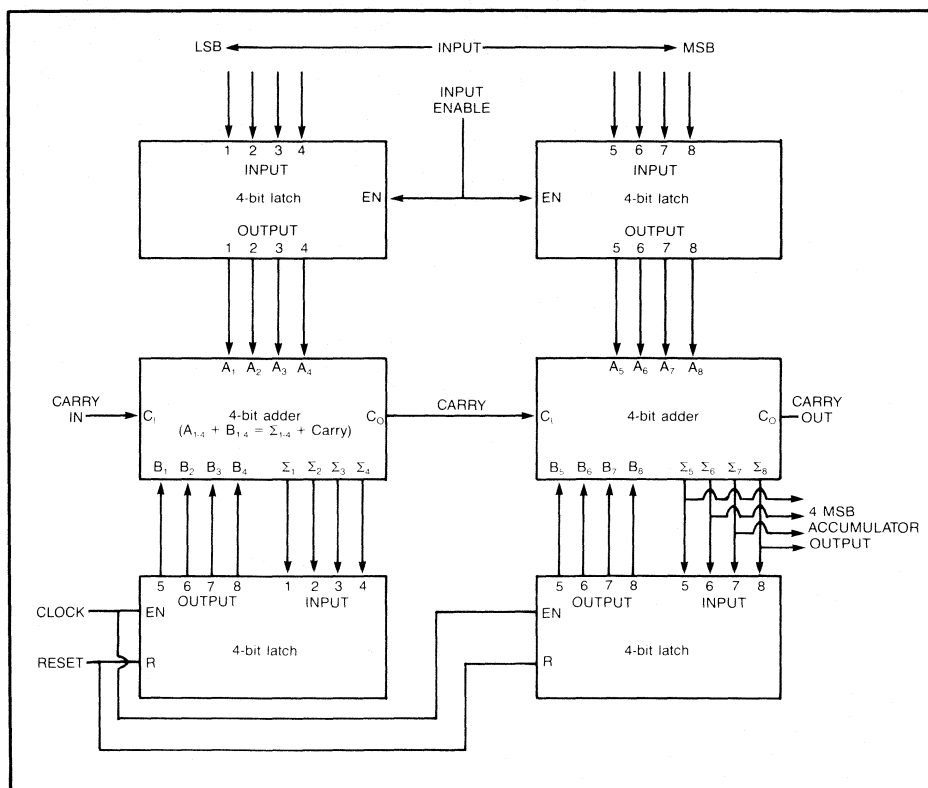


Figure 1. An 8-bit accumulator using 4-bit latches and adders, with registered inputs and 4 MSB output.

size) is entered via latches and transferred to the adders with an INPUT ENABLE command. Until a new input word is enabled, the adders will increment the sum in steps the size of the input number. This example has a four-MSB (most significant

bits) output to mimic the SCX-256's 12 MSB output from a 24-bit input.

Figure 1, above, demonstrates the accumulator process. The input word has been left fixed and the carry functions are not used:

Start count = 0
 Input word = 00101001 (number 41)

Clock Cycle	8-bit Sum	4 MSB Output
1	00101001 (41)	0010 (2)
2	01010010 (82)	0101 (5)
3	01111011 (123)	0111 (7)
4	10100100 (164)	1010 (10)
5	11001101 (205)	1100 (12)
6	11110110 (246)	1111 (15)
7	00011111 (31)	0001 (1)

Note: The sum is really 100011111 (287), but with no carry the 9th bit is dropped: The sum is always the eight LSB (least significant bits).

8	01001000 (72)	0100 (4)
---	---------------	----------

If the four MSB output is used to address a read-only memory (ROM), a sequence of stored values can be recovered at a rate determined by the input word.

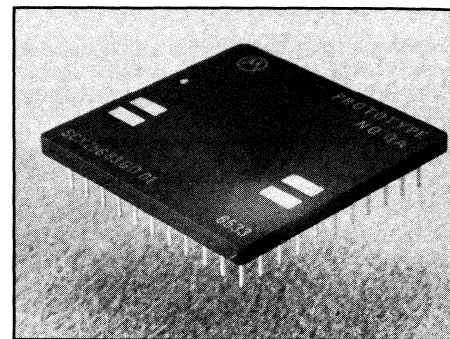
Direct digital frequency synthesis uses the sequential recovery of data in ROM. An accumulator such as the SCX-256 generates outputs which address a ROM containing the values of a sine wave in binary form. These ROM values form the input to a digital-to-analog converter

(DAC) whose output is a step-by-step approximation of a sine wave at a frequency determined by the input word to the accumulator. The accuracy of the output depends on the resolution (number of bits) of the ROM and DAC. For example, a 512×8 bit ROM and an 8-bit DAC with $\pm 1/2$ LSB accuracy will reproduce a sine wave with 0.4% accuracy.

SCX-256 Description

The SCX-256 is a 24-bit ECL level accumulator. The design includes 24 registered inputs with independent loading of the 12 MSB and 12 LSB. Outputs are fully registered 12 MSB of the accumulated sum. Internal adding takes place on the clock rising edge; reset is asynchronous. Transparent latches allow inputs to be loaded either synchronously or asynchronously. Carry input and output functions are available for cascading two or more devices. The SCX-256 requires 750 mA at standard ECL supply voltage. The clock rate is guaranteed to be 70 MHz, with 100+ MHz typical.

Although developed specifically for direct digital synthesizers, the SCX-256 can be used for other fast arithmetic and digi-



The Sciteq SCX-256 accumulator.

tal signal processing applications, like digital filters and fast Fourier transform. Although similar functions can be achieved using discrete ECL devices, the SCX-256 will eliminate the critical board layout required for large ECL designs, improving speed and reducing glitches. With the introduction of the SCX-256, Sciteq has given design engineers a lot of performance in a small package... and a lot of potential applications. 11

ANSI Committee Studying Voluntary EMI Susceptibility Standards.

Will Soon Release First Report on TV/VCR Immunity

By Gary A. Breed

The 1982 Amendment to the Communications Act of 1934 gave the FCC authority to regulate EMI susceptibility of electronic equipment. Continuing a policy of deregulation, however, the FCC insisted that the parties involved develop voluntary standards. In response to the Congressional mandate for regulation and the FCC's wishes, an ad hoc committee was formed under the aegis of ANSI committee C63. The members of the committee represent manufacturers, testing laboratories, the Electronic Industries Association (EIA) and the American Radio Relay League (ARRL). The first report from this committee on television and VCR immunity is in final draft stage, and should be ready for review by the full C63 committee at their mid-November meeting in Washington. Don Heirman of AT&T Information Systems, chairman of the group, indicated the report should be released by the end of this year.

The committee has been studying TV and VCR susceptibility to interference received by direct radiation or accompanying the desired signal through the antenna lead. Their report will address EIA Interim Standards IS-10, "Immunity of TV Tuners to Internally Generated Harmonic Interference From Signals in the Band, 535 kHz to 30 MHz," and IS-16, "Immunity of Television Receivers and Video Cassette Recorders to Direct Radiation from Radio Transmission, 0.5 - 30 MHz." These two documents represent earlier proposed standards in this area and the committee report is said to contain no major deviation from them. Results of an EIA-commissioned study by the National Bureau of Standards on conducted interference via outside leads may be included in the report. The NBS study has been

completed and results should be available for the November C63 meeting.

A spokesman for the FCC expressed satisfaction with the voluntary regulation efforts, noting that the process saves the FCC time and money and should result in standards acceptable to everyone because compromises are being worked out during the process. According to all parties involved, cooperation has been very good despite the diverse interests of the groups represented. One example of compromise is the selection of a statistical "average case" analysis rather than either a lenient model or a worst-case situation.

Some committee members noted the difficulty presented by VCRs, where HF signal processing circuitry is sensitive to radiated interference. TV IF circuits were also mentioned as an area requiring additional engineering to achieve EMI protection. Everyone contacted emphasized the need for continued work, not only on TVs, VCRs and home electronics but in commercial areas. Hugh Turnbull, ARRL Atlantic Division Director, pointed out that cordless telephones, security devices, and other low-power RF devices need attention. Part 15 of the FCC Rules and Regulations covers radiation by these devices, but their immunity to interference has not been addressed. Other users of the RF spectrum, whether they are "closed circuit" or have internal circuits operating at radio frequencies, have potential EMI problems and will require study. Another area the committee must address is Channel 6 interference from Educational FM broadcasters. The FCC recently released revised allocation standards for FM channels in the vicinity of Channel 6 facilities, but has left TV receiver standards to the ad hoc committee.

Eb Tingley of the EIA Consumer Electronics Group emphasized the need for international cooperation to implement new standards. Offshore companies may perform all engineering and manufacturing outside the U.S. and must be aware of new developments. U.S. representatives have been involved in EMI standards discussions in Australia and Europe, sharing the results of work done here and encouraging international development of standards and test procedures.

In its proper role of evaluating only engineering issues, this committee has not addressed the *cost* of achieving EMI immunity. The increase in the price of a TV due to additional shielding is unknown. Line filters, extra bypassing and mechanical redesign will certainly add to the cost of production and consumers must understand the protection offered by these changes. Fortunately, consumer awareness of the nature of interference seems to be improving. Frivolous complaints to the FCC have decreased, and overall interference complaints have not grown at the same rate as the increase in sales of consumer equipment.

It is easy to overstate the significance of this first effort at major voluntary regulation of EMI. It is only a first step, not a set of final standards. Television sets and VCRs may be the largest group of consumer electronics, but with many other devices yet to be examined, work on EMI immunity standards will continue for a long time. Success of this voluntary regulation effort requires industry commitment, international cooperation and consumer awareness. The alternative is a return to the difficult process of FCC regulation, an idea unattractive to everyone involved. [E]

Excess Insertion Loss at the Input Ports of a Combiner Hybrid

By Earnest A. Franke
E-Systems, ECI Division

Combining circuits for multiple power amplifiers require inputs with proper phase and amplitude relationships. The repair or replacement of circuit components may alter the gain or phase shift characteristics of one portion of the system, causing a change from the original design parameters. This article presents a discussion of the excess losses that are a result of deviation from ideal phase and amplitude of the signals to be combined.

An RF designer measures all the components for a power amplifier consisting of a power splitter, two or more amplifier modules and a power combiner, only to find that the overall gain is less than the sum of the gains and losses of the components. Or, a technician replaces a defective transistor in a paired amplifier and discovers that the total gain is not what he expected, even after assuring himself that separately both halves worked perfectly. Each person expects the total power from a hybrid combiner to be the sum of the inputs after considering any mismatch losses. With an examination of effects of amplitude and phase imbalance, one discovers why the difference power ended up in the isolation resistor connected to the hybrid combiner.

Power Combining and Imbalance

Power combining may be considered on one of two general levels: the device level and the circuit level. Device level combining is accomplished by clustering several devices in a region whose extent is small compared with the operating wavelength. Transistor vendors have continually increased the available output power from a single package until the device is package limited. Combining several transistor dice within the same package eventually runs into problems of impedance matching, concentrated heat dissipation and reactance interaction (power hogging). By directly paralleling two transistors, the resistive part of the input and the output load impedance decreases, yield-

ing a higher Q, lower bandwidth part. The advantage of using a hybrid power combiner centers around the isolation achieved when combining the outputs of the two devices. With power shared by many elements, the summing technique provides more reliability than a single solid state element operating at high power. The stability of combined power transistors is enhanced by this isolation, as the reactive components of one transistor do not affect the other transistor, which is effectively in parallel.

In radio frequency amplifiers formed by effectively placing two transistors in parallel by using hybrid power combiners, there will always be some phase and amplitude imbalance at the input ports when using the typical combiner techniques shown in Fig. 1. Typically, transistors are selectively paired at the factory to limit gain difference at some median operating point and frequency to less than 1 dB. There is also some imbalance due to the

type and tolerance of the splitter hybrid. The phase imbalance of the output power of two transistors is a result of component tolerances in the matching networks, process control for manufacturing the semiconductor itself and the fact that several vendors may be second-sourcing the transistor itself. Typically the phase distribution for a part which must be acceptance tested in a wideband circuit is less than $\pm 15^\circ$. The use of automated wire bonding and wafer processing has lowered this deviation significantly.

3 dB Hybrid Coupler Performance

Electrical parameters of the hybrid splitter/combiner of concern to the amplifier designer are insertion loss, amplitude balance and phase balance. The insertion or excess loss is the amount of attenuation, in excess of signal coupling losses, of an input signal from a matched source to a matched output termination. The coupling loss for an equal-split hybrid is 3.01 dB.

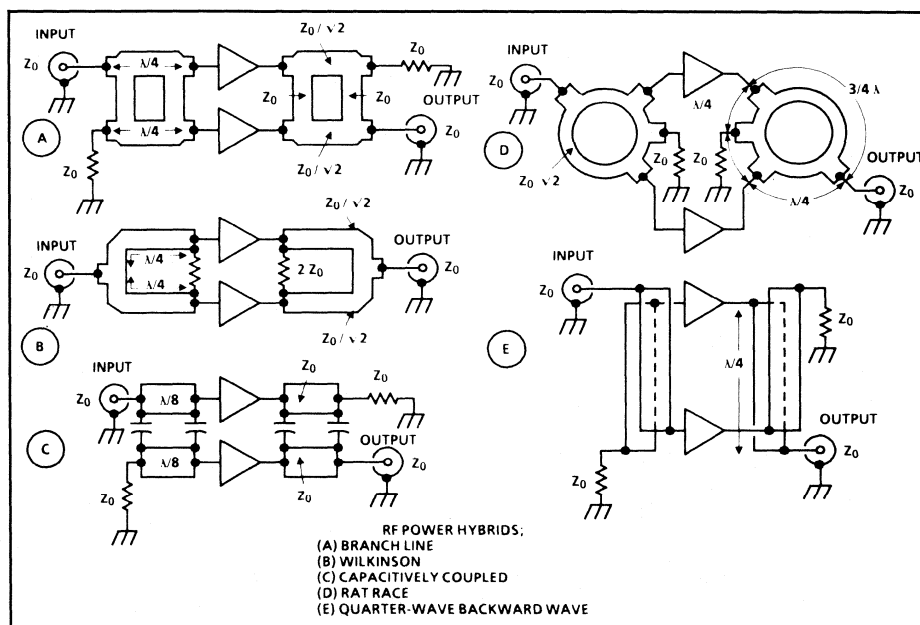


Figure 1. Power Combining using RF Power Hybrids

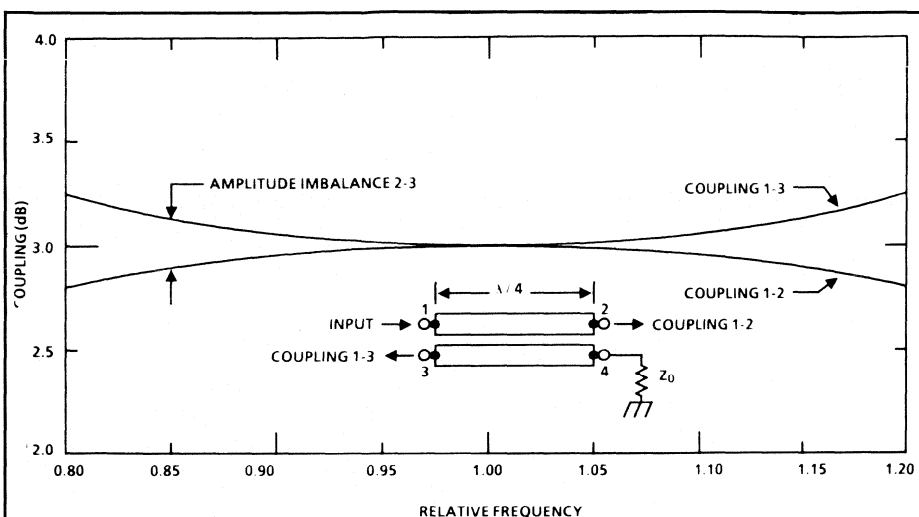


Figure 2. Coupling for a Backward Wave Coupled Hybrid

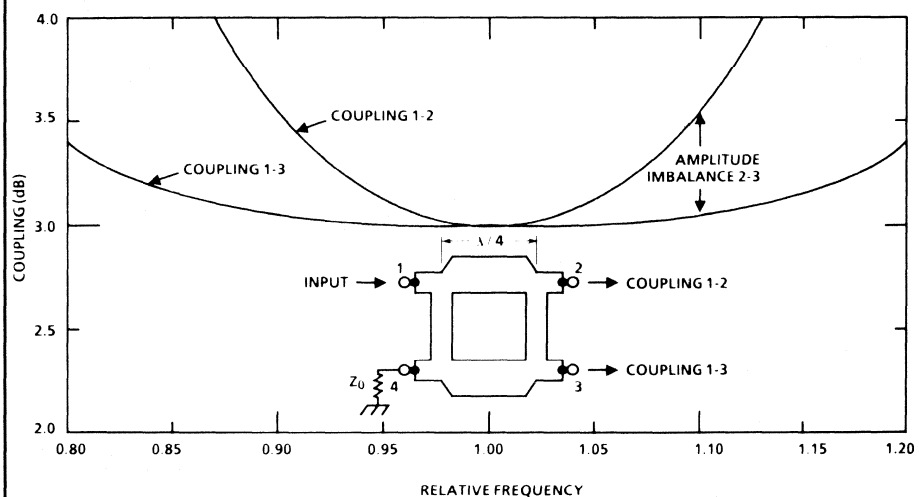


Figure 3A. Coupling of a Single-Section Branch Line Hybrid

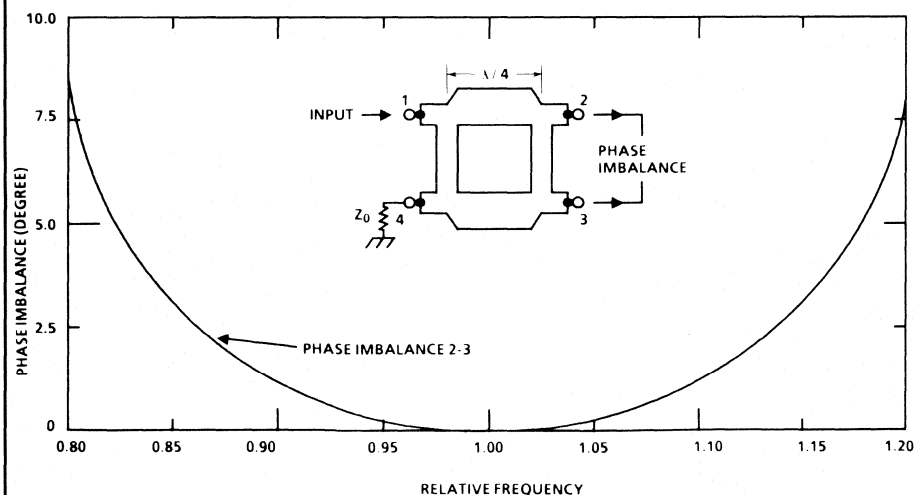


Figure 3B. Phase Imbalance for a Branch Line Hybrid

One-half the input power appears at each output port of a 3 dB hybrid splitter. The amplitude balance is the difference in attenuation between the two output signals when fed from a common input, generally expressed as a maximum variation over the specified operating range. The difference in phase between two output signals fed from a common input is known as phase balance or phase tracking.

Some performance tradeoffs may be made between these parameters. The principal tradeoff naturally deals with simplicity and frequency range. The ability to reproduce a coupler inexpensively in microstripline form on common printed circuit board can be very important. For single frequency applications requiring bandwidths less than 10%, the insertion loss of a manufactured hybrid can be held quite low, with the amplitude balance degrading rapidly away from the center frequency. Octave bandwidth designs typically display slightly more insertion loss but the amplitude balance is held tighter. Amplitude balance may also be improved, at the sacrifice of increased overall loss, by increasing the number of sections contained within each hybrid.

A single-section, quarter-wave, quadrature hybrid for example displays a theoretical amplitude imbalance of 0.44 dB at the upper and lower operating frequencies (Fig. 2) over a 40% bandwidth. The phase balance however, is quite good. Theoretically the outputs remain in quadrature (90° difference) over the above bandwidth. Experimentally the phase imbalance can be held to less than $\pm 1^\circ$. The amplitude and phase balance of other 3 dB hybrids is not as good. The popular branch line hybrid (Fig. 3A and 3B) displays an amplitude imbalance of 1.84 dB at the band edges and 8.3° phase imbalance at the same $\pm 20\%$ bandwidth points. The capacitively coupled hybrid formed by two eight-wave transmission lines (Fig. 4A and 4B) has an amplitude imbalance of over 6 dB at the upper operating frequency and nearly 5 dB at the lower operating frequency. The phase imbalance is also quite high, 8.4° at the bottom and 22.3° at the top of the same relative bandwidth.

The rat race hybrid resembles the branch line hybrid with an additional half-wave transmission line added (Fig. 5A). The rat-race is a reciprocal four-port device that can provide two in-phase signals when fed from its sum port and two 180° out-of-phase signals when fed from its difference port. The push-pull output ports differ by a nominal 180° and exhibit an amplitude imbalance of 1.8 dB and a phase imbalance of 13° (Fig. 5B)

over the 40% bandwidth. The equal-phase outputs for an input at port 4 show an amplitude imbalance of 1.7 dB and a phase imbalance of 11°.

An equal-phase hybrid, such as the Wilkinson coupler (Fig. 6) displays excellent amplitude and phase balance over a moderate bandwidth because of its symmetry. Any imbalance is due to construction or termination imperfections.

Excess Insertion Loss

The primary concern of excess combiner insertion loss for amplitude and phase imbalance appears in an amplifier when only one of the two paired power transistors is replaced. The replacement transistor probably will not come from the same wafer lot as the original transistor, nor even possibly from the same vendor. The evidence of amplitude and phase imbalance may be first noted by increased power dissipation in the isolation resistor of the output hybrid combiner. The output power and gain will also be reduced slightly.

The insertion loss due to phase and amplitude imbalance is:

$$\text{Excess Insertion Loss} = 10 \log_{10} \left[0.5 + \frac{\sqrt{P_r} \cos \theta}{1 + P_r} \right] \text{ dB} \quad (1)$$

or

$$\text{Excess Insertion Loss} = 10 \log_{10} \left[0.5 + \frac{10^{\frac{P_{dB}}{20}} \cos \theta}{1 + 10^{\frac{P_{dB}}{10}}} \right] \text{ dB} \quad (2)$$

where

P_r = relative ratio of the input powers

P_{dB} = input power ratio in decibels

θ = relative phase angle between the input signals.

This excess insertion loss also may be broken into two terms to study independently the effects of amplitude and phase imbalance. If the input powers are exactly equal but the phase angles differ, then the equation for the excess insertion loss for phase imbalance reduces to:

$$\text{Excess Insertion Loss} = 10 \log_{10} \left[0.5 + \frac{\cos \theta}{2} \right] \text{ dB} \quad (3)$$

as shown in Fig. 7. If the two input powers to a hybrid have equal phase angles but unequal amplitudes, then the equation for excess insertion loss due to amplitude imbalance reduces to:

$$\text{Excess Insertion Loss} = 10 \log_{10} \left[0.5 + \left(\frac{\sqrt{P_r}}{1 + P_r} \right) \right] \text{ dB} \quad (4)$$

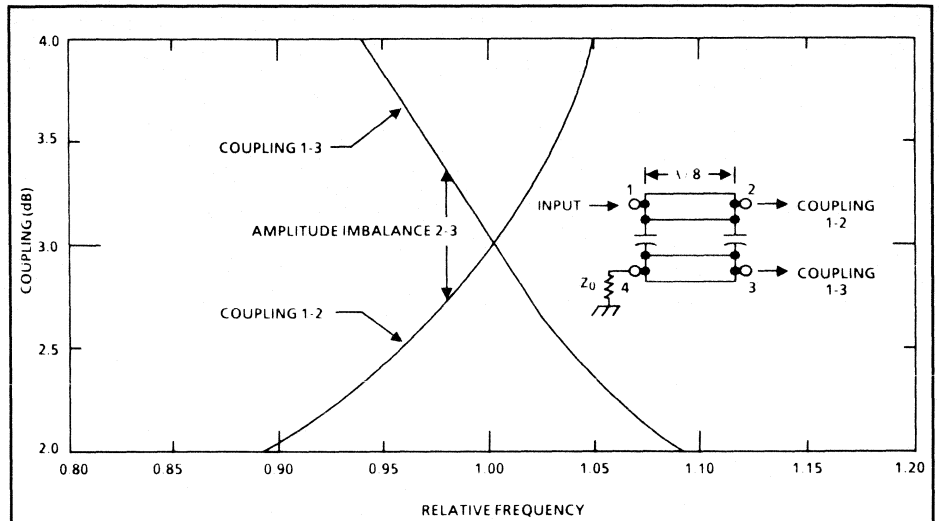


Figure 4A. Coupling for a Capacitively-Coupled Hybrid

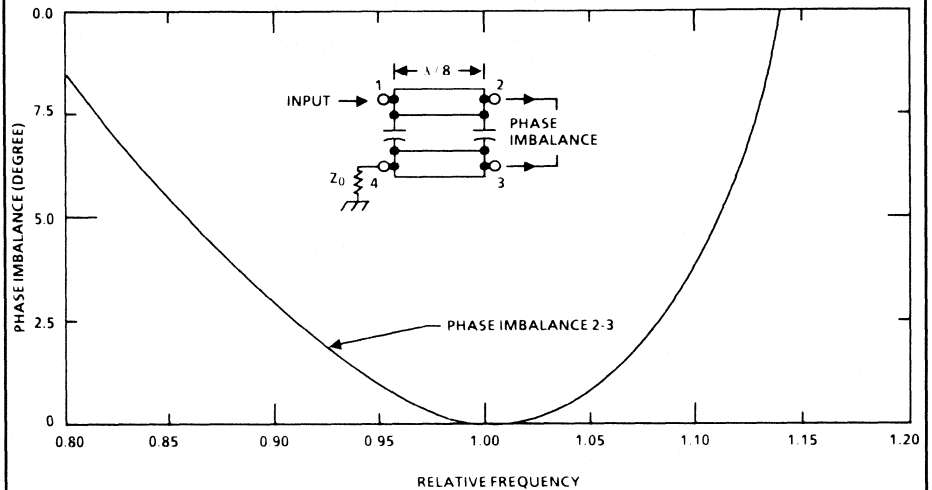


Figure 4B. Phase Imbalance for a Capacitively-Coupled Hybrid

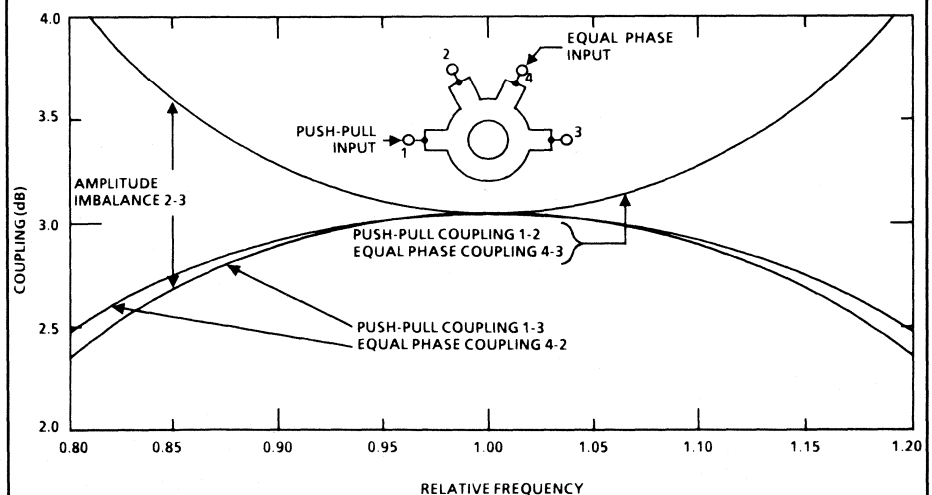


Figure 5A. Coupling for a Rat Race Hybrid

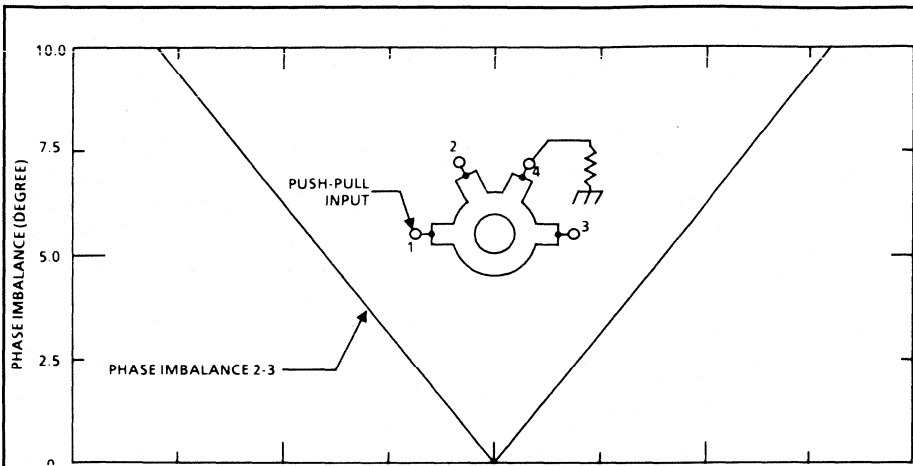


Figure 5B. Phase Imbalance for a Push-Pull Rat Race Hybrid

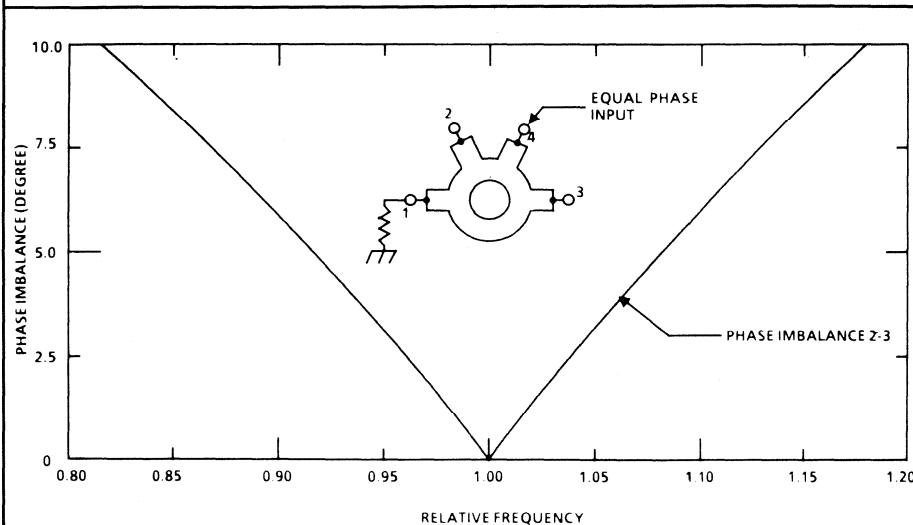


Figure 5C. Phase Imbalance for an Equal-Phase Rat Race Hybrid

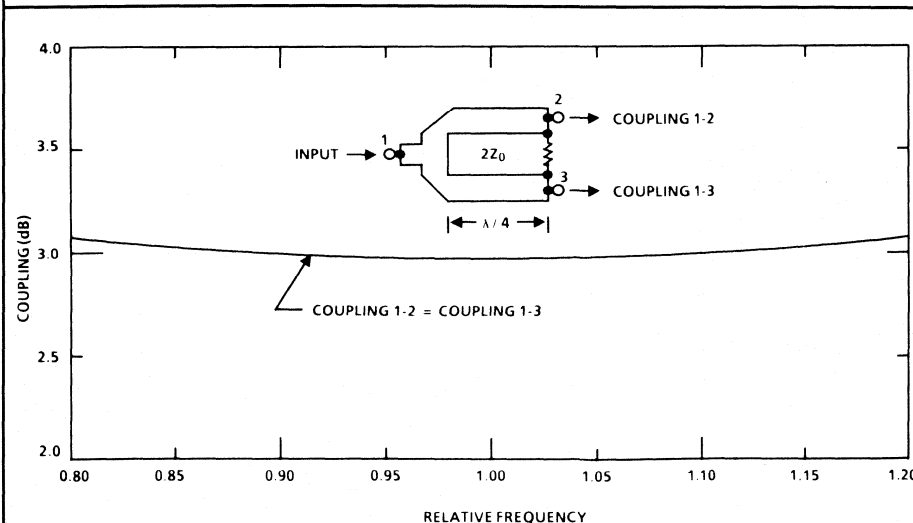


Figure 6. Coupling of a Wilkinson Hybrid

Excess Insertion Loss =

$$10 \log_{10} \left[0.5 + \frac{\sqrt{10 \frac{\text{PdB}}{20}}}{1 + 10 \frac{\text{PdB}}{10}} \right] \text{ dB}$$

as shown in Fig. 8.

Derivation of Excess Combining Loss

The output power for a single input to a 3 dB hybrid combiner is:

$$P_{\text{out}} = P_{\text{in}}/2 \text{ and an output voltage } V_{\text{out}} = V_{\text{in}}/\sqrt{2}$$

The resultant voltage vector V_{out} for input voltage vectors V_A and V_B according to the Argand phasor diagram of Fig. 9A by the law of cosines is:

$$(V_{\text{OUT}})^2 = \left(\frac{V_A}{2}\right)^2 + \left(\frac{V_B}{2}\right)^2 - 2\left(\frac{V_A}{2}\right)\left(\frac{V_B}{2}\right)\cos\theta$$

$$= 1/2 \left[V_A^2 + V_B^2 - 2V_A V_B \cos\theta \right] \quad (5)$$

where the angle θ is the relative phase imbalance between the two input voltages.

Using the identity $\cos(180^\circ - \theta) = -\cos\theta$:

$$(V_{\text{OUT}})^2 = 1/2 \left[V_A^2 + V_B^2 + 2V_A V_B \cos\theta \right] \quad (6)$$

From this equation the resultant output voltage is shown to be composed of two voltages V_A and V_B plus an interference term which is equal to $2 V_A V_B$ when the phase imbalance is zero. When the phase imbalance is 90° the interference term is destructive.

Next, one input signal is chosen as the reference voltage and the coordinate system is normalized and centered on that vector:

$$(V_{\text{OUT}})^2 = 1/2 \left[\left(\frac{V_A}{V_A}\right)^2 + \left(\frac{V_B}{V_A}\right)^2 + 2 \left(\frac{V_A}{V_A}\right)\left(\frac{V_B}{V_A}\right)\cos\theta \right] \quad (7)$$

$$V_{\text{OUT}}^2 = 1/2 \left[1 + \left(\frac{V_B}{V_A}\right)^2 + 2 \left(\frac{V_B}{V_A}\right)\cos\theta \right] \quad (8)$$

The normalized output power is equal to the square of the rms voltage across the termination impedance:

$$P_{\text{OUT}} = \frac{V_{\text{OUT}}^2}{2Z} =$$

$$\frac{1}{4Z} \left[1 + \left(\frac{V_B}{V_A}\right)^2 + 2 \left(\frac{V_B}{V_A}\right)\cos\theta \right] \quad (9)$$

The total available input power to the hybrid combiner is:

$$P_{\text{IN}} = P_A + P_B$$

The normalized input power sum is:

$$P_{IN} = \left(\frac{V_A}{V_A} \right)^2 + \left(\frac{V_B}{V_A} \right)^2 / 2Z \quad (10)$$

Finally with the ratio of the individual input powers P_A and P_B defined as:

$$P_r = P_B/P_A = (V_B)^2/(V_A)^2 \quad (11)$$

then the ratio of the output power to the available input power, assuming equal input and output impedances, is:

$$P_{OUT}/P_{IN} = \frac{1}{2Z} \frac{[1 + P_r + 2\sqrt{P_r} \cos \theta]}{(1 + P_r)} \quad (12)$$

The excess insertion loss due to amplitude imbalance (P_r) and phase imbalance (θ) is:

$$P_{OUT}/P_{IN} = \frac{1 + P_r + 2\sqrt{P_r} \cos \theta}{2(1 + P_r)} \quad (13)$$

Excess Insertion Loss =

$$10 \log_{10} (P_{OUT}/P_{IN}) = 10 \log \left[0.5 + \left(\frac{\sqrt{P_r}}{1 + P_r} \right) \cos \theta \right] \quad (14)$$

The resultant phase angle (ϕ) of the output signal is simply derived from the phasor diagram (Fig. 9B). The tangent of the resultant phase angle is:

$$\tan \phi = \frac{V_B \sin \theta}{V_A + V_B \cos \theta} = \frac{\sin \theta}{(V_A/V_B) + \cos \theta} \quad (15)$$

$$\theta = \tan^{-1} \left[\frac{\sin \theta}{\frac{P_{dB}}{10} + \cos \theta} \right] \quad (16)$$

Typical Losses

Examination of the curves showing excess loss as a function of amplitude and phase imbalance indicates that the loss is low even for moderate differences in amplitude and phase. For an amplitude imbalance P_{dB} of 1 dB the reduction in output power compared to the sum of the input powers is only 0.014 dB (a reduction of 0.33%). A worst case imbalance of 2 dB results in a 0.057 dB loss (1.3% reduction). For a phase imbalance θ of 30° the insertion loss would be 0.30 dB (a reduction of 7.2%).

Let's consider a 100 watt power amplifier module composed of two 50 watt transistors. If we consider a 2 dB power imbalance, the power in one transistor will be +47 dBm (50 watts) and +45 dBm (31.5

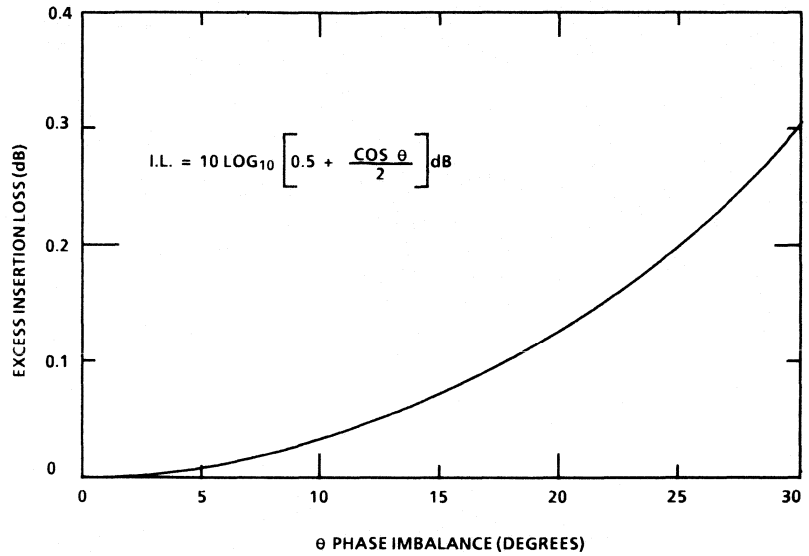


Figure 7. Excess Insertion Loss Due to Phase Imbalance

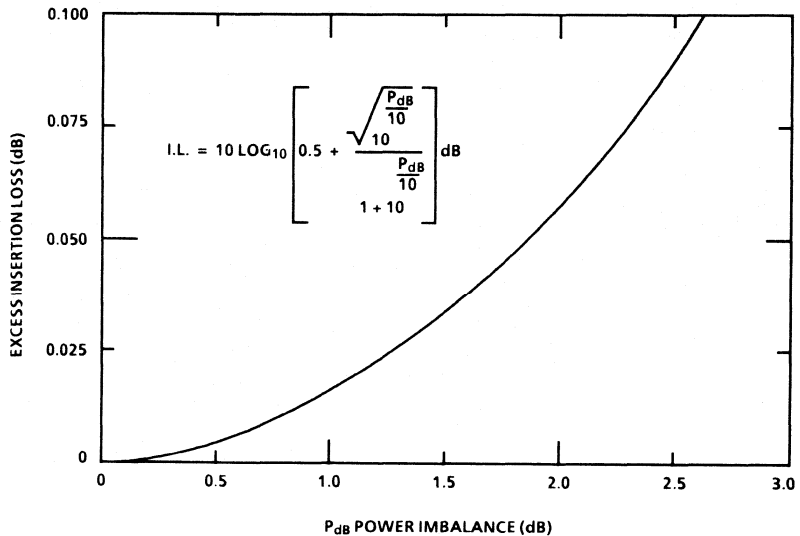


Figure 8. Excess Insertion Loss Due to Amplitude Imbalance

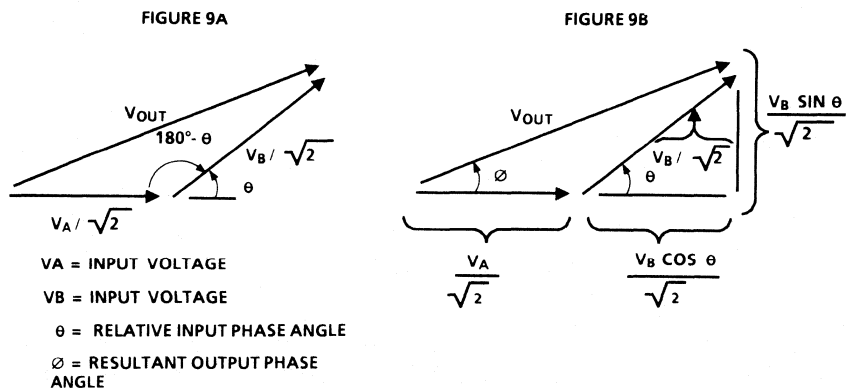


Figure 9. Derivation of Excess Combiner Insertion Loss

watts) in the other. The output power with this amplitude imbalance would be the sum of two powers minus the excess insertion loss due to imbalance:

$$P_{OUT} = P_1 + P_2 - I.L. (P_r) = 80.5 \text{ watts}$$

Approximately one watt from the original sum of 81.5 watts is lost in the isolation resistor because of amplitude imbalance.

Now for the same amplifier let's consider that the two input powers also have a phase difference of 30°. The output power would then be:

$$P_{OUT} = 80.5 \text{ watts} - I.L. (\theta) = 75.1 \text{ watts}$$

Thus, for an amplitude imbalance of 2 dB and a phase imbalance of 30° approximately 6.4 watts of power would be lost out of a possible 81.5 watts of input power to the final combiner, a reduction of 0.35 dB or 8%.

Measured Results

The total losses through a hybrid power combiner consist of the mismatch losses, losses in each path, and excess losses due to phase and amplitude imbalance. Pairs of experimental hybrids (quadrature, Wilkinson, branch-line) were combined to verify the excess losses due to phase and amplitude imbalance. A variable length transmission line was placed in one leg of the coupled hybrid to simulate an unequal amplifier phase delay (Fig. 10). Attenuators were also placed in each leg to simulate unequal amplifier gain. The expected loss just due to attenuators placed in each leg would then be:

$$\text{Loss} = 10 \log_{10} \left[\frac{1}{0.5 \left(\frac{-\text{Atten1}}{10} + \frac{-\text{Atten2}}{10} \right)} \right] \text{ dB}$$

where Atten 1 = Attenuation in one leg
Atten 2 = Attenuation in the other leg

The total measured loss was indeed equal to the sum of the insertion loss due to attenuators placed in each leg and the ex-

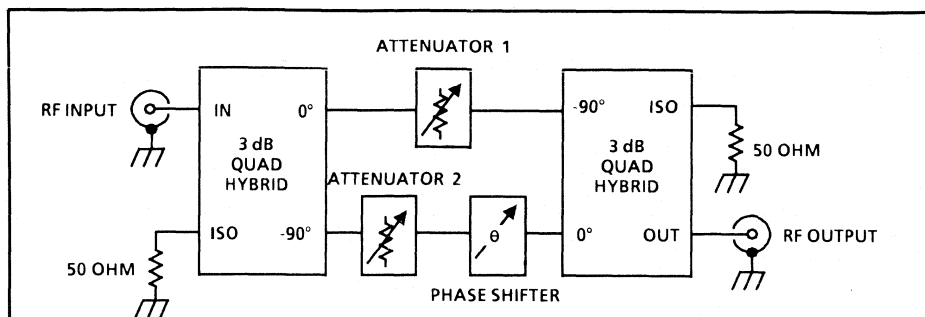


Figure 10. Combiner Loss Measurement Set-Up

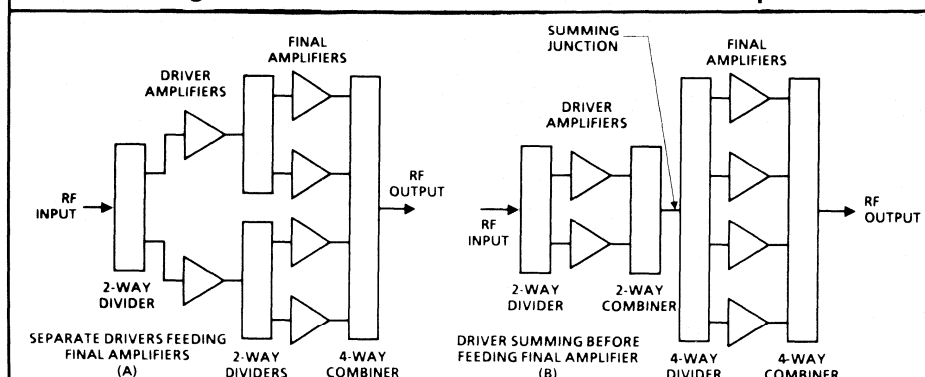


Figure 11. Summing of Gain Stages

cess insertion loss due to amplitude imbalance.

The phase was measured on each of eight UHF amplifier modules. These amplifier modules consisted of two balanced transistors using quadrature hybrids at the input and output. The gain and phase variations reported below are normalized about a collector supply voltage of +28 VDC, a bias voltage of +0.5 VDC, a flange temperature of +25°C, and a power level of 125 watts. (See box below.)

Reduction of Insertion Loss Due to Unbalance

The additional insertion loss due to amplitude and phase imbalance following the replacement of one damaged transistor can be minimized in several ways. First, the repair technician could replace both transistors with a paired replacement set that has been matched for gain. Next the design engineer might include a variable phase shift network in one side of the

combiner amplifier. If one side of the amplifier were designed to contain less phase shift than the other side, an adjustable phase shifter could be added to account for differing phase delays between the devices. The phase imbalance could be optimized by simply adjusting for minimum detected power at the isolation port of the combiner hybrid.

Finally, excess summing losses can be controlled for long amplifier chains by summing after each stage of amplification as illustrated in Fig. 11. If the driver amplifiers are unequal in gain or phase then this driver output power difference would be further amplified by the final amplifiers before being absorbed in the output 4-way power combiner isolation resistor. By adding a 2-way combiner at the output of the driver amplifier (Fig. 11B) the power is summed before splitting to feed the final amplifiers. Thus, any phase or amplitude difference is absorbed at a lower power level. This design requires an additional 2-way combiner and divider, but the phase and amplitude balance of the drive signal to the final amplifiers is improved. [E]

VARIABLE	VARIATION	MEASURED GAIN DEVIATION	MEASURED PHASE DEVIATION
Collector Supply Voltage	+26 to +30 VDC	-0.3 to +0.3 dB	-4 to -3
Base Supply Voltage	+0.4 to +0.6 VDC	-0.6 to +1.0 dB	+4 to -1
Flange Temperature	-40 to +100 C	+0.4 to -1.1 dB	+2 to -4
Power Level	50 to 150W	+0.2 to -0.1 dB	+5 to -2

About the Author

Ernie Franke is a Member of Technical Staff at E-Systems, ECI Division, P.O. Box 12248, M/S 28, St. Petersburg, FL 33733.

The Close-Field Probe: A Powerful EMI Troubleshooting Tool

A hand-held probe can find localized emission sources within equipment.

By Mark Terrien
Hewlett-Packard Company

The increasing world-wide regulation of electromagnetic radiation is forcing design engineers to be more concerned than ever about minimizing radiated and conducted emissions. Methods are needed to detect and locate EMI problems during the product-design cycle to avoid costly re-design at the production stage. Unfortunately, many design centers do not have in-house EMI testing facilities and designers have no way of detecting emissions problems early, when they are easiest to fix. Even when such facilities are available, the measurement methods cannot always locate sources of high emissions within the equipment, making it difficult for the designer to solve EMI problems. This article describes the Hewlett-Packard 11940A Close-Field Probe and its use in identification and troubleshooting of EMI problems.

There are a variety of radiating sources in electronic equipment including analog oscillators, digital clocks and microprocessors. The sources and their surrounding metallic support structures directly control the radiation pattern when placed in an unshielded enclosure. When placed in a shielded enclosure, the enclosure itself controls the radiation pattern. In both cases, the task for the troubleshooter is to locate the major radiators in the equipment. However, most EMI testing methods measure total radiated field strengths without determining the physical location of the major radiators. A device that measures radiated emissions with repeatable spatial accuracy would be a powerful troubleshooting tool. With such a device, the circuit designer could identify problem radiators in a new product prototype and the mechanical engineer

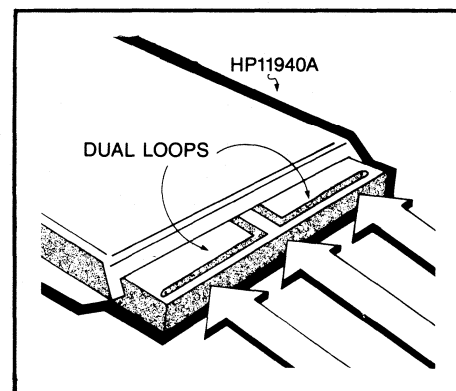


Figure 2. Probe orientation for maximum coupling to the magnetic field.

could evaluate the effectiveness of the enclosures and shields being designed for the new product.

There are several descriptions in the literature of balanced shielded loop antennas for measuring magnetic fields (1,2,3). These antennas are shielded from electric field components to reduce errors in the output signal from stray capacitive coupling to nearby sources. It is this parasitic coupling that limits the repeatability of the electromagnetic field measurement. The spatial resolution of these antennas is limited because of the size of

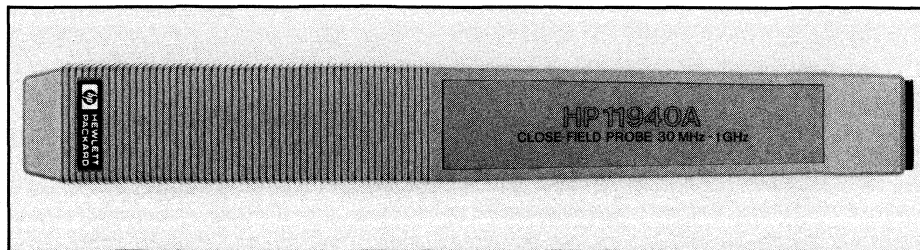
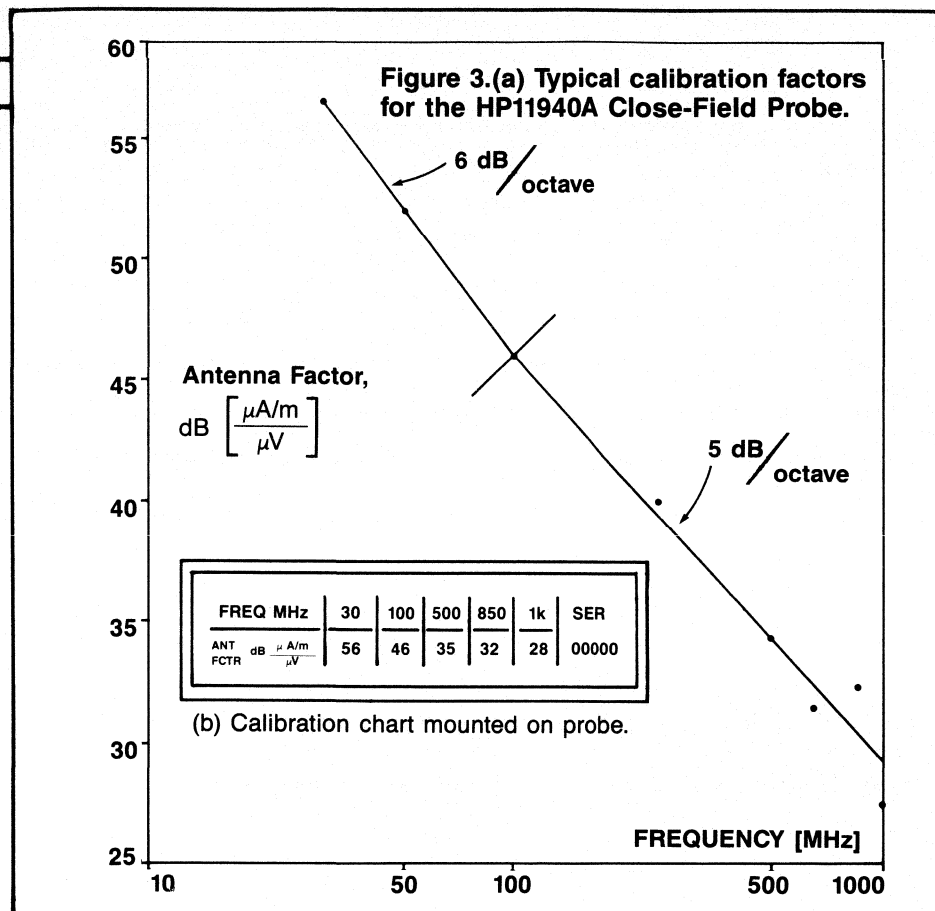


Figure 1. The HP 11940A Close-Field Probe.



the shield, and the bandwidth is limited by the frequency response of the balun used to match the probe to a measuring instrument's input. Such radiation monitors are also used to measure emissions near an enclosure and when cabled with high impedance, non-metallic lines, the stray capacitive coupling is reduced. However, because radiation monitors rectify the RF voltage for a DC output, frequency information is lost.

A new commercial product for accurately locating emission sources is the HP 11940A Close-Field Probe, shown in Fig.



Figure 4. Searching for electromagnetic energy leaks at seams of an enclosure.

1. This device is a balanced magnetic field sensor that provides an output voltage proportional to the strength of the magnetic field at its tip. A dual-loop configuration and balun provide rejection of the common-mode currents created by electric field coupling to both of the loops. (Fig. 2.) The balun itself provides 30 dB (typical) of common-mode rejection from 30 MHz to 1 GHz. This common-mode rejection makes the probe insensitive to electric-field components, yielding very repeatable measurements.

The Close-Field Probe is supplied with a calibration accurate to ± 2 dB in a 377 ohm field impedance (see Fig. 3). Using appropriate modeling, this calibration allows the prediction of radiated signal strength at a specified distance from the equipment (4). The probe is small and lightweight making it easy to probe around an enclosure or cabling and accurately locate emission "hot spots." As shown in Fig. 4, the probe tip is held very close to the potential radiating points, such as the seams of the enclosure. When the tip of the probe is on a "hot spot," the radiated field magnetically couples to the probe and produces a larger output voltage.

Since the probe preserves frequency information, it is ideally used with a spectrum analyzer. The spectrum analyzer accurately displays the frequency and amplitude of the emission to help the troubleshooter track down its source. The Close-

Field Probe and spectrum analyzer can be used to diagnose EMI problems in these design areas:

1) By the circuit designer on the lab bench.

2) By the EMI test engineer to find emission sources in equipment being tested for the design team.

3) By the mechanical designer to evaluate the relative shielding effectiveness of new enclosures and shielding structures.

The third application requires a tracking generator, whose output signal radiates from a small antenna placed inside the enclosure being tested. The probe is then used to "sniff" along the enclosure's seams and openings in search of electromagnetic energy leaks. This application is described in an article published in the July/August 1984 issue of *RF Design* (5).

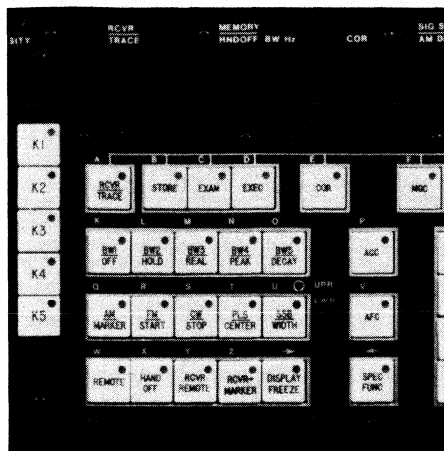
The Close-Field Probe can also be used as a localized magnetic field source for locating susceptibility problems on a circuit board. It is a reciprocal device; that is, a voltage fed into the unit will create a magnetic field at the loops. For this application, the maximum input power is 0.5 W with a typical worst-case VSWR of 3:1. The probe can be used effectively by the circuit designer, mechanical engineer and EMI test engineer to troubleshoot EMI problems early in the design cycle and avoid costly re-design. [7]

About the Author

Mark Terrien is a development engineer for EMI measuring equipment at Hewlett-Packard, Signal Analysis Division, Santa Rosa, CA 95401. He has a BS in Physics from the University of Wisconsin (Milwaukee) and an MSEE from the University of Wisconsin (Madison).

References

1. Libby, L.L., "Special Aspects of Balanced Shielded Loops," proceedings of the IRE, Vol. 34, September 1946, pgs. 641-646.
2. Roleson, S., "Evaluate EMI Reduction Schemes with Shielded-loop Antennas," *EDN*, May 17, 1984, pgs. 203-207.
3. Whiteside, H., and King, R.W., "The Loop Antenna as a Probe," *IEEE Transactions on Antennas and Propagation*, May 1964, pgs. 291-297.
4. Terrien, M., "Far-field Amplitude Estimation of General Electromagnetic Radiators from Close-Field Electromagnetic Compatibility," Boston, August 1985.
5. Jerse, T., "Low Transfer Impedance — A Key to Effective Shielding," *RF Design*, July/August 1984.

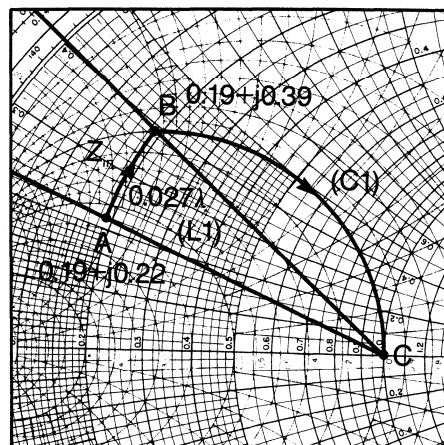


Cover

This month's cover features a new multiple receiver controller by Watkins-Johnson Company, Special Products Division, Gaithersburg, Maryland. The setting represents various military vehicles that might carry the WJ-8610A, which helps monitor and control intercept receivers in dense signal environments.

Features

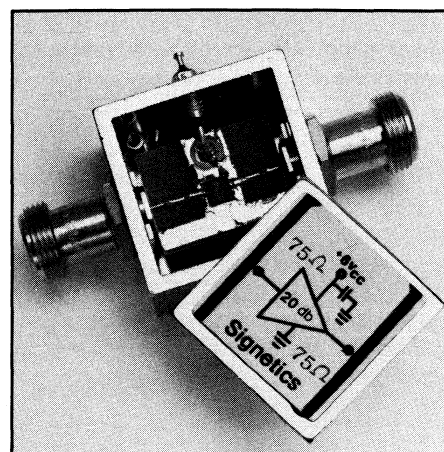
- 21 Microstrip High Power Amplifier Design**
This article reviews the fundamentals of microstripline design techniques using an L-Band (1650 MHz) 45 watt amplifier as a design example. — Alan K. Tam
- 29 Special Report: The Military Uses of RF**
This month's Special Report examines a few new uses of RF technology with significant military implications. The military is becoming increasingly interested in the below-microwave frequencies for reliable communications under hostile conditions. This report looks at three distinct applications of RF technology.
- 49 High Frequency Amplifier IC Simplifies Design**
One of a growing number of matched 50/75 ohm "building block" components, Signetics' latest product, the NE5205, is a 20 dB gain monolithic amplifier usable to 600 MHz. — Tom DeLurio



Departments

Designer's Notebook — Engineering Use of Spreadsheet Languages

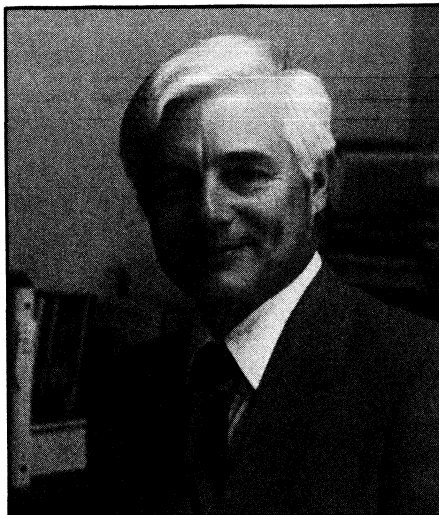
- 54** Writing a new program for each new application may not be necessary with a personal computer and a good spreadsheet program. The author describes how to use spreadsheets for engineering computations. — Pat O'Neil
- 58 RFI/EMI Corner — Power Line Filter Considerations**
Eliminating conducted RFI/EMI requires a power line filter. Based on information from Curtis Industries, this article provides a basic understanding of filter requirements. — Gary Breed



- 6 Editorial
- 8 Viewpoint
- 12 Letters
- 14 News
- 19 Courses
- 20 Calendar
- 60 New Products
- 72 New Literature
- 76 Classified Advertising
- 78 Advertisers Index
- 79 Info/Card

R.F. DESIGN (ISSN: 0163-321X USPS: 453-490) is published monthly plus one extra issue in August. December 1985, Volume 8, No. 13. Copyright 1985 by Cardiff Publishing Company, a subsidiary of Argus Press Holdings, Inc., 6530 S. Yosemite Street, Englewood, CO 80111 (303) 694-1522. Contents may not be reproduced in any form without written permission. Second-Class Postage paid at Englewood, CO and at additional mailing offices. Subscription office: 1 East First Street, Duluth, MN 55802, (1-800-346-0085). Domestic subscriptions are sent free to qualified individuals responsible for the design and development of communications equipment. Other subscriptions are: \$22 per year in the United States; \$29 per year in Canada and Mexico; \$33 (surface mail) per year for foreign countries. Additional cost for first class mailing. Payment must be made in U.S. funds and accompany request. If available, single copies and back issues are \$5.50 each (in the U.S.). This publication is available on microfilm/fiche from University Microfilms International, 300 N. Zeeb Road, Ann Arbor, MI 48106 USA (313) 761-4700. POSTMASTER & SUBSCRIBERS: Please send address changes to: R.F. Design, P.O. Box 6317, Duluth, MN 55806.

The Benefits of Military Electronics Development



*By James N. MacDonald
Editor*

Normally, this magazine does not cover the military electronics scene, even though many of our readers design military equipment. We concentrate on design ideas and techniques, not on systems. Sometimes, however, a subject is so interesting we cannot resist the temptation to draw our readers' attention to it, even if it does not show them how to design something better or solve a problem. The guiding philosophy in such circumstances is whether thinking about some new developments in the field might help engineers keep up with changes that could affect their career.

This kind of thought process took place as we worked on this month's Special Report. We started out to write about interesting, little-known uses of RF in industry and the military. We discovered so much going on that we finally decided to limit the subject to military uses of RF. But as we looked at the material available we began to say, "This is interesting, but how

does it really help an engineer do a better job?" The result is three contributed articles describing electronic operations applicable to many military devices.

One thing our research pointed out is how much the civilian community benefits from military electronics development. The receiver controller featured on our cover is especially suitable for monitoring signals in a military environment. A Watkins-Johnson engineer pointed out that it could also be used to locate and monitor surreptitious radio signals within a large city. It could be used to track terrorist groups or drug runners. Potentially, any illegal communications network could be monitored with such a system.

Frequency-hopping techniques seem to be solely a military use of the technology, but the technique might also be used for secure business communications. We do not know to what extent commercial and government communications are being intercepted, but it would be naive to assume they are not. Most sensitive communications are encrypted, but encryption can be defeated unless it is quite sophisticated. Technology cannot stand still, even in the civilian sector.

So, we have not fulfilled the promise in last month's editorial to write about industrial uses of RF in this month's Special Report. We hope to be able to describe such uses in a future issue, because they are interesting. We also hope, however, that we will never lose the flexibility to change the focus of our Special Reports to best serve our readers' needs.

*James N.
MacDonald*

Microstripline High Power Amplifier Design

By Alan K. Tam
Space & Communications Group
Hughes Aircraft Company

Most available RF/microwave Computer Aided Design (CAD) software has been developed for small signal amplifier applications. Touchstone from EEsof and Super-Compact from Compact Engineering are widely used by microwave circuit designers. Such programs are powerful tools for designers who synthesize, analyze and optimize active and passive circuits to meet their specific needs. Many microwave microstripline Low Noise Amplifiers (LNAs) and intermediate power amplifiers ($P_{OUT} \leq +20$ dBm) have been designed using CAE/CAD software. Yet, little software has been developed for large signal amplifier design.

The Smith chart graphical approach for effective microstripline High Power Amplifier (HPA) design is demonstrated by the author, using a proven L Band HPA design example to illustrate the technique.

The objective of this design was a narrow-band 1.6 GHz ± 10 MHz telemetry transmitter HPA meeting the following requirements:

Power Gain	≥ 7 dB
Power Output	≥ 45 W (CW)
Efficiency	$\geq 45\%$
Input VSWR	$\leq 1.5:1$
Load Mismatch	$\infty:1$ at all phase angles
In Band Spurs	≤ -60 dBc
2nd Harmonics	≤ -25 dBc
Subharmonics	≤ -35 dBc
Vcc	+28 VDC
Temperature Range	-40°C to $+75^\circ\text{C}$

There are a few key steps that the designer should be aware of regarding microwave power devices and performance tradeoff considerations. Successful high performance HPA design requires an understanding of the electrical characteristics of the power devices. For instance, a bipolar device can deliver more RF power than its GaAs FET counterpart when operated in the L Band. A common base device has better output VSWR, ruggedness and stability at lower frequencies but has less gain than a common emitter

FREQUENCY (GHz)	Z_{in} (Ω)	Z_{cl} (Ω)
1.50	8.6+j13.0	12.1-j3.9
1.55	7.8+j11.7	9.5-j2.7
1.60	8.5+j11.1	8.6-j4.3
1.65	9.5+j11.0	7.2-j5.0
1.70	7.8+j11.7	8.6-j4.3

Table 1. MSC 1517-25M published input/output impedance data

device. Furthermore, internally matched devices offer wider operating bandwidth, higher efficiency and larger series input and output impedance to the microwave circuit designer. The MSC 1517-25M device from Microwave Semiconductor Corp., a flange mounted device, was chosen accordingly in this empirical example.

It is important to review some practical circuit design rules that microwave engineers need to follow in order to achieve maximum efficiency and reliability:

Always operate the device within its Safe Operating Area (SOA) by not exceeding the maximum breakdown voltage BV_{CBO} and current I_{CBO} ratings.

The junction-to-case thermal resistance θ_{jc} should be as low as possible for maximum heat transfer under RF operation. Thermal compound should be placed between the bottom side of the flanged package and the ground surface of the housing.

The housing ground surface, always critical for microwave class 'C' amplifier operation, should be polished to avoid any ground loop problems.

Teflon, Fiberglass, Duroid, E10 ceramic and alumina circuit board/substrate materials can be used depending upon the individual application and considerations of cost, performance and reliability.

The specified torque should be used to secure the power device on the unit housing.

Design Implementation Using the Immittance Chart

The series input and output impedances at 1.64 GHz are taken from the manufacturer's data in Table 1:

$$Z_{IN} = (9.5 + j11.0) \text{ ohm}$$

$$Z_{OUT} = (7.2 - j5.0) \text{ ohm}$$

Normalized impedance with respect to a 50 ohm system are:

$$Z_{IN} = (0.19 + j0.22) \text{ ohm}$$

$$Z_{OUT} = (0.14 - j0.10) \text{ ohm}$$

To begin the actual design, normalize the series input and output impedances and plot them directly on the immittance chart (an opposed admittance Smith chart superimposed on the standard impedance Smith chart). For simplicity, a single section low-pass input matching network was used, which is adequate for narrow band amplifier applications ($\leq 5\%$ BW).

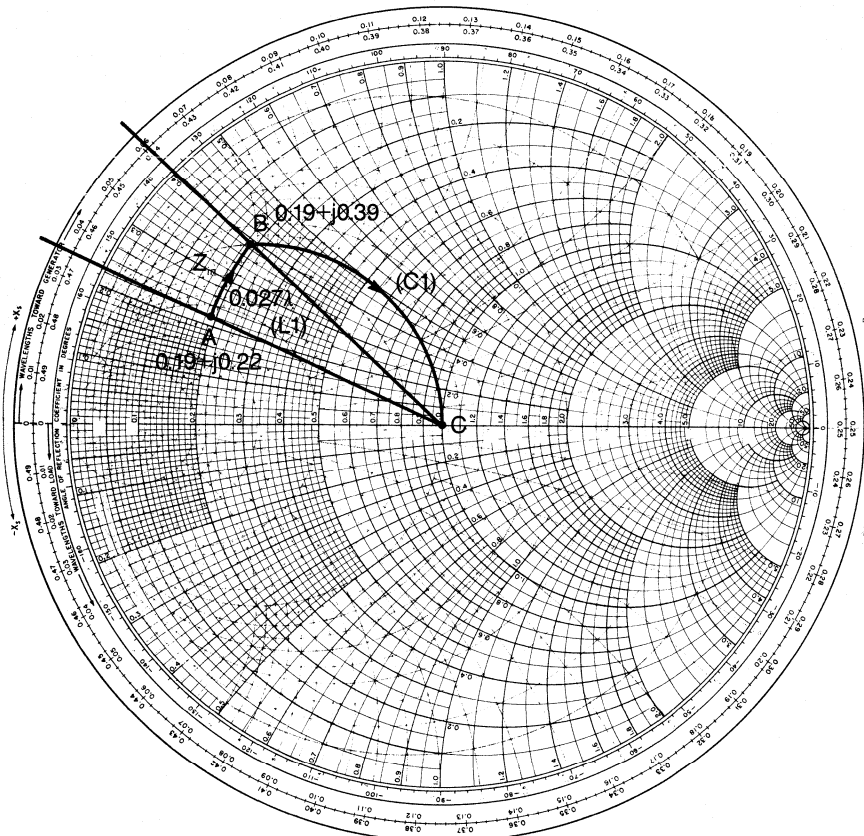


Figure 1. MSC AM-1517-25 input match at 1.65 GHz

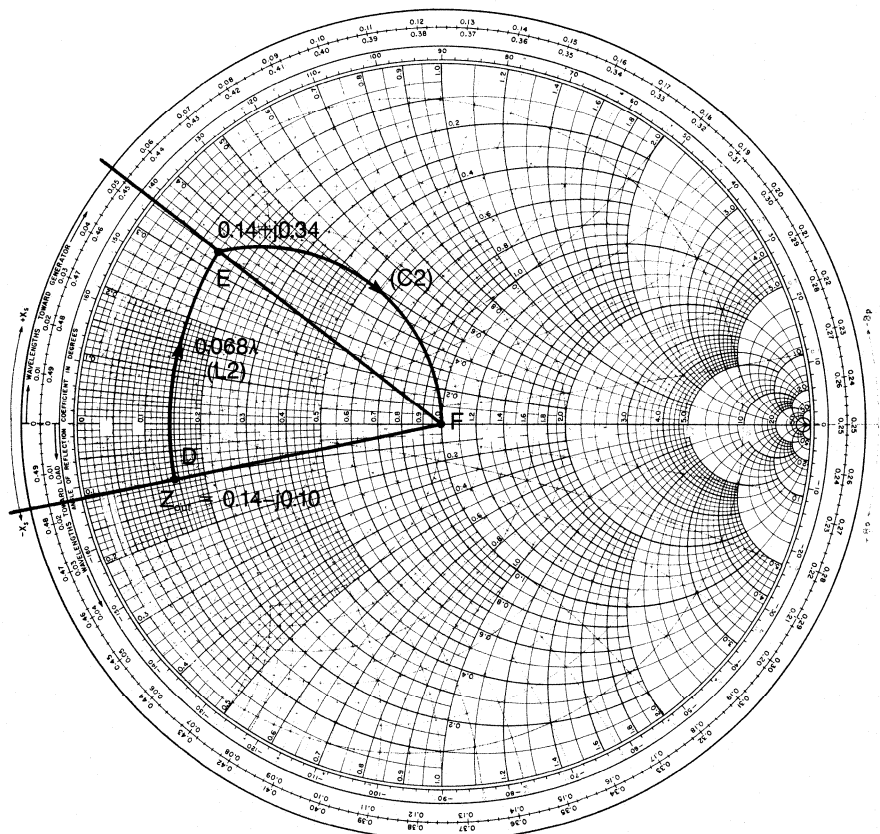


Figure 2. MSC AM-1517-25 output match at 1.65 GHz

Referring to Figs. 1 and 2, L1 and C1 are the input matching elements and L2 and C2 are the respective output matching elements.

L1 and C1 are identified as arcs AB and BC in Fig. 1. The electrical wavelength at 1.64 GHz on a 31 mil Teflon fiberglass board with a relative dielectric constant of 2.10 is given by:

$$\lambda = \frac{C}{\epsilon f} = \frac{1.18 \times 10^{10} \text{ in/sec}}{2.10 (1.64 \times 10^9 \text{ Hz})} = 4.97 \text{ inch}$$

With this data, line widths were obtained using Compact.

For the input matching network, the electrical length of the 50 ohm transmission line used as L1 is read from arc AB of Fig. 1 as 0.027λ or 0.134 inch. C1 will be designed as a double-sided open stub rather than a lumped capacitor to provide lower loss, lower cost and better reproducibility. From experience, the characteristic impedance of an open stub should be ranged from 10 ohms to 25 ohms and the overall electrical length should be less than a quarter wavelength. The impedance of C1 as derived from arc BC of Fig. 1 is $40 \text{ mmho} = 25 \text{ ohms}$ (Z_{C1}). The actual impedance of C1 will be doubled due to the double-sided open stub design, so $Z_C = 2Z_{C1} = 50 \text{ ohms}$. Dimensions of the stub (Fig. 3) are determined using the equation:

$$Z_C = -jZ_0 \cot \theta, \text{ where} \quad (1)$$

$$Z_C = \text{capacitive reactance}$$

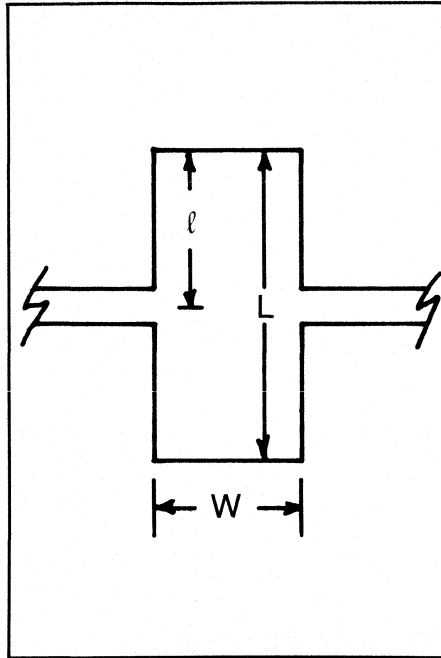


Figure 3. Double-sided open stub dimensions

Z_0 = characteristic impedance of stub (w)

θ = electrical length of ℓ

Rearranging (1), and setting $Z_0 = 19\Omega$:

$$\theta = \tan^{-1} \frac{Z_0}{Z_C} = \tan^{-1} \frac{19\Omega}{50\Omega} =$$

$$\tan^{-1} (0.38) = 21.0^\circ$$

Convert to inches, using:

$$\ell = \frac{\theta \lambda}{2\pi} = \frac{(21.0^\circ) (4.97 \text{ in.})}{360^\circ} = 0.290 \text{ in.}$$

$$L = 2 \ell = 0.580 \text{ in.}$$

$W = 0.30 \text{ in.}$, for $Z_0 = 19\Omega$ (using Compact)

The $\lambda/4$ high impedance ($Z_0 \cong 80\Omega$) microstripline is incorporated as a shunt inductor to form a DC return path, since the power device is packaged in a common base configuration.

The Output Matching Network design can be accomplished using the same approach. L2, the electrical length of arc DE of Fig. 2, is found to be 0.068λ or 0.338 inch. The impedance of C2, arc EF of Fig. 2 is 19.2 ohms. Again, for a double-sided open stub, $Z_C = 2Z_{C2} = 38.4\Omega$.

If we set $Z_0 = 11\Omega$ and use (1),

$$\theta = \tan^{-1} \frac{Z_0}{Z_C} = \tan^{-1} \frac{11\Omega}{38.4\Omega}$$

$$\ell = \tan^{-1} (0.286) = 16.0^\circ$$

Again, convert to inches,

$$\ell = \frac{\theta \lambda}{2\pi} = \frac{16.0^\circ (4.97 \text{ inch})}{360^\circ} = 0.220 \text{ inch}$$

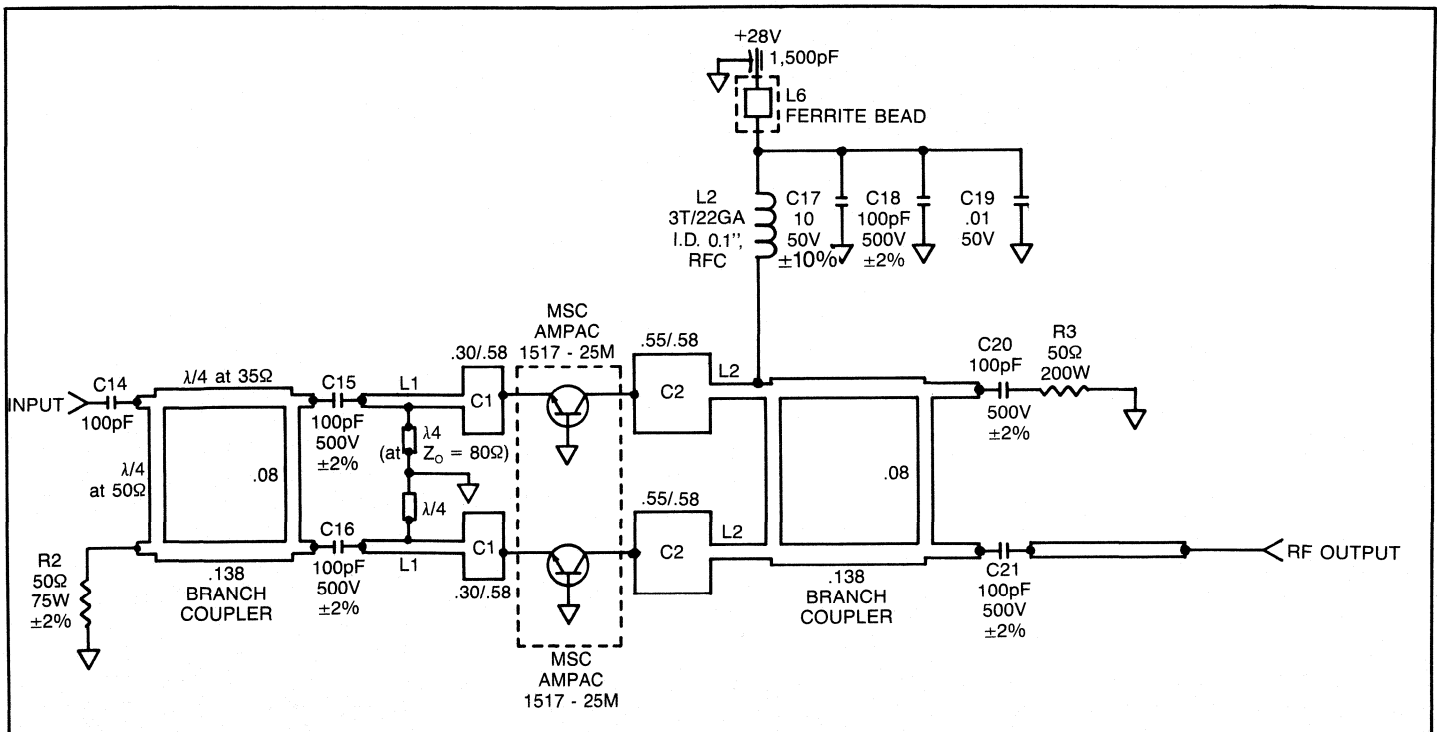


Figure 4. Schematic diagram (layout dimensions)

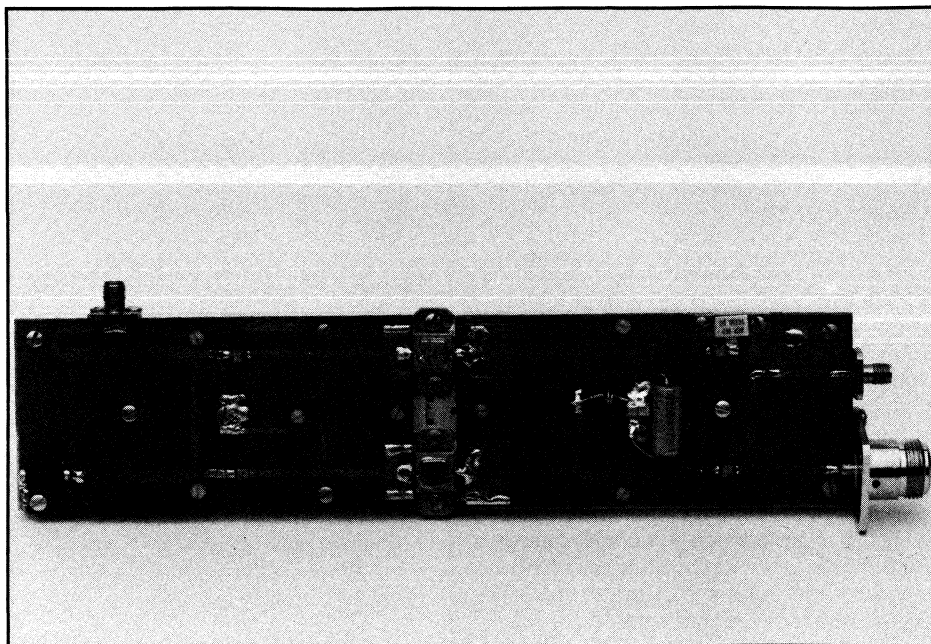


Figure 5. Photo of the completed amplifier

$$L = 2 \ell = 0.440 \text{ inch}$$

$$W = 0.55 \text{ in, for } Z_0 = 11\Omega$$

A power combining technique using two quadrature hybrids was adapted for this amplifier. In order to achieve the required 45W minimum power output, two identical 25W class 'C' amplifier stages were paralleled. The quadrature hybrid is essentially a branch coupler in which the series arms are $1/4\lambda$ long 50 ohm transmission lines and the shunt arms are $1/4\lambda$ long 35.2 ohm transmission lines. The hybrid's function is to split the input and combine the output power while maintaining low VSWR and good isolation. Power devices used in this configuration should be a matched pair with the same DC characteristics to minimize unbalanced power sharing. By using this method the 2nd harmonic component is also greatly reduced compared to a single-ended design. Refer to Figs. 4 and 5, the schematic diagram and the photograph of the unit for layout techniques. Power terminations being used for input and output hybrids should be able to withstand the heat dissipation under RF operation. The ones used are made out of thick film materials which are mounted on the BeO substrate for good heat conduction.

The actual performance data of the completed amplifier is tabulated in Table 2. The performance goals were met using these design techniques.

This immittance chart graphical approach is practical and time saving. The

Frequency (MHz)	1,650	1,640	1,630
Pin (+dBm)	40	40	40
P _{OUT} (+dBm)	47	47	47
Efficiency (77)	44%	43%	43%
Power Gain (dB)	7	7	7
Return Loss (dB)	≤-20	≤-20	≤-20
Spurs (dBc)	<-60	<-60	<-60
2nd Harmonics (dBc)	<-35	<-35	<-35
3rd Harmonics (dBc)	<-35	<-35	<-35
4th Harmonics (dBc)	<-40	<-40	<-40
I _{CC} at + 28 VDC (Amp)	4.08	4.14	4.13

Table 2. L/Band HPA performance data.

actual results indicate that the input matching network design was perfect, but the output matching was slightly off and the open stub C2 needed to be tuned by adding 6° more electrical length on both sides. This shows that error could be introduced by variations of DuPont Teflon® Fiberglass PCB's dielectric constant, the physical alignment of the output section circuit boards during assembly, or other electrical and mechanical variations. The overall impedance matching design values agreed very closely with the final microstrip layout dimensions. rf

About the Author

Alan Tam is Section Head, Microwave Product Design of the Space & Communications Group, Hughes Aircraft Company, P.O. Box 92919, M.S. S72/T301, Los Angeles, CA 90009. His telephone number is (213) 618-2312.

Military Uses of RF

A look at a multiple-receiver controller system, the use of noise to calibrate and test military electronics, and frequency-hopping by direct-digital synthesis.

During the recent hijacking of an Italian passenger ship a shortwave listener overheard President Reagan in Air Force One talking about the incident with Secretary of Defense Weinberger in another aircraft. (Although the listener was called a ham in newspaper accounts, it is doubtful that the president and the secretary were using an amateur frequency, so SWL would be a more accurate term, whether or not the listener had an amateur license).

White House spokesman Larry Speakes acknowledged that the communication did occur and that the President did not use a secure communications link because there was not enough time to coordinate the two systems. Apparently, the president weighed the risk of an overheard conversation against the time factor and decided the risk was small. His communications specialists undoubtedly knew the conversation could be overheard. In fact, it probably was heard by

other SWLs who did not report it to the press.

The occurrence is a reminder of the major problem with complex communication technology. The more elements involved in the link the more difficult the system is to use. Although it was not a factor in this event, each separate element that processes communications is one more place where communications can fail.

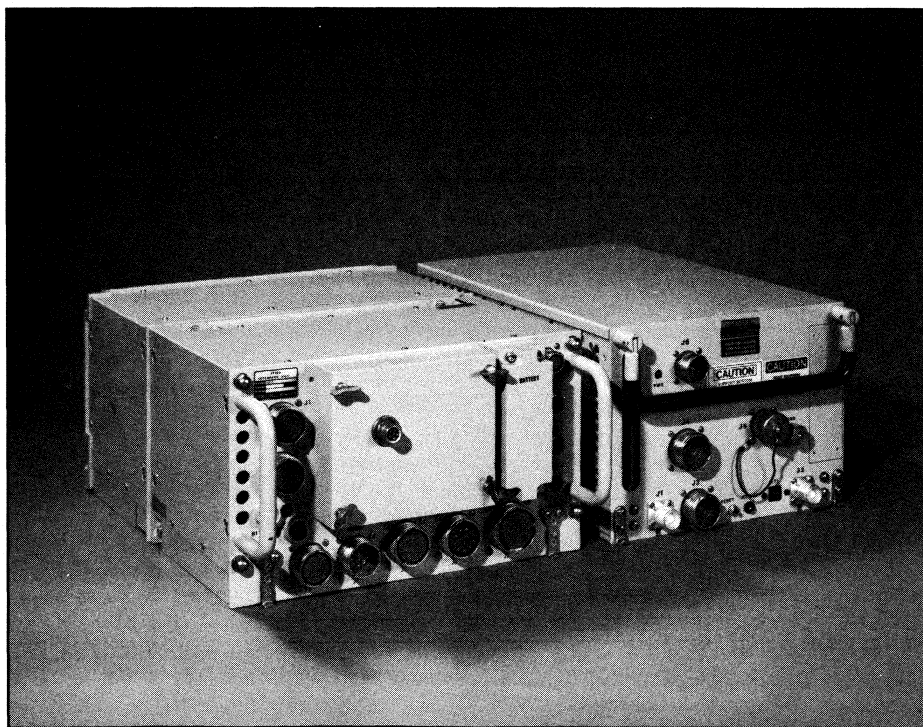
This is one reason military planners are still relying heavily on HF communications. If a major war lasts more than a few days we will probably be bouncing radio signals off the ionosphere instead of satellites. The birds won't be there anymore.

Research runs throughout the lower RF spectrum, from ELF for submarine communications to UHF for video and data transfer, and it is of interest to all military branches. Successful propagation of RF has been well researched, although much remains to be learned about the ionosphere. Most research seems to be directed toward frequency agility to avoid jamming and signal encryption to avoid information compromise. Both research areas bring digital signal processing into the RF field.

This month's Special Report covers a few applications where digital signal processing is enhancing the performance of military communications equipment. Digital design is becoming more and more a part of RF design, and we hope RF design engineers are keeping on top of this trend.

The first article describes the device featured on the cover, Watkins-Johnson Company's new multiple receiver controller, the WJ-8610A. Following up on last month's Special Report, the next article is a brief description of the use of noise in modern communications. The third describes frequency-hopping control by direct-digital synthesis.

— James N. MacDonald



The Joint Tactical Information Distribution System (JTIDS) Class 2 terminal being produced by Singer's Kearfott Division and Collins Government Avionics Division of Rockwell International for the U.S. Army provides complete tactical information exchange for air defense systems and will be integrated with the Army's Position Location Reporting System. The terminal integrates many communications functions, reducing the weight and size required, and provides real-time, high-capacity, jam-resistant information exchange between combat units within its 300 nautical mile range.

Controlling Multiple VHF/UHF Receiver Systems

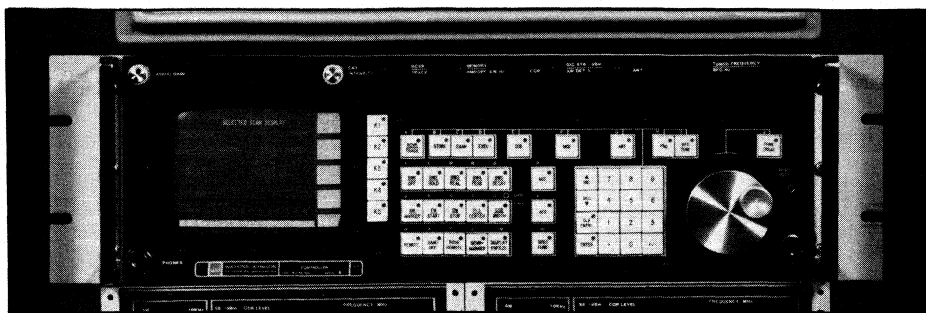
By C.E. Dexter and
T.W. Goodell,
Special Projects Division
Watkins-Johnson Co.

As the number of digitally controlled receivers in use at multiple-receiver collection sites grows, the system designer faces a difficult decision in the choice of a controller. If a computer or even a microprocessor is chosen as the multiple-receiver controller, the user has to develop required software. This often proves to be impractical for small collection systems. In a large collection system operated in dense signal environments, a computer appears to be ideal as a multiple-receiver controller. However, in very dense, high-activity signal environments, a central computer can be overloaded with service requests and response commands from a large number of frequency-scanning receivers. In this situation, data collection and operational decisions may be impaired unless some decisions and basic receiver-type routine functions are removed from the computer.

A multiple-receiver controller operating between the central computer and collection receivers can ease the computer workload while providing rapid response to receiver demands. The controller not only expands the communication link, IEEE-488 or other, it also buffers data from the receivers. Many auxiliary functions, such as generating a digitally refreshed display spectrum for a scanned frequency band or queuing intercepted signals also may be handled by the controller. The controller CRT presents a menu-driven alphanumeric display of the status of all receivers and permits operator intervention and control in the event of a central computer failure.

The number of receivers serviced by a central computer can be limited by the number of available bus locations and by the overall system response time. Short duration events such as "pop up" transmissions require rapid system response to such signal parameters as frequency, modulation type and percentage, and signal strength. System response time is limited by both the time required to acquire the signal and the time required to service the active receiver over the bus. All receivers on the bus may require nearly simultaneous requests for service while in the SCAN mode. So much time can be spent on this task that the computer cannot perform its primary analysis function.

Fig. 1 illustrates this problem. In this



system, a single computer monitors 60 receivers over an IEEE-488 bus. A bus expander is needed to increase the number of devices per controller to more than 14. The time required to interrogate each receiver for just-tuned frequency is over half a second. Short duration signals cannot be observed or logged by the computer.

A controller between the computer and receiver can do much to relieve this problem. In Fig. 2 the bus expanders have been replaced with receiver controllers. Each controller monitors 10 receivers and reports wanted activity to the computer. With a single command string, the computer can determine the status of up to six receivers, achieving a six-fold reduction in communication time. System programmers can control blocks of receivers with a few simple commands, as opposed to individually servicing each receiver. Distributed processing and the specialized features of the controller simplify programming of system tasks.

System reliability need not be totally dependent upon the proper operation of a single piece of equipment. In some systems the computer may not be needed at all. Often the controller alone is a better choice since it is much more friendly than a computer, while still retaining most computer features. A system controller consists of a microcomputer, keyboard and CRT display. It varies little in these respects from an Apple computer, and is less powerful than an IBM PC. What separates this microcomputer from the others is the unique front panel and the software. The front panel looks and acts like a receiver, even though the receiver is remotely located. The handoff receiver is selected, and the operator may tune and listen to signal activity while watching for any activity on the CRT screen from other receivers with signals present.

The software makes the hardware think it is a controller. Special routines call up each receiver through the IEEE-488 bus and control it or update its status on the

alphanumeric CRT screen. Other software routines set up the parameters for putting a number of receivers in the scan mode. Each receiver gets a start frequency, stop frequency and step size. Unwanted signals may be locked out. The controller accepts the 50 dB log video information from the receiver and displays each receiver scan on a digitally refreshed trace on an X-Y CRT. The operator may observe a wide range of signal activity throughout the spectrums selected, place a cursor over the signal of interest with the frequency tuning knob and assign it to a handoff receiver. The headphones and any signal monitor in the system are then connected to this receiver. The operator can listen and select an appropriate IF bandwidth and detection mode before leaving this receiver to the audio recorder. Each signal of interest can be handed off using the cursor control until all receivers are in use.

Other software-controlled auxiliary routines can be chosen, such as antenna select and receiver labeling. Background software tasks aid the operator in distinguishing which receiver has what options and range. Therefore, single sideband signals cannot be accidentally handed off in a receiver without the SSB option.

Some complicated signals or a group of signals may require detailed analysis by an operator. A good handoff receiver with pan sector can ease the analysis task. Pan sector shows the operator a wide panoramic view of signal activity, while a sector of that view is also displayed. An operator can then take the time to use all the features of that versatile receiver to make decisions. Several types of special demodulators such as PSK, FSK and TDM can be used to analyze the signal further.

Auxiliary Functions of the Controller

The controller is capable of far more than receiver control. Other functions as-

sociated with a multiple receiver system, such as audio and video routing and signal-monitor switching, can be a part of the controller's job. Spectrum surveillance through panoramic displays can aid the operator in selecting a signal of interest to pass to a monitoring receiver. To implement this panoramic display, the controller sends the scan parameters to a receiver (start and stop frequency, step size, etc.). The receiver does not stop on the signals, but sends the log video back to the controller.

Another important function of the controller is to let the system computer or operator know when any component or receiver on the bus is malfunctioning. Most good receivers have a built-in test but are unable to distinguish a broken antenna cable from poor sensitivity. The controller queries the BITE function on each receiver and presents the status to the operator or computer. Next, a system test is performed by tuning all receivers to several known transmitted frequencies and comparing signal parameters from each receiver and auxiliary circuits. Any malfunction is reported to the operator, through the alphanumeric CRT, or to the system computer.

The controller can aid the operator in finding certain signals with unique modulation characteristics. Upon acquiring a signal the receiver sends a service request to the controller. The controller asks the receiver for the modulator parameters, such as peak AM, peak deviation, FM offset, etc. The controller compares these parameters with special signal characteristics stored in memory and alerts the operator to a match. Scanning scenarios like this can easily skip standard commercial signals and only stop on signals of sonobuoys, transponders and other transmitters of interest. The receiver signal parameters can also be read directly from the alphanumeric CRT.

Management of Fast-Scan Spectrum Data

A very important auxiliary function of the controller is to manage the many different options, IF bandwidths and frequency ranges of receivers in the system. The controller can display several configuration tables to the operator. By using other menus, such as signal parameter presentations, the operator can hand off wide-spectrum signals to receivers configured with the wider IF bandwidths.

Several types of receivers are available for rapid signal acquisition using IFM, microscan and channelized technology. This article considers only performance typical to a scanning or frequency-step-

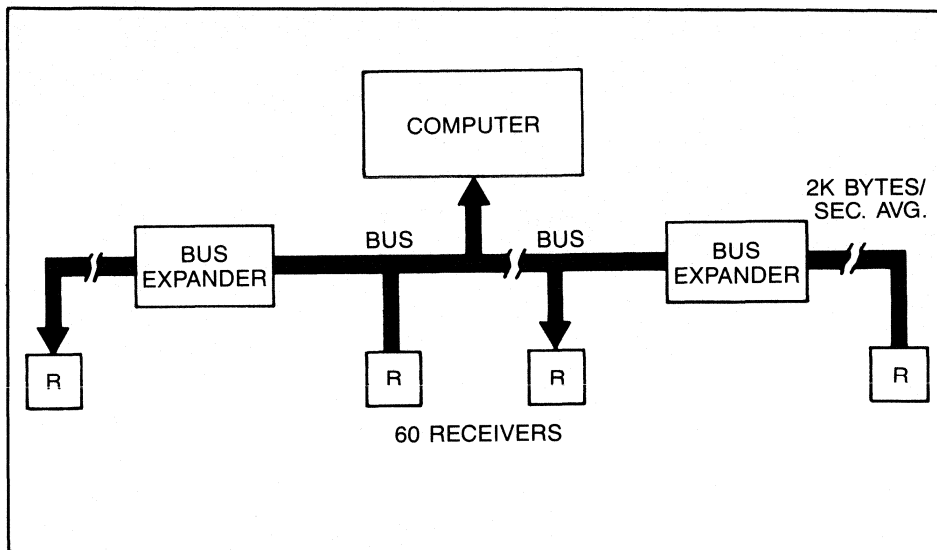


Figure 1. Receiving system without a controller

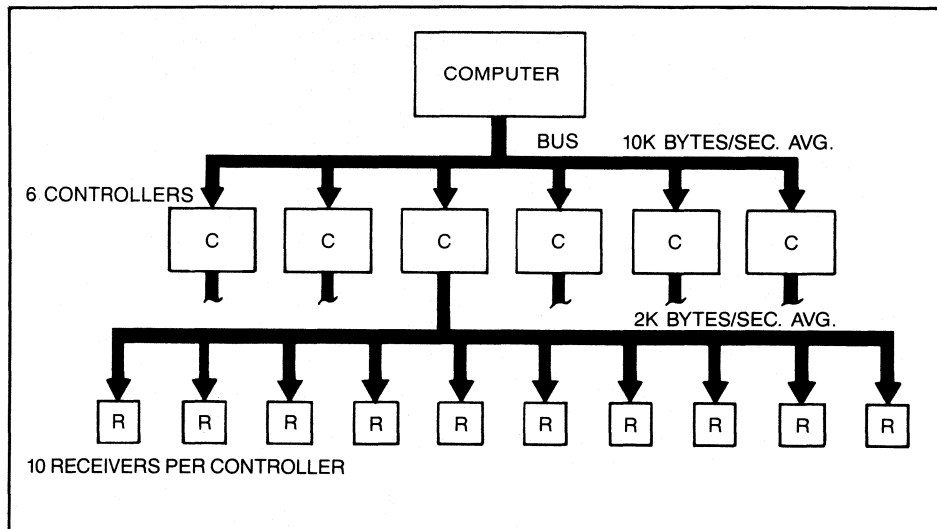


Figure 2. Receiving system with a controller

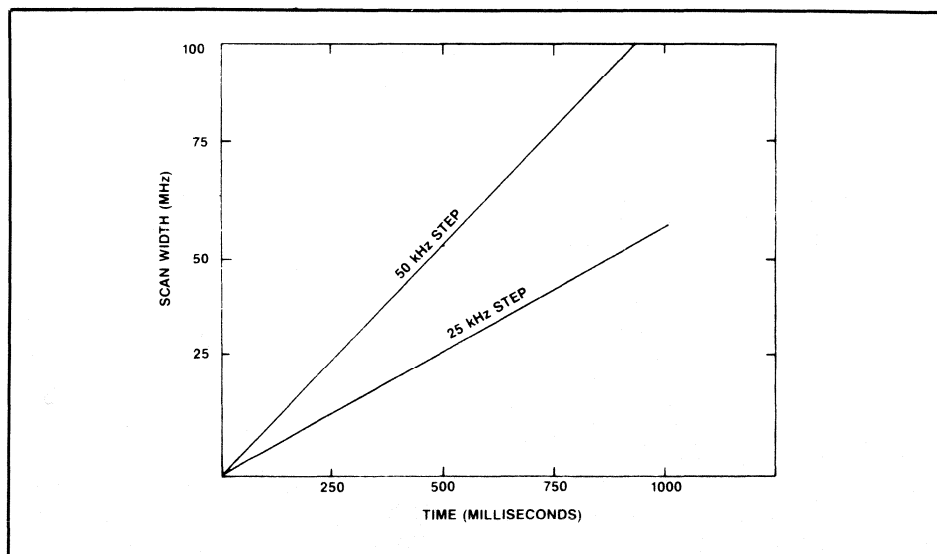


Figure 3. Typical scan speed

stepping superheterodyne receiver.

Ideally, the superheterodyne receiver chosen for a fast-scanning application should be frequency-synthesized and microprocessor controlled. The Fast Scan/Step operation then may be largely software based, using an internal microprocessor. The required time-per-frequency point can be expected to be approximately 400 microseconds. If frequency steps equal to the IF bandwidth being used are taken, a 50 MHz spectrum can be scanned in less than one second with IF bandwidths as narrow as 25 kHz. Fig. 3 shows the relationship of spectrum width, IF bandwidth and scan time. The following example illustrates the scan speed performance to be expected with this type of narrowband superheterodyne receiver.

Assume a requirement to scan a 50 MHz spectrum using an IF bandwidth of 50 kHz. The number of frequency steps will be:

$$\frac{\text{Scan Width}}{\text{IF BW}} = \frac{50 \times 10^6}{50 \times 10^3} = 1 \times 10^3 \text{ Steps}$$

Approximate time per frequency step is 400 microseconds:

$$\begin{aligned} \text{Steps} \times \text{Time/Step} &= \\ (1 \times 10^3) \times (400 \times 10^{-6}) &= \\ 400 \times 10^{-3} \text{ Seconds} \end{aligned}$$

Number of 5 MHz crossings will be:

$$\frac{\text{Scan Width}}{5 \text{ MHz}} = \frac{50 \times 10^6}{5 \times 10^6} = 10$$

Approximate time for ten 5 MHz crossings at 3 milliseconds per crossing is:

$$10 \times 3 \text{ milliseconds} = 30 \text{ milliseconds}$$

Total approximate scan time will be 430 milliseconds for the 50 MHz scan, using a 50 kHz step size.

Approximately 430 milliseconds is required only if the scanning receiver does not stop on signals encountered. If the receiver must stop on signals above a selected level, additional time will be required. The additional time may vary from 100 microseconds to a few milliseconds, depending on the routine initiated; i.e., AFC to center signal in IF passband, AGC to adjust receiver gain; comparison, measurement for recognition of signal or modulation characteristics, etc. Many, if not all, of these routines can be programmed into the microprocessor resident in each receiver. However, more versatility and flexibility can be achieved if most of these functions or routines are assigned to additional microprocessor capability in a multiple receiver controller.

Using Noise to Advantage in Military Systems

By Tony Ramsden
Micronetics, Inc.

Noise as an Interfering Source

The performance of any system will inevitably suffer in some way from the effects of interference from the environment it operates in. For military systems this is often particularly important, so some way has to be found to simulate different levels of interference and generate a measure of susceptibility.

Since there is usually no prior knowledge of the form or character of the interference, noise is usually the quickest way of finding the weakest point in the system. Sometimes the form of the interfering signal can be predicted, in which case noise that is colored or superimposed on a coherent signal is more appropriate. A particular example of this occurs in digital transmission, which is relatively impervious to noise unless it occurs at the same transmission rate, a likely occurrence if adjacent cables are carrying similar traffic.

Noise as a Calibration Reference

Perhaps the most common application of noise is a calibrated noise source used in conjunction with a Noise Figure Meter, which provides a measure of the sensitivity performance of receivers. Here the levels of signal and noise are extremely low, so an accurate reference of level is essential to the measurement. For such tests the noise being produced by the front end of the receiver is matched to a reference

noise source (Fig. 1) by monitoring the receiver output to see how much noise has to be added to increase the output by 3 dB. Since the noise source is accurately calibrated in terms of level and frequency, it is a short step to derive the sensitivity or "noise figure" of the receiver.

These same principles can be extended to the measurement of amplifier and system performance, expanding the applications to almost all electronic systems. Of special interest in the military is the use of built in noise sources (part of the move to BITE, built-in-test-equipment), which now measure the performance of critical amplifiers and receivers continuously on aircraft and in space vehicles and, should it become necessary, even rearrange their functional order.

Noise to Simulate Channel Loading

The logical way to determine if a communications link is working is to test it fully loaded with voice, data, etc., and check it under the most unfavorable operating conditions. It was discovered in the 1950s that White noise simulated actual traffic and of course was much more controllable. The White Noise Test Set has since become the internationally accepted way of determining the performance of all broadband frequency division multiplex systems.

"White" indicates that the spectral density is constant across the band under

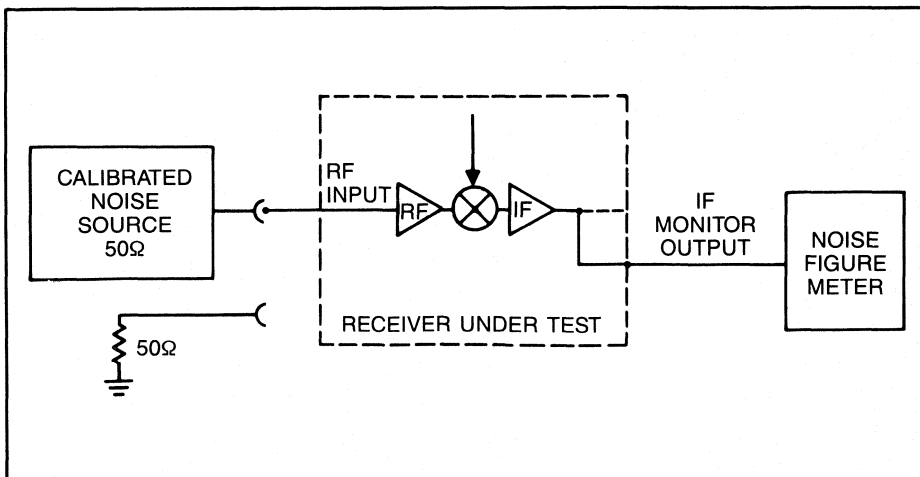


Figure 1. Use of calibrated noise source to measure receiver front end performance

study, while "Gaussian" is a measure of the distribution probability that amplitude peaks reach a certain level. (It is interesting to note that both are capitalized, "Gaussian" after the well known 19th Century German mathematician Karl Frederick Gauss, but also "White" allegedly after R.W. White and J.S. Whyte of the British Post Office, who in 1955, pioneered the use of flat broadband noise to measure interchannel crosstalk on multichannel telephone systems.)

White noise from a Noise Generator is limited to the bandwidth of the system under test and fed to the baseband input at a standard reference level, equivalent to a light channel loading. "Quiet" channels are introduced into the baseband using band stop filters. A narrow band receiver tuned to these frequencies can measure how much noise and intermodulation is being introduced by the transmission system. The test is repeated at higher and higher input levels until the system goes into overload and performance crashes. This is then repeated with other band stop filters, so results are obtained for frequencies at the top, middle and low ends of the baseband. The graphs generated, generally known as "bucket curves," reveal valuable information on the distortions present and direct the user to where they are being introduced.

Noise to Evaluate A/D Converters

Every time an analog signal is digitized errors are introduced, since the continuous function never has a precisely corresponding code. There is always a "quantizing" error which appears at the output as noise. If the digital transmission path is essentially error free, no additional noise will be added to the system until the codes are returned to their original analog form in the D/A converter. It is therefore very important to check the performance of digital modems most critically.

Most A/D converters have compression characteristics built into them, so the signal-to-quantizing noise is essentially constant over the operating range of the analog input. Not to do this would produce very poor performance at low input levels, which would have only a few levels allocated to them. Such compression was once done with a continuous curve; however, with today's components it is more easily performed digitally, where the slope of the characteristic is modified at specific levels, known generally as segmented companding.

When it comes to measuring quantization noise, sine waves once again have severe limitations, although this time the problem is that its amplitude distribution

rather than its frequency distribution is so unlike the real signal. Think of the peak of the sine wave as its level is increased. As it meets a new quantizing level the error will be minimal, while between levels it will be at a maximum. The resulting graph will therefore resemble rolling hills, useful for determining if all the quantizing levels are operating, but at the cost of making a vast number of measurements. This problem is further compounded when one adds segmented compression, which effectively superimposes a further range of hills on an already complex graph.

Once again, White noise can simplify testing, since it builds a Gaussian level distribution into each measurement, effectively "blurring" the effects of both quantum step and slope transition. The resulting smooth curve can then be accurately constructed from a relatively few measurements. This technique has been applied to PCM telephone systems for some time; however, its extension to the testing of higher frequency A/D converters, common in the military, is only recently being realized. One problem has been the lack of suitable test equipment, which was li-

mitted to White Noise Test Sets designed to evaluate basebands with top frequencies of 13.388 MHz. A few sets were introduced with wider bandwidths, but at a considerable premium in price.

Micronetics' Noise Generators fitted with appropriate band stop filtering meet the demands of this market. With the significant advances in intermodulation performance in the past few years, spectrum analyzers can now make the required measurements with little, if any, pre-filtering, eliminating the need for a specialized receiver.

References

White, R.W. and J.S. Whyte, "Equipment for Measurement of Interchannel Crosstalk and Noise on Broadband Multichannel Telephone Systems," *The Post Office Electrical Engineers Journal*, Vol. 48, Part 3 (October 1955), pp. 26-31.

Tant, M.J., "The White Noise Book," Marconi Instruments, Allendale, N.J., 1974.

"Bucket Curves — Part 1 & 2" G.T. & E. Lenkurt Demodulator, March/April 1976.

Schneider, S., "A Noise Nomograph," *RF Design*, June 1985.

Frequency-Hopping with Direct-Digital Synthesis

By Henry Eisenson
Scitec Electronics

Frequency synthesizers can be judged by any of several criteria and the relative weight of those parameters is determined by the application. In some cases, spectral purity is the overwhelming factor — in others it might be size alone. In every design situation, however, there is usually some combination of tradeoffs because no one methodology is ideal. In many technologies, including military communications and radar, one of the most important criteria is the speed with which the synthesizer can "hop" from one frequency to another, its switching speed.

Of the three synthesis architectures, each has its advantages and disadvantages. PLL is clean and broadband but requires extreme complexity (multiple loops) to generate high resolution, and this technique is ponderous in a world that measures time in fractions of a microsecond. Mix/filter can be clean and broadband, but is complex and costly because of the multitude of reference frequencies that must be generated. The third alternative is direct-digital synthesis (DDS).

With DDS a frequency control word (binary or BCD) controls an accumulator that refers to a program on PROMs to define the signal output. That signal is fed to a D/A converter, the output of which is smoothed (and the clock signal removed) by a low-pass filter. The result is compact, fast and perfectly phase-continuous when frequencies change.

A DDS is driven by a single reference clock, the frequency of which helps determine the output frequency range of the device. Information theory says that two samples per Hz is sufficient to perfectly reconstruct a waveform: therefore, output of the synthesizer is theoretically limited to exactly one-half the clock rate. In fact, that sampling rate is not achievable and the actual output frequency limit of a DDS is always slightly less than half the clock rate.

The limit of today's technology permits a DDS to be clocked at about 76 MHz, with logic and PROMs setting the limit. The maximum output frequency from such a unit is about 38 MHz, though in

practice this is limited to under 35 MHz. Fortunately, the device provides both high resolution and switching speed that is many times faster than any alternative. The operation and very nature of a DDS permits it to change frequencies in a period equal to one clock tick plus the delay introduced by the output lowpass filter. In operation, such a DDS switches between any two frequencies in less than 70 nanoseconds.

Special features, including quadrature output, high-resolution phase rotation, phase reset to 0° and output gating, are all easy with a DDS because control and processing both occur in the digital domain. Because of the way a DDS constructs the output waveform, high resolution is practical and inexpensive. It is relatively easy to achieve a milliHertz, a microHertz, or even a femtoHertz, with no important collateral penalties. The dif-


ference appears in the accumulation and logic portions of the machine as a few more ICs. The nature of a DDS also permits remarkable phase noise; in baseband some designs demonstrate <-136 dBc/Hz offset. Spurious output derives primarily from glitch energy in the D/A converter, and present designs are generally limited to about -60 dBc. In many DDS applications where maximum bandwidth and switching speed are design goals -45 dBc spurs is a more realistic objective. The major limitations of a DDS, then, are bandwidth and spurious energy in the output.

Many programs can benefit from synthesizers that exploit the high resolution and fast switching of a DDS while achieving the operating range of one of the more conventional architectures. Hybridization does exactly that. When PLL and DDS techniques appear in the same synthesizer, the result can offer high resolution, compact size, low cost and extraordinary reliability because of the predominance of the digital component.

When mix/filter and DDS are combined, the result is speed. In an industry that defines "fast" as anything under 20 microseconds, the speed of a DDS creates many new opportunities for the design engineer.

The simplest exploitation of the hybrid concept mixes the output of the DDS with an LO and filters the result. This architecture can take advantage of the DDS, moving its operation to a new center frequency. It is practical to use 20 MHz of the output of a 30 MHz bandwidth DDS, mix it with an LO in the VHF range and filter the result. Such a synthesizer can cover any 20 MHz sector of VHF with high resolution, very fast switching, small size and excellent reliability.

As one example, a 100-120 MHz synthesizer can be built with 4 Hz resolution, 150 nanosecond switching, and excellent spectral characteristics. With the clock and the LO references supplied to it, such a product can be expressed in only 24 square inches. It might then become one module of a much more complex synthesizer designed to operate in the microwave region. If the end result must operate in C-band, for instance, it is a relatively simple matter to continue the upconversion as required. Each mix/filter stage can impose a delay due to the characteristics of the filters used. With sufficiently wide-band filters these penalties are minimized.

Using such hybrid architecture, it is quite possible to design a microwave synthesizer with switching in a fraction of a microsecond, which defines today's state-of-the-art in frequency hopping. 

High Frequency Amplifier IC Simplifies Design

By Tom DeLurio
Signetics Corporation

The incorporation of a complete sub-system in one package is the direction taken by many RF component manufacturers. The design engineer has a whole new category of "super components" to understand and incorporate into his designs. The Signetics NE5205 amplifier described here is a recently introduced product of this type. Although used to describe one product, the author's information is useful for understanding many similar devices.

In the past, most RF and high frequency designers had to settle for discrete or hybrid solutions to their amplification problems. Most of these solutions re-

quired design compromises in order to use high frequency gain stages, including high power consumption, large component count, impedance matching transformers, large packages with heat sinks and high parts cost. A new part has been developed which incorporates a wide-band amplifier on a single monolithic chip that has 50/75 ohm input and output impedances, is internally compensated, and needs no external components when applying AC coupled signals.

The NE5205 is a high frequency amplifier with a fixed insertion gain of 20 dB into a 50 or 75 ohm matched impedance system. The NE5205 block diagram and corresponding gain-bandwidth character-

istics are shown in Fig. 1. It can be seen that the insertion gain is flat to ± 0.5 dB from DC to 475 MHz and has a -3 dB frequency greater than 600 MHz.

The device has a single ended non-inverting input and a single ended output. The NE5205 operates with a single supply of 6 V and only draws 25 mA of supply current, compared to hybrid parts which range from 12 V and up with a supply current of 85 mA. The noise figure is 4.8 dB in a 75 ohm system and 6 dB in a 50 ohm system with lower noise versions available in the future.

Since the part is incorporated on one die, capacitance is minimized. The die size is small enough to fit into an 8-pin

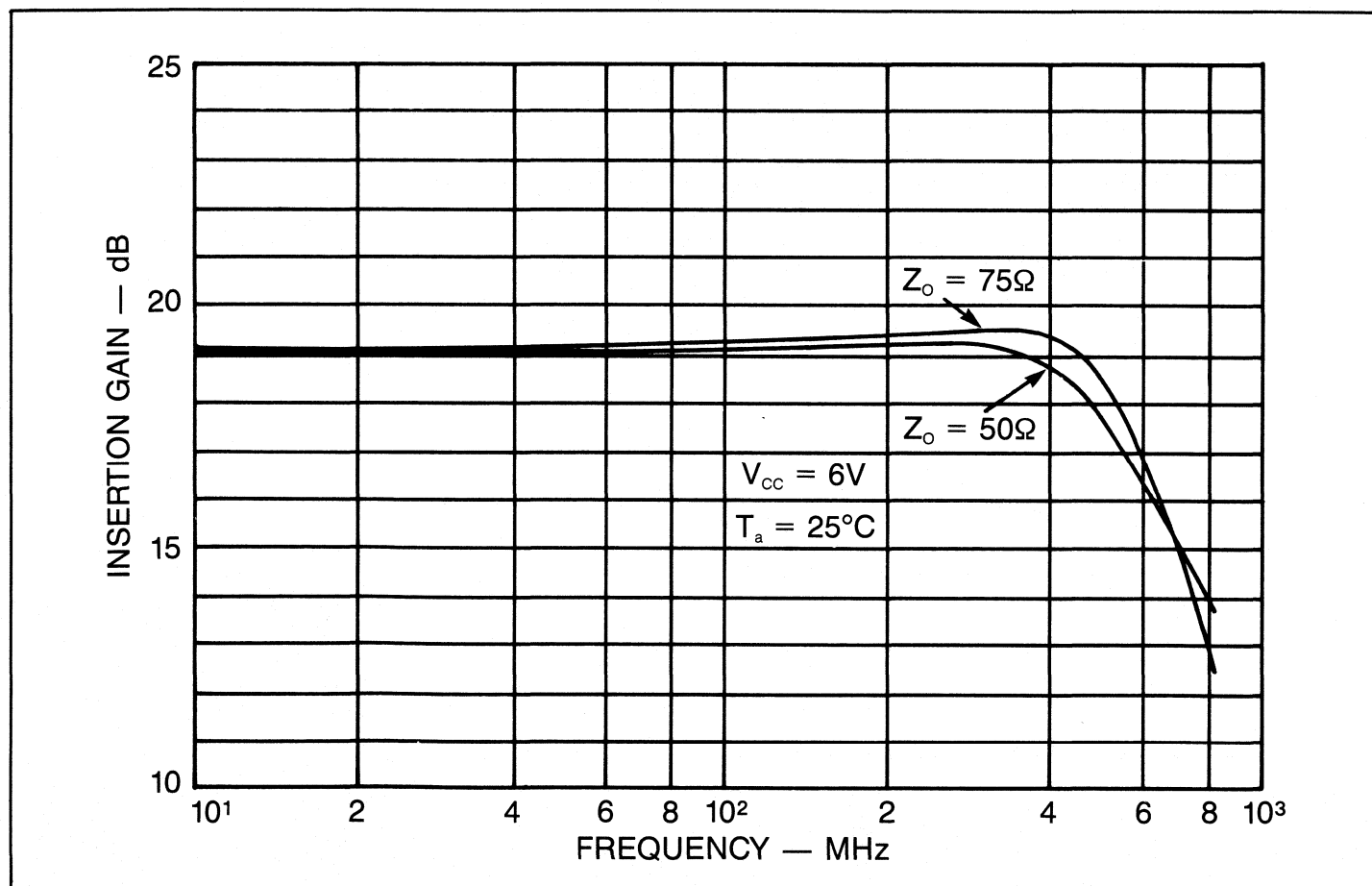


Figure 1. Insertion gain vs. frequency (S_{21})

small-outline (SO) package. The smaller size of the SO package is beneficial to board layout, and the inherent smaller lead inductances of the package are important for high frequency operation. The SO package can operate over commercial and industrial temperature ranges from -40°C to $+85^{\circ}\text{C}$. A TO-46 metal can is available with a case connection for RF grounding which increases the -3 dB frequency range to 650 MHz . The metal can is hermetically sealed and can operate over the full -55 to $+125^{\circ}\text{C}$ range. Plastic and ceramic DIP packages are also available.

The amplifier has very good distortion specifications. The second and third order intermodulation intercepts are $+24\text{ dBm}$ and $+17\text{ dBm}$, respectively, representing the low-level linearity of the NE5205. When operating with a 6V power supply, the output is biased at 3.3V , and at 100 MHz the NE5205 can swing approximately $1.4\text{V}_{\text{p-p}}$ into a 50 ohm load. Under

these conditions, the saturated output power is $+7\text{ dBm}$. If used with larger loads, the output swing will increase but the system will not be matched.

The VSWR of the input and output is less than 1.5 across the entire DC to 600 MHz -3 dB bandwidth of the NE5205. This represents the part's good impedance matching to the corresponding 50 or 75 ohm system. The NE5205 is well-suited for 75 ohm cable television applications such as decoder boxes, satellite receiver/decoders, front-end amplifiers for TV receivers, amplified splitters and antenna amplifiers.

The device is also well matched for 50 ohm test equipment such as signal generators, oscilloscopes, frequency counters, and all kinds of signal analyzers. Other 50 ohm applications include mobile radio, CB radio, and other communications equipment. The NE5205 can also be used in data/video transmission, broadband LANs (Local Area Networks) and

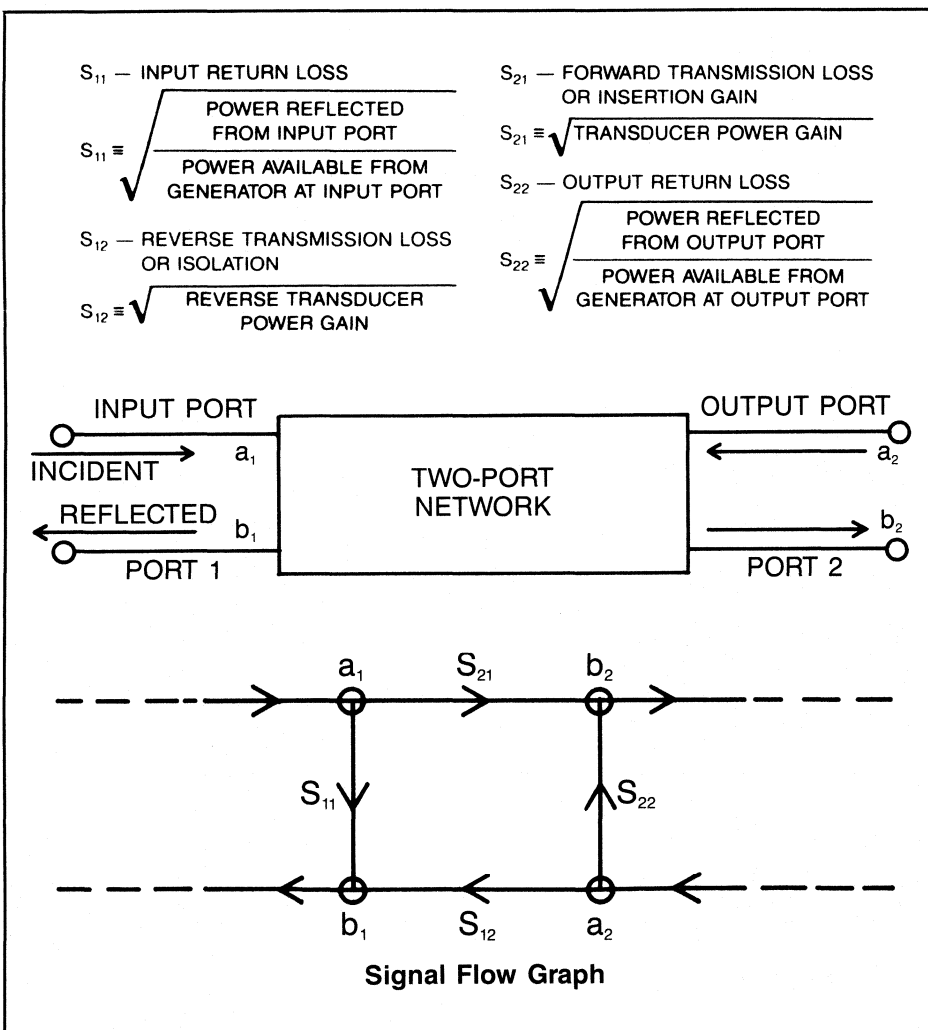
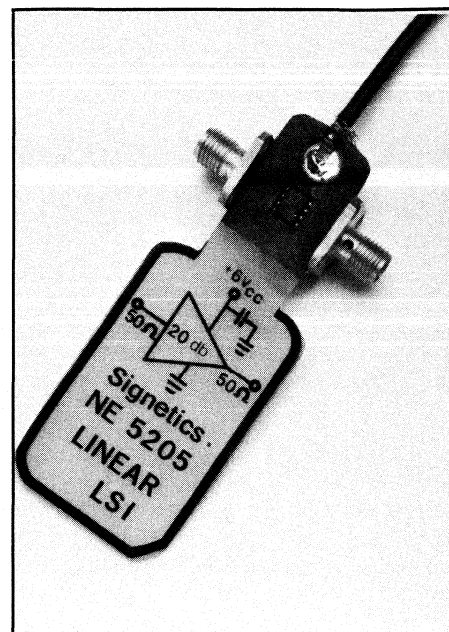


Figure 2. Scattering parameter definitions for a two-port system

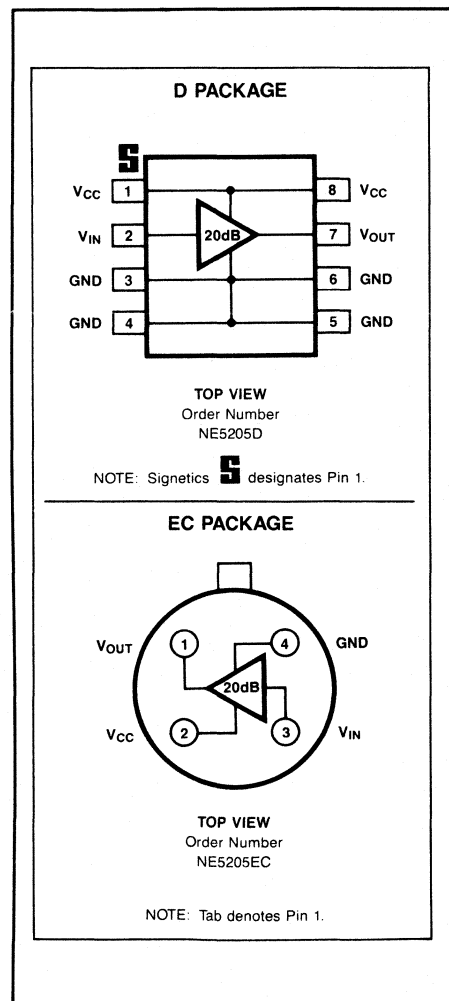


Fig. 3 — Pinout diagrams of the NE5205.

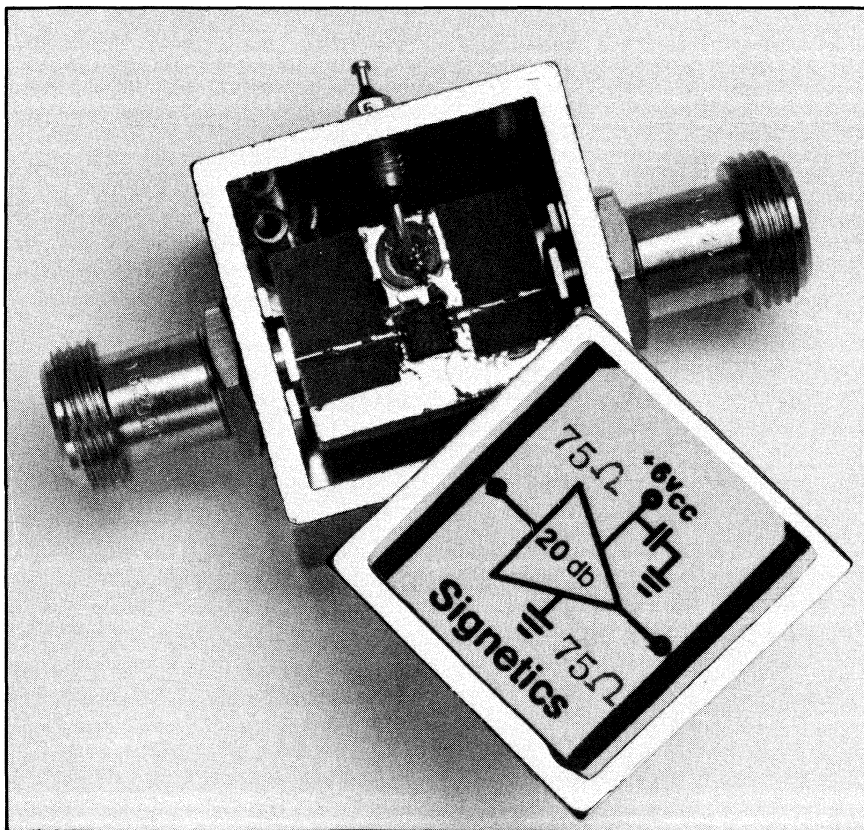
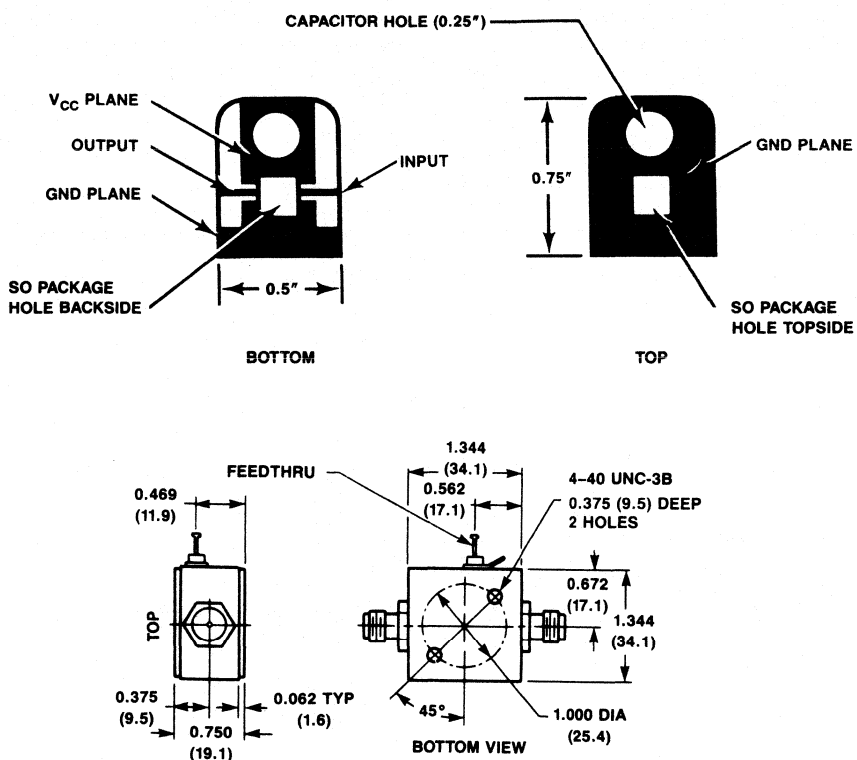


Figure 4. Evaluation board layout

telecom in general.

Scattering Parameters

The primary specifications for the NE5205 are listed as S-parameters. They are measurements of incident and reflected voltages and currents or "powers" between the source, amplifier and load as well as transmission losses and gains. S-parameters are measured with the device connected between a 50 or 75 ohm matched load and the corresponding source. These are the actual operating conditions for the part and a realistic test of its capabilities.

The definitions for scattering parameters for a two-port network in which the NE5205 is tested are in Fig. 2. The notations a_1 and a_2 represent incident waves and b_1 and b_2 are the reflected waves and are the basis for the measurements.

There are commercially available test systems that will do S-parameter tests. Signetics uses a Hewlett-Packard system that incorporates the following equipment:

- 9845A — Desktop Computer
- 8505A — Network Analyzer
- 8503B — S Parameter Test Set — 75 ohm
- 3455A — Digital Voltmeter
- 8501A — Storage — Normalizer
- 8503A — S Parameter Test Set — 50 ohm
- 6002A — DC Power Supply

The test jig for the surface mount small outline package is available and is discussed below. The software that controls the testing is designed for a production type system. It can be used for PASS/FAIL readout or for full data log. A copy of the "test key" listing the tests, conditions and limits used in the program is available from Signetics.

Evaluation Boards

The evaluation board shown in Fig. 4 produces excellent results although it does not employ microstriplines. This is primarily used as an inexpensive solution to measuring the performance of the part or prototyping. This board has been tested and has performed satisfactorily compared to testing the part in a special test jig. Performance data is provided with the NE5205 data sheet.

Both 50 and 75 ohm boards are available with boxes and various connectors (SMA, N, F and BNC) in kit form from Advanced Analog Systems Corporation.

Signetics has helped design production-type test fixtures to accept the small outline (SO) package in either a 50 or 75 ohm system. The fixture exhibits excellent VSWR specifications, less than 1.1 within the NE5205 frequency range. The test

socket is built into a PC board similar to the one shown in Fig. 4, housed in a massive brass housing and unique receptor mechanism to enable the user to test SO devices without any solder connection in

a shielded environment. The 50 ohm system uses female SMA type connectors, and the 75 ohm system utilizes female N type connectors. They are both available from Megarate Test Products Sales.

Applications

Because the NE5205 is a complete design, it can be used in any 50 or 75 ohm system with few external components and little compensation for oscillation or matching networks. The NE5205 can be used not only as an amplifier but also as a buffer and driver. It can be used in instrumentation applications to buffer and drive other circuits such as balanced mixers and analog to digital converters. The NE5205 can be used as a gain stage and buffer when there are losses or mismatches due to passive elements used as filters (Fig. 5). In all these applications, the S-parameter tests can be used to verify correct impedance matching and design.

If more gain is needed, the amplifiers can be cascaded as shown in Fig. 6. Test show that a 40 dB gain stage can be designed this way with minimal loss in frequency response.

Another interesting application is to use the NE5205 as a remote antenna amplifier. In Fig. 7 the NE5205 is AC coupled to a 75 ohm antenna and TV receiver input connection through a 75 ohm coax cable. A DC voltage of 6V to 8V is connected to the 75 ohm cable and decoupled from the receiver with an additional DC blocking capacitor. To power up the amplifier, the DC is tapped off the line with an RF choke and a power supply decoupling capacitor. This system will give the signal from the antenna an extra 20 dB gain and increase the apparent sensitivity of the TV receiver.

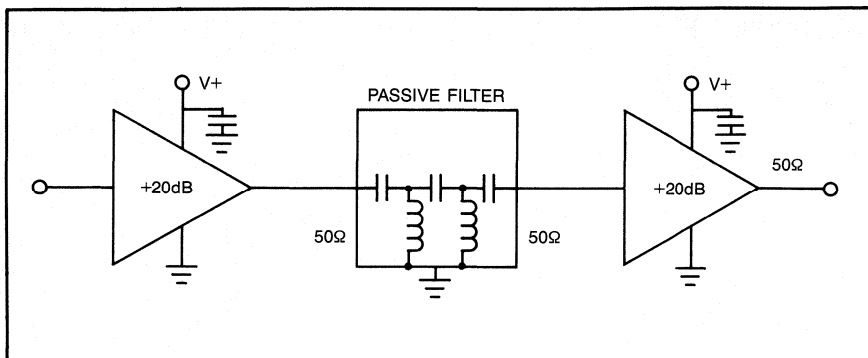


Figure 5. Buffering and driving a passive or SAW filter

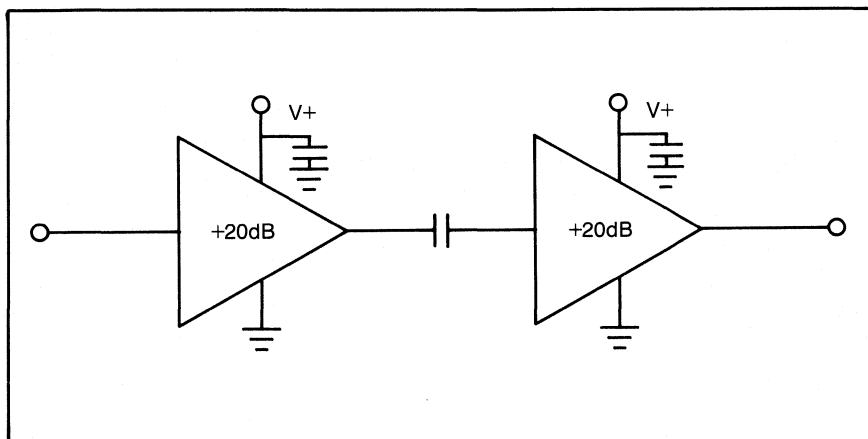


Figure 6. Cascading two amplifiers for a 40 dB gain

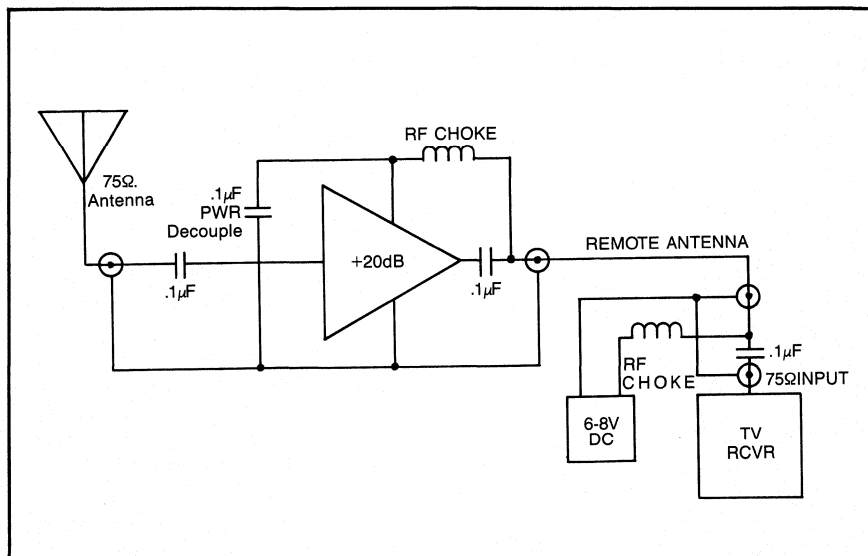


Figure 7. The NE5205 as an antenna amplifier

For more information about the products mentioned in this article, circle the following INFO/CARD numbers:
 NE5205, INFO/CARD #125
 Signetics, Inc. NE5205 Evaluation Kit,
 Advanced Analog
 Systems, Inc. INFO/CARD #124
 Production Test Fixture,
 Megarate Test
 Product Sales INFO/CARD #123

Additional Reading on Scattering Parameters

For more information regarding S-parameters, please refer to:

High-Frequency Amplifiers, Ralph S. Carson, University of Missouri, Rolla, John Wiley & Sons, Inc., 1985.

S-Parameter Techniques for Faster, More Accurate Network Design, H.P. App Note 95-1, Richard W. Anderson, 1967, HP Journal.

S-Parameter Design, H.P. App Note 154, 1972. 

Engineering Use of Spreadsheet Languages

By Pat O'Neil
Motorola Government Electronics Division

The growing use of personal computers by design engineers has created a demand for software specific to their needs. The great diversity of engineering applications may never be completely served by software suppliers, and engineers will continue to write their own programs. Author O'Neil presents a method of using currently available spreadsheet software for engineering computations, saving time that would be spent writing separate programs for each new application.

Recently there has been a great deal of discussion among the readers of *RF Design* regarding the qualities of BASIC versus the various calculator based languages. This discussion has centered around machine availability and portability rather than the actual ease of programming, because each of these languages is relatively easy to program if the user is fluent in the particular language he is using.

For those with access to computers there is another alternative: spreadsheets. The use of spreadsheet languages offers a new level of programming ease and interaction, a quality which has long been recognized in the financial and management worlds, but which seems to have been largely overlooked by the engineering community.

Spreadsheet Operation

To see what has made the spreadsheet so popular and useful, let us write a trivial program to manipulate Ohm's Law. Each cell of the spreadsheet may contain a label, a number, or a formula. Let us use labels first. We can write across the top of the sheet (Fig. 1) the letters E, I, R in cell locations A1, B1, C1. In line 2 we write in location A2 the number 4 (volts) and in location B2 the number 2 (amps). In location C2 we can write (A2/B2). What appears on the screen in cell C2 is the number 2 (ohms). If we move the cursor back to A2 and change the number to 10, the number in C2 immediately changes to 5.

Of course, the example is trivial but illustrates the power that can be used if the output were, for example, linewidths and spacings for a 7-pole Chebyshev parallel line filter. By entering all the appropriate

formulae and constants in spreadsheet cells, such a filter can be designed for any frequency and bandwidth simply by entering the required frequency and bandwidth in the appropriate cells, so that the line widths, line lengths, and spacings immediately appear on the screen. Such a program can be written in BASIC, TI-59, HP-41, Pascal, etc., but only by actually trying the spreadsheet can one appreciate just how much quicker and easier the spreadsheet is to program, debug and utilize.

As another example, Fig. 3 shows a spreadsheet programmed to display the results of a program originally written in BASIC in May/June 1984 *RF Design* to calculate the optimum terminations for an unconditionally stable amplifier (1). Figure 3 shows the output as calculated for the

example used by the authors. So far, there appears to be no advantage to the use of a spreadsheet instead of BASIC. But what happens if we change *gr* to 0.1 mS instead of 0? Look at the output of Fig. 4. "ERROR" flashes everywhere. (Notice that *C* is now greater than 1). If *gr* is $-1E-3$, look at Fig. 5. The gain has dropped to 19.3 dB. The instantaneous nature of these answers greatly facilitates interaction with the calculations as compared with BASIC or calculator programs which require re-entry of all the data and "run" to get the answers.

In addition, since the mechanics of getting hard copy are already provided in the spreadsheet language, a simple command will print out the entire sheet for documentation. In fact, one of the main advantages of spreadsheets is that the

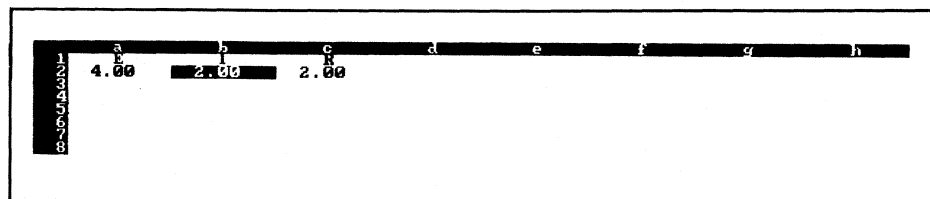


Figure 1. Trivial Ohm's Law calculation

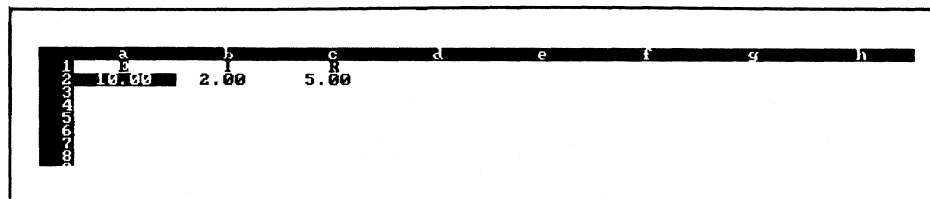


Figure 2. Trivial Ohm's Law calculation changed to 10 volts

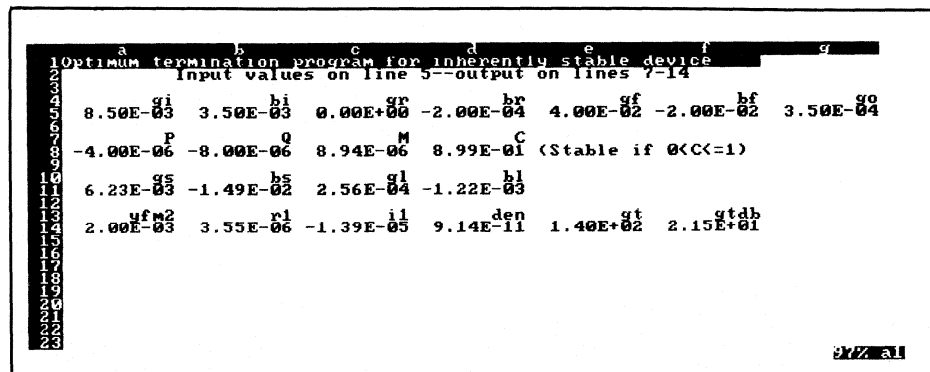


Figure 3. Linvill stability calc sheet



Figure 4. Linvill stability calc sheet: unstable case



Figure 5. Linvill stability calc sheet: stable case



Figure 6. Use of spreadsheet graphics

language provides all the input/output support that often comprises more than half the code of a traditional program.

As a final example Fig. 6 shows a spreadsheet program which utilizes simple graphics to illustrate the behavior of the function being calculated. Nearly all spreadsheets offer this simple level of graphics, and some, such as Lotus® and SuperCalc®, offer much more graphics power. This graphics I/O capability is built into the language and is easily accessed without complex programming.

Engineering Spreadsheets

To be sure, not all spreadsheets are useful to the engineering world, primarily because many of them are oriented toward business application. To be useful for engineering a spreadsheet language must contain trigonometric functions, logarithmic and exponential functions, scientific notation and the other normal expressions useful to engineers. In view of the original applications of the first spreadsheet, the foresight of the authors in including these functions is remarkable, and their scientific education undoubtedly influenced this choice. However, later imitators of VisiCalc have not always been so broadminded and have often substituted financial functions for engineering functions.

Spreadsheets useful for scientific work include but are not limited to:

VisiCalc	MyCalc
SuperCalc	MultiPlan
Lotus 1-2-3	PerfectCalc

Others which are NOT suitable include financial spreadsheets such as:

CalcStar	ScratchPad
ProCalc	MicroPlan


The best bet is to go to a local dealer and try a program to make sure it has all the needed functions.

If one has access to a suitable spreadsheet, many calculation programs used frequently are more easily done on the spreadsheet. Almost any calculations that do not involve repetitive loops can be programmed in "calc." Engineers who are familiar with this use of spreadsheets seldom reach for pencil, paper, and calculator for a long series of calculations — they reach for the spreadsheet disk. I might add that there exists no engineer who has not had to prepare a budget or fill out an expense account, and the spreadsheet obviously excels at these necessary chores. Using a good engineering oriented spreadsheet program can frequently make engineering programming and calculations easier and more convenient than other computer languages.

About the Author

Pat O'Neil is Section Manager, Communications Research Facility, Secure Communications Operations at the Government Electronics Division of Motorola, Inc., P.O. Box 1417, Scottsdale, AZ 85252.

References

1. Hertling, D.R. and R.K. Feeney, "Basic Program for Designing an RF Amplifier Using an Inherently Stable Device," *RF Design*, May/June 1984, pp. 56-61. 

Power Line Filter Considerations

By Gary A. Breed

With the increasing regulation of RFI/EMI radiation and susceptibility, and with the growing use of the RF spectrum, design engineers need to understand power line filter performance for reduction of conducted RFI/EMI. The need for proper filter selection at the design stage is more important than ever, since the FCC has stated that any change in the design or construction of FCC-regulated equipment will require re-certification! The designer must not only select a filter based on performance, but must also work with purchasing and supply personnel to assure that the unit selected will be available in production quantities.

With the help of Pete McDonnell of Curtis Industries, Inc., basic technical considerations and selection guidelines for power line filters are presented here.

At first glance, selecting a power line filter seems to be an uncomplicated task, but there are many factors to be considered, both obvious and subtle. First, the engineer must answer the pertinent questions about the interference to be eliminated: Is the power supply linear or switching type? What frequency and amplitude is the internally-generated energy? What types of EMI is the equipment susceptible to? Is the unwanted energy coupled in the common mode (line to ground) or differential mode (line to line)? Once these questions are answered, filter requirements can be determined.

Electrical specifications of power line filters include voltage, current, line frequency and temperature range information, plus mechanical and environmental requirements. The agency approval needs (UL, CSA or VDE) should be identified, as well as any additional testing that might be desired. Finally, the needed attenuation specifications and the operating impedance of the filter should be identified. With this information, a properly performing filter can be obtained.

Typically, a power line filter is a two- or three-pole lowpass filter with minimal loss at 60 Hz and a stopband above 10 kHz.

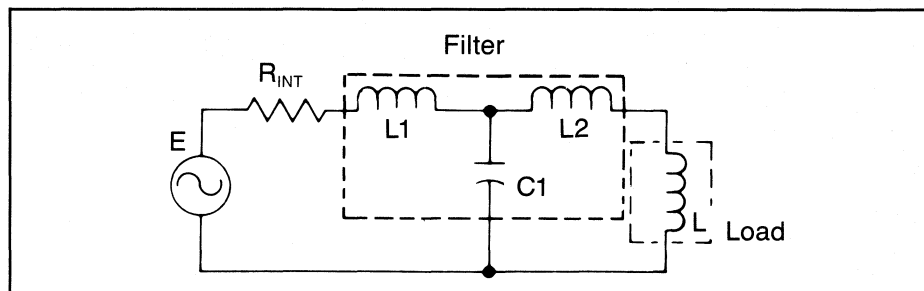


Figure 1. Three-pole filter, inductive load

The filter attenuation specifications must be understood, however, to get the expected performance. Most manufacturers use line impedance stabilization networks to determine their published performance data. A specific design is not likely to present the same impedance to the filter under operating conditions. Also, if the load is capacitive or inductive, shunt capacitors or series inductors in the power line filter will effectively become part of the load impedance. A three-pole filter with an inductor in series with an inductive load (Fig. 1) will perform as a two-pole network (Fig. 2), with RF attenuation less than expected.

Collaboration is needed between the equipment designer and the filter manufacturer. Some filter companies, including Curtis Industries, have in-house test facilities which can be used to measure per-

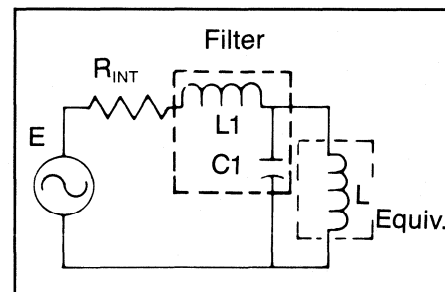
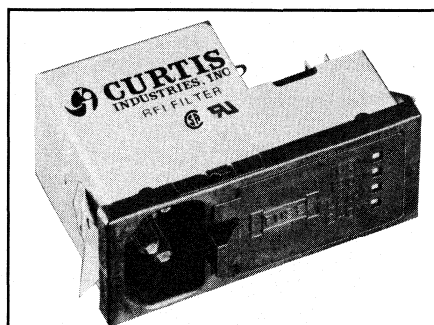


Figure 2. Effective circuit of Fig. 1, with L2 and load combined

formance of a particular filter/equipment combination. Often, a custom filter or modification of a stock design may be needed to achieve required EMI performance. Filter manufacturers emphasize their ability to handle such requirements with ease, recognizing that stock filters will not meet all requirements.

Finally, it pays to be familiar with the current status of filter products. New products and features are always being introduced. For example, complete power entry assemblies are now available, combining power cord connector, fuse, line voltage selector and line filter in a single unit. Such an assembly can save labor costs on the assembly line.

Like every other component designed into a product, power line filter selection requires the engineer to know his product's requirements and the capabilities of prospective suppliers. rf



Integrated power-entry assembly, combining socket, fuse, voltage selector and EMI filter in one unit.